Novel Secondary Metabolites from Endophytic Marine-derived Fungi

Dissertation

zur

Erlangung des Doktorgrades (Dr. rer. nat.)

der

Mathematisch-Naturwissenschaftlichen Fakultät

der

Rheinischen Friedrich-Wilhelms-Universität Bonn

vorgelegt von

Celso Almeida

aus

Lissabon, Portugal

Bonn 2011

Angefertigt mit Genehmigung der Mathematisch-Naturwissenschaftlichen Fakultät
der Rheinischen Friedrich-Wilhelms-Universität Bonn

1. Gutachterin	:	Prof. Dr. G. M. König
2. Gutachterin	:	Prof. Dr. E. Kostenis

Tag der Promotion	:	15. Februar 2011
Erscheinungsjahr	:	2011

Vorveröffentlichungen der Dissertation/In Advance Publications of the Dissertation

Teilergebnisse aus dieser Arbeit wurden mit Genehmigung der Mathematisch-Naturwissenschaftlichen Fakultät, vertreten durch die Mentorin/Betreuerin der Arbeit, in folgenden Beiträgen vorab veröffentlicht:

Parts of this study have been published in advance by permission of the Mathematisch-Naturwissenschaftlichen Fakultät, represented by the supervisor of this study:

Publikationen / Research Papers

Almeida C., Eguereva E., Kehraus S., Siering C. and König G.M., Hydroxylated Sclerosporin Derivatives from the Marine-derived Fungus *Cadophora malorum, J. Nat. Prod.*, **2010**, *73* (3), pp 476–478.

Almeida C., Elsaedi S., Kehraus S. and König G. M., Novel Bisabolane Sesquiterpenes from the Marine-derived Fungus *Verticillium tenerum*, *Nat. Prod. Commun*. **2010**, 5(4), 507-10.

Almeida C., Part N., Kehraus S. and König G. M., Stachylines A – D from the Sponge-derived Fungus *Stachylidium* sp. (*accepted by Journal of Natural Products*).

Almeida C., Kehraus S., Prudêncio M. and König G. M., Marilones A – J, Unusual Phthalides from the Sponge-derived Fungus *Stachylidium* sp. (*submitted to European Journal of Organic Chemistry*).

Almeida C., Kehraus S., Dimas K., Gütschow M. and König G. M., Marilines A – D, Novel Phthalimidines from the Sponge-derived Fungus *Stachylidium* sp. (*In preparation)*

Almeida C., Kehraus S. and König G. M., Novel Furyl Derivative from the Sponge-derived Fungus *Stachylidium* sp. (*In preparation*).

Almeida C., Kehraus S. and König G. M. Novel bioactive peptides from the Sponge-derived Fungus *Stachylidium* sp. (*In preparation*).

Tagungsbeiträge/Research Presentations

Almeida C., Kehraus S., König G. M., Hydroxylated derivatives of a rare cadinane-type sesquiterpene isolated from a cytotoxic *Wardomyces inflatus* extract. Poster presented at the 7th Natural Products Joint Meeting of AFERP, ASP, GA, PSE & SIF, August 3-8, 2008, Athens, Greece.

Almeida C., Kehraus S., König G. M., Hydroxylated derivatives of a rare cadinane-type sesquiterpene isolated from a cytotoxic *Wardomyces inflatus* extract. Poster presented at the Joint Meeting of the Deutsche Pharmazeutische Gesellschaft (DPhG), October 8-11, 2008, Bonn, Germany.

Almeida C., König G. M., Novel secondary metabolites from the sponge-derived fungus *Stachylidium* sp.; tracking bacterial endosymbionts. Oral presentation at the 50th Annual Meeting of the American Society of Pharmacognosy, June 27-July 1, 2009, Honolulu, Hawaii.

Almeida C., König G. M., Novel Secondary Metabolites from the Sponge-Derived Fungus *Stachylidium* sp.; Tracking Bacterial Endosymbionts. Poster presented at the 6th European Conference on Marine Natural Products, July 19 - 23, 2009, Porto, Portugal.

Almeida C., Kehraus S., Dimas K., and König G. M., Marilines A – D, Novel Phthalimidines from the Sponge-derived Fungus *Stachylidium* sp. Poster presented at the International Conference New Biotrends in Green Chemistry, December 1-2, 2010, Dortmund, Germany.

To my mother, Marilia, and father, Benjamim

Acknowledgements

I wish to express my sincere gratitude and admiration to my supervisor Prof. Dr. G. M. König for the expert guidance, encouragement and kind support during the course of this project. I would like to thank her for providing excellent scientific advice, working facilities, for letting me express my creativity, and especially for understanding and guidance in unexpected personal difficulties that arose during the research. I have nothing else than to be proud and consider to be a truly privilege to have performed a PhD under the orientation of Prof. Dr. G. M. König.

Special thanks go to Prof. Dr. E. Kostenis for officiating as second referee.

Many specific tasks involved in this study were performed in cooperation with other members of the Institute for Pharmaceutical Biology, Uni Bonn. For this work cordial thanks go to:

Dr. Stefan Kehraus for indispensable help concerning the implementation and interpretation of special NMR experiments, for proofreading manuscripts and thesis, and for providing friendly, professional laboratory support during all phases of this study. I would also like to express my extreme admiration for the NMR interpretation skills of Dr. Kehraus.

Ekaterina Eguereva for introducing me to the work with marine-derived fungi. Also thanks for recording all LC-MS spectra and friendly talks during the research.

Edith Neu for conducting agar diffusion assays and for being such a friendly person.

Natalja Part, for her outstanding lab work and for being a good friend.

E. Gassen for friendly assistance and for resolving all administrative questions.

I would like to thank all members of the Institute for Pharmaceutical Biology, University of Bonn, present or past for cooperation and friendship, with special regards to Hendrik Greve and Ana Kralj for the great help in the first year in the lab.

Extra-special thanks go to Sanem Insu Tezkan, words cannot describe her existance.

As for Rita Roque, Rui Branco and Paulo Figueiredo, thank you for making the days in Germany so special, I met you here but the friendship will be for life.

Also for Maria Laura Vinuela which will be in my heart for the rest of my life.

Another thanks goes to Ricardo Baptista Lopes, long time friend that is allways there when i return to Portugal.

A final thankfull word for “pre-PhD“ personalities, namely Dr. Rob Verpoorte (Leiden University, The Netherlands) for all the knowledge given during my Masters, and Dr. Artur Silva

(Aveiro University, Portugal) for teaching exquisidly the basics of NMR spectroscopy to a biologist, which was essencial for this PhD work.

Financial support for this project was provided by FCT (Fundação para a Ciencia e Tecnologia, Portugal) and is gratefully acknowledged.

International scientific cooperation acknowledgements. I thank the efforts of Dr. K. Dimas (Biomedical Research Foundation of Academy of Athens, Greece) for the cytotoxicity assays, Prof. Dr. M. Gütschow (Institute for Pharmaceutical Chemistry, University of Bonn, Germany) for performing the panel of proteases inhibition assays, Dr. L. Meijer (Protein Phosphorylation & Disease, CNRS, Roscoff, France) for performing the protein kinases assays and Dr. C. Pannecouque (Rega Institute for Medical Research, Leuven, Belgium) for performing the HIV-1 and HIV-2 antiviral assays; I also kindly thank Dr. M. Prudêncio (Malaria Unit, Institute for Molecular Medicine, University of Lisbon, Portugal) for performing the antiplasmodial activity assays, Indra Bergval (KIT Biomedical Research, Royal Tropical Institute, Amsterdam, Netherlands) for performing the *M. tuberculosis* activity assays, Dr. Marc Diederich (LBMCC, Luxembourg) for performing the NF-kB activity assays, Dr. Steinar Paulsen (University of Tromsø, MabCent, Tromsø, Norway) for performing the anti-diabetic activity assays and Dr. K. Shimokawa (Department of Chemistry, Nagoya University, Japan) for performing the 3T3-L1 murine adipocytes assay; the Ki determinations and antagonist functional data that was generously provided by the National Institute of Mental Health's Psychoactive Drug Screening Program, Contract # HHSN-271-2008-00025-C (NIMH PDSP). The NIMH PDSP is directed by Bryan L. Roth MD, PhD at the University of North Carolina at Chapel Hill and Project Officer Jamie Driscol at NIMH, Bethesda MD, USA; I kindly thank also the remaining antiviral tests performed by the U.S. National Institute of Health which were supported by contracts NO1-A1-30048 (Institute for Antiviral Research, IAR) and NO1-AI-15435 (IAR) from Virology Branch, National Institute of Allergic and Infectious Diseases, NIAID; also a thankful word for Dr. M. Engeser and Dr. B. Sondag (Kekulé-Institute for Organic Chemistry and Biochemistry, University of Bonn) for the High Resolution Mass Spectrometry efforts. Synthetic reference compounds for CD spectra comparison with verticonols A/B were kindly provided by Dr. Kenji Mori, Emeritus Professor from the University of Tokyo, Japan; special thanks to Carsten Siering (Kekulé Institute for Organic and Inorganic Chemistry, University of Bonn) for CD spectral measurements and invaluable discussions.

Table of contents **Page**

Abbreviations

°C	degrees Celsius
1D	one dimensional
2D	two dimensional
$[\alpha]^{T}_{D}$	specific rotary power, sodium D-line (589 nm); T: temperature
δ	NMR chemical shift [ppm]
λ	wavelength [nm]
µ	micro (10^{-6})
µg	10^{-6} gram
µl	10^{-6} liter
µM	10^{-6} molar, micromolar (= 10^{-6} mol/L)
ν	wave number [cm^{-1}]
ASW	artificial seawater
ATR	attenuated total reflection
AU	absorbance units
BMS	biomalt salt medium
br	broad (in connection with NMR data)
c	concentration
C 18	C-18 modified silica gel
calcd	calculated
CD	circular dichroism
$CDCl_3$	chloroform-*d*
CD_3CN	acetonitrile-d_3
CD_3OD	methanol-d_4
CH_2Cl_2	dichloromethane (DCM)
CH_3CN	acetonitrile
conc.	concentration
COSY	correlated spectroscopy
cm	10^{-2} meter
CZ	Czapek medium
d	doublet (in connection with NMR data)
DAD	diode array detector

DCM	dichloromethane
DEPT	distortionless enhancement by polarization transfer
dmol	10^{-1} mol
DNA	deoxyribonucleic acid
EC_{50}	half maximal effective concentration (drug concentration causing 50% of maximal effect)
e.g.	example given (for example)
EI	electron ionization
ESI	electron spray ionization
et al.	et alii [Lat.]: and others
EtOAc	ethyl acetate
EtOH	ethanol
g	gram
GI	growth inhibition
h	hour
H_3BO_3	boric acid
HMBC	heteronuclear multiple-bond correlation
HMGCoA	hydroxymethylglutaryl-CoA
HPLC	high performance liquid chromatography
HR	high resolution
HSQC	heteronuclear single quantum correlation
Hz	Hertz
H_2O	water
IC_{50}	half maximal inhibitory concentration (drug concentration causing 50% inhibition)
i.e.	that is
IR	infrared
J	spin-spin coupling constant [Hz]
kDa	kilo Dalton (= 10^3 Dalton)
L	liter
LC	liquid chromatography
leu	leucine
m	meter

m	multiplet (in connection with NMR data)
m/z	mass-to-charge ratio (in connection with mass spectrometry)
mdeg	millidegrees
Me	methyl
MeOH	methanol
MeOD	methanol-d_4
mg	10^{-3} gram
MHz	megahertz
min	minute
mL	10^{-3} liters
mm	10^{-3} meters
mM	10^{-3} molar, millimolar (= 10^{-3} mol/L)
mol. wt.	molecular weight [g/mol]
MYA	malt yeast agar medium
MS	mass spectrometry
NaOH	sodium hydroxide
n.d.	not determined
NH_4Ac	ammonium acetate
nm	10^{-9} meter
NMR	nuclear magnetic resonance
no	number
NOE	nuclear Overhauser effect
NOESY	nuclear Overhauser effect spectroscopy
NP	normal phase silica gel
NRPS	non-ribosomal peptide synthetase
p	pentet (in connection with NMR data)
PDA	photodiode-array
PE	petroleum ether
pH	potentia hydrogenii
PKS	polyketide synthase
ppm	parts per million
q	quartet (in connection with NMR data)
qC	quaternary carbon

ROESY	rotating frame Overhauser effect spectroscopy
RP	reversed phase
RT	room temperature
s	singlet (in connection with NMR data)
sec	second
Si	silica gel
sp.	species
spp.	species (plural)
sxt	sextet (in connection with NMR data)
t	triplet (in connection with NMR data)
TLC	thin layer chromatography
UV	ultraviolet
VIS	visible
VLC	vacuum-liquid chromatography
X-ray	Röntgen-ray

1. Introduction

Nature has evolved over time to produce a bewildering diversity of secondary metabolites. Based on empirical observations and folklore, natural product extracts were the first, and for a long time, the only medicines available to mankind. Although according to the WHO, 80% of the world's population - primarily those of developing countries - rely on plant-derived medicines for their healthcare, they are largely supplanted by pharmaceutical ingredients in the Western world. Furthermore, the dependence upon natural products is no longer obligatory and many drugs are purely synthetic small molecules or manufactured biologics such as vaccines, antibodies, and recombinant proteins (Gurib-Fakim, 2006; Ganesan, 2008).

1.1. Role of Natural Products in Pharmaceutical Sciences

The seminal discoveries leading to the use of pure drug substances occurred in the 18th and 19th centuries. In 1785 William Withering published his treatment of heart patients with cardiotonic foxglove extract, also known as digitalis (Aronson, 1985). This treatment led to the discovery of digoxin (Smith, 1930), and has been used to treat arrhythmia and congestive heart failure. In 1806 Freidrich Serturner (Schmitz, 1985) analyzed opium poppy and isolated morphine, used in pain therapy. The pharmacology of the small molecule morphine enabled an understanding of the opiate receptors subtypes, of the endorphin and enkephalin pathways (Ignelzi, 1980), and ultimately led to the development of analogs as therapy for pain. In 1897 Felix Hoffmann, working with the Bayer Company, synthesized aspirin from salicylic acid in willow bark (Bosch and Banos, 1998). People had been using the extract from willow bark prepared as a tea for centuries to treat rheumatism and headache. After structure optimization with an acetylation reaction to mask the phenol of salicylic acid, Aspirin was born. Using salicylic acid as a pharmacologic tool, it was possible to delineate the mechanisms of inflammation (Vane, 1971) and subsequently to design and test a battery of new nonsteroidal anti-inflammatory agents, including acetaminophen, ibuprofen, and naproxen. Although mycophenolic acid was the first fungal secondary metabolite obtained from *Penicillium glaucoma* as early as 1896 (see Bérdy, 2005), it is a well-known story that in 1928, Alexander Fleming discovered penicillin in mold (Bennett

and Chung, 2001). The discovery of penicillin and its impact on the treatment and understanding of infectious disease did more for human health than any other single discovery. The small molecule penicillin enabled the study of antibiotic action and infection to the point that countless penicillin and cephalosporin could be synthesized and studied for the treatment of various strains of bacteria and in response to antibiotic resistance (Ghuysen 1997). An understanding of infectious disease was achieved, and an entirely new therapeutic approach was born.

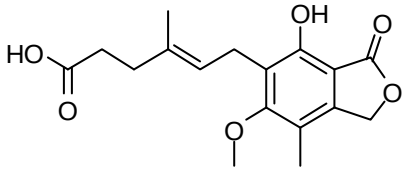

mycophenolic acid

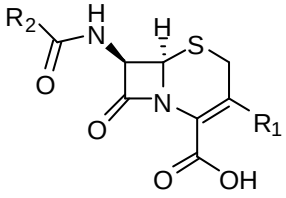

core structure of cephalosporins

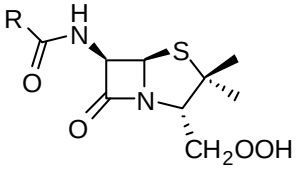

core structure of penicillins

1.2. **Natural products as pharmaceutical drugs in the 20th century**

Natural products continued to play a major role, and endogenous chemicals, such as the steroids, prostaglandins, and peptide hormones, provided the pharmaceutical industry with additional natural inspiration for drug discovery during the 20th century (Gaudilliere, 2005). The most recent survey covering the period 1981–June 2006 of molecules discovered post-1970 lists a total of 1184 new chemical entities (NCEs) receiving approval as pharmaceutical drugs (Newman and Cragg, 2007). Of these, 52% have a natural product connection, 18% are biologics, and 30% purely synthetic. The meta-analysis of this list made by Ganesan (2008) reveals a total of 24 unique natural product chemotypes that led at least to one approved drug (Table 1). A priori, natural products should undergo an iterative cycle of pharmacological improvement, as their evolutionary reason for existence is not for use as a therapeutic agent (Ganesan, 2008). Though, among the 24 leads in Table 1, 17 progressed to an approved drug with no modification. Another six natural products were modified by semisynthesis and only the β-lactam SQ26,180 was replaced by a synthetic analog.

Table 1. The 24 natural products discovered since 1970 that led to an approved drug in 1981–2006, (Ganesan, 2008)

Lead, year	Chemical class	Origin	Drug, year	Rank*
Validamycin, 1970	Oligosaccharide	Actinomycete	Acarbose, 1990	357
			Voglibose, 1994	
Midecamycin, 1971	Macrolide	Actinomycete	Miocamycin, 1995	
Pseudomonic acid, 1971	Polyketide	Bacteria	Mupirocin, 1985	436
Taxol, 1971	Diterpene	Plant	Paclitaxel, 1993	81
			Docetaxel, 1995	123
Cephamycin C, 1971	β-lactam	Actinomycete	Moxalactam, 1982	
			Cefotetan, 1984	
			Cefbuperazone, 1985	
Coformycin, 1974	Nucleoside	Actinomycete	Pentostatin, 1992	
Echinocandin B, 1974	Cyclopeptide	Fungus	Caspofungin, 2001	293
			Micafungin, 2002	
			Anidulafungin, 2006	
Mizoribine, 1974	Nucleoside	Fungus	Mizoribine, 1984	
Rapamycin, 1974	Polyketide	Actinomycete	Sirolimus, 1999	434
			Everolimus, 2004	
			Zotarolimus, 2005	
Compactin, 1975	Polyketide	Fungus	Lovastatin, 1984	264
			Simvastatin, 1988	2
			Pravastatin, 1989	41
			Fluvastatin, 1994	195
			Atorvastatin, 1997	1
			Cerivastatin, 1997	
			Pitavastatin, 2003	71
			Rosuvastatin, 2003	
Cyclosporine A, 1975	Cyclopeptide	Fungus	Ciclosporin, 1983	122
Lipstatin, 1975	Polyketide	Actinomycete	Orlistat, 1987	277
Bestatin, 1976	Peptide	Actinomycete	Ubenimex, 1987	
Thienamycin, 1976	β-lactam	Actinomycete	Imipenem, 1985	247
			Meropenem, 1994	231
			Panipenem, 1994	
			Faropenem, 1997	
			Biapenem, 2002	
			Ertapenem, 2002	
			Doripenem, 2005	
Artemisinin, 1977	Sesquiterpene	Plant	Artemisinin, 1987	
			Artemether, 1987	
			Artenusate, 1987	
			Artheether, 2000	
Forskolin, 1977	Diterpene	Plant	Colforsin, 1999	
Plaunotol, 1977	Diterpene	Plant	Plaunotol, 1987	
Avermectib B_1a, 1979	Polyketide	Actinomycete	Ivermectin, 1987	
SQ26,180, 1981	β-lactam	Actinomycete	Aztreonam, 1984	
			Carumonam, 1988	
Spergualin, 1981	Peptide	Bacteria	Gusperimus, 1994	
Arglabin, 1982	Sesquiterpene	Plant	Arglabin, 1999	
FK506, 1984	Polyketide	Actinomycete	Tacrolimus, 1993	103
Daptomycin, 1986	Cyclodepsipeptide	Actinomycete	Daptomycin, 2003	
Calicheamicin γ_1, 1988	Polyketide	Actinomycete	Gemtuzumab, 2000	

*final column gives the ranking among the global top 500 drugs of 2006, according to IMS Health.

Although leadfinding new bioactive carbon skeletons is essential for the development of new drugs, known successful lead compounds continue to give us optimized pharmaceutically approved drugs or currently in clinical trials. Two of these examples are Larotaxel (XRP9881) and Cabazitaxel (XRP6258), novel taxoid compounds that appear to be potent microtubule stabilizers (NCI Drug Dictionary: Larotaxel. http://www.cancer.gov/Templates/drugdictionary.aspx?CdrID=42554. Accessed 1 December 2010; Engels *et al.*, 2005). Larotaxel and Cabazitaxel are active in cell lines resistant to doxorubicin, vinblastine, paclitaxel, and docetaxel (Gelmon *et al.*, 2000; Fumoleau *et al.*, 2005). Both compounds appear to cross the blood-brain barrier (Sessa *et al.*, 2002). Furthermore, Larotaxel shows *in vivo* synergy in combination with doxorubicin, cisplatin, vinorelbine, and trastuzumab (Vrignaud *et al.*, 2005; Vrignaud *et al.*, 2007). Larotaxel is currently in phase III trials in patients with advanced pancreatic cancer and in patients with advanced bladder cancer. Cabazitaxel is also currently in a phase III trial in patients with hormone-refractory prostate cancer following docetaxel-based therapy. (http://www.oncology.sanofi-aventis.com. Accessed 1 December 2010).

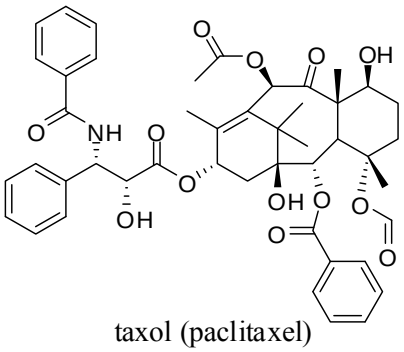

taxol (paclitaxel)

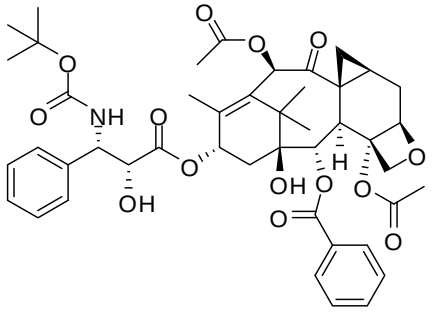

larotaxel

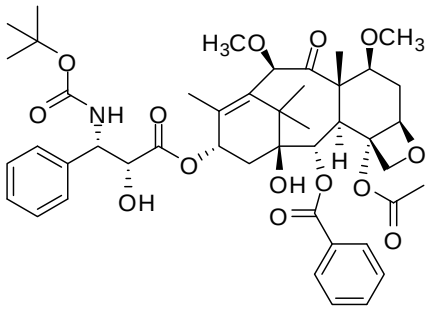

cabazitaxel

1.3. Terrestrial Fungal-derived Natural Products as Pharmaceutical Drugs

A wide range of pharmaceutically significant compounds belonging to all structural classes were found to be produced by fungi (Mutschler *et al*., 2008). Since the discovery of the fungal metabolite penicillin by Fleming in 1928 and its subsequent development as antibiotic drug, secondary metabolites of fungal origin have been proved to be an important source for new pharmaceuticals and drug lead compounds, as shown by the presently bestselling pharmaceutical drugs, the fungal-derived statins, cholesterol-lowering drugs based on inhibition of HMG-CoA reductase which are widely consumed daily and play an important role in lowering the risk of cardiovascular disease (Laws *et al.*, 2004).

Besides the mentioned fungal-derived compounds in Table 1 (compound discovery post-1970), other fungal metabolites that are present on the pharmaceutical market should be mentioned, such as semi-synthetic or synthetic penicillins and cephalosporins, the alkaloid ergotamine (Ergo-Kranit®), the antibiotic polyketide griseofulvin (Likuden M®), the immunosuppressive mixed-biosynthesized compound mycophenolate mofetil (CellCept®, derivative of mycophenolic acid) used for preventing renal transplant rejection as well as the antibacterial terpenoid fusidic acid (Fucidine®) (Hamilton-Miller, 2008; Buttler, 2005),

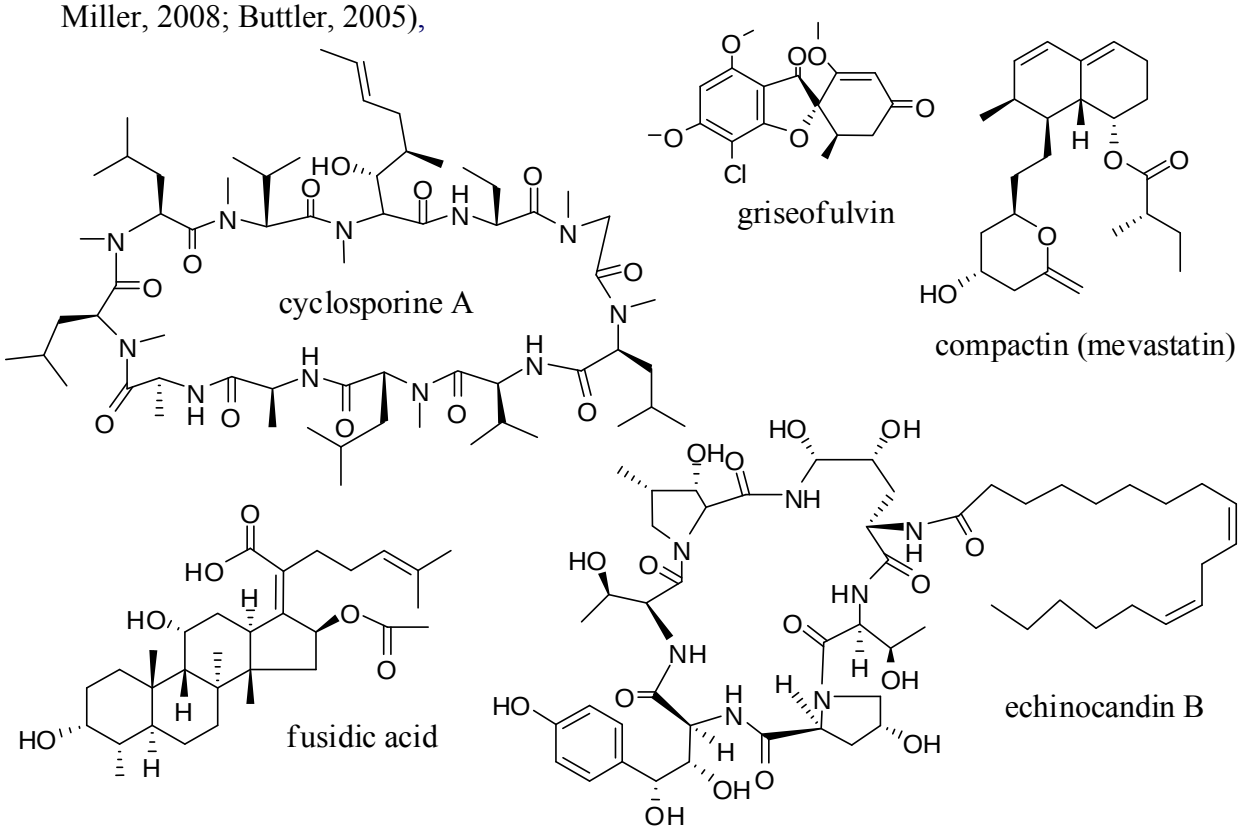

A class of antimicrobial agents that remained largely undeveloped for human clinical use is the pleuromutilins (Hunt, 2000). These antimicrobials are derivatives of the naturally occurring pleuromutilin produced by *Pleurotus mutilus*, an edible mushroom. In veterinary practice, tiamulin and valnemulin (two semisynthetic pleuromutilin analogs) are used for the control and treatment of serious infections in swine (Hunt, 2000, Brooks *et al.* 2001). Recently, retapamulin, a semisynthetic pleuromutilin compound was approved in the U.S. and Europe for the treatment of skin infections (Daum *et al.*, 2007; Jacobs, 2007; Laustsen *et al.*, 2008). Retapamulin has a unique mode of action, selectively inhibiting the elongation phase of bacterial protein synthesis at a unique site on the prokaryotic ribosome (Hunt, 2000). This antibacterial drug currently shows no target-specific cross-resistance to other classes of antibiotics and has potent activity *in vitro* against *Staphylococcus aureus* and *Streptococcus pyogenes*, including strains that are resistant to ß-lactams, macrolides and quinolones, as well as strains that are resistant to current topical therapies including fusidic acid and mupirocin (Bouchillon *et al.*, 2005; McCloskey *et al.*, 2005; Stevens *et al.*, 2005).

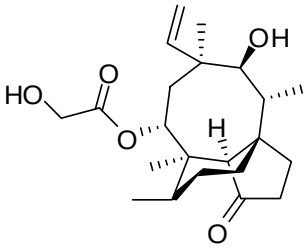

pleuromutilin

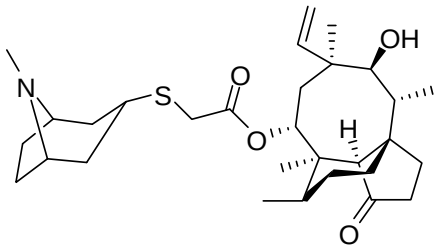

retapamulin

But to date, fungal metabolites or derivatives thereof have not been launched as anticancer chemotherapeutics. Interestingly, several plant-derived anti-cancer agents are being reported to be produced from endophytic fungi isolated from the original plant sources. Stierle and coworkers have demonstrated in 1993, that the well-established and world's bestselling anticancer drug taxol from the plant *Taxus brevifolia*, is also produced by the endophytic fungus *Taxomyces andreanae* (Stierle et al., 1993). In the meantime, taxol was discovered as product of many various endophytic fungi (Yang *et al.*, 1994; Wang *et al.* 2000; Ji *et al.*, 2006). Also recently the aryl tetralignan podophyllotoxin has been reported to be produced by endophytes, namely

Phialocephela fortinii, isolated from the rhizomes of the host plant *Podophyllum peltatum* (Eyberger *et al.*, 2006). Podophyllotoxin, which was originally isolated from the rhizoma of *Podophyllum peltatum*, is a valuable natural product as precursor for several therapeutic agents, including the anticancer drugs etoposide, teniposide and etoposide phosphate (Canel *et al.*, 2000). In other recent reports, camptothecin was also found to be produced by endophytic fungi (Puri *et al*., 2005; Strobel & Daisy, 2003; Strobel *et al*., 2004). There is an urgent demand for other sources than the primary source plant, whose wild populations are being destroyed more and more and the pharmaceutical demand will not be covered anymore if no other sources are made available (Eyberger *et al.*, 2006).

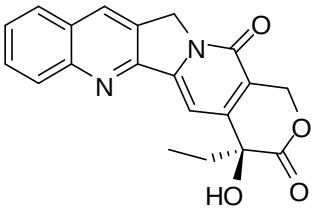

camptothecin

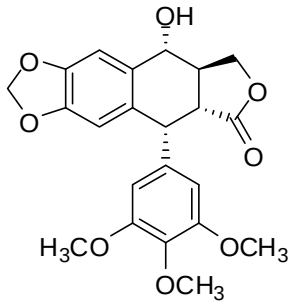

podophyllotoxin

1.4. Compounds from Terrestrial Fungi in Clinical Trials

There are currently two fungal-derived molecules that serve as templates for analogs used in clinical trials, fumagillin and illudin S (Buttler, 2005). Fumagillin arises from a mixed sesquiterpenoid (C15-nucleus) and polyketidic (C10 side chain) biosynthesis and is produced by the fungus *Aspergillus fumigatus* (Birch & Hussain, 1969). It has been the template for analogues undergoing oncological clinical trials. Fumagillin is an angiogenesis inhibitor, which suppresses the formation and growth of new blood vessels, namely the angiogenesis, by direct blocking endothelial cell proliferation (Ingber *et al.,* 1990). Semi-synthetic derivatives, such as TNP-470, PPI-2458 and CKD-732 entered clinical trials for the treatment of breast, prostate, and brain cancer, as well as Kaposi sarcoma (Kruger & Figg, 2000, Lee *et al.*, 2004; Kim *et al*., 2007, Bernier *et al*., 2005; Chun *et al.,* 2005; Ingber *et al*., 1990). TNP-470 acts through an irreversible binding to methionine aminopeptidase 2, which then leads to intracellular signalling interference (Zhang *et al.*, 2006; Lu *et al.*, 2006). Although clinical trials of the fumagillin derivative PPI-2458 against cancer were later terminated (Buttler, 2008), the

same antiproliferative mechanism of action might be used for the treatment of rheumatoid arthritis, and PPI-2458 has been investigated towards this disease. Furthermore, fumagillin has been proven to be highly active as antimicrosporidial agent in mice (Didier *et al.*, 2006) and has been found to inhibit HIV-1 viral protein R (VPR) activity (Asami *et al.*, 2006). Preliminary evidence has recently been put forward that angiogenesis inhibitors also inhibit the growth of atherosclerotic plaques (Moulton, 1999). Remarkably, fumagillin was approved for use in the treatment of intestinal microsporidiosis in France in 2005, a disease caused by the parasite *Enterozytozoon bieneusi*, which is of major concern to immunocompromised patients as it can cause diarrhoe (Burton, 2002; Alvarado *et al.*, 2009).

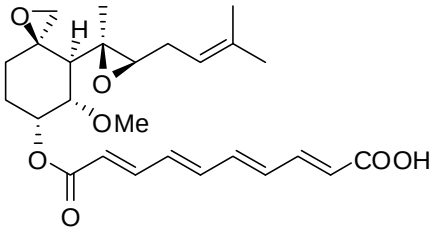

fumagillin

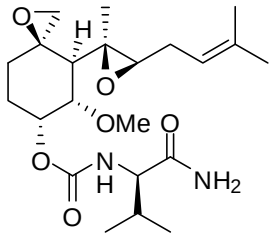

PPI-2458

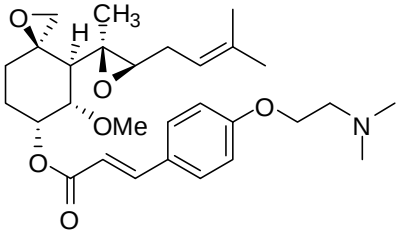

CKD-732

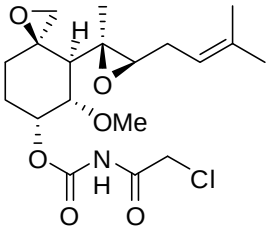

TNP-470

Another anticancer lead compound of fungal origin is the sesquiterpene illudin S, which was first isolated from the basidiomycete *Omphalotus illudens* (formerly *Clitocybe illudens*) and was shown to be extremely cytotoxic against the human leukemia cell line HL-60 *in vitro* (IC_{50} = 3 ng/mL), but exhibiting a low therapeutic index in mouse xenograft solid tumor systems (Anchel *et al.*, 1950; McMorris & Anchel, 1965; McMorris *et al.*, 1996). Though, the improved semi-synthetic compound irofulven has a significantly superior therapeutic index in comparison to the parent natural product illudin S and possesses selectivity towards human tumor cells in which apoptosis is induced (e.g. MV522 lung carcinoma cell assay with an IC_{50} value of 73 nM for irofulvene), with only a marginal apoptotic effect on normal human cells (Baekelandt, 2002; Woynarowska *et al.*, 2000, McMorris 2001). Irofulvene possesses a greater

efficacy than illudin S due to its slower and more selective action. It has entered phase I and II clinical trials against several types of cancer (Seiden *et al.*, 2006).

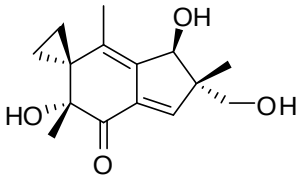

iIlludin S

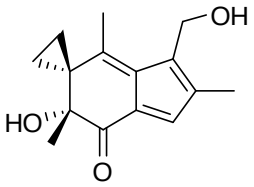

irofulven

1.5. Marine Natural Products as Pharmaceutical Drugs

The marine ecosystem, covering more than 70 % of the planet's surface, is home to an immense diversity of life. Though, due to the extreme depth of the oceans, they represent more than 99 % of our planet's natural habitat when setting the terrestrial habitat up to 100 m of height (Schuh, 2008). Marine natural products are conspicuously absent in table 1, as their systematic exploration became widespread only recently. In the United States there are three FDA approved marine-derived drugs, namely cytarabine, vidarabine and ziconotide. Currently, trabectedin has been approved by the European Agency for the Evaluation of Medicinal Products (EMEA), and is completing key Phase III studies in the US for approval. The current clinical pipeline includes 13 marine-derived compounds that are either in Phase I, Phase II or Phase III clinical trials (Mayer *et al.*, 2010).

Table 2, Marine-derived compounds in clinical development and approved as pharmaceutical drugs (Mayer *et al.*, 2010)

Clinical status	Compound name	Structural class	Origin	Disease area
Approved	Cytarabine, Ara-C	Nucleoside	Sponge	Cancer
	Vidarabine, Ara-A	nucleoside	Sponge	Antiviral
	Ziconotide	Peptide	Snail	Pain
	Trabectedin (ET-743) (EU registered only)	Alkaloid	Tunicate	Cancer
Phase III	Eribulin Mesylate (E7389)	Macrolide	Sponge	Cancer
	Soblidotin (TZT 1027)	peptide	Bacterium	Cancer
Phase II	DMXBA (GTS-21)	Alkaloid	Worm	Cognition/Schizophrenia
	Plinabulin (NPI-2358)	Diketopiperazine	Fungus	Cancer
	Plitidepsin	Depsipeptide	Tunicate	Cancer
	Elisidepsin	Depsipeptide	Mollusc	Cancer
	PM1004	Alkaloid	Nudibranch	Cancer
	Tasidotin, Synthadotin (ILX-651)	Peptide	Bacterium	Cancer
	Pseudopterosins	Diterpene glycoside	Soft coral	Wound healing
Phase I	Bryostatin 1	Polyketide	Bryozoa	Cancer
	Hemiasterlin (E7974)	Tripeptide	Sponge	Cancer
	Marizomib (Salinosporamide A; NPI-0052)	Beta-lactone-gamma lactam	Bacterium	Cancer

A recent development in the area of antitumor agents from natural sources was the approval of the alkaloid trabectedin for advanced soft tissue sarcoma (Verweij, 2009) and patients with relapsed platinum-sensitive ovarian cancer (Yap *et al.*, 2009) by the EMEA (European Medicines Agency) in September 2007 (http://www.emea.europa.eu). Currently the product is being developed in Phase II trials in breast, lung, prostate and pediatric cancer, and Phase III trials for first-line therapy in STS (Mayer *et al.,* 2010). Yondelis® is being developed and marketed by Pharmamar (http://www.pharmamar.com/products.aspx). Trabectedin, was originally isolated from a marine invertebrate, the tunicate *Ecteinascidia turbinata* which was found in the Caribbean and Mediterranean sea (Rinehart, *et al.* 1990, Wright, *et al.* 1990), but is now produced semi-synthetically (Cuevas *et al*., 2000; Newman *et al*., 2000; Rinehart *et al*., 1990; Wright *et al*., 1990; http://www.pharmamar.com). Trabectedin binds guanine-specific to the minor groove of DNA, but its precise mechanism of action remains poorly understood (Herrero *et al*., 2006; Pommier *et al*., 1996).

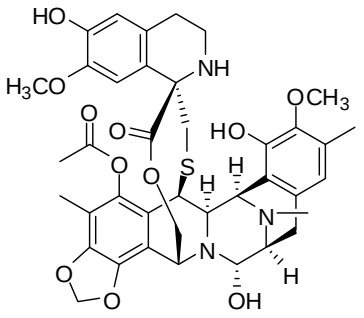

trabectedin (ET-743, Yondelis)

Cytarabine (Ara-C, developed by Bedford Laboratories, http://www.bedfordlabs.com/, and Enzon Pharmaceuticals, http:// www.enzon.com/), is a synthetic pyrimidine nucleoside which was developed from spongothymidine, a nucleoside originally isolated from the Caribbean sponge *Tethya crypta* (Newman *et al.*, 2009). Cytarabine is an S-phase specific antimetabolite cytotoxic agent, which when converted intracellularly to cytosine arabinoside triphosphate competes with the physiologic substrate deoxycitidine triphosphate, thus resulting in both inhibition of DNA polymerase and DNA synthesis. Cytarabine received FDA approval in 1969. FDA-labeled indications for conventional cytarabine are treatment of acute lymphocytic leukemia, acute myelocytic leukemia, blast crisis phase of chronic myelogenous leukemia, meningeal leukemia (Thomas, 2009; Absalon *et al.*, 2009; MARTINDALE, 2009) and intrathecal treatment of lymphomatous meningitis.

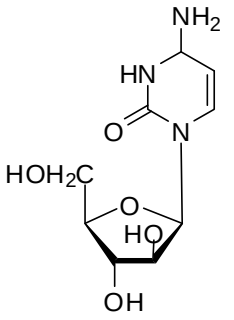

Cytarabine (Ara-C)

Vidarabine (Ara-A) is a synthetic purine nucleoside which was developed from spongouridine, a nucleoside originally isolated from the Caribbean sponge *Tethya crypta* (Newman, *et al.*, 2009), and which is currently obtained from *Streptomyces antibioticus*. Adenine arabinoside inhibits viral DNA polymerase and DNA synthesis of herpes, vaccinia and varicella zoster viruses. Although its marketing status is currently listed as discontinued by the FDA in the US market, vidarabine (Vira-A1) received FDA approval in 1976. FDA-labeled indications for conventional vidarabine (Vira-A ophthalmic ointment, 3%) are treatment of acute keratoconjunctivitis, recurrent epithelial keratitis caused by herpes simplex virus type 1 and 2, and superficial keratitis caused by herpes simplex virus that has not responded to topical idoxuridine (Herplex1) (MARTINDALE, 2009). Vidarabine (Vira-A1), previously marketed by King Pharmaceuticals (http://www.kingpharm.com/) was discontinued in June of 2001 by an executive decision, possibly associated with the lower therapeutic window of vidarabine relative to newer antiviral compounds currently on the market (Mayer *et al.*, 2010).

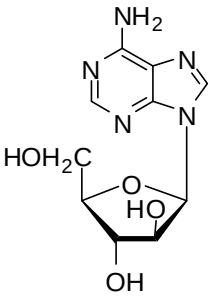

Vidarabine (Ara-A)

Ziconotide (Prialt®, Elan Corporation, PLC (http://www.elan.com/therapies/products/prialt.asp) is the synthetic equivalent of a naturally occurring 25-amino acid peptide, ω-conotoxin MVIIA, originally isolated from the venom of the fish-hunting marine snail *Conus magus* (Olivera, 2000). Receiving FDA-approval in 2004, Ziconotide is a potent analgesic with a completely novel mechanism of action (Bingham *et al.*, 2010; Kerr and Yoshikami, 1984). Various subtypes of voltage-gated calcium channels have been identified in the nervous system. Ziconotide reversibly blocks N-type calcium channels located on primary nociceptive afferent nerves in the superficial layers of the dorsal horn of the spinal cord. Binding of ziconotide to presynaptic N-type calcium channels reduces the release of excitatory neurotransmitter release from the primary afferent nerve terminals (Miljanich, 2004; McGivern, 2006). Tolerance to drug effects is a major limiting factor in opiate-based therapies; unlike opiates, ziconotide does not produce tolerance (Wang *et al.*, 2000; Gaur *et al.*, 1994). Ziconotide is currently used for the management of severe chronic pain in patients with cancer or AIDS (Staats *et al.*, 2004; Rauck *et al.*, 2009), for whom intrathecal (IT) therapy is warranted, and who are intolerant or refractory to other treatments, such as systemic analgesics, adjunctive therapies or IT morphine.

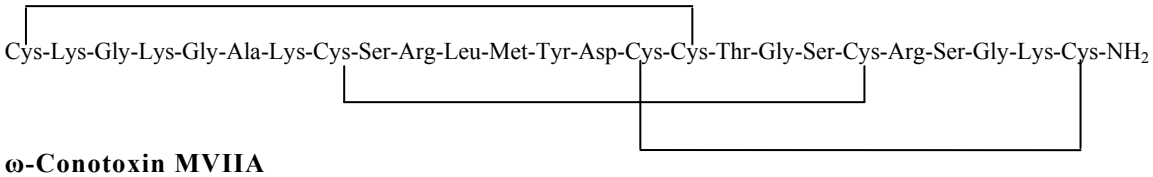

ω-Conotoxin MVIIA

1.6. Marine-derived fungal compounds in clinical trials

As interests have turned to marine microorganisms, marine fungi have proved to be a rich and promising source of novel bioactive natural products. Most of these microorganisms grow in a unique and extreme habitat and therefore have the capability to produce unusual secondary metabolites. It is believed that the metabolites possibly act as a chemical defense adaptation of fungi competing for substrates. The production of these unique secondary metabolites by marine fungi is most likely due to their adaptation to a very distinct set of environmental pressures (Bhadury *et al*., 2006).

Although some marine-fungal compounds are in pre-clinical trials, the most promising marine-fungal derived analogue in clinical trials is the anticancer agent plinabulin which is based on the diketopiperazine halimide (also known as phenylahistidin), isolated from the fungus *Aspergillus ustus* (Kanoh *et al.*, 1997). Initially halimide was isolated as a mixture of enantiomers, but the (-) enantiomer alone exhibited a 50-fold increase of *in vitro* antitumor activity against human cancer cell lines, along with inhibition of tubulin polymerisation by interacting with the colchicine-binding site on tubulin (Kanoh *et al*., 1999a & 1999b).

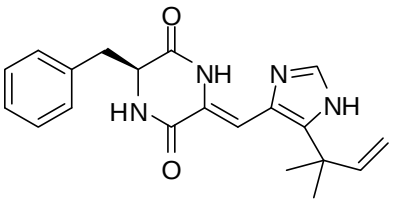

(-)-halimide

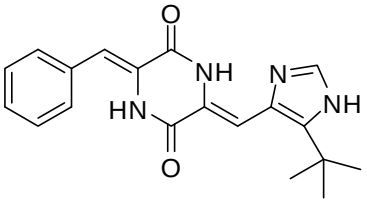

plinabulin

To optimise biological activity, a series of 200 synthetic analogues were generated by the company Nereus Pharmaceuticals, San Diego, U.S.A., and finally led to compound NPI-2358 (Plinabulin), which is since 2009 in Phase II clinical studies as a vascular disrupting agent against advanced non-small cell lung cancer refractory to current therapy (http://www.nereuspharm.com). A recent study showed that plinabulin acts moreover as a tumor vascular-disrupting agent by inducing rapid depolymerisation of existing microtubules in the highly proliferating tumor vascular endothelial cells, as evidenced by *in vitro* assays with human umbilical vein endothelial cells (HUVECs) (Nicholson *et al*., 2006). Tumor vascular-disrupting agents thereby attack established tumor blood vessels, resulting in occlusion of vasculature in the tumor, which induces tumor cell hypoxia and finally necrosis.

2. Scope of the present study

Due to the rapidly increasing number of pathogenic bacteria, viruses and tumor cells that possess resistance towards established therapies, lead structures for the development of new drugs are in high demand.
Marine microorganisms, such as fungi often occur associated with macroorganisms like algae, sponges or tunicates and produce secondary metabolites with novel structures and potential pharmaceutical significance.

The goal of this study was the evaluation of new natural products of marine-derived fungi in order to find novel lead structures for drug development, with a focus on anticancer leads. To achieve this aim seven fungal strains living associated with marine algae and sponges were cultivated during 40 to 60 days, and the extracts tested for bioactivity. Subsequently, the natural products were isolated, their structures determined and their bioactivity established.

The research relies in tracing active principles from the selected extracts by performing NMR guided fractionation, together with the application of various preparative chromatographic systems (e.g., VLC, HPLC). The structure elucidation of the obtained pure compounds relies on interpretation of 1D and 2D NMR spectroscopic data, as well of mass spectrometry data, UV, IR and CD spectra.
Additionally, the isolated compounds can be submitted to a vast panel of biological assays, such as antimicrobial, antiplasmodial, antidiabetic, antiinflammatory, antiviral or psychoactive activity, amongst others.

3. General Methodology

3.1. General Experimental Procedures

Optical rotations were measured on a Jasco DIP 140 polarimeter. UV and IR spectra were obtained employing a Perkin-Elmer Spectrum BX instrument. CD spectra were recorded in MeOH at room temperature using a JASCO J-810-150S. All NMR spectra were recorded in MeOD, $CDCl_3$ or $(CD_3)_2CO$ employing a Bruker Avance 300 DPX spectrometer. Spectra were referenced to residual solvent signals with resonances at $\delta_{H/C}$ 3.35/49.0 for MeOD, $\delta_{H/C}$ 7.26/77.0 for $CDCl_3$ and $\delta_{H/C}$ 2.04/29.8 for $(CD_3)_2CO$. HREIMS were recorded on a Finnigan MAT 95 spectrometer. HRESIMS were recorded on a Bruker Daltonik micrOTOF-Q Time-of-Flight mass spectrometer with ESI source. HPLC was carried out using a system composed of a Waters 515 pump together with a Knauer K-2300 differential refractometer. HPLC columns were from Knauer (250 x 8 mm, 5 µm, Eurospher-100 Si and 250 x 8 mm Eurospher-100, C18, 5 µm, flow rate 2 mL/min) and from Macherey-Nagel (Nucleodur C18 EC Isis and Nucleodur C18 Sphinx RP, both with 250 x 4.6 mm, 5 µm, flow rate 1 mL/min).
Merck silica gel 60 (0.040–0.063 mm, 70-230 mesh) was used for vacuum liquid chromatography (VLC). Columns were wet-packed under vacuum using petroleum ether (PE). Before applying the sample solution, the columns were equilibrated with the first designated eluent. Standard columns for crude extract fractionation had dimensions of 13 x 4 cm.

3.2. Fungal material:

Marine-derived fungus *Stachylidium* sp. was isolated from the sponge *Callyspongia* sp. cf. *C. flammea* and identified by Dr. P. Massart and Dr. C. Decock from the Belgian coordinated collections of microorganisms of the Catholic University of Louvain, (BCCM/MUCL). A specimen is deposited at the Institute for Pharmaceutical Biology, University of Bonn, isolation number “293K04”, running number “220”.

The marine-derived fungus *Cadophora malorum* (Kidd & Beaumont) W. Gams was isolated from the green alga *Enteromorpha* sp. and identified by P. Massart and C. Decock, BCCM/MUCL, Catholic University of Louvain, Belgium. A specimen is deposited at the Institute for Pharmaceutical Biology, University of Bonn, isolation number "SY3-1-1MIT", running number "417".

The marine-derived fungus *Verticillium tenerum* was isolated from an unknown alga and identified by Isabelle Charue, BCCM/MUCL, Catholic University of Louvain, Belgium. A specimen is deposited at the Institute for Pharmaceutical Biology, University of Bonn, isolation number "293K04", running number "780".

3.3. Methodology for the performed bioactivity assays

The referred compounds were tested in antibacterial (*Escherichia coli*, *Bacillus megaterium*), antifungal (*Mycotypha microspora*, *Eurotium rubrum*, and *Microbotryum violaceum*), and antialgal (*Chlorella fusca*) assays as described by Schulz *et al.*, 1995 and Schulz *et al.*, 2002.

Compounds were tested towards a panel of proteases including chymotrypsin, trypsin, human leukocyte elastase (HLE), papain, porcine cease, and acetylcholine esterase as described by Neumann, *et al.*, 2009.

Compounds were tested for protein kinases inhibition assays (DYRK1A and CDK5) according to Bettayeb *et al.*, 2008.

The triglyceride accumulation inhibition in the 3T3-L1 murine adipocytes assay were performed as described by Shimokawa *et al.*, 2008.

Cytotoxic activity assay against a panel of 5 cancer cell lines, NCI-H460/lung, A549/lung, MCF7/breast and SF268/CNS and CAKI/renal at the 100 µM level was performed according to Saroglou *et al*., 2005 and Monks *et al.*, 1991.

Compounds were tested for antiplasmodial activity assay against *Plasmodium berghei* as described by Prudêncio *et al.*, 2008.

The sporogenic activity assay was performed according to Kitahara *et al.*, 1984 and Sawai *et al.*, 1985.

Inhibition of the viral HIV-1 and HIV-2 induced cytopathogenic effect in MT-4 cells assays were performed according to Pannecouque *et al*., 2008 and Zhan *et al*., 2008.

Severe Acute Respiratory Syndrome coronavirus (SARS) assays were performed according to Kumaki *et al.*, 2008.

The Herpes Simplex Virus-2 (HSV-2) activity assay methods are described by Harden *et al.*, 2009.

The Respiratory Syncytial virus (RSV) activity assays were conducted according to Barnard *et al.*, 1993 and Barnard *et al.*, 1997.

Two influenza viruses (Flu A and Flu B) activity assays were performed as described by Sidwell and Smee, 2000.

Hepatitis B virus assay was performed according to Sells *et al*., 1998 and Korba and Gerin, 1992.

The Epstein-Barr virus (EBV) assay was performed according to Smee *et al.*, 1997.

The activity assays against two strains of antibiotic resistant *Mycobacterium tuberculosis* were performed according to Bauer *et al.*, 1966.

The methodology for the inhibition of the NF-kB protein complex is described by Schumacher *et al.*, 2010.

The compounds were tested against a panel of anti-diabetic activity assays as described by Marrapodi and Chiang, 2000, Dey *et al.*, 2007 and Seale *et al.*, 1997.

The agonistic/antagonistic binding assays against a panel of forty four psychoactive receptors (activity considered with at least 50 % inhibition at the 10 μM level against 5HT1A, 5HT1B, 5HT1D, 5HT1E, 5HT2A, 5HT2B, 5HT2C, 5HT3, 5HT5A, 5HT6, 5HT7, Alpha1A, Alpha1B, Alpha1D, Alpha2A, Alpha2B, Alpha2C, Beta1, Beta2, Beta3, BZP Rat Brain Site, D1, D2, D3, D4, D5, DAT, DOR, Gaba A, H1, H2, H3, H4, KOR, M1, M2, M3, M4, M5, MOR, NET, SERT, Sigma1, Sigma2). Ocasionally the compounds were also tested for specific receptors, i.e., CB1, CB2, GabaB, NMDA-PCP site, Oxytocin, PBR, mGluR5_Rat Brain, V1A, V1B and V2. All experimental procedures are desribed by the assay provider at http://pdsp.med.unc.edu/UNC-CH%20Protocol%20Book.pdf.

4. Marilines A – D, Novel Phthalimidines from the Sponge-derived Fungus *Stachylidium* sp.

Abstract

The marine-derived fungus *Stachylidium* sp. was isolated from the sponge *Callyspongia* cf. *C. flammea.* Chemical investigation of the bioactive fungal extract led to the isolation of the novel phthalimidine derivatives marilines A - D (**1**-**4**). The absolute configuration of the enantiomeric compounds **1** and **2** was assigned by means of theoretical Circular Dichroism calculations. The skeleton of marilines A - D is most unusual, and its biosynthesis is suggested to require unusual biochemical reactions in fungal secondary metabolism. Both enantiomers marilines A and B (**1**, **2**) inhibited human leucocyte elastase (HLE) with an IC_{50} value of 0.86 μM, and acetylcholinesterase (AChE) with IC_{50} values of 0.18 μM (offset = 49 %) and 0.63 μM (offset = 54 %), respectively.

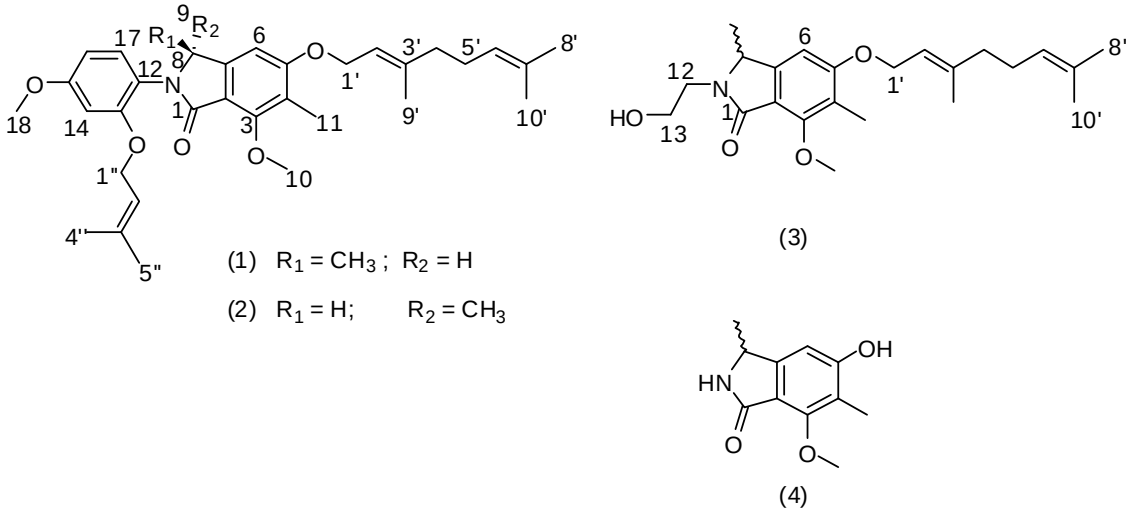

Figure 1. Structural Formulae of Compounds **1 – 4**

Introduction

Inspired by the impressive level of biodiversity in the marine environment, the pharmacological potential of natural products from marine organisms has been investigated enthusiastically (Glaser and Mayer, 2009). Phthalimidines are secondary metabolites mostly isolated from fungi, but also reported from plants and bacteria. Fungal-derived phthalimidines are described as having a wide spectrum of bioactivities, e.g. the phytotoxic activity of cichorine, a metabolite isolated from *Alternaria cichorii* and *Aspergillus silvaticus* that causes necrotic lesions in Russian knapweed (Kawahara *et al.*, 1988; Stierle *et al.*, 1993). Porritoxin is known to be a non-specific toxin isolated from *Alternaria porri*, inhibiting the growth of lettuce and stone-leek roots, two important commercial plants (Suemitsu *et al.*, 1992; Suemitsu *et al.*, 1995; Horiuchi *et al.*, 2003; Horiuchi *et al.*, 2002; Moreau *et al.*, 2006). Stachybocins and spirodihydrobenzofuranlactams were isolated from *Stachybotrys* sp. and are reported to possess endothelin receptor antagonistic effects. The latter has also HIV-1 protease inhibitory properties (Ogawa *et al.*, 1995; Roggo *et al.*, 1996). The antifungal pestalachlorides isolated from *Pestalotopsis adusta* (Li *et al.*, 2008), the aldose reductase inhibitors salfredins from *Crucibulum* sp. (Matsumoto *et al.*, 1995) or the cytotoxic hericenone B isolated from *Hericium erinceum* (Kawagishi *et al.*, 1990) additionally demonstrate the broad spectrum of bioactivity found for fungal-derived phthalimidine-like structures.

During our search for new natural products produced from the marine-derived fungus *Stachylidium* sp., four novel pthalimidine derivatives, marilines A-D, were isolated from a culture grown on agar-biomalt medium supplemented with artificial sea salt. Albeit phthalimidine-like structures are not rare, the structural skeleton of marilines A - D is most unusual, and its biosynthesis is suggested to require unique reactions in fungal secondary metabolism. Marilines A-D were tested in a broad range of assays to determine their biological activity. Both enantiomers, marilines A and B (**1**, **2**) inhibited human leucocyte elastase (HLE) with the same potency (IC_{50} 0.86 µM). Acetylcholinesterase (AChE) was inhibited with an IC_{50} of 0.18 µM (offset = 49 %) and 0.63 µM (offset = 54 %), for marilines A and B, respectively. Compounds **1** and **2** also showed weak antiplasmodial and antiproliferative activity, and were antagonistic in several assays employing psychoactive receptors.

Results

Compounds **1** and **2** were initially obtained and analysed as a mixture of enantiomers. The molecular formula was deduced by accurate mass measurement (HREIMS) to be $C_{33}H_{43}NO_5$, requiring thirteen degrees of unsaturation. The ^{13}C NMR and DEPT135 spectra contained 33 carbon resonances, including nine resulting from methyl groups, seven from *sp*^{2} methines, one from a *sp*^{3} methine, further four signals from methylene groups and 12 resonances were assigned to quaternary carbons. ^1H NMR and ^1H-^1H COSY spectra showed four resonance signals in the aromatic region (δ 6.95 s, 6.67 d, 6.56 dd, 7.19 d) indicating together with ^{13}C NMR and ^1H-^{13}C HMBC data the presence of two benzylic moieties, one of them 1,2,4- and the other penta-substituted (Tables 1, 2 and Appendix - 2D NMR Tables). Furthermore, the molecule was found to contain three 1,1,2-substituted double bonds (δ_C 120.6, 141.5, 124.6, 132.0, 120.8, 137.9), which were part of a mono- and a hemiterpene moiety. The C-1' to C-10' part of the molecule was deduced from two proton coupling spin systems, the first from H-2' to H_2-1' and H_3-9', and the second ranged from H-4' through to H_3-10' and H_3-8'. ^1H-^{13}C HMBC data correlated H_3-9' to C-2', C-3' and C-4', which disclosed the structure of this terpenoid fragment. Based on literature comparisons (Tanaka *et al.*, 1985) we established the configuration of the $\Delta^{2'/3'}$ as *E*. ^1H NMR resonance signals that arose from the hemiterpene unit C-1'' to C-5'' included two singlet methyl resonances, i.e. CH_3-4''(δ_H 1.68, brs) and CH_3-5''(δ_H 1.67, brs), both with ^1H-^{13}C HMBC correlations to C-3'' and the *sp*^{2} methine CH-2'' (δ_H 5.35). H-2'' coupled to the oxygenated methylene protons H_2-1'', thus completing this partial structure.

A ^{13}C NMR signal at δ 57.5 (CH-8) was found to be characteristic for a carbon neighboring a nitrogen atom, which according to its chemical shift in the ^{15}N NMR spectrum (δ_N 132.4) was part of an amide functionality. The ^1H-^1H COSY showed correlations from H-8 to H_3-9. Furthermore, ^1H-^{13}C HMBC spectra showed correlations between H-8 and the carbonyl carbon C-1, as well as to C-6, C-7 and C-2 of the penta-substituted aromatic ring. ^1H-^{13}C HMBC correlations between H_3-9 and C-7 as well as ^1H-^{15}N HMBC correlations between H_3-9 and the amide nitrogen (see Appendix - Complete 2D NMR data) gave evidence for a phthalimidine skeleton, i.e. the C-1 to C-9 part of the structure. One of the substituents of the aromatic ring of the phthalimidine moiety was established to be a methyl group (CH_3-11, δ_H 2.12, s), which was positioned at C-4 as deduced from HMBC correlations (Tables 1 and 2). The quaternary carbons

C-3 and C-5 have ^{13}C NMR shifts typical for aromatic carbons bound to oxygen. The methoxyl group OCH_3-10 was established to be located at C-3, as evident from ^{1}H-^{13}C HMBC correlations. CH_2-1' of the monoterpene moiety was attached to oxygen as concluded from the chemical shifts of C-1' (δ_C 66.2) and H_2-1' (δ_H 4.68 and 4.72). H_2-1' showed long range heteronuclear coupling with C-5 of the aromatic ring via an oxygen bridge, thus placing the terpene moiety at C-5. The latter deduction was also supported by ^{1}H-^{1}H NOESY correlations from H_2-1' to H-6.

Further three resonance signals in the ^{1}H NMR spectrum resulted from a tri-substituted benzene ring. H-16 and H-17 (J = 8.6 Hz) were placed in *ortho* position to each other, while H-14 and H-16 (J = 2.6 Hz) were *meta*-positioned. ^{1}H-^{13}C HMBC correlations from H_2-1'' to C-13 and from OCH_3-18 to C-15 showed that the oxygenated quaternary aromatic carbons C-13 (δ_C 156.8) and C-15 (δ_C 160.8) were connected with a hemiterpene (C-1'' to C-5'') and a methoxyl moiety (OCH_3-18), respectively. ^{1}H-^{1}H NOESY correlations of H_3-18 to H-14 and H-16, and of H_2-1'' to H-14 confirmed the position of these substituents. ^{1}H-^{15}N HMBC measurements showed two distinct correlations from H_3-9 and H-17 to the nitrogen atom (δ_N 132.4), evidencing that the tri-substituted benzene ring is connected at C-12 to the phthalimidine nucleus. ^{1}H-^{1}H NOESY correlations from H-17 to H_3-9 and to H-8 confirmed the structure. Compounds **1** and **2** have the same planar structure, but differ concerning their configuration at C-8, i.e. they are enantiomers. We propose the trivial names mariline A (**1**) and B (**2**) for these compounds.

The molecular formula of **3** was deduced by accurate mass measurement (HRESIMS) to be $C_{23}H_{33}NO_4$, requiring eight degrees of unsaturation. The C-1 to C-8 and C-1' to C-10' parts of the molecule were established to be identical to those of compounds **1** and **2** based on ^{13}C and ^{1}H NMR, as well as ^{1}H-^{13}C HMBC and ^{1}H-^{1}H COSY spectra (Tables 1, 2 and Appendix - 2D NMR tables) The structure of **3** however, was missing the second aromatic ring and instead an ethyl-1-ol moiety was linked to the nitrogen atom. This was evidenced by heteronuclear long range correlations from H_2-12 to C-8 and C-1 through the nitrogen atom. Furthermore, the methylene CH_2-13 showed proton coupling with CH_2-12, whereby the ^{13}C NMR shift of C-13 indicated that it was connected to a hydroxy group (δ_C 61.7). This completed the planar structure of compound **3**, for which we propose the trivial name mariline C.

The molecular formula of **4** was deduced by accurate mass measurement (HRESIMS) to be $C_{11}H_{13}NO_3$, requiring six degrees of unsaturation. NMR data (Tables 1, 2 and Appendix - 2D NMR tables) suggested the presence of a phthalimidine nucleus with most substituents on the aromatic ring as present in **1**, **2** and **3**. Compound **4**, however possessed a free hydroxy group, which was confirmed by an IR absorption band at 3346 cm^{-1}. The latter was placed at C-5 (δ_C 162.3), which was clearly an oxygenated aromatic carbon atom. Spectroscopic data for compound **4** did not show any signals for a substituent on the nitrogen atom, which is thus present as an NH group. We propose the trivial name mariline D for **4**.

Table 1. ^{13}C NMR Spectroscopic Data for Compounds **1** – **4**

	1 & 2	**3**	**4**
position	δ_N, δ_C, mult.[a, b, c]	δ_C, mult.[a, b, c]	δ_C, mult.[a, b,c]
N	132.4, N		
1	166.2, qC	167.3, qC	171.7, qC
2	116.4, qC	116.3, qC	114.5, qC
3	157.2, qC	156.9, qC	158.4, qC
4	119.4, qC	119.3, qC	118.9, qC
5	161.9, qC	161.7, qC	162.3, qC
6	101.8, CH	101.8, CH	105.0, CH
7	150.0, qC	150.0, qC	152.1, qC
8	57.5, CH	56.9, CH	53.2, CH
9	19.4, CH_3	18.9, CH_3	20.8, CH_3
10	62.1, CH_3	62.1, CH_3	62.5, CH_3
11	8.8, CH_3	8.8, CH_3	8.6, CH_3
12	120.1, qC	43.6, CH_2	
13	156.8, qC	61.7, CH_2	
14	101.2, CH		
15	160.8, qC		
16	105.5, CH		
17	131.9, CH		
18	55.7, CH_3		
1'	66.2, CH_2	66.2, CH_2	
2'	120.6, CH	120.6, CH	
3'	141.5, qC	141.5, qC	
4'	40.1, CH_2	40.1, CH_2	
5'	27.0, CH_2	27.0, CH_2	
6'	124.6, CH	124.6, CH	
7'	132.0, qC	132.1, qC	
8'	25.8, CH_3	25.8, CH_3	
9'	16.7, CH_3	16.7, CH_3	
10'	17.7, CH_3	17.7, CH_3	
1"	66.1, CH2		
2"	120.8, CH		
3"	137.9, qC		
4"	18.2, CH_3		
5"	25.7, CH_3		

[a] acetone-d_6 (**1**, **2**, **3**) , and MeOD (**4**) 300/75.5 MHz. [b] Assignments are based on extensive 1D and 2D NMR experiments (^1H-^{13}C, ^1H-^{15}N HMBC, HSQC, COSY). [c] Implied multiplicities determined by DEPT.

Table 2. ^{1}H NMR Spectroscopic Data for Compounds **1** – **4**

	1 & **2**	**3**	**4**
position	δ_H[a, b] (*J* in Hz)	δ_H[a, b] (*J* in Hz)	δ_H[a, b] (*J* in Hz)
N			
1			
2			
3			
4			
5			
6	6.95, s	6.92, s	6.68, s
7			
8	4.97, q (6.8)	4.62, q (6.8)	4.53, q (6.8)
9	1.27, d (6.8)	1.44, d (6.8)	1.42, d (6.8)
10	3.99, s	3.98, s	3.95, s
11	2.12, s	2.09, s	2.15, s
12		a: 3.33, dt (14.0, 5.5) b: 3.85, dt (14.0, 5.5)	
13		3.71, m	
14	6.67, d (2.6)		
15			
16	6.56, dd (2.6, 8.6)		
17	7.19, d (8.6)		
18	3.81, brs		
1'	a: 4.68, dd (6.6, 12.3) b: 4.72, dd (6.6, 12.3)	a: 4.65, dd (6.6, 12.3) b: 4.71, dd (6.6, 12.3)	
2'	5.53, t (6.6)	5.51, t (6.6)	
3'			
4'	2.12, m	2.12, m	
5'	2.14, m	2.14, m	
6'	5.10, t (6.6)	5.10, t (6.6)	
7'			
8'	1.63, brs	1.63, brs	
9'	1.77, brs	1.76, brs	
10'	1.59, brs	1.58, brs	
1"	a: 4.54, dd (6.6, 12.0) b: 4.58, dd (6.6, 12.0)		
2"	5.35, t (6.6)		
3"			
4"	1.68, brs		
5"	1.67, brs		

[a] acetone-d_6 (**1**, **2**, **3**) , and MeOD (**4**), 300/75.5 MHz. [b] Assignments are based on extensive 1D and 2D NMR experiments (^{1}H-^{13}C, ^{1}H-^{15}N HMBC, HSQC, COSY).

Stereochemistry

Compounds **1-4** possess a single chiral carbon, i.e. C-8. The measurement of specific optical rotations yielded in all cases a value close to zero, and furthermore, CD measurements produced only marginal CD effects. The structure of the molecules suggested a CD effect at around 260 nm due to the proximity of the chiral center to the chromophore. It was thus assumed that we may have obtained racemic mixtures. In the case of marilines A and B (**1**, **2**) this was confirmed by chromatographic separation of the enantiomers using chiral HPLC. The enantiomers **1** and **2** were isolated from three independent cultures and found to be present in ratios of approximately 3:2, 3:7 and 1:1 as deduced from the final weights obtained.

We found several previously reported cases of racemization reactions on natural products with a chiral center in lactam, lactone and dihydrofuran rings (Harper *et al.*, 2003; Li *et al.*, 2008; Strobel, *et al.*, 2002; Wolfgang and Kund, 1990), which suggested a post-biosynthetic racemization also for **1** or **2**. This racemization could occur via a resonance stabilized cationic intermediate, as previously described for similar compounds (Harper *et al.*, 2003; Li *et al.*, 2008). Especially noteworthy is a previous literature report on the easy racemization of the phthalimidine-like compound pagoclone (Stuck *et al*., 2003). It was reported that this isoindolinone already racemized at low basic or acidic conditions and moderately elevated temperatures. Racemization of pagoclone was found to be optimal with 0.005N KOH at 50 ºC for 2h, and suggested to occur via a retro-Michael/Michael reaction. This type of reaction is, however unlikely to occur in the case of **1** and **2**. Nevertehless, to evaluate whether racemization occured during the extraction and isolation process, enantiomerically pure marilines A and B were subjected to increasing concentrations of KOH and HCl as outlined in the experimental section, however even harsh conditions produced no racemization as evidenced by chiral HPLC analysis.

CD spectra of **1** and **2** were measured and opposite CD effects were discerned for the enantiomers (Figure 2).

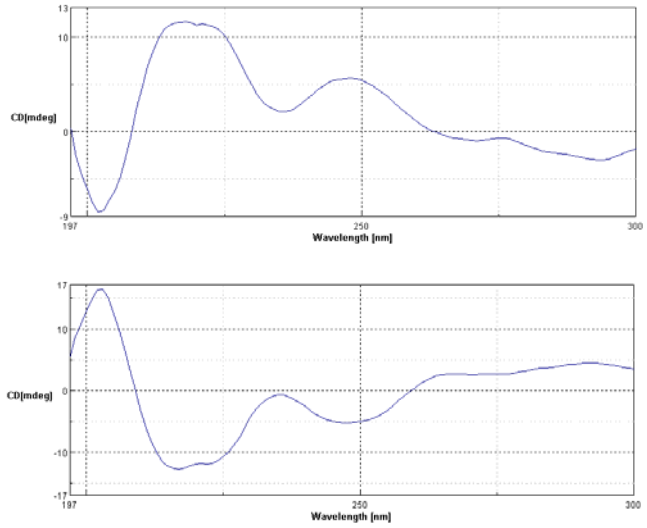

(Compound **1**)

(Compound **2**)

Figure 2. CD spectra of compound **1** (mariline A) and **2** (mariline B)

The configuration at C-8 is currently being elucidated by theoretical CD calculations.

Compounds **3** and **4** were also collected as racemic mixtures, as no effects in CD spectra and no optical rotation values were obtained. Exhaustive attempts to separate the enantiomers with three different chiral stationary HPLC columns were unsuccessful.

Biological activity

Marilines A and B inhibited the protease HLE with an IC_{50} value of 0.86 μM for both enantiomers. Acetylcholinesterase (AChE) activity was inhibited with an IC_{50} value of 0.18 μM (offset = 49 ± 3 %) for mariline A and 0.63 μM (offset = 54 ± 3 %) for mariline B. The large offset (i.e. a remaining activity in the presence of inhibitor) in the AChE inhibition assay probably means that the compounds do not bind to the protease active site. When performing calculations with equations which do not considers the offset, marilines A and B have IC_{50} values of 4.4 and 6.6 μM, respectively. Mariline C (**3**) showed no activity toward the proteases HLE and AChE at the 10 μM level (see Appendix - Bioactivity results). Compound **4** was not tested in these assays, due to the small amounts isolated. Marilines A-D were assayed towards further proteases and found to be inactive (see Appendix - Bioactivity results).

Mariline A was tested against five cancer cell lines and exhibited a mean GI_{50} of 24.44 μM, whilst mariline B was tested against 19 cancer cell lines and showed a GI_{50} of 5.00 μM. The observed antiproliferative pattern of mariline B did not correlate with that of any of the standard antiproliferative compounds with known mechanism of action as deduced by COMPARE analyses. The first match on the standard agents database (correlation 0.427) was rhizoxin, a metabolite produced by a bacteria associated with a fungus (see see Appendix - Bioactivity results). Mariline C (**3**) and D (**4**) were also evaluated for cytotoxic activity against a panel of 5 cancer cell lines (NCI-H460/lung, A549/lung, MCF7/breast and SF268/CNS and CAKI/renal at the 100 μM level) and mariline C exhibited low antiproliferative activity with an GI_{50} of 48.32 μM, while mariline D exhibited no activity.

Marilines A-C were shown to have antiplasmodial activity against *Plasmodium berghei* with an IC_{50} of 6.68 μM, 11.61 μM and 13.84 μM, respectively.
Marilines C and D showed also antagonist activity on the canabinoid receptor CB_2 with K_i values of 5.97 μM and 5.94 μM, respectively.
Mariline B further exhibited antagonist activity against the histamine receptor H2 with a K_i value of 5.92 μM, the dopamine receptor DAT with a K_i value of 5.63 μM and the adrenergic receptor $Beta_3$ with a K_i value of 5.63 μM (see Appendix - Bioactivity results).

Mariline A and B were further evaluated for inhibition of the protein kinases DYRK1A and CDK5 assays (tested at 10 mM dose) and for the inhibition of further proteases: Chymotrypsin, trypsin, papain and acetylcholine esterase (tested at the 100 μM level), but showed no activity.
Mariline B (**2**) was tested against two antibiotic resistant *Mycobacterium tuberculosis*, strains MTB72 and R46 (tested at the 50 μg/mL disc level), but did not show relevant activity.

Discussion

Compounds with a related phthalimidine (isoindolinone) nucleus as found for **1** – **4** are known from fungal metabolism, however they all lack the methyl group at C-8. The structurally most simple phthalimidines possess an unsubstituted nitrogen atom as found in mariline D (**4**), i.e. 6-hydroxy-4-methoxy-5-methylphthalimidine (cichorine) (Kawahara *et al.*, 1988; Stierle *et al.*, 1993), zinnimidine (Suemitsu et al, 1995), duricaulic acid (Achenbach et *al.*, 1985), memnobotrin A and the related staybotrylactam (Jarvis et al., 1999) and the more complex xylactam (Wang et al, 2005). Reported N-substituted phthalimidines include compounds with a phenylethyl (Kawagishi *et al.*, 1990; Nozawa *et al.*, 1997), ethyl-1-ol (Horiuchi *et al.*, 2003; Horiuchi *et al.*, 2002) or a carbonic acid (Ogawa et al, 1995, Matsumoto *et al.*, 1995) moiety attached. Of these, examples of fungal phthalimidines structurally related to marilines A and B (**1**, **2**) include hericenone B and stachybotrin C (Kawagishi *et al.*, 1990; Nozawa *et al.*, 1997), both with a phenylethyl moiety connected to the nitrogen atom. In compounds **1** and **2**, however the nitrogen is substituted with a derivatised phenyl ring, hitherto only present in a similar way in the phthalimidine structure clitocybin A (Kim et al, 2008). Porritoxin, porritoxin sulfonic acid (Horiuchi *et al.*, 2003; Horiuchi *et al.*, 2002), memnobotrin B (Jarvis *et al.*, 1999) and stachybotramide (Ayer *et al.*, 1993) contain an N-ethyl-1-ol moiety and are structurally related to mariline C (**3**) (all related structures are depicted in see Appendix – Spectroscopic data supporting information)

Racemization

8*R* and 8*S* enantiomers of phthalimidines are described for pestalachloride A, where a 2,4-dichloro-5-methoxy-3-methylphenol moiety is attached to the chiral carbon C-8 (Li *et al.*, 2008). Also, the isobenzofuranone isopestacin was found to occur as a racemic mixture (3*R*/3*S*), with diverging configuration at the carbon neighbouring the lactone functional group (Strobel, *et al.*, 2002). A similar case is the dihydro isobenzofuran derivative pestacin, which occurs as a racemic mixture of 1*R* and 1*S* enantiomers, whereby the chiral carbon C-1 is in α-position to the oxygen in the dihydrofuran ring (Harper *et al.*, 2003). Racemization in the case of pestalachloride A, isopestacin and pestacin was proposed to occur after biosynthesis via resonance stabilized cationic

intermediates. Based on structural considerations a similar mechanism may be feasible for **1** and **2**, however less favoured since the substituent at C-8 is a methyl group whereas in pestalachloride A (and in a similar fashion in isopestacin and pestacin) an aromatic moiety is located at the respective position. Since racemization does not occur when marilines A or B are exposed to different reaction conditions, it may be concluded that both enantiomers are products of the biosynthetic process and not of post-biosynthetic racemization reactions.

Hypothesis on Biosynthesis

Phthalimidine nucleus/Carbon skeleton/Origin of nitrogen:

Compounds **1**-**4** are phthalimidine derivatives and related to their oxygen-containing counterparts named phthalides, which are more common in nature (Lin *et al.*, 2005). Biosynthetic studies focusing on phthalide structures, e.g. for mycophenolic acid (Bedford *et al.*, 1973) or for phthalide-like metabolites isolated from *Talaromyces flavus* (Ayer and Racok, 1990) were previously performed by means of feeding experiments with labeled precursors, evidencing the tetraketide nature of the phthalide nucleus. Compounds **1**-**4**, possess the basic skeleton of the tetraketide 3-methyl-orsellinic acid, however the acetate-derived methyl group in orsellinic acid would be replaced by an ethyl group in the precursor molecules of **1**-**4** (Geris and Simpson, 2009) (Figure 3). To our knowledge no biosynthetic studies were performed for phthalimidine-like molecules. Phthalimidine biosynthesis, however most probably involves similar polyketide-type reactions as known for phthalides.

The most unusual structural characteristic of the phthalimidine derivatives **1**-**4** is the methyl substituent at C-8. The latter seems to require either, a propionate starter unit (see A in Figure 3) or a methylation (e.g. via a SAM-dependent methyl-transferase) at C-8 (see B in Figure 3). A third possibility would be the loss of a carbon atom from a pentaketide intermediate (not depicted in Figure 3). To our knowledge to date, these types of reaction are not known in fungal polyketide metabolism.

Methylation (see B in Figure 3) would occur most probably at the acetate starter unit, because the methylene carbons in the poly-ß-keto acid would be more prone as the site of attack for a SAM-dependent methyl-transferase than the terminal methyl group of the starter unit (see B in Figure 3). A somewhat similar case represents the myxobacterial

metabolite myxovirescin A, isolated from *Myxococcus xanthus*, where methylation of the starter unit was also found. In this case feeding studies and the overall organization of the myxovirescin A gene cluster suggested that the biosynthesis of this compound takes place firstly by fusion of an acetate unit with a malonate, followed by methylation, reduction and hydroxylation to produce the starter unit 2-hydroxyvalerianic acid (Simunovic *et al.*, 2006). For the cyanobacterial compound homoanatoxin-a, the incorporation of a SAM-mediated methyl group is suggested to occur in a similar fashion (Namikoshi *et al.* 2004).

Incorporation of an intact propionate starter unit (see A in Figure 3) has been reported for a number of bacterial metabolites, e.g. anthracycline antibiotics such as aclarubicin, or doxorubicin (Fujii and Ebizuka, 1997). Umezawa *et al*. showed that the common anthracycline intermediate aklavinone, a metabolite isolated from *S. galilaeus*, is derived from propionyl-CoA and nine malonyl-CoA extender units (Yoshimoto *et al.*, 1981). The best-studied use of a propionate as starter is for daunorubicin from *S. peucitus* and its C14-hydroxylated derivative doxorubicin from *S. coeruleorubicus*, which are among the most important antitumor antibiotics in current use (Hutchinson, 1997; Grim *et al.*, 1994). With regard to the biosynthetic origin of propionyl-CoA, it is proposed that the primer is derived from multiple sources such as amino acid catabolism and degradation of odd-numbered fatty acids, but decarboxylation of methylmalonyl-CoA appears to be less likely (Weissman *et al.*, 1998).

It appears that the type of reactions probably involved in the formation of marilines, to date was only found in bacteria. Hence, these data open up interesting questions on why biosynthetic steps reported for bacteria are encountered in fungal metabolism. Preliminary studies in our laboratory indicate the presence of bacteria associated with the mycelium of the investigated fungus (data not shown).

The origin of the nitrogen atom of the lactam ring in phthalimidines is probably derived from amino acid metabolism. Based on the structural characteristics in several phthalimidines this seems quite obvious, e.g. staplabin analogues containing serine, phenylalanine, leucine or tryptophan partial structures (Geris and Simpson, 2009). Similarly, the nitrogen precursor of hericenone B and stachybotrin C (Kawagishi *et al.*, 1990; Nozawa *et al.*, 1997) with a phenylethyl moiety connected to the nitrogen atom, is probably phenylalanine or tyrosine.

For marilines A and B (**1, 2**) it seems likely that 4-hydroxyaniline, produced via chorismic acid and p-amino-benzoic-acid (Sasaoka *et al.*, 1980; Tsuji *et al.*, 1981; Tsuji *et al.*, 1985a; Tsuji *et al.*, 1985b;) (Figure 2 and Appendix – Spectroscopic data supporting information) may be the precursor for the C-12 to C-17 comprising aromatic ring and the nitrogen atom. Incorporation studies of chorismic acid and 4-amonobenzoic acid into the 4-hydroxyaniline moiety of N-(γ-glutamyl)-4-hydroxyaniline in *Agaricus bisporus* supports the formation of aniline derivatives in fungi (Tsuji *et al.*, 1985a; Tsuji *et al.*, 1985b). Furthermore, several dihydroxyaniline derivatives are known to be produced in fungal metabolism, e.g. 4-hydroxy-2-methoxyacetanilide isolated from a spruce fungal endophyte and *Aspergillus* sp. (Findlay *et al.*, 2003) (see depicted structures in Appendix - Spectroscopic data supporting information). Regarding mariline C (**3**), the N atom may originate from ethylamine (see Figure 3), previously reported to be biosynthetically derived through decarboxylation of alanine (Takeo, 1974; Deng *et al.*, 2008). For mariline D (**4**), glutamine, glutamate or ammonia may introduce the nitrogen atom.

The carbon skeleton of marilines A and B could be considered unprecedented, due to the existence of the unique extra-methyl group at C-8 amongst all known phthalides/phthalimidines. Feeding experiments are under way in order to determine the building blocks for these most unusual molecules.

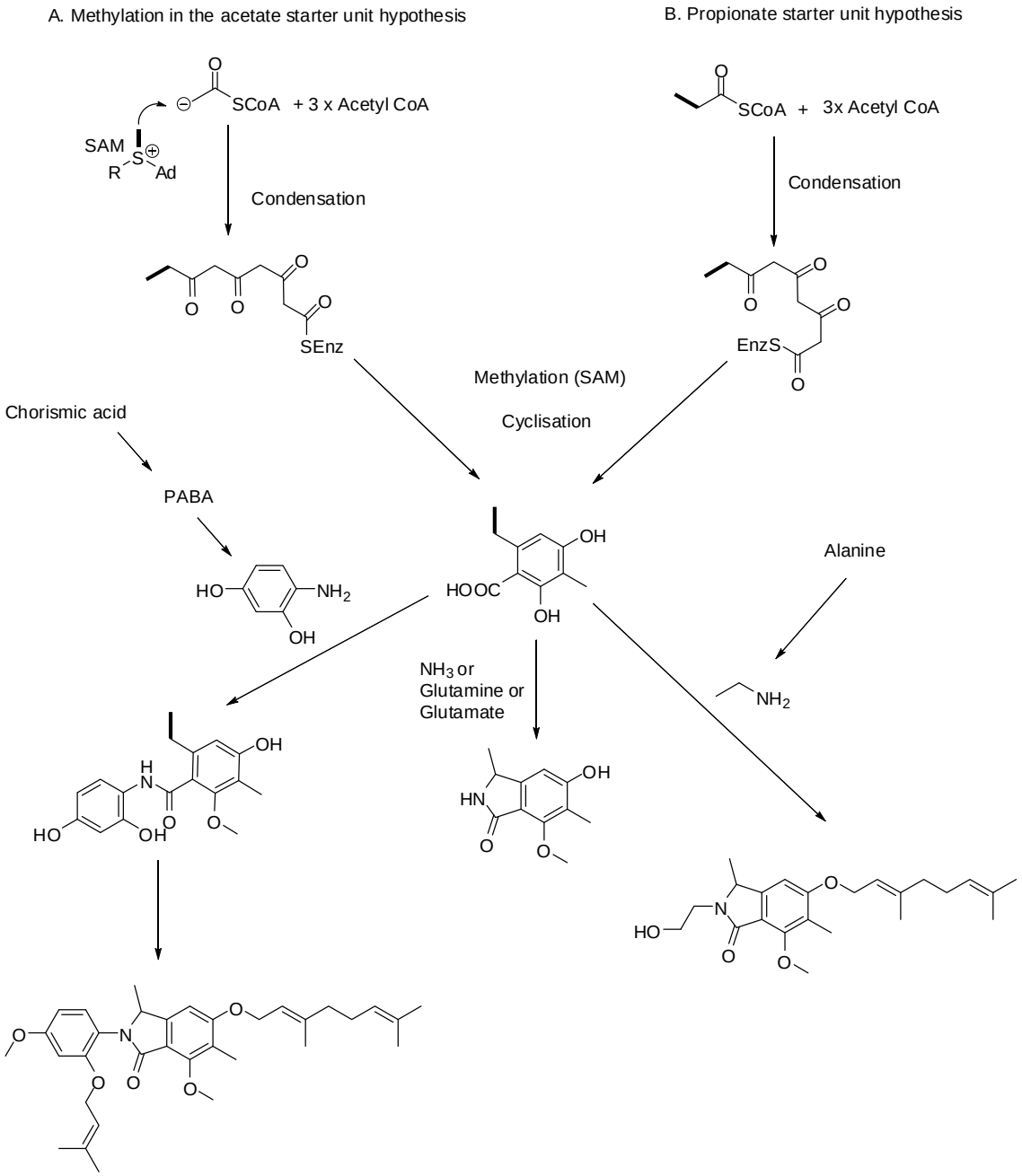

Figure 3. Proposed biosynthetic pathways for Mariline A – D.

It is worthwhile to mention that marilines were produced solely on solid biomalt medium supplemented with sea salt, whereas in other media such as Czapek or YPM no phthalimidines were formed. In all four individual culture experiments on biomalt medium supplemented with sea salt, marilines A and B were isolated, whilst marilines C and D were separated only once and in low amounts. The fungus was also not able to grow on biomalt without a sea salt supplement.

Bioactivity

The most interesting activity obtained from the multitude of bioactivity tests was found towards human leukocyte elastase (HLE). This serine protease that has been associated with several pathological conditions including cystic fibrosis, rheumatoid arthritis and infectious diseases (Bieth *et al.*, 1998) HLE is further considered to be the primary source of tissue damage associated with such inflammatory diseases as pulmonary emphysema and adult respiratory distress syndrome (Vender, 1996; Chua and Laurent, 2006; Pham, 2006; Taggart *et al.*, 2005). Small molecular weight HLE inhibitors could be therapeutically useful in the treatment of such diseases, and a number of inhibitors are currently in development (Esper and Martin, 2005; Abbenante and Fairlie, 2005).

Experimental section

General Experimental Procedures. See chapter 3 - General methodology. Specifically for marilines A-B, to separate enantiomeric mixtures the HPLC column Lux Cellulose-1 from Phenomenex (250 x 4.5 mm; 5 μm) was used with a flow rate of 1 mL/min (hexane : isopropanol 90:10). The ^{1}H-^{15}N HMBC spectrum was referenced externally to urea (^{15}N chemical shift is reported relative to liquid ammonia).

Fungal material. See chapter 3 - General methodology.

Culture, extraction and isolation. Compounds **1** to **4** were isolated from two different cultures of *Stachylidium sp.*, a first with 12 L and a second with 10 L media volume. Both were performed on an agar-biomalt medium (biomalt 20g/L, 15 g/L agar) supplemented with sea salt during 2 months (12 L culture) and 40 days (10 L culture). An extraction with 5 L EtOAc yielded 5.9 g and 2.1 g of extract, respectively, which were subjected to VLC fractionation in a silica open column using a gradient solvent system with petroleum ether - acetone at 10:1, 5:1, 2:1, 1:1, 100 % acetone and 100 % MeOH, resulting thus 6 VLC fractions for each culture. Compounds **1** and **2** were isolated from both cultures, being hereby described the 12 L culture isolation procedures. Compound **4** was isolated from the first culture (12 L), whilst compound **3** was isolated from the second culture (10 L).

Compounds **1** and **2** were isolated from VLC 2, followed by HPLC fractionation using petroleum ether - acetone 11:1 (fraction 2 of 7) and RP-HPLC fractionation using 90 %

MeOH (fraction 3 of 4, 12.6 mg, t_R 31 min). The racemic mixture was then separated using a Phenomenex Lux Cellulose-1 HPLC column using hexane : isopropanol 90:10 (Mariline A, 7.2 mg, t_R 21 min; Mariline B, 4.8 mg, t_R 29 min).
Compound **3** was isolated from VLC 4, followed by HPLC fractionation using petroleum ether - acetone 9:2 (fraction 5 of 7, 2.6 mg, t_R 48 min)
Compound **4** was isolated from VLC 4, followed by HPLC fractionation using petroleum ether - acetone 2:1 (fraction 4 of 7), followed by RP-HPLC with an Macherey-Nagel Ísis column using 30 % MeOH (fraction 2 of 3, 1.4 mg, t_R 7 min).

Mariline A (1): colorless oil (600 µg/L 0.12 %); $[\alpha]_D^{23}$ +14 (*c* 0.225, acetone); UV (MeOH) λ_{max} 219 nm (log ϵ 4.11), 268 (log ϵ 3.73); IR (ATR) ν_{max} 3330 (br), 2925, 1668, 1605 cm^{-1}; ^1H NMR and ^{13}C NMR (Tables 1 and 2); LREIMS *m/z* 533.3 $(M)^+$; HREIMS calcd. *m/z* 533.3141 for $C_{33}H_{43}NO_5$ $(M)^+$, found 533.3139; CD (*c* 2.8×10^{-4} mol/L, MeOH) λ (Δε) = 202 (-9.0), 218 (+12.4), 248 (+6.1), 298 (-3.2).

Mariline B (2): colorless oil (400 µg/L, 0.08 %); $[\alpha]_D^{23}$ -14 (*c* 0.175, acetone); UV (MeOH) λ_{max} 219 nm (log ϵ 4.1), 268 (log ϵ 3.7); IR (ATR) ν_{max} 3330 (br), 2925, 1668, 1605 cm^{-1}; ^1H NMR and ^{13}C NMR (Tables 1 and 2); LREIMS *m/z* 533.3 $(M)^+$; HREIMS calcd. *m/z* 533.3141 for $C_{33}H_{43}NO_5$ $(M)^+$, found 533.3139; CD (*c* 3.1×10^{-4} mol/L, MeOH) λ (Δε) = 202 (+15.8), 218 (-12.2), 248 (-5.2), 293 (+4.3).

Mariline C (3): white amorphous solid (260 µg/L, 0.124 %); UV (MeOH) λ_{max} 207 nm (log ϵ 4.46), 262 nm (log ϵ 3.95); IR (ATR) ν_{max} 3391 (br), 2926, 1664, 1607 cm^{-1}; ^1H NMR and ^{13}C NMR (Tables 1 and 2); LRESIMS *m/z* 388.5 $(M+H)^+$; HRESIMS calcd. *m/z* 410.2302 for $C_{23}H_{33}NO_4Na$ $(M+Na)^+$, found 410.2290; no CD spectra revealed the presence of a racemic mixture.

Mariline D (4): amorphous solid (108 µg/L, 0.022 %); UV (MeOH) λ_{max} 216 nm (log ϵ 3.90), 259 nm (log ϵ 3.71); IR (ATR) ν_{max} 3346 (br), 2926, 1670, 1610 cm^{-1}; ^1H NMR and ^{13}C NMR (Tables 1 and 2); LRESIMS *m/z* 206.0 $(M-H)^-$, *m/z* 207.9 $(M+H)^+$; HRESIMS calcd. *m/z* 230.0788 for $C_{11}H_{13}NO_3Na$ $(M+Na)^+$, found 230.0786; no CD spectra revealed the presence of a racemic mixture.

Racemization experiments. Racemization experiments were based on literature data (Stuck *et al*., 2003)., where racemization of a phthalimidine nucleus was achieved with very low acidic/alkaline concentrations (0.0005 M KOH). Each experiment contained 200 µg of mariline A dried on a stream of N_2 in a glass vial which was suspended in 400 µL solution with the following conditions: a) water, b) 0.0005 M KOH, c) 0.0025 M KOH, d) 0.5 M KOH, e) 0.0005 N HCl, d) 0.5 N HCl. 200 µg mariline B were also tested at the range of 0.5 N KOH. All samples were then incubated in a water bath at 55 ºC for 2 hours, after which they were neutralized with the same molar proportion of acid/alkaline solution. After drying the sample in gaseous nitrogen the samples were injected in a HPLC chiral phase column with the same solvent system used to separate the enantiomers marilines A and B for detection of racemization (see General Experimental Procedures).

Biological activity assays. See chapter 3 - General methodology.

5. Marilones A – J, Unusual Phthalides from the Sponge-derived Fungus *Stachylidium* sp.

Abstract

The marine-derived fungus *Stachylidium* sp. was isolated from the sponge *Callyspongia* sp. cf. *C. flammea.* Culture on a biomalt medium supplemented with sea salt led to the isolation of eight new phthalide derivatives with unusual structural motives, i.e. marilones A – J (**1**-**8**, **10**, **11**), and the known compound silvaticol (**9**). In the epimeric compounds **10** and **11** the phthalide (=isobenzofuranone) nucleus is modified to an isobenzofuran ring with ketal and acetal functionality. The skeleton of marilones A, B, D and F-J is most unusual, and its biosynthesis is suggested to require unusual biochemical reactions considering fungal secondary metabolism. Marilone A (**1**) was found to have antiplasmodial activity against *Plasmodium berghei* with an IC_{50} of 12.1 μM. Marilone B (**2**) showed selective antagonistic activity towards the serotonin receptor 5HT2B with a K_i value of 7.7 μM.

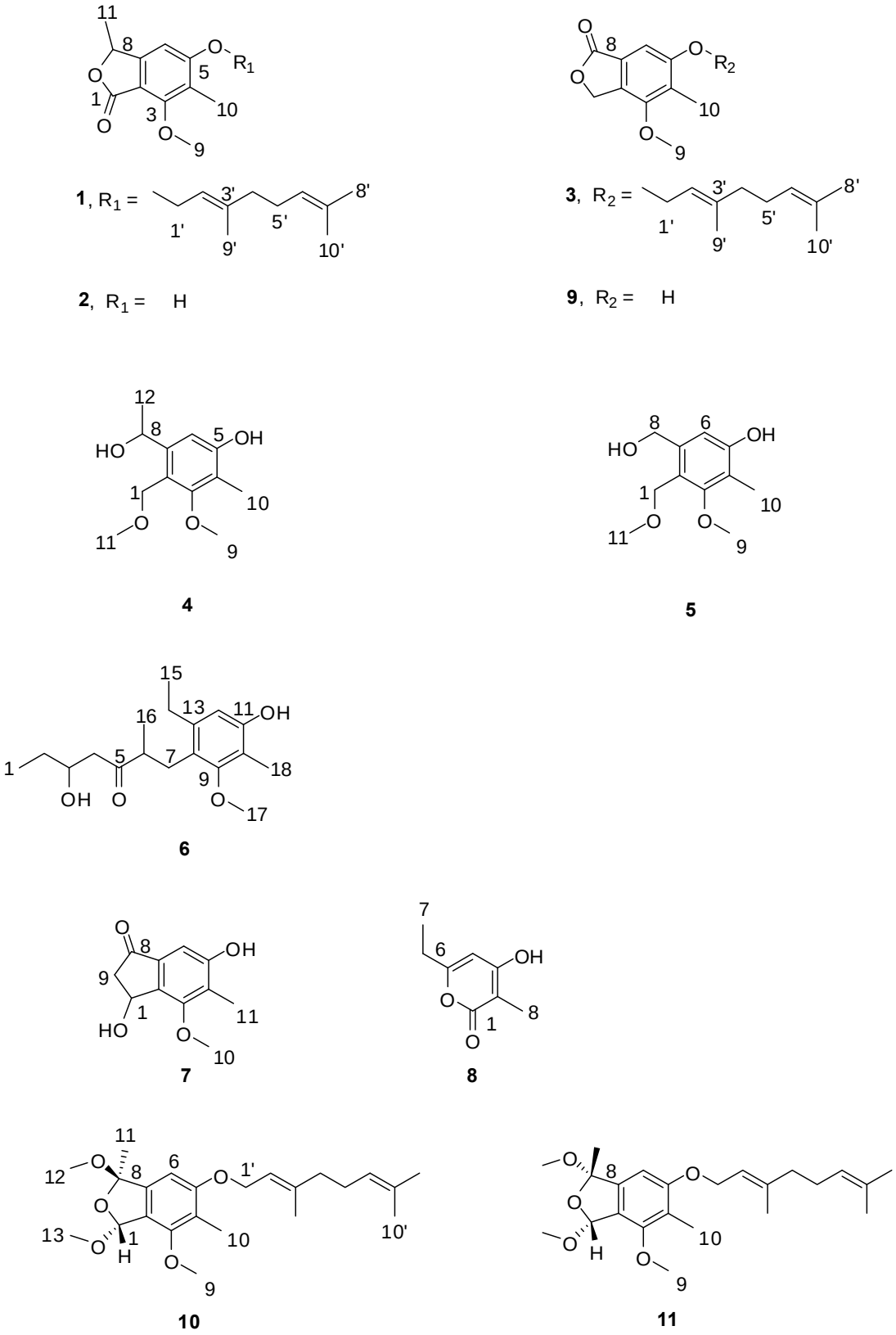

Figure 1. Secondary metabolites **1 – 11** isolated from *Stachylidium* sp.

Introduction

Phthalides are a class of structurally most diverse secondary metabolites with more than 180 naturally occurring compounds described (Lin *et al.*, 2005). They are produced by a wide range of organisms, i.e. marine and terrestrial fungi belonging to genera such as *Aschochyta* (Seibert *et al.*, 2006), *Aspergillus* (Fujita *et al.*, 1984; Achenbach *et al.*, 1985), *Alternaria* (Suemitsu *et al.*, 1995; Kawahara *et al.*, 1988), *Penicillium* (Smith, 1952), *Hericium* (Kawagishi *et al.*, 1990) or *Talaromyces* (Ayer and Racok, 1990), but also by plants and liverworts (Lin *et al.*, 2005).
Phthalides exhibit an equally broad spectrum of bioactivity, including modulation of the central nervous system, protection against brain eschemia, modulation of platelet aggregation and cardiac function, inhibition of smooth muscle cell proliferation, anti-angina activity, smooth muscle relaxation, as well as antibacterial, antifungal, antiviral and phytotoxic activity (Lin *et al.*, 2005). The medically most important member of this family of natural products is mycophenolic acid, firstly isolated from *Penicillium brevicompactum*, and used in form of its derivative mycophenolate mofetil as an immunosupressant drug (Dewick, 2009).

During our search for new natural products produced from the marine-derived fungus *Stachylidium* sp., several structurally unusual phthalide derivatives, i.e. marilones A - J, were isolated from a culture on agar-BMS media supplemented with artificial sea salt (Scheme 1). Albeit phthalide-like structures are not rare, the structural skeleton of marilones A, B, D, F - J is most unusual, and its biosynthesis is suggested to require unique reactions in fungal secondary metabolism. Marilone A (**1**) exhibited antiplasmodial activity against *Plasmodium berghei* with an IC_{50} of 12.1 µM. Marilone B (**2**) showed a specific antagonistic effect on the serotonin receptor 5HT2B with a K_i value of 7.7 µM.

Results

The molecular formula of **1**, was deduced by accurate mass measurement (HREIMS) to be $C_{21}H_{28}O_4$, requiring eight degrees of unsaturation. The ^{13}C NMR and DEPT135 spectra contained 21 carbon resonances, including six resulting from methyl groups,

three from sp^2 methines, one from a sp^3 methine, whereas further three signals resulted from methylene groups and eight resonances were assigned to quaternary carbons (Tables 1, 2 and Appendix – Complete 2D NMR data). The ^{1}H NMR spectrum of **1** displayed a singlet resonance for the aromatic methine (6-CH) at δ 6.95 indicating together with UV and ^{13}C NMR data the presence of a penta-substituted benzene ring. The methyl group 10-CH_3 (δ_C 8.8) was linked to C-4 of the aromatic ring due to heteronuclear long range correlations of the methyl protons with C-3, C-4 and C-5. The methoxyl group 9-OCH_3 (δ_H 3.98) had a heteronuclear long range correlation to C-3 of the aromatic ring, thus clearly delineating it's position. Besides the aromatic proton 6-H, the ^{1}H NMR spectrum showed two further resonance signals in the downfield shifted region (δ_H 5.52 and 5.09) indicating together with ^{13}C NMR and ^{1}H-^{13}C HMBC data the presence of a geranyl substituent. The C-1' to C-10' part of the molecule was deduced from two proton coupling spin systems observed in the ^{1}H-^{1}H COSY spectrum, namely 1'-H_2 to 2'-H (J = 6.6 Hz) and 4'-H_2 to 6'-H through 5'-H_2. ^{1}H-^{13}C HMBC data showed correlations from 9'-H_3 to C-2', C-3' and C-4', and from methyl protons 8'-H_3 and 10'-H_3 to C-6'and C-7', disclosing a geranyl fragment. Based on literature comparisons we established the configuration of $\Delta^{2'/3'}$ as *E* (Tanaka *et al.*, 1985). The aromatic quaternary carbon C-5 (δ_C 164.2) had a carbon resonance indicating a connection to an oxygen atom. The monoterpenyl substituent was established to be connected to C-5 through an oxygen atom due to heteronuclear long range correlations of 1'-H_2 (δ_H 4.69, 4.74) to C-5.

The ^{1}H-^{13}C HMBC spectrum exhibited a correlation from 6-H to C-8. Furthermore, the ^{13}C NMR resonance of C-8 at δ 77.0 was found to be characteristic for a carbon bound to an oxygen atom. The ^{1}H-^{1}H COSY spectrum showed a coupling of 8-H with 11-H_3 (J = 6.6 Hz), and the ^{1}H-^{13}C HMBC spectrum contained correlations from 8-H to C-6, C-7 and C-2 of the penta-substituted aromatic ring, as well as to the carbonyl carbon C-1. Ring double bond equivalents required a second ring within compound **1**, and together with heteronuclear correlations of 8-H to C-1 and the carbon resonance of C-1 at δ_C 168.2 indicating the presence of a carbonyl group, gave evidence for a C-8-methylated phthalide skeleton, i.e. the C-1 to C-11 part of the structure. Since the resonance signal for 6-H did not show heteronuclear long range correlations to that of the carbonyl C-1, but correlated with the sp^3 methine C-8, the carbonyl group was assigned at C-1. This way, a phthalide-nucleus identical to that of the known natural product nidulol was formed.[6] To further prove that the carbonyl group is positioned at C-1 and not at C-8 of

1, ^{1}H NMR spectra of **1** were compared with those of nidulol, silvaticol (**9**) and derivatives (see Appendix – Spectroscopic data supporting information). The latter are known regioisomeric phthalides with the carbonyl group at C-1 and C-8, respectively. Differences in ^{1}H NMR resonances can be discerned especially for 6-H, resonating at δ_H 6.59 ($CDCl_3$) for nidulol and δ_H 7.04 ($CDCl_3$) for silvaticol (Kawahara *et al.*, 1988). The ^{1}H NMR spectrum of **1** (δ_H 6.54 in $CDCl_3$) was shown to be similar to that of nidulol and the nidulol derivative, 5-(3',3'-dimethylallyloxy-7-methoxy-6-methylphthalide with 6-H resonating at δ_H 6.62 (see Appendix – Spectroscopic data supporting information and Suemitsu *et al.*, 1995). For compound **1** the trivial name marilone A is suggested.

The molecular formula of **2** was deduced by accurate mass measurement (HREIMS) to be $C_{11}H_{12}O_4$, requiring six sites of unsaturation. The NMR spectral data (see Tables 1, 2 and Appendix – Complete 2D NMR data) indicated that compound **2** is identical to **1**, except for the missing geranyl moiety attached to the hydroxy group at C-5. We propose the trivial name marilone B for compound **2**.

The molecular formula of **3**, was deduced by accurate mass measurement (HREIMS) to be $C_{20}H_{26}O_4$, requiring eight degrees of unsaturation. The spectroscopic data of **3** revealed that the compound is very similar to **1** (Tables 1, 2 and Appendix – complete 2D NMR data). In contrast to compound **1**, however, resonance signals for a methylene group, i.e. 1-CH_2 (δ_C 68.9) were found in the NMR spectra, instead of those for a methine (8-CH) and methyl group (11-CH_3) as in **1**. The resonance signal for 6-H did not have a heteronuclear long range correlations to C-1, but correlated with the carbonyl carbon C-8. Hence, the carbonyl group in **3** was assigned to be located at C-8, thus, forming a phthalide-nucleus as present in silvaticol (**9**). For compound **3**, the name marilone C is suggested.

The molecular formula of **4**, was deduced by accurate mass measurement (HRESIMS) to be $C_{12}H_{18}O_4$, requiring four sites of unsaturation. The NMR spectroscopic data (Tables 4, 5 and Appendix – complete 2D NMR data) indicated again a penta-substituted benzene ring identical to that in **1-3**. A ^{1}H NMR coupling from the methine 8-H to 12-H_3 (J = 6.3 Hz) was discerned in the ^{1}H NMR spectrum, whereas C-8 had a carbon shift (δ_C 65.9) characteristic for oxygen substitution. The methoxyl function 11-OCH_3 was connected to the methylene 1-CH_2 as deduced from heteronuclear long range

correlations of the methoxyl protons to C-1. Compound **4** is thus a monocyclic compound, for which we propose the trivial name marilone D.

The molecular formula of **5**, was deduced by accurate mass measurement (HRESIMS) to be $C_{11}H_{16}O_4$, requiring four sites of unsaturation. The structure of **5** was found to be almost identical to that of **4** (Tables 4 and 5 and Appendix – complete 2D NMR data). The only difference between them was discerned to be the substitution of C-8. In case of compound **4** this carbon was substituted with the methyl group (12-CH_3), whereas in compound **5** C-8 was an oxygenated methylene group. Consequently, the ^{1}H NMR spectrum of **5** exhibited a singlet resonance for a methylene group at δ_H 4.64. We propose the trivial name marilone E for compound **5**.

The molecular formula of **6** was deduced by accurate mass measurement (HRESIMS) to be $C_{18}H_{28}O_4$, requiring five sites of unsaturation. The ^{13}C NMR and DEPT135 spectra indicate the presence of 18 resonances, including five for methyl, four *sp*^{3} methylene, one *sp*^{2} methine, two *sp*^{3} methine groups and six for quaternary carbons (see Table 3). Compound **6** has the close to identical penta-substituted aromatic ring as found for **1**-**5** (notice: carbons/hydrogens have different number assignment), as proven by ^{1}H-^{13}C HMBC correlations from 12-H to C-8, C-10, C-11, C-13 and C-14. The methyl group 15-CH_3 was attached to the *sp*^{3} methylene 14-CH_2, completing the substituent at C-13. Based on ^{1}H-^{13}C HMBC and ^{1}H-^{1}H COSY correlations we found that the aromatic substituent at C-8 was an aliphatic chain giving rise to two ^{1}H-^{1}H spin systems, interrupted by a ketone functionality (C-5, δ_C 214.8). The ^{1}H-^{1}H COSY spectrum revealed a spin system ranging from 1-H_3 to 4-H_2, including the hydroxylated 3-H (δ_H 3.85), and from 6-H to 16-H_3 and 7-H_2. 4-H_2, 6-H, 16-H_3 and 7-H_2 displayed heteronuclear long range correlations to the ketone carbon C-5 and thus connected the partial structures that were deduced from ^{1}H coupling data. Heteronuclear long range correlations also cleared the connection of 7-CH_2 to C-8 of the aromatic ring. For compound **6** the name marilone F is suggested.

The molecular formula of **7** was deduced by accurate mass measurement (HRESIMS) to be $C_{11}H_{12}O_4$, requiring six sites of unsaturation. Spectroscopic data clearly suggested, that compound **7** shares the penta-substituted aromatic ring with compounds **1**-**6**. The *sp*^{3} methine 1-CH displayed a ^{13}C NMR resonance signal typical for a carbon bound to

oxygen (δ_C 67.1) and showed ^{1}H-^{1}H coupling with 9-H_2 (J = 6.5 and 1.6 Hz). 1-H had heteronuclear long range correlations with C-2, C-3 and C-7 of the aromatic ring, suggesting that it is connected to C-2 of the aromatic moiety. All of the protons, 1-H, 6-H and 9-H_2 had heteronuclear long range couplings to a carbonyl carbon (C-8, δ_C 206.4), which is thus connected to C-7 of the aromatic ring. Thus, in **7** the second ring is not heterocyclic, and cyclisation during biosynthesis probably involved the C-11 methyl carbon of **1** to give the methylene group 9-CH_2 in **7**. For compound **7** the name marilone G is suggested.

The molecular formula of **8** was deduced by accurate mass measurement (HREIMS) to be $C_8H_{10}O_3$, requiring four sites of unsaturation. The ^{13}C NMR and DEPT135 spectra included eight resonances, i.e. two for methyl, one for a sp^2 methine, and one further resonance for a sp^3 methylene group. Further four resonances were due to quaternary carbons, which thus made up half of the carbons encountered in the molecule (see compound spectroscopic data). The methyl protons 7-H_3 coupled with 6-H_2 (J = 7.5 Hz) as evident from ^{1}H NMR data, and both had heteronuclear long range correlations with C-5, the latter being a quaternary carbon connected to oxygen (δ_C 164.9). The methyl group 8-CH_3 had heteronuclear long range correlations with C-1, C-2 and C-3, and was assigned at C-2 (δ_C 98.2). C-3 was characterized by a downfield shifted carbon resonance, which indicated it to be connected to oxygen (δ_C 165.6). The HMBC correlations of 4-H and 8-H_3 to C-3 placed this hydroxylated quaternary carbon between C-2 and C-4. The quaternary carbon C-1 (δ_C 166.0) was identified as being part of a carboxylic functionality, also evidenced by an IR absorption at 1645 cm^{-1}. Consideration of the molecular formula required compound **8** to be monocyclic. Thus, C-1 was connected to C-5 through an oxygen atom forming a six-membered lactone ring. We propose the trivial name marilone H for compound **8**, which is already described as a synthetic compound (Suzuki *et al.*, 1973).

Spectroscopic data of **9** were determined to be identical to those of silvaticol (see Appendix – Spectroscopic data supporting information and Kawahara *et al.*, 1988).

The molecular formulae of **10** and **11** were deduced by accurate mass measurement (HREIMS) and found to be identical, i.e. $C_{23}H_{34}O_5$, requiring seven degrees of unsaturation. The ^{13}C NMR and DEPT135 spectra contained 23 carbon resonances,

including eight resulting from methyl, three from sp^2 methines, one from a sp^3 methine and three from methylene groups, whereas eight resonances were assigned to quaternary carbons. 1D and 2D NMR spectroscopic data of both compounds revealed that the penta-substituted aromatic ring and the substituents at C-3, C-4 and C-5 were identical to those in **1** and **3** (Tables 1, 2 andAppendix – Complete 2D NMR data).

Compounds **10** and **11** have the same planar structure, but differ in stereochemistry. For clarity in the description of the structure elucidation, only the spectroscopic data of **10** will be described initially. The NMR spectra revealed signals for three methoxyl groups 9-OCH_3, 12-OCH_3 and 13-OCH_3 (δ_C at 59.8, 49.7 and 54.2, respectively). Heteronuclear long range correlations from 12-H_3 and 13-H_3 to C-8 and C-1, respectively allowed to locate the methoxyl moieties at the respective carbons. The carbons C-1 (δ_C at 105.4) and C-8 (δ_C at 111.4) displayed strongly downfield shifted resonances for sp^3 carbons, indicating that both of them were connected to two oxygen atoms.

The methine proton 1-H, had heteronuclear long range correlations to C-3, C-7 and C-8, making the presence of a furan ring with a ketal and an acetale functionality most likely. HMBC couplings from 11-H_3 with C-7 and C-8 connected this methyl group to C-8. Differences between **10** and **11** were established to be related to the configuration at C-8. This was evident from different NOE interactions. Namely, in **10** the protons of the methyl group 11-CH_3 had a NOE correlation with 13-OCH_3, whilst 12-OCH_3 at C-8 had a NOE correlation with 1-H. In **11** the NOE correlations were the opposite, i.e. 11-CH_3 correlates with 1-H and 13-OCH_3 correlates with 12-OCH_3 (see Figure 2).

Initially, it seemed likely, that compounds **10** and **11** are artifacts of compound **1,** probably produced during extraction and isolation by methanolysis. However, heating of compound **1** for two hours at 50 ºC in methanol did not produce **10** and **11**. For compounds **10** and **11** the names marilone I and J are suggested, respectively.

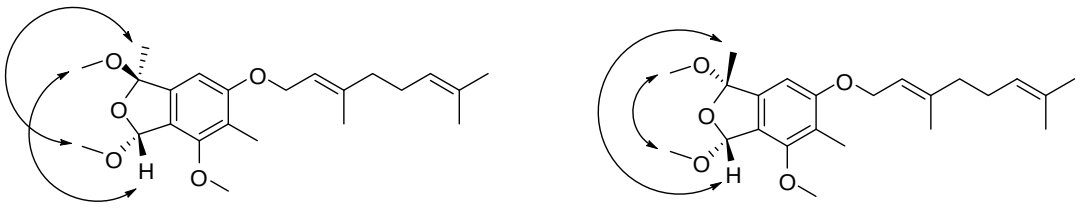

(3) (4)

Figure 2. Key NOE correlations for compounds **10** and**11**

Table 1. ^{13}C-NMR spectroscopic data for compounds **1**, **2**, **3**, **10** and **11**.

	1	**3**	**10**	**11**	**2**
position	δ_C, mult.[a, b]	δ_C, mult.[a, b]	δ_C, mult.[a, b]	δ_C, mult.[a, b]	δ_C, mult.[a, b]
1	168.2, qC	68.9, CH_2	105.4, CH	104.8, CH	168.2, qC
2	110.0, qC	128.4, qC	121.4, qC	121.5, qC	109.1, qC
3	158.0, qC	153.9, qC	154.8, qC	154.9, qC	158.9, qC
4	120.4, qC	124.8, qC	119.0, qC	119.2, qC	118.8, qC
5	164.2, qC	159.7, qC	160.4, qC	160.4, qC	163.2, qC
6	100.8, CH	102.0, CH	100.2, CH	100.2, CH	103.6, CH
7	154.2, qC	125.8, qC	141.7, qC	141.3, qC	153.9, qC
8	77.0, CH	171.1, qC	111.4, qC	110.8, qC	76.6, CH
9	62.1, CH_3	59.3, CH_3	59.8, CH_3	59.8, CH_3	62.0, CH_3
10	8.8, CH_3	9.8, CH_3	9.3, CH_3	9.3, CH_3	8.6, CH_3
11	20.9, CH_3		28.1, CH_3	27.8, CH_3	21.0, CH_3
12			49.7, CH_3	50.5, CH_3	
13			54.2, CH_3	55.5, CH_3	
1'	66.5, CH_2	66.4, CH_2	66.1, CH_2	66.2, CH_2	
2'	120.1, CH	120.5, CH	120.8, CH	120.9, CH	
3'	142.1, qC	141.6, qC	141.1, qC	141.1, qC	
4'	40.1, CH_2	40.1, CH_2	40.1, CH_2	40.1, CH_2	
5'	26.9, CH_2	26.9, CH_2	27.0, CH_2	27.0, CH_2	
6'	124.6, CH	124.6, CH	124.6, CH	124.7, CH	
7'	132.1, qC	132.1, qC	132.0, qC	132.0, qC	
8'	25.8, CH_3	25.8, CH_3	25.8, CH_3	25.8, CH_3	
9'	16.7, CH_3	16.7, CH_3	16.6, CH_3	16.7, CH_3	
10'	17.7, CH_3	17.7, CH_3	17.7, CH_3	17.7, CH_3	

[a]Acetone-d_6 (**1, 2, 3, 10, 11**), 75.5 MHz. [b]Implied multiplicities determined by DEPT.

Table 2. ^{1}H-NMR spectroscopic data for compounds **1**, **2**, **3**, **10** and **11**.

	1	**3**	**10**	**11**	**2**
position	δ_H[a, b] (*J* in Hz)	δ_H[a, b] (*J* in Hz)	δ_H[a, b] (*J* in Hz)	δ_H[a, b] (*J* in Hz)	δ_H[a, b] (*J* in Hz)
1		5.50, s	6.32, s	6.02, s	
2					
3					
4					
5					
6	6.95, s	7.03, s	6.60, s	6.59, s	6.75, s
7					
8	5.43, q (6.6)				5.37, q (6.6)
9	3.98, s	3.96, s	3.90, s	3.89, s	3.98, s
10	2.09, s	2.15, s	2.07, s	2.06, s	2.10, s
11	1.54, d (6.6)		1.62, s	1.55, s	1.48, d (6.6)
12			2.85, s	2.94, s	
13			3.38, s	3.50, s	
1'	a: 4.69, dd (6.6, 12.1) b: 4.74, dd (6.6, 12.1)	4.71, d (6.6)	4.64, d (6.6)	4.63, d (6.6)	
2'	5.52, t (6.6)	5.51, t (6.6)	5.48, t (6.6)	5.48, t (6.6)	
3'					
4'	2.10, m	2.10, m	2.08, m	2.07, m	
5'	2.13, m	2.14, m	2.11, m	2.11, m	
6'	5.09, m	5.10, m	5.11, m	5.10, m	
7'					
8'	1.63, br s	1.63, br s	1.64, br s	1.64, br s	
9'	1.76, br s	1.78, br s	1.75, br s	1.75, br s	
10'	1.58, br s	1.58, br s	1.59, br s	1.58, br s	

[a]Acetone-d_6 (**1, 2, 3, 10, 11**), 300 MHz. [b] Assignments are based on extensive 1D and 2D NMR experiments (HMBC, HSQC, COSY).

Table 3. 1D and 2D NMR spectroscopic data for compound **6**

position	δ_C, mult.[a, b, e]	δ_H[a, b] (*J* in Hz)	COSY[a, c]	HMBC[a, d]
1	10.1, CH_3	0.85, t (7.3)	2	2, 3
2	30.6, CH_2	1.35, m	1, 3	1, 3
3	69.4, CH	3.85, m	2, 4	1
4	49.5, CH_2	a :2.41, dd (4.4, 16.5)	3, 4b	2, 3, 5
		b: 2.51, m	4a	2, 3, 5
5	214.8, qC			
6	48.1, CH	2.87, m	7a, 7b, 16	5, 7, 8, 16
7	29.8, CH_2	a: 2.81, m	6, 7b	5, 6, 8, 9, 13, 16
		b: 2.53, m	6, 7a	5, 6, 8, 9, 13, 16
8	122.1, qC			
9	159.2, qC			
10	115.6, qC			
11	155.6, qC			
12	111.5, CH	6.51, s		8, 10, 11, 14
13	141.9, qC			
14	26.3, CH_2	2.52, m	15	8, 12, 13, 15
15	15.8, CH_3	1.10, t (7.5)	14	13, 14
16	15.9, CH_3	0.94, d (6.7)	6	5, 6, 7
17	60.4, CH_3	3.65, s		9
18	9.4, CH_3	2.08, s		9, 10, 11

[a]Acetone-d_6, 300/75.5 MHz. [b] Assignments are based on extensive 1D and 2D NMR experiments (HMBC, HSQC, COSY). [c] Numbers refer to proton resonances. [d] Numbers refer to carbon resonances. [e] Implied multiplicities determined by DEPT.

Table 4. ^{13}C-NMR spectroscopic data for compounds **4** and **5**

	4	**5**
position	δ_C, mult.[a, b]	δ_C, mult.[a, b]
1	66.1, CH_2	66.9, CH_2
2	119.6, qC	120.3, qC
3	159.3, qC	160.0, qC
4	116.1, qC	117.5, qC
5	157.1, qC	157.9, qC
6	108.5, CH	111.6, CH
7	147.2, qC	141.4, qC
8	65.9, CH	62.6, CH_2
9	61.8, CH_3	62.2, CH_3
10	9.1, CH_3	9.2, CH_3
11	57.8, CH_3	58.1, CH_3
12	25.4, CH_3	

[a] Acetone-d_6 (**4**), MeOD (**5**), 75.5 MHz. [b]Implied multiplicities determined by DEPT.

Table 5. ^{1}H-NMR spectroscopic data for compounds **4** and **5**

	4	**5**
position	$\delta_H{}^a$ (*J* in Hz)	$\delta_H{}^a$ (*J* in Hz)
1	a: 4.39, d (9.9) b: 4.43, d (9.9)	4.53, s
2		
3		
4		
5		
6	6.91, s	6.77, s
7		
8	5.06, q (6.3)	4.64, s
9	3.67, s	3.74, s
10	2.09, s	2.15, s
11	3.32, s	3.42, s
12	1.33, d (6.3)	

[a]Acetone-d_6 (**4**), MeOD (**5**), 300 MHz.

Stereochemistry

Compounds **1**, **2** and **4** possess a single chiral center at C-8. The measurement of the specific optical rotation for these compounds yielded values close to zero, and furthermore, the CD measurements showed hardly any CD effect for the referred compounds. The latter was expected at around 260 nm due to the proximity of the chiral center to the chromophoric penta-substituted benzene ring. We thus assumed the presence of racemic mixtures for these chiral compounds. Extensive trials to separate the enantiomers employing three different HPLC chiral stationary phases were performed, but unsuccessful. However, the presence of racemic mixtures was proven for the analogous, nitrogen-containing compounds, i.e. ptthalimidine derivatives isolated from the same fungus (Almeida *et al.*, unpublished data).

The chiral centre C-1 in compound **7** also seems to be present in *R* and *S* configuration, since measurements of optical rotation yielded values close to zero.

Biological activity

Marilones A, B and C (**1**-**3**) were tested for antiplasmodial activity, and marilone A exhibited an IC_{50} of 12.1 μM against *Plasmodium berghei* (see Appendix – Bioactivity results). Interestingly, marilone C (**3**) showed no activity at the 25 μM level, indicating that the methyl group 11-CH_3 and/or the position of the ketone functionality is essential for this bioactivity.

Marilones A, B, C, D (**1**-**4**) and I (**10**) were tested for cytotoxic activity toward three cancer cell lines (NCI-H460, MCF7 and SF268). Marilone A and C (**1**, **3**) showed weak antiproliferative activity with an average GI_{50} of 36.7 and 26.6 μM, respectively (seeAppendix – Bioactivity results).

Marilone B (**2**) and H (**8**) were assayed in a panel of 44 psychoactive receptors, including 11 serotonin receptors, and marilone B showed specific antagonistic effect on the serotonin receptor 5HT2B with a K_i value of 7.7 μM.

Marilones A, B and C were tested in protein kinases (DYRK1A and CDK5) inhibition activity assay, inhibition of the viral HIV-1 and HIV-2 induced cytopathogenic effect in MT-4 cells, in antibacterial (*Escherichia coli*, *Bacillus megaterium*), antifungal (*Mycotypha microspora*, *Eurotium rubrum*, and *Microbotryum violaceum*), and antialgal (*Chlorella fusca*) assays at the 50 μg/mL disc level, they were evaluated for

inhibition of the following panel of proteases: Chymotrypsin, trypsin, the protease elastase HLE, papain, porcine cease and acetylcholine esterase (tested at the 100 μM level) but exhibited no activity in any of these tests.

Marilones A and C were also evaluated against 3-T3-L1 murine adipocytes assay and exhibited no activity.

Marilones A and B were evaluated against three sub-types of Influenza A virus (H1N1, H5N1 and H3N2), Influenza B virus (Flu B) and exhibited no activity.

Marilone A was evaluated against the Severe Acute Respiratory Syndrome coronavirus (SARS) and Hepatitis B virus but did not show any activity.

Marilone B was evaluated against the Herpes Simplex Virus-2 (HSV-2) and the Respiratory Syncytial virus (RSV) and exhibited no activity.

Marilones A and D were further tested against two antibiotic resistant *Mycobacterium tuberculosis* strains, MTB72 and R46 (tested at the 50 μg/mL disc level), but did not show any relevant activity.

Marilones C, G and H were tested in a panel of anti-diabetic activity assays: PPAR ligand assay, PPAR co-activator assay, PTP-1B inhibitor assay and glucose uptake assay (both 3T3-l1 cells and primary rat/mouse adipocytes, tested at the 100 μM dose), but did not show any activity.

Marilones C, G, H and E were tested for the inhibition of the NF-kB protein complex assay (at the 100 μM), but did not show any activity.

Discussion

Similar molecules and biosynthesis

Phthalide derivatives are compounds of the polyketide metabolism, which are common in nature (Lin *et al.*, 2005). Secondary metabolites **1** and **2** discovered in the marine-derived *Stachylidium* sp. were found to be derivatives of the natural product nidulol, whilst compound **3** was a derivative of silvaticol (**9**) (see Appendix – Spectroscopic data supporting information), formerly described from the fungus *Aspergillus silvaticus* (Kawahara *et al.*, 1988). Nidulol and silvaticol (**9**) are regioisomeric compounds and differ in terms of the position of the carbonyl group, which either is placed *peri* to the aromatic hydrogen as in **3** and **9**, or it is *peri* positioned to the aromatic methoxyl moiety, e.g. in **1** and **2**. The here investigated *Stachylidium* species is thus able to

produce both types of phthalides, which are suspected to differ significantly in terms of their biosynthesis (Figure 3).

Whereas compound **3** is simply the O-prenylated form of silvaticol (**9**), the nidulol derivatives **1** and **2** are distinguished by an additional methyl substituent (11-CH_3) at C-8. In terms of biosynthesis, i.e. polyketide metabolism, this substitution is most unusual and unique amongst all the known phthalides. The non-phthalide compounds of the *Stachylydium* metabolites, i.e. **4**, **6-8**, also share this structural characteristic of an additional carbon atom (C-12 in **4**, C-15 in **6**, C-9 in **7**, C-7 in **8**), which is hard to explain by the usual fungal polyketide metabolism.

Biosynthetic studies focusing on phthalide structures, e.g. for mycophenolic acid (Bedford *et al.* 1973), nidulol and silvaticol (Ayer and Racok, 1990), were previously performed by means of feeding experiments with labeled precursors, evidencing the tetraketide nature of the phthalide nucleus (Figure 2). Compounds **1-7**, possess a basic skeleton which is related to that of the well known tetraketide 3-methyl-orsellinic acid (Geris and Simpson, 2009). Closing of the lactone ring would for compounds **1** and **2** require the oxidation of C-8 to obtain a hydroxy group, which subsequently could form a lactone with the C-1 carboxyl group (Figure 3A). In contrast to that for **3** and **9**, a reduction of the C-1 carboxyl group to an alcoholic function and an oxidation of C-8 to a carboxylic function would be required (Figure 3B).

Most intriguing however is, that in compounds **1**, **2**, **4**, **6** and probably also **7** the acetate-derived methyl group 8-CH_3 in the methyl orsellinic acid precursor would be replaced by an ethyl group (Figure 3). Thus, biosynthesis seems to require either, a propionate starter unit (see C in Figure 3) or a methylation (e.g. via a SAM-dependent methyl-transferase) at C-8 (see D in Figure 3). A third possibility would be the loss of a carbon atom from a pentaketide intermediate (not depicted in Figure 3). To our knowledge, to date these types of reactions are not known in fungal polyketide metabolism. Feeding experiments are under way in order to determine the building blocks for these most unusual molecules.

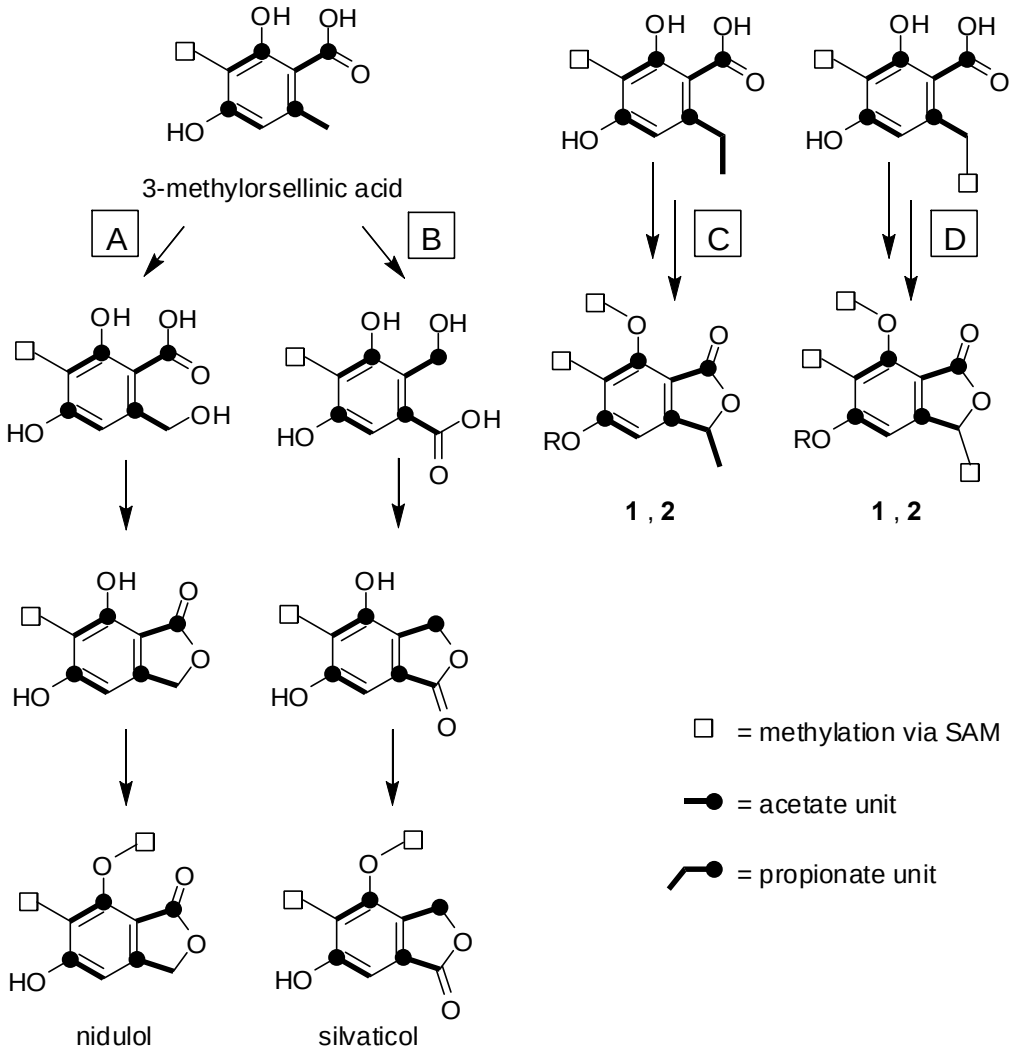

Figure 3. Tetraketide nature of the phthalides nidulol (A) and silvaticol (B), and hypothetical biosynthetic pathways (C, D) for marilones A and B (**1**, **2**).

It is worthwhile to mention that marilones were produced solely on solid biomalt medium (BMS) supplemented with sea salt, whereas in other media such as Czapek or YPM no phthalides were formed.

Experimental Section

General Experimental Procedures. See chapter 3 - General methodology.

Fungal material. As described in chapter 3 - General methodology.

Cultivation, extraction and isolation. Compounds **1**-**9** were isolated from a 60 days culture (12 L) of *Stachylidium* sp. on an agar-biomalt medium supplemented with sea salt (BMS). An extraction with 5 L EtOAc yielded 5.9 g of extract which was subjected to a VLC fractionation in an open column using silica as solid phase and a gradient solvent system with petroleum ether - acetone of 10:1, 5:1, 2:1, 1:1, 100 % acetone and 100 % MeOH, resulting in six VLC fractions. Compounds **10** and **11** were isolated from a second 10 L culture on BMS (cultivation time: 60 days), from which 1.0 g extract was obtained.

Compounds **1** and **3** were isolated from VLC fraction 1. VLC fraction 1 was fractionated using petroleum ether – acetone 90:1 and 10:1 in order to eliminate fatty acid content of the sample. The VLC fraction 10:1 was subjected to NP-HPLC fractionation using petroleum ether – acetone 30:1 to yield a mixture of both compounds (sub-fraction 4 of 7). Further fractionation using MeOH - H_2O 8:2 (RP-HPLC, Isis column) yielded compound **1** (sub-fraction 1 of 2; 19 mg, t_R 13 min) and compound **3** (sub-fraction 2 of 2; 14.2 mg, t_R 15 min).

Compounds **2** and **9** were isolated from VLC fraction 2, followed by NP-HPLC fractionation using PE-acetone 11:1 to yield a mixture of both compounds (fraction 6 of 7). Further fractionation using 40 % MeOH / 60 % H_2O (RP-HPLC, Isis column) yielded compound **2** (fraction 1 of 2; 5.2 mg, t_R 35 min) and the know compound **9**, silvaticol (fraction 2 of 2; 5.6 mg, t_R 38 min).

Compound **4** was isolated from VLC fraction 3, followed by NP-HPLC fractionation using petroleum ether - acetone 5:1 (fraction 4 of 10). This sub-fraction was further purified using 50 % MeOH / 50 % H_2O (RP-HPLC, Isis column; fraction 2 of 4, 4.2 mg, t_R 10 min).

Compound **5** was isolated from VLC fraction 3, followed by NP-HPLC fractionation using petroleum ether - acetone 5:1 (fraction 7 of 10). This sub-fraction was further purified using 50 % MeOH / 50 % H_2O (RP-HPLC, Isis column; fraction 2 of 4, 4 mg, t_R 3 min).

Compound **6** was isolated from VLC fraction 2, followed by NP-HPLC fractionation using petroleum ether - acetone 11:1 (fraction 3 of 7). This sample was further fractionated with 90 % MeOH / 10 % H_2O (RP-HPLC, Isis column, fraction 2 of 4, 1.5 mg, t_R 15 min)

Compound **7** was isolated from VLC fraction 3, followed by NP-HPLC fractionation using petroleum ether - acetone 5:1 (fraction 9 of 10). This sub-fraction was further

purified using 50 % MeOH / 50 % H_2O (RP-HPLC, Isis column; fraction 1 of 4). Finally we reached purification using 30 % MeOH / 70 % H_2O (RP-HPLC, Isis column, fraction 6 of 6, 2.5 mg, t_R 14 min).

Compound **8** was isolated from VLC fraction 3, followed by NP-HPLC fractionation using petroleum ether - acetone 5:1 (fraction 3 of 10). This sub-fraction was further separated using petroleum ether - acetone 13:1 (fraction 3 of 4), which was finally purified with 40 % MeOH / 60 % H_2O using RP-HPLC (fraction 2 of 2, 5.8 mg, t_R 12 min).

Compounds **10** and **11** were isolated in a second culture in the same procedures as for compounds **1** and **2**, except the last RP-HPLC fractionation which was performed with 85 % MeOH /15 % H_2O (compound **10**, sub-fraction 1 of 2; 1.6 mg, t_R 9 min and compound **11**, sub-fraction 2 of 2; 1.7 mg, t_R 11 min).

In two other cultures of the same fungus in the same medium (2 months; 40 days), only marilone A and marilone C were detected (both in quantities lower than 2.5 mg).

Marilone A (1): transparent oil (1.6 mg/L, 0.32 %); UV λ_{max} (MeOH)/nm: 219 (log ε 4.38), 261 (log ε 2.95); IR (ATR) ν_{max} 2964, 1745, 1603 cm^{-1}; ^1H NMR and ^{13}C NMR (Tables 1 and 2); LREIMS *m/z* 344.2 $(M)^+$; HREIMS calcd. for $C_{21}H_{28}O_4$ $(M)^+$ *m/z* 344.1988, found 344.1996.

Marilone B (2): white amorphous solid (0.4 mg/L, 0.09 %); UV λ_{max} (MeOH)/nm: 215 (log ε 4.09), 260 (log ε 2.83); IR (ATR) ν_{max} 3238 (br), 2931, 1708, 1601 cm^{-1}; ^1H NMR and ^{13}C NMR (Tables 1 and 2); LREIMS *m/z* 208.1 $(M)^+$; HREIMS calcd. for $C_{11}H_{12}O_4$ $(M)^+$ *m/z* 208.0736, found 208.0737.

Marilone C (3): transparent oil (1.3 mg/L, 0.27 %); UV λ_{max} (MeOH)/nm: 223 (log ε 4.10), 255 (log ε 2.80); IR (ATR) ν_{max} 2921, 1760, 1619 cm^{-1}; ^1H NMR and ^{13}C NMR (Tables 1 and 2); LREIMS *m/z* 330.2 $(M)^+$; HREIMS calcd. for $C_{20}H_{26}O_4$ $(M)^+$ *m/z* 330.1831, found 330.1833.

Marilone D (4): white amorphous solid (350 µg/L, 0.068 %); UV λ_{max} (MeOH)/nm: 212 (log ε 4.04), 226 (log ε 3.82), 271 (log ε 3.27); IR (ATR) ν_{max} 3338 (br), 2929, 1610, 1458, 1414 cm^{-1}; ^{1}H NMR and ^{13}C NMR (Tables 3 and 4); LRESIMS *m/z* 224.9 $(M-H)^-$; HRESIMS calcd. for $C_{12}H_{18}O_4Na$ $(M+Na)^+$ *m/z* 249.1097, found 249.1101.

Marilone E (5): white amorphous solid (333 µg/L, 0.068 %); UV λ_{max} (MeOH)/nm: 210 (log ε 4.25), 229 (log ε 3.94), 276 (log ε 3.18); IR (ATR) ν_{max} 3347 (br), 2929, 1602, 1457, 1418 cm^{-1}; ^{1}H NMR and ^{13}C NMR (Tables 3 and 4); LRESIMS *m/z* 211.1 $(M-H)^-$; HRESIMS calcd. for $C_{11}H_{16}O_4Na$ $(M+Na)^+$ *m/z* 235.0941, found 235.0948.

Marilone F (6): white amorphous solid (125 µg/L, 0.025 %); $[\alpha]_D^{23}$ -33 (*c* 0.1, MeOH); UV λ_{max} (MeOH)/nm: 206 (log ε 4.14), 275 (log ε 3.12); IR (ATR) ν_{max} 3361 (br), 2929, 1702, 1609, 1457, 1407 cm^{-1}; ^{1}H NMR and ^{13}C NMR (Table 5); LRESIMS *m/z* 307.6 $(M-H)^-$, *m/z* 309.5 $(M+H)^+$; HRESIMS calcd. for $C_{18}H_{28}O_4Na$ $(M+Na)^+$ *m/z* 331.1880, found 331.1886.

Marilone G (7): white amorphous solid (208 µg/L, 0.042 %); UV λ_{max} (MeOH)/nm: 220 (log ε 4.17), 266 (log ε 3.73); IR (ATR) ν_{max} 3268 (br), 2930, 1697, 1605 cm^{-1}; ^{1}H NMR (MeOD): 1-H: δ 5.54, dd (1.6, 6.5); 6-H: δ 6.87, s; 9-H_a: 3.08, dd (6.5, 19.1); 9-H_b: 2.50, dd (1.6, 19.1); 10-H_3: 4.01, s; 11-H_3: 2.23, s; ^{13}C NMR (MeOD): CH-1, δ 67.1; qC-2, δ 139.4; qC-3, δ 158.4; qC-4, δ 128.1; qC-5, δ 159.8; qC-6, δ 103.3; qC-7, δ 137.2; qC-8, δ 206.4; CH_2-9, δ 48.4; CH_3-10, δ 61.1; CH_3-11, δ 10.0; (2D NMR in Appendix – Complete 2D NMR data); LRESIMS *m/z* 206.9 $(M-H)^-$; HRESIMS calcd. for $C_{11}H_{11}O_4$ $(M-H)^-$ *m/z* 207.0652, found 207.0650.

Marilone H, 5-ethyl-3-hydroxy-2-methyl-pyran-1-one (8): amorphous solid (0.483 ug/L, 0.098 %); UV λ_{max} (MeOH)/nm: 207 (log ε 4.05), 285 (log ε 3.69); IR (ATR) ν_{max} 3330 (br), 2929, 2674, 1645, 1578 cm^{-1}; ^{1}H NMR (acetone-d_6): 4-H: δ 6.02, s; 6-H_2: δ 2.42, q (7.5); 7-H_3: δ 1.13, t (7.5); 8-H_3: δ 1.81, s; ^{13}C NMR (acetone-d_6): qC-1, δ 166.0; qC-2, δ 98.2; qC-3, δ 165.6; CH-4, δ 99.1; qC-5, 164.9; CH_2-6, δ 27.1; CH_3-7, δ 11.3; CH_3-8, δ 8.5; (2D NMR in Appendix – Complete 2D NMR data); LRESIMS *m/z* 153.1 $(M-H)^-$, HREIMS calcd. for $C_8H_{10}O_3$ $(M)^+$ *m/z* 154.0630, found 154.0628.

Marilone I (10): white amorphous solid (160 µg/L, 0.084 %); UV λ_{max} (MeOH)/nm: 214 (log ε 4.09), 272 (log ε 2.98) IR (ATR) ν_{max} 2930, 1610, 1463 cm^{-1}; ^{1}H NMR and ^{13}C NMR (Tables 1 and 2); LREIMS *m/z* 330.2 $(M)^{+}$; HREIMS calcd. for $C_{23}H_{34}O_5$ $(M)^{+}$ *m/z* 390.2406, found 390.2417.

Marilone J (11): white amorphous solid (170 µg/L, 0.089 %); UV λ_{max} (MeOH)/nm: 214 (log ε 4.10), 272 (log ε 2.98); IR (ATR) ν_{max} 2925, 1610, 1464 cm^{-1}; ^{1}H NMR and ^{13}C NMR (Tables 1 and 2); HREIMS calcd. for $C_{23}H_{34}O5$ $(M)^{+}$ *m/z* 390.2406, found 390.2412.

Methodology for the performed biological assays. As described in chapter 3 - General methodology.

6. Stachylines A – D from the Sponge-derived Fungus *Stachylidium* sp.

Abstract

The marine-derived fungus *Stachylidium* sp. was isolated from the sponge *Callyspongia* cf. *C. flammea.* Four new, putatively tyrosine-derived and O-prenylated natural products, stachylines A – D (**1** – **4**), were obtained from the fungal extract. The structures of **1** – **4** were elucidated based on extensive spectroscopic analyses. The absolute configuration of compound **2** was established by Mosher's method. Stachyline A (**1**) possesses a rare terminal oxime group and occurs as an interchangeable mixture of *E*/*Z*- isomers.

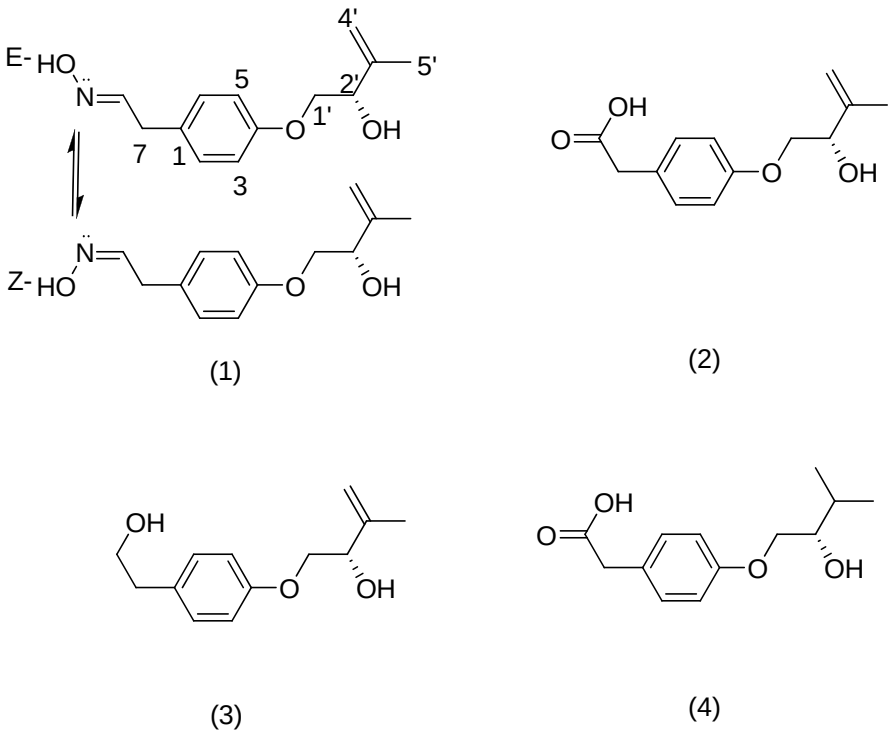

Figure 1. Structure formulae of Compounds **1 - 4**

Introduction

The marine environment harbours approximately half of the global biodiversity and is estimated to contain between 3 and 500 million different species, offering an almost infinite resource for novel compounds (Tziveleka *et al.*, 2003). Among these organisms marine-derived fungi became known as prolific producers of structurally most intriguing compounds (Bhadury *et al.*, 2006). In general, tyrosine derivatives have only rarely been reported from fungi, and in most cases such compounds were obtained from strains originating from environmentally extreme habitats, e.g. tyrosol carbamate which was isolated from the deep-water fungus *Arthrinium* sp. (Sashidhara *et al.*, 2009). *Phytomyces* sp., producing O-prenylated tyrosine derivatives, is an extremophile collected from an acid mine waste rich in toxic metals (Stierle *et al.*, 2003). Another unusual case is aspergillusol A, an α-glucosidase inhibitor obtained from the sponge-derived fungus *Aspergillus aculeatus* which is reported to be the only known fungal tyrosine derivative to possess an oxime group (Ingavat *et al.*, 2009).
Secondary metabolites with an oxime substituent are rare, and most of the reported examples have potent bioactivity, e.g. the actinomycete-derived nocardicins displayed strong antibiotic activity (Hashimoto *et al.*, 1976), and brevioxime from *Penicillium brevicompactum* inhibited the biosynthesis of insect juvenile hormones (Amade *et al.*, 1993). *P. olsonii* produced 2-(4-hydroxyphenyl)-2-oxoacetaldehyde oxime (PHBA) which regenerated phosphorylated cholinesterase (Moya *et al.*, 1997). The oxime geometrical isomers collismycins A and B were isolated from *Streptomyces* sp. MQ22 which inhibited dexamethasone glucocorticoid receptor binding (Shindo *et al.*, 1994).

During our search for new cytotoxic natural products an extract of the marine-derived fungus *Stachylidium* sp. was found to be active. During chromatographic separations it became clear that this fungus produces a vast array of secondary metabolites with intriguing structural features, among them the four novel, putatively tyrosine-derived and O-prenylated natural products, stachylines A – D (**1 - 4**). Stachyline A (**1**) is distinguished by an oxime terminal group, probably derived through biosynthetic reactions similar to those known for cyanogenic glycosides and nocardicin A formation (Cimino *et al.*, 1975; Isaaki *et al.*, 1993; Bjarnholt and Møller, 2008; Kelly and Townsend, 2002; Kelly and Townsend, 2002). The molecules were evaluated in a number of biological assays, to date however no considerable activity was detected.

Results

The RP-18 HPLC chromatogram of **1** contained two peaks (ratio 1:1), which when re-injected after their individual isolation, again resulted in the same chromatogram. This result suggested that compound **1** exists as a mixture of interchangeable isomers. NMR spectra also presented two sets of data, one for each isomer (see Tables 1 and 2). For clarity in the description of the structure elucidation, only one set of data will be considered initially.

The molecular formula of **1** was deduced by accurate mass measurement (HREIMS/HRESIMS) to be $C_{13}H_{17}NO_3$, requiring six sites of unsaturation. The ^{13}C NMR and DEPT135 spectra showed the presence of thirteen resonances for one methyl, five sp^2 methine, one sp^3 methine, one sp^2 methylene, two sp^3 methylene groups and three quaternary carbons (see Tables 1 and 2). The UV maximum at 276 nm indicated the presence of an aromatic moiety, whereas an IR absorption at around 3300 cm^{-1} arose from a hydroxy group in the molecule.

^1H NMR and ^1H-^{13}C HSQC data (see Tables 1 and 2) included two resonances for magnetically equivalent protons, i.e. H-2/H-6 and H-3/H-5 resonating at δ_H 7.17 and 6.88, respectively. This spectroscopic feature was interpreted as characteristic for a *para*-substituted aromatic ring. From the same spectra the presence of an exomethylene moiety, CH_2-4', was evident (δ_H 4.89, 5.08; δ_C 112.1). The ^{13}C NMR spectrum showed two resonances for carbons connected to oxygen atoms, namely at δ_C 72.1 (C-1') and 73.9 (C-2') (see Table 1), and the protons attached to these carbon atoms, H_2-1' and H-2' were coupled as evidenced by ^1H-^1H COSY correlations. ^1H-^1H COSY correlations indicated the presence of another spin system between H_2-4' and H_3-5'. The partial structures deduced from these two spin systems were connected making use of ^1H-^{13}C HMBC correlations. Thus, correlations from H_3-5' to C-2', C-3' and C-4' delineated an unsaturated and hydroxylated isoprene unit (see Appendix – Complete 2D NMR data). This was confirmed by further heteronuclear long range correlations from H_2-4' to C-3' and C-2'. ^1H-^{13}C HMBC correlations between H-1' to qC-4 showed that the isoprene unit was connected via C-4 to the *para*-substituted aromatic moiety. Due to the downfield shift of C-1' and C-4 (δ_C 72.1, 158.5) connection of both parts of the molecule occurred through an oxygen atom.

According to the molecular formula, the second substituent on the aromatic ring of **1** must have the composition C_2H_4NO. ^{1}H-^{13}C HMBC correlations could be detected from the aromatic protons H-2/H-6 to the methylene carbon C-7, making the connection of the second side chain via C-1 most likely. Through an ^{1}H-^{1}H COSY experiment, the methylene protons CH_2-7 were shown to be part of a spin system including H-8 (δ_H 6.73), whereby the latter was bound to an sp^2 hybridized carbon. The remaining presence of a nitrogen, oxygen and proton atom was assigned to an unusual oxime moiety (see Tables 1 and 2). The latter is known to be able to adopt interchangeable configurations (Tennant *et al.*, 1979). *E*- and *Z*- isomers in the case of **1** presented clearly distinguishable NMR shifts for the C-8 to C-2/C-6 part of the molecules (see Tables 1 and 2). The assignment of NMR shifts for the *E*- and *Z*- isomers was supported using the ACD NMR predictor software (ACD/Labs®). The configuration at C-2' of compound **2** was found to be *S* as deduced by Mosher's method. Based on the negative optical rotation of compound **1**, which was also observed for **2**, and the close biosynthetic relationship between both compounds, the *S* configuration is also proposed for C-2' of **1** (see Figure 2). For compound **1** the trivial name *E*- and *Z*-stachyline A is proposed.

The molecular formula of **2** was deduced by accurate mass measurement (HREIMS) to be $C_{13}H_{16}O_4$, requiring six sites of unsaturation. The ^{13}C and ^{1}H NMR spectra were closely related to those of compound **1** (see Table 2). One of the substituents on the aromatic ring was again an O-prenyl moiety as in **1**, also connected via qC-4 and C-1' (see Tables 1, 2 and Appendix – complete 2D NMR data). The second substituent on the aromatic ring of **2** was however, different and established by interpretation of ^{1}H-^{13}C HMBC long range correlations. Thus, the methylene protons H_2-7 had a heteronuclear coupling with C-2 and C-6 of the aromatic ring. Additionally, H_2-7 had HMBC long range correlations to the quaternary carbon C-8, which according to its characteristic ^{13}C NMR resonance was part of a carboxylic acid group (δ_C 173.0). Compound **2** was thus an O-prenylated phenyl acetic acid.

The absolute configuration at C-2' was determined by modified Mosher's method. The evaluation of the corresponding ^{1}H-^{13}C HSQC NMR spectra revealed differences of the proton shifts between the (*S*)- and (*R*)-MTPA esters (see Figure 2 and Appendix – complete 2D NMR data). The calculated differences in chemical shifts [δ of protons in the (*S*)-MTPA-ester minus δ of the corresponding protons in the (*R*)-MTPA-ester] led to the assignment of the (*S*)-absolute configuration for C-2′. Since compounds **1** - **4** all

showed a negative specific optical rotation, it was assumed that they all share the (*S*-) configuration at C-2'. Compound **2** is an O-prenylated phenyl acetic acid, for which we propose the trivial name stachyline B.

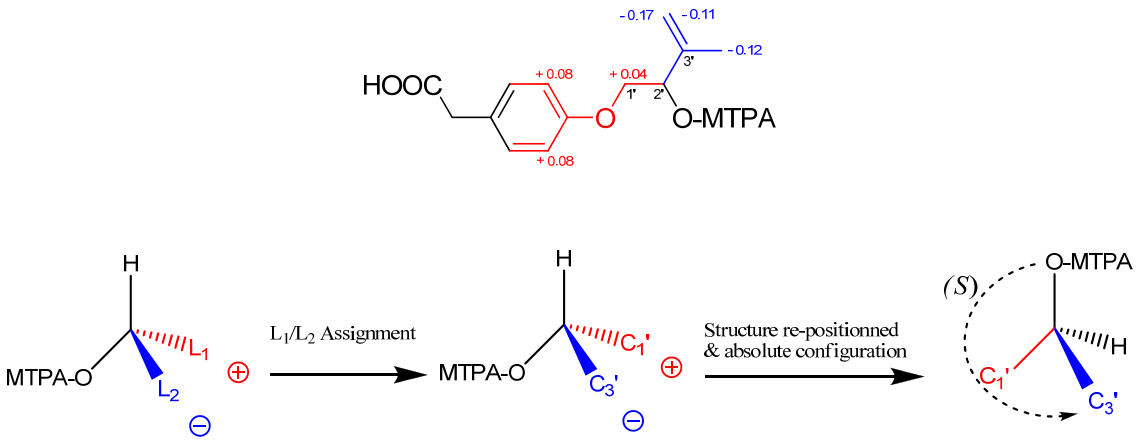

Figure 2. Deduction of the absolute configuration at C-2′ using modified Mosher's method with Δ^{S-R} values of MTPA-esters of compound 2.

The molecular formula of **3** was deduced by accurate mass measurement (HREIMS) to be $C_{13}H_{18}O_3$, requiring five sites of unsaturation. 1D and 2D NMR data of **3** were closely similar to those of **2** (see Tables 1, 2 and Appendix – Complete 2D NMR data), except for the absence of resonances for the carboxylic acid group in the ^{13}C NMR spectrum and the presence of an additional resonance for a sp^3 methylene group. The latter had a downfield shifted ^{13}C NMR resonance (δ_C 64.1), which evidenced connection to an oxygen atom. Thus, **3** can be regarded as the C-8 reduction product of **2**, for which the trivial name stachyline C is suggested.

The molecular formula of **4** was deduced by accurate mass measurement (HRESIMS) to be $C_{13}H_{18}O_4$, requiring five sites of unsaturation. 1D and 2D NMR spectroscopic data of compound **4** exhibited many identical features when compared with those of **2** (see Tables 1, 2 and Appendix – complete 2D NMR data). A difference, however concerned the exo-methylene proton signals which were absent in the ^1H NMR spectrum of **4**, whilst signals for a methyl (H_3-4', δ_H 0.97) and a methine group were present (H-3', δ_H 1.86). ^1H-^1H COSY correlations confirmed the structure, since a spin system connected all atoms within the isoprene unit from H_2-1' to H_3-5' and H_3-4' (see Table 2 and Appendix – complete 2D NMR data). For compound **4** the trivial name stachyline D is proposed.

Table 1: ^{13}C NMR Spectroscopic Data for Compounds **1 - 4**.

	1*	**2**	**3**	**4**
position	δ_C, mult.[a, b, c]	δ_C, mult.[a, b, c]	δ_C, mult.[a, b,c]	δ_C, mult.[a, b, c]
1	130.1, qC	128.0, qC	132.5, qC	127.9, qC
2	130.5, CH	131.2, CH	130.7, CH	131.2, CH
3	115.5, CH	115.3, CH	115.2, CH	115.2, CH
4	(*Z*-), 158.5, qC | (*E*-), 158.7, qC	158.8, qC	158.3, qC	159.0, qC
5	115.5, CH	115.3, CH	115.2, CH	115.2, CH
6	130.5, CH	131.2, CH	130.7, CH	131.2, CH
7	(*Z*-), 31.0, CH_2 | (*E*-), 35.4, CH_2	40.5, CH_2	39.4, CH_2	40.4, CH_2
8	(*Z*-), 150.0, CH | (*E*-), 149.7, CH	173.0, qC	64.1, CH_2	173.2, qC
1’	72.1, CH_2	72.1, CH_2	72.1, CH_2	71.6, CH_2
2’	73.9, CH	73.9, CH	74.0, CH	74.6, CH
3’	146.1, qC	146.1, qC	146.2, qC	31.6, CH
4’	112.1, CH_2	112.1, CH_2	112.0, CH_2	17.7, CH_3
5’	18.7, CH_3	18.8, CH_3	18.8, CH_3	19.4, CH_3

[a]acetone-$_{d6,}$ 75.5 MHz. [b]Assignments are based on extensive 1D and 2D NMR experiments (HMBC, HSQC, COSY, see Appendix – 2D NMR complete data). [c] Implied multiplicities determined by DEPT. *Carbon resonances were attributed to the (*Z*-) or (*E*-) configuration, according to ACD/NMR Predictor® software.

Table 2. ^{1}H NMR Spectroscopic Data for Compounds **1 - 4**.

	1*	**2**	**3**	**4**
position	$\delta_H{}^{a,b}$ (*J* in Hz)	$\delta_H{}^{a,b}$ (*J* in Hz)	$\delta_H{}^{a,b}$ (*J* in Hz)	$\delta_H{}^{a,b}$ (*J* in Hz)
1				
2	(*Z*-), 7.17, d (8.4) | (*E*-), 7.13, d (8.4)	7.20, d (8.4)	7.13, d (8.4)	7.19, d (8.4)
3	6.88, d (8.4)	6.87, d (8.4)	6.84, d (8.4)	6.87, d (8.4)
4				
5	6.88, d (8.4)	6.87, d (8.4)	6.84, d (8.4)	6.87, d (8.4)
6	(*Z*-), 7.17, d (8.4) | (*E*-), 7.13, d (8.4)	7.20, d (8.4)	7.13, d (8.4)	7.19, d (8.4)
7	(*Z*-), 3.60, d (5.5) | (*E*-), 3.39, d (6.2)	3.51, br s	2.72, t (7.1)	3.52, br s
8	(*Z*-), 6.73, t (5.5) | (*E*-), 7.40, t (6.2)		3.68, t (7.1)	
1'	a: 4.01, dd (3.7, 9.5)	a: 4.01, dd (4.0, 9.8)	a: 4.00, dd (4.3, 9.8)	a: 4.00, dd (4.0, 9.8)
	b: 3.90, dd (7.3, 9.5)	b: 3.90, dd (7.2, 9.8)	b: 3.89, dd (7.2, 9.8)	b: 3.89, dd (6.6, 9.8)
2'	4.39, m	4.40, dd (4.0, 7.2)	4.39, dd (4.3, 7.2)	3.68, m
3'				1.86, m
4'	a: 4.89, br s	a: 4.88, br s	a: 4.89, br s	0.97, d (6.8)
	b: 5.08, br s	b: 5.08, br s	b: 5.09, br s	
5'	1.78, s	1.79, s	1.79, s	0.97, d (6.8)

[a]acetone-d_6, 300 MHz. [b]Assignments are based on extensive 1D and 2D NMR experiments (HMBC, HSQC, COSY see Appendix – 2D NMR complete data). *Proton resonances were attributed to the (*Z*-) or (*E*-) configuration, according to ACD/NMR Predictor® software.

Further compounds isolated were established to be known molecules, including etrogol (**5**) (Stierle *et al.,* 2003), tyrosol (**6**) (Hashimoto *et al.,* 1976), phenyl acetic acid (**7**) (Nair and Burke, 1988), benzoic acid (**8**) (Chen, 1958) and *para*-hydroxyphenyl acetic acid (**9**) (Chen, 1958; Crowden and Ralph, 1961).

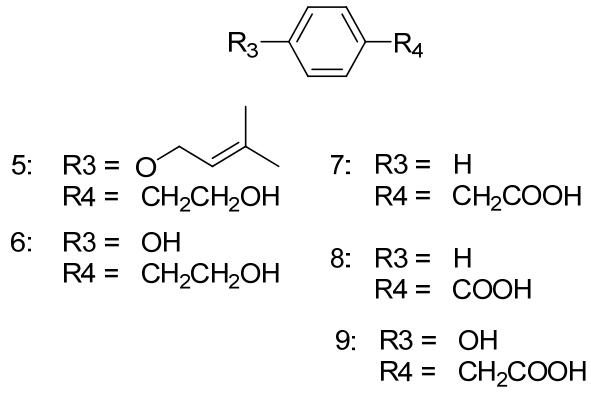

Figure 3. Structural formulae of the known compounds **5 - 9**

Biological activity

Stachyline A, B and C (**1, 2, 3**) were evaluated for cytotoxic activity against a panel of 3 cancer cell lines (NCI-H460, MCF7 and SF268, tested at the 100 μM dose), but did not show activity.

Stachyline A and B (**2**) were tested each against a panel of forty four psychoactive receptors, namely 5ht1a, 5ht1b, 5ht1d, 5ht1e, 5ht2a, 5ht2b, 5ht2c, 5ht3, 5ht5a, 5ht6, 5ht7, Alpha1A, Alpha1B, Alpha1D, Alpha2A, Alpha2B, Alpha2C, Beta1, Beta2, Beta3, BZP Rat Brain Site, D1, D2, D3, D4, D5, DAT, DOR, Gaba A, H1, H2, H3, H4, KOR, M1, M2, M3, M4, M5, MOR, NET, SERT, Sigma1, Sigma2, (activity considered with at least 50 % inhibition at the 10 μM level), but exhibited no potent activity. One could mention though the 48.3 % antagonistic effect of Stachyline B specifically against the Adrenergic receptor Alpha 2C (at 10 μM dose, quadruplicate measurements).

Stachylines C (**3**) and D (**4**) were also tested against five dopamine receptors (D1 – D5) but also did not show activity.

Stachyline A (**1**) was tested in antibacterial (*Escherichia coli*, *Bacillus megaterium*), antifungal (*Mycotypha microspora*, *Eurotium rubrum*, and *Microbotryum violaceum*), antialgal (*Chlorella fusca*) assays at a dose of 50 μg/ml disc level but did not show activity.

Stachyline B (**2**) was further tested in protein kinases DYRK1A and CDK5 inhibition activity assay (tested at 10 mM dose), for antiplasmodial activity assay against *Plasmodium berghei* (tested at 25 μM single dose), against two antibiotic resistant *Mycobacterium tuberculosis* strains, MTB72 and R46 (tested at the 50 μg/ml disc level), for the inhibition of the NF-kB protein complex assay (at the 100 μM) and in a panel of anti-diabetic activity assays: PPAR ligand assay, PPAR co-activator assay, PTP-1B inhibitor assay and glucose uptake assay (both 3T3-l1 cells and primary rat/mouse adipocytes, tested at the 100 μM dose) but did not show activity in any of the tests.

Stachyline D (**3**) was evaluated against Influenza B virus (tested at 100 μg/mL dose) and for the inhibition of the viral HIV-1 and HIV-2 induced cytopathogenic effect in MT-4 cells (tested at the 50 μg/mL dose) but did not show activity.

Discussion

Stachylines A-D are presumably tyrosine-derived metabolites, a group of compounds rarely encountered in fungal metabolism. The oxime group in compound **1** is even more intriguing. Phenylpyruvic acid oxime derivatives (Isaaki *et al.,* 1993), brominated tyrosine-derived compounds like the bastadins and psammaplins (Calcul *et al.,* 2010), as well as biosynthetically possibly related nitrile containing metabolites (Flemming, 1999) occur in marine sponges. The *Stachylidium* sp. used for this investigation was isolated from a marine sponge.

It was observed that the configuration of the oxime moiety in compound **1** was labile, and upon chromatographic isolation of the *E*- and *Z*-isomers, respective isomerisation took place instantaneously. None of the isomers seemed to be thermodynamically more stable under the prevailing conditions, since a 1:1 ratio of isomers was obtained (see Appendix – Spectroscopic data supporting information). In contrast to that, the geometrical isomers collismycin A and B from *Streptomyces* sp. MQ22 were reported to be not interchangeable in many organic solvents and at room temperature. Only by heating in *ortho*-dichlorobenzene at 120 °C they were gradually interchangeable (Shindo *et al.,* 1994). For 2-(4-hydroxyphenyl)-2-oxoacetaldehyde oxime (PHBA) isolated from *Penicillium olsonii*, the *E*-configuration was described without mentioning any isomerisation reactions (Amade *et al.,* 1993).

Although the oxime functional groups are rare in natural products they occur in a variety of phyla, e.g., sponges, bacteria, fungi, and plants. Tyrosine-derivatives with an oxime moiety were found in actinomycetes, such as the β-lactam antibiotic nocardicin A from *Nocardia uniformis* (Hashimoto *et al.,* 1976). Higher plants are also capable of producing oxime groups, since the biosynthesis of glucosinolates and cyanogenic glycosides, e.g. dhurrin from *Sorghum bicolor* proceeds via aldoximes (Bjarnholt and Møller, 2008; Flemming, 1999; Akazawa *et al*., 1960; Sibbesen *et al*., 1995). From these studies, oximes can be regarded as biosynthetic precursors of nitriles. Aspergillusol A was reported to be the first fungal tyrosine-derivative with an oxime moiety (Ingavat *et al*., 2009), however a previous publication had described the isolation of 2-(4-hydroxyphenyl)-2-oxoacetaldehyde oxime (PHBA) from *Penicillium olsonii* (Amade *et al*., 1993). Hence, the current report is the third one of a fungal tyrosine-derived oxime derivative.

Concerning the biosynthesis of naturally occurring oximes it is not clear which isomer is produced initially. The aldoxime intermediate in the biosynthesis of the cyanogenic glycoside dhurrin has been reported to initially have the *E*-configuration, subsequently undergoing non-enzymatic isomerisation (Bjarnholt and Møller, 2008; Sibbesen *et al.* 1995). Nocardicin A with Z-oxime configuration is thought to be preferentially produced over the *E*-configurated nocardicin B, due to favourable intramolecular hydrogen-bonding in biosynthetic intermediates (Kelly and Townsend, 2002; Kelly and Townsend, 2005). In the case of bastadins and psammaplins, it was assumed that the *Z*-oxime configuration is initially produced during biosynthesis, followed by isomerisation to the thermodynamically more favored *E*-isomers during extraction and isolation of the compounds (Calcul *et al.*, 2010).

Stachylines A-D are proposed to be biosynthetically derived from tyrosine (Figure 4). For stachyline A the biosynthetic process may be similar to that of cyanogenic glycosides, e.g. dhurrin, in that the precursor tyrosine is N-hydroxylated by CYP 450 enzymes to N,N-dihydroxytyrosine and subsequently decarboxylated and dehydrated to form an aldoxime (Bjarnholt and Møller, 2008). A similar pathway was described for the norcardicin biosynthesis (Kelly and Townsend, 2002; Kelly and Townsend, 2005).

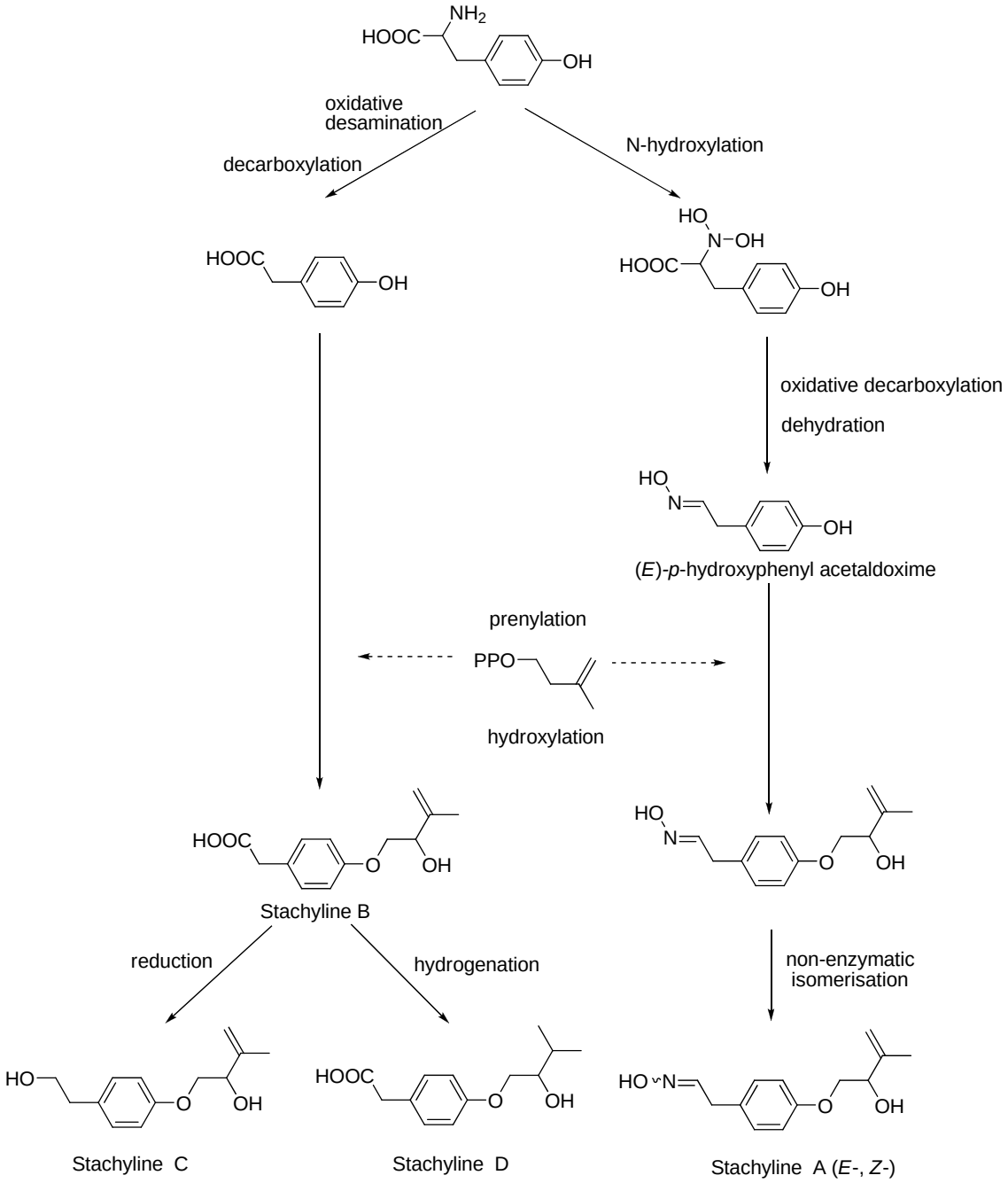

Figure 4. Proposed biosynthesis of stachylines A – D.

Experimental section

General Experimental Procedures. See chapter 3 - General methodology.

Fungal material. See chapter 3 - General methodology.

Culture, extraction and isolation. Compounds **1** to **4** were isolated from three different cultures of *Stachylidium* sp. The first and second culture comprised 12 L and 10 L of agar-biomalt medium (biomalt 20 g/L, 15 g/L agar) supplemented with sea salt incubated for 2 months (12 L) and 40 days (10 L) in Fernbach flasks at room temperature. The third culture was performed with 9.6 L liquid YPM medium (yeast extract 5 g/L, peptone from YPM 3 g/L, mannitol 25 g/L) incubated for 10 days. An extraction with 5 L EtOAc yielded 5.9 g, 2.1 g and 1.0 g of extract, respectively which were subjected to a VLC fractionation on silica gel, using a step gradient solvent system with petroleum ether - acetone from 10:1, 5:1, 2:1, 1:1 to 100 % acetone and, subsequently 100 % MeOH, resulting in 6 VLC fractions for each culture. Compounds **2** and **3** were isolated from the first culture (12 L), whilst compound **4** was isolated from the second culture (10 L) and compound **1** was isolated from the third culture (YPM medium). The known compounds **6** and **9** were isolated from the first culture and the know compounds **5**, **7** and **8** from the first and third culture (isolation described for the YPM culture).

Compound **1** was isolated from VLC fraction 3 by NP-HPLC separation using petroleum ether - acetone (7:1) to yield 6 fractions. Sub-fraction 3 and 4 corresponded to a mixture of isomers of compound **1** (*E*- and *Z*-, 4.4 mg), which was again separated by RP-HPLC using 50 % MeOH (t_R 11 min and 15 min), but immediately formed the initial mixture of isomers in a ratio of 1:1. Compounds **2** and **3** were isolated from VLC fraction 3 by NP-HPLC using petroleum ether - acetone (11:2) to yield 10 fractions. Further RP-HPLC fractionation with sub-fraction 5 using 50 % MeOH yielded 5 more sub-fractions, in which sub-fraction 4 was a mixture of compounds **2** and **3**. Finally, we performed NP-HPLC fractionation using petroleum ether - acetone (7:1) to afford compound **2** (fraction 1 of 2, 4.1 mg, t_R 19 min) and compound **3** (fraction 2 of 2, 2.2 mg, t_R 26 min). Compound **4** was isolated from VLC fraction 4, followed by HPLC fractionation using petroleum ether - acetone (9:2; sub-fraction 2 of 7) which was further purified using RP-HPLC with 60 % MeOH (fraction 2 of 4, 1.8 mg, t_R 10 min).

Etrogol (**5**) was isolated from VLC fraction 3, followed by HPLC fractionation using petroleum ether - acetone (7:1) to yield 5 sub-fractions. Sub fraction 1 was further purified using petroleum ether - acetone (7:1) to yield pure etrogol (fraction 3 of 3, 3.1 mg, t_R 26 min). Tyrosol (**6**) was isolated from VLC fraction 3 followed by HPLC fractionation using petroleum ether - acetone (5:1) to yield 10 fractions. Further RP-HPLC fractionation with sub-fraction 6 using 30 % MeOH yielded the pure compound

(fraction 3 of 7, 2.5 mg, t_R 19 min). Phenyl acetic acid (**7**) and benzoic acid (**8**) were isolated from VLC fraction 3, followed by HPLC fractionation using petroleum ether - acetone (11:1) to yield 5 fractions. Benzoic acid was present in fraction 2 (7.9 mg, t_R 16 min) and phenylacetic acid in fraction 3 (11.2 mg, t_R 25 min). *Para*-hydroxyphenyl acetic acid (**9**) was isolated from VLC fraction 3 followed by HPLC fractionation using petroleum ether - acetone (5:1) to yield 10 fractions. Further RP-HPLC fractionation with sub-fraction 6 using 30 % MeOH yielded the pure compound (fraction 4 of 7, 1.8 mg, t_R 27 min).

Stachyline A, mixture of *E*-/*Z*-isomers, 1:1 (**1**)**:** white amorphous solid (458 µg/L, 0.43 %); $[\alpha]_D^{23}$ -15 (*c* 0.29, MeOH); UV (MeOH) λ_{max} (log ε) 225 nm (3.60), 222 nm (2.84), 276 nm (2.76) ; IR (ATR) ν_{max} 3300 (br), 2922, 1610, 1510 cm^{-1}; ^1H NMR and ^{13}C NMR (Tables 1 and 2 and Appendix – Complete 2D NMR data); ESIMS *m/z* 236.1 $[M+H]^+$; HREIMS *m/z* 235.1208 $[M]^+$ (calcd. for $C_{13}H_{17}NO_3$, *m/z* 235.1208); HRESIMS *m/z* 258.1125 $[M+Na]^+$ (calcd. for $C_{13}H_{17}NNaO_3$, *m/z* 258.1101).

Stachyline B (2): white amorphous solid (340 µg/L, 0.07 %); $[\alpha]_D^{23}$ - 12 (*c* 0.33, MeOH); UV (MeOH) λ_{max} (log ε) 204 nm (3.35), 227 nm (3.75), 276 nm (3.05), 283 nm (2.75); CD (*c* 1.06 × 10^{-6} mol/L, MeOH), λ (Δε) = 197 (+ 1.78); IR (ATR) ν_{max} 3364 (br), 2929, 1610, 1511 cm^{-1}; ^1H NMR and ^{13}C NMR (Tables 1 and 2 and Appendix – Complete 2D NMR data); EIMS *m/z* 236.1 $[M]^+$; HREIMS *m/z* 236.1051 $[M]^+$ (calcd. for $C_{13}H_{16}O_4$, *m/z* 236.1049).

Stachyline C (3): white amorphous solid (183 µg/L, 0.04 %); $[\alpha]_D^{23}$ - 16 (*c* 0.33, MeOH); UV (MeOH) λ_{max} (log ε) 205 nm (3.43), 225 nm (3.85), 277 nm (2.95), 283 nm (2.95); CD (*c* 1.25 × 10^{-6} mol/L, MeOH) λ (Δε) = 199 (+ 1.94); IR (ATR) ν_{max} 3235 (br), 2937, 2551, 1685, 1509 cm^{-1}; ^1H NMR and ^{13}C NMR (Tables 1 and 2 and Appendix – Complete 2D NMR data); EIMS *m/z* 222.1 $[M]^+$; HRESIMS *m/z* 245.1162 $[M+Na]^+$ (calcd. for $C_{13}H_{18}NaO_3$, *m/z* 245.1148).

Stachyline D (**4**): white amorphous solid (180 µg/L 0.09 %); $[\alpha]_D^{23}$- 6 (*c* 0.12, MeOH); UV (MeOH) λ_{max} (log ε) 205 nm (3.86), 226 nm (3.86), 276 nm (3.08), 283 nm (2.90); IR (ATR) ν_{max} 3265 (br), 1687, 1512 cm^{-1}; ^1H NMR and ^{13}C NMR (Tables 1 and 2 and

Appendix – Complete 2D NMR data); ESIMS *m/z* 237.1 $[M-H]^-$; HRESIMS *m/z* 261.1096 $[M+Na]^+$ (calcd. for $C_{13}H_{18}NaO_4$, *m/z* 261.1097).

Preparation of the (*R*)- and (*S*)-MTPA esters of compound 2. The secondary alcohol (1 eq, 1 mg, 4.23 x 10^{-6} μmol) was dissolved with the corresponding MTPA-Cl (10 eq) in an adequate quantity of deuterated pyridine and DMAP (1 eq) in an NMR tube. The reaction was followed by ^{1}H-NMR to observe the downfield proton shift of H-2'. After 1 hour reaction time, the final ^{1}H-NMR was recorded, the sample dried and re-dissolved in D-acetone for ^{1}H-^{13}C HSQC measurements. The $\Delta^{(S-R)}$ values between (*S*)- and (*R*)-MTPA esters were recorded with the help of both ^{1}H-NMR and ^{1}H-^{13}C HSQC (see Figure 1 and Appendix - Spectroscopic data supporting information).

Bioassays. See chapter 3 - General methodology.

7. Novel Furyl Derivative from the Sponge-derived Fungus *Stachylidium* sp.

Abstract

The marine-derived fungus *Stachylidium* sp. was isolated from the sponge *Callyspongia* sp. cf. *C. flammea.* One new furyl derivative, 2-(furan-3-yl)acetic acid (**1**) were isolated from the fungal extract which was obtained from a agar-BMS medium supplemented with artificial sea salt. The structure of **1** was elucidated based on extensive spectroscopic analysis. Three further and known furyl derivatives, namely 1-(furan-2-yl)ethane-1,2-diol (**2**), furan-2,5-diyldimethanol (**3**) and 2-furoic acid (**4**) were found.

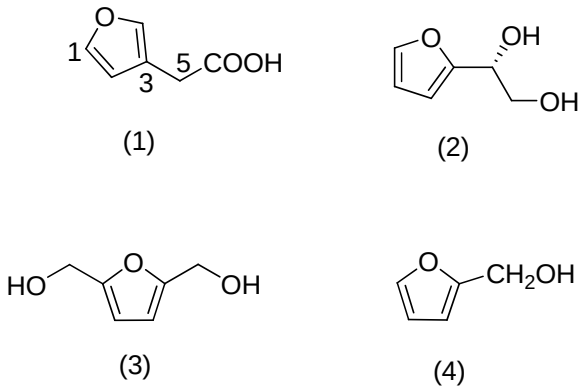

Figure 1. Structures of Compounds **1 - 4**

Introduction

Interactions that occur between organisms are often mediated by small molecules, e.g. *N*-acyl-homoserine lactones, 2-heptyl-3-hydroxy-4-quinoline (PQS) (Dudler and Eberl, 2006; Camili and Bassler, 2006). In addition to controlling the production of active compounds in bacteria, there is a growing number of reports indicating that small molecules like *N*-acyl-homoserine lactones autoinducers modulate gene expression of eukaryotic organisms (Sperantio, 2004; Shinner *et al.*, 2005).

Furyl derivatives are also found in a wide taxonomical range of bacterial and fungal species. Methyl 2-furancarboxylate is found in *Loktanella* (Dickschat *et al.*, 2005), while the related compound 2-acetylfuran (Andreae, 1990) is a metabolite of myxobacteria (Dickschat *et al.*, 2004; Dickschat *et al.*, 2005a), *Streptomyces citreus* (Pollak and Berger, 1996) and marine bacteria (Dickschat *et al.*, 2005b). Interestingly, the typical fungal metabolite 3-methylfuran has been reported from three *Streptomyces* strains (Schöller *et al.*, 2002; Schulz and Dickschat, 2007), whereas the regioisomer 2-methylfuran is reported from *Thermoactinomyces* (Wilkins, 1996).

During our search for new natural products produced from the marine-derived fungus *Stachylidium sp.*, one new (**1**) and three known furyl derivatives (**2** – **4**) were isolated from a culture of this fungus on agar-BMS media supplemented with artificial sea salt.

Structure elucidation

The molecular formula of **1** was established by HREIMS to be $C_6H_6O_3$, requiring four sites of unsaturation. The ^{13}C NMR and DEPT135 spectra indicated the presence of six resonances, including three sp^2 methines, one sp^3 methylene and two quaternary carbons (Compound Spectroscopic Description and Table 1). The three methine protons were assigned to be part of a furyl moiety. H-1 and H-4 have downfield shifted proton resonances in the ^1H-NMR spectra, indicating that the furyl oxygen atom is placed between them. H-2 was placed next to H-1 making use of ^1H-^1H-COSY correlations. Key heteronuclear long range correlations from the sp^3 CH_2-5 to the furyl carbons C-2, C-3, C-4 and the carboxyl carbon C-6 (δ_c 172.3) completed the assignment of **1** as 2-(furan-3-yl)acetic acid**.** Compound **1** is a new natural products but was previously synthesized (Paolucci and Rosini, 2007; Kassianidis *et al.*, 2005).

The structure of the furyl derivatives **2**, **3** and **4** was established to be namely 1-(furan-2-yl)ethane-1,2-diol (**2**) , furan-2,5-diyldimethanol (**3**) and 2-furoic acid (**4**), respectively by comparison of spectroscopic data with those previously reported for these natural products (Lu *et al.*, 2008, Schneider *et al.*, 1996; Hong *et al.*, 1981).

Table 1. 1D and 2D NMR spectroscopic data for compound **1**

position	δ_C, mult.[a, b, e]	δ_H[a, b] (*J* in Hz)	COSY[a, c]	HMBC[a, d]
1	143.6, CH	7.476, m	2	2, 3, 4
2	112.5, CH	6.43, s (br)	1	1, 3, 4, 5
3	119.1, qC			
4	141.3, CH	7.482, m	5	1, 2, 3, 5
5	30.6, CH_2	3.45, s	4	2, 3, 4, 6
6	172.3, qC			

[a] CD_3COCD_3, 300/75.5 MHz. [b] Assignments are based on extensive 1D and 2D NMR experiments (HMBC, HSQC, COSY). [c] Numbers refer to proton resonances. [d] Numbers refer to carbon resonances. [e] Implied multiplicities determined by DEPT.

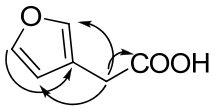

(**1**)

Figure 2. Key HMBC correlations of compound **1**

Biological activity assays

(*R*)-1-(furan-2-yl)ethane-1,2-diol (**2**) were tested for antiplasmodial activity assay against *Plasmodium berghei* (tested at 25 µM single dose), in antibacterial (*Escherichia coli*, *Bacillus megaterium*), antifungal (*Mycotypha microspora*, *Eurotium rubrum*, and *Microbotryum violaceum*), antialgal (*Chlorella fusca*) assays at a dose of 50 µg/ml disc level but did not show any activity.

Compounds **1** – **4** are currently being tested for agonistic/antagonistic quorum sensing effect in the bacterial species *Chromobacterium violaceum*.

Discussion

Small molecules like furyl derivatives are widely present in fungal and bacterial extracts (Dickschat *et al.*, 2004; Dickschat *et al.*, 2005a; Dickschat *et al.*, 2005b; Pollak and Berger, 1996; Schöller *et al.*, 2002; Schulz and Dickschat, 2007), and they could work in the quorum sensing responsible for eukaryotic-bacterial as well as bacterial-bacterial chemical interactions, (Dudler and Eberl, 2006). Interestingly, peptides, phthalides and phthalimidines indicating the presence of bacterial metabolism were isolated from the same fungal extract (unpublished data). We are currently undergoing studies to identify the possible origin of these compounds, as well as the possible interaction/origin of the hereby reported furyl derivatives.

Experimental section

General Experimental Procedures. See chapter 3 - General methodology.

Fungal material. See chapter 3 - General methodology.

Culture, extraction and isolation. Compounds **1** and **2** were isolated from two different cultures of *Stachylidium sp.*, the first and second performed on 12 L and 10 L respectively of agar-biomalt medium (biomalt 20g/L, 15 g/L agar) supplemented with sea salt during 2 months (12 L) and 40 days (10 L). An extraction with 5 L EtOAc yielded respectively 5.9 g and 2.1 g of extract which were subjected to a VLC fractionation in a silica open column using a gradient solvent system with petroleum ether - acetone at 10:1, 5:1, 2:1, 1:1, 100% acetone and 100% MeOH, resulting thus 6 VLC fractions from each culture. Compound **2**, **3** and **4** were isolated from the first culture (12 L), whilst compound **1** was isolated from the second culture (10 L).
Compound **1** was isolated from VLC fraction 3, followed by HPLC fractionation using petroleum ether - acetone 5:1 (sub-fraction 2 of 10) which was further purified using NP-HPLC with petroleum ether - acetone 9:1 (fraction 3 of 4, 3.2 mg, t_R 21 min).

Compound **2** was isolated from VLC fraction 3, followed by HPLC fractionation using petroleum ether - acetone 5:1 (sub-fraction 7 of 10) which was further purified by HPLC reverse phase fractionation using 50% MeOH (sub-fraction 1 of 4). Finally we used RP-HPLC using 10% MeOH to yield the pure compound (fraction 2 of 7, 3.1 mg, t_R 4 min).

Compound **3** was isolated from VLC fraction 3, followed by HPLC fractionation using petroleum ether - acetone 5:1 (sub-fraction 7 of 10) which was further purified by HPLC reverse phase fractionation using 50% MeOH (sub-fraction 1 of 4). Finally we used RP-HPLC using 10% MeOH to yield the pure compound (fraction 3 of 7, 2.6 mg, t_R 4 min).

Compound **4** was isolated from VLC fraction 3, followed by HPLC fractionation using petroleum ether - acetone 5:1 (sub-fraction 7 of 10) which was further purified by HPLC reverse phase fractionation using 50% MeOH (sub-fraction 1 of 4). Finally we used RP-HPLC using 10% MeOH to yield the pure compound (fraction 4 of 7, 1.6 mg, t_R 4 min).

2-(furan-3-yl)acetic acid (**1**): white amorphous solid (320 µg/L 0.152 %); UV (MeOH) λ_{max} 206 nm (log ϵ 3.76); IR (ATR) ν_{max} 2907 (Br), 1693 cm^{-1}; ^1H NMR [H-1, δ 7.476, m; H-2, δ 6.43, s (br); H-4, δ 7.482, m; H-5, δ 3.45, s] and ^{13}C NMR (C-1, δ 143.6, CH; C-2, δ 112.5, CH; C-3, δ 119.1, qC; C-4, δ 141.3, CH; C-5, δ 30.6, CH_2; C-6, δ 172.3, qC; 2D NMR in Table 1); LRESIMS *m/z* 124.9 $(M-H)^-$; HRESIMS calcd. *m/z* 125.0233 for $C_6H_5O_3$ $(M-H)^-$, found 125.0240.

Methodology for the performed biological assays. See chapter 3 - General methodology.

8. Endolides A – J, N-methylated Peptides from the Sponge-derived Fungus *Stachylidium* sp.

Abstract

Marine organisms are rich sources of structurally diverse bioactive compounds. Recently, a great deal of interest has been expressed regarding marine-derived bioactive peptides because of their numerous health beneficial effects (Kim and Wijesekara, 2010).

During our search for new natural products produced from the marine-derived fungus *Stachylidium sp.*, ten novel cyclic N-methylated peptides, Endolides A – J, were isolated from the extract of the fungus. These peptides (structure formulae not shown) are currently undergoing absolute configuration analysis by means of the advanced Marfey's method and X-ray crystallography. We have already submitted Endolides A - J to a total of 311 individual biological activity assays, in such areas like cytotoxicity, antimicrobial, antiviral, antiplasmodial, psychoactive or anti-inflammatory activity, amongst others.

9. Hydroxylated Sclerosporin Derivatives from the Marine-derived Fungus *Cadophora malorum*†

Abstract

The marine-derived fungus *Cadophora malorum* was isolated from the green alga *Enteromorpha* sp. Growth on a biomalt medium supplemented with sea salt yielded an extract from which we have isolated sclerosporin and four new hydroxylated sclerosporin derivatives, namely 15-hydroxysclerosporin (**2**), 12-hydroxysclerosporin (**3**), 11-hydroxysclerosporin (**4**) and 8-hydroxysclerosporin (**5**). The compounds were evaluated in various biological activity assays. Compound **5** showed a weak fat-accumulation inhibitory activity against 3T3-L1 murine adipocytes.

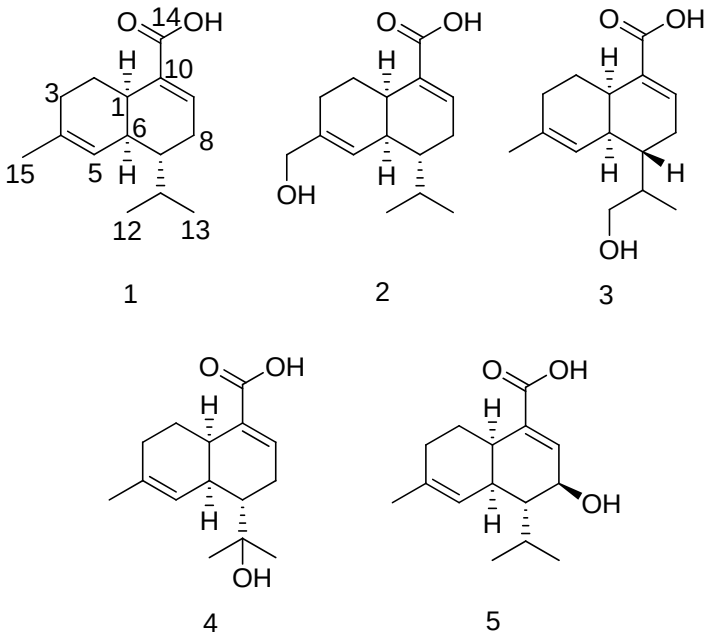

Figure 1. Structure formulae of compounds **1 - 5**

Introduction

In recent years, research on the chemistry of marine organisms has experienced a tremendous increase, due to the need for compounds possessing bioactivity with possible pharmaceutical application or other economically useful properties (Anderson *et al.*, 2000). From these organisms, marine fungi are recognized as a valuable source for new and bioactive secondary metabolites that have the potential to lead to innovations in drug therapy (Haefner, 2003). Sclerosporin is a rather rare antifungal and sporogenic cadinane-type sesquiterpene (Katayama *et al.*, 1983; Datta *et al.*, 2007). This substance, initially isolated from *Sclerotinia fruticula* showed an induction of asexual arthrospore formation in fungal mycelia (Katayama *et al.*, 1983; Kitahara *et al.*, 1984). Interestingly, its (-)-form isolated from *Diplocarpon mali* did not showed sporogenic activity towards *S. frutícula* (Kitahara *et al.*, 1984; Sawai *et al.*, 1985).

During our search for new natural products produced from the marine-derived fungus *Cadophora malorum*, (+)-sclerosporin (**1**) and four new hydroxylated sclerosporin derivatives (**2** – **5)** were isolated from a spore culture on agar-BMS media supplemented with artificial sea salt.

Results and Discussion

The molecular formulae of compounds **2** - **5** were deduced by HREIMS to be identical, *i.e*. $C_{15}H_{22}O_3$, indicating five degrees of unsaturation. The ^{13}C NMR spectra for all four compounds showed 15 closely similar resonance signals, evidencing that each of the compound belonged to the same structural type. In each case a ^{13}C NMR downfield shifted resonance signal at δ 168 – 170 was found, typical for a carboxylic acid functionality (C-14), whereas a further resonance signal at around δ 70 indicated a hydroxy substituted methylene for compounds **2** and **3**, a hydroxy substituted methine for compound **5**, and for compound **4** a hydroxylated quaternary carbon (see Tables 1-2, respectively). IR spectroscopic measurements showed a broad absorption band at 3300 cm^{-1} for **2** - **5**, also confirming the presence of a hydroxy substituent in each case.
^1H-^1H COSY data for **2** revealed a spin system ranging from H_2-3 via H-1 and H-6 to H_2-9 and to H_3-12/H_3-13, thus outlining major parts of the planar structure. Protons H_2-

15 showed a ^{1}H-^{1}H long range coupling to H-5, which together with an HMBC correlation from H_2-15 to C-3 and from H-5 to C-6 completed the first ring of **2**. HMBC correlations from H-9 to C-14 connected the carboxylic acid moiety with C-10, which in turn had to be bound to C-1 due to a HMBC correlation from H-1 to C-10 and to C-9. The planar structure of compound **2** was thus that of sclerosporin (**1**) hydroxylated at C-15.

Sclerosporin itself was also obtained during this study. The molecular formula of **1** was deduced by accurate mass measurement (HREIMS) to be $C_{15}H_{22}O_2$. The final structure of **1** was identified as that of the known compound (+)-sclerosporin by comparing its NMR data and optical rotation with published values (Datta *et al.*, 2007; Kitahara *et al.*, 1984).

The carbon skeleton of compounds **3** - **5** and the position of the double bonds were also found to be identical to that of **1,** as deduced from 1D and 2D NMR analyses. All compounds are thus cadinane type sesquiterpenes with a sclerosporin nucleus (see Tables 1-2) and differ merely concerning the site of hydroxylation.

The position of the hydroxy group in **3** and **4** was established making use of ^{1}H-^{1}H COSY and HMBC data. Thus, in **3** the ^{13}C NMR resonance signal for C-12 (δ 64.9) was shifted downfield, and H-12 (δ 3.52) showed coupling with H-11, placing the hydroxy substituent at C-12. The ^{13}C NMR spectrum of **4** exhibited a downfield shifted quaternary carbon (δ 72.6, C-11) along with singlet proton resonances for the methyl groups CH_3-12/CH_3-13 in the ^{1}H NMR spectrum, thus the hydroxy substituent had to be placed at C-11. The ^{13}C NMR spectrum of **5** exhibited only two resonances for methylene groups (C-2, C-3) instead of three such moieties as in **2** - **4**. Instead of the methylene group CH_2-8 in **2** – **4,** in **5** a methine group resonating at δ 68.7 and δ 4.13 in the ^{13}C and ^{1}H NMR spectra respectively was found. The ^{1}H-^{1}H COSY spectrum revealed correlations between H-8 and H-9 as well as H-7, positioning the hydroxy substituent in **5** at C-8. The planar structures of **2** - **5** were thus established to be 15-hydroxysclerosporin (**2**), 12-hydroxysclerosporin (**3**), 11-hydroxysclerosporin (**4**) and 8-hydroxysclerosporin (**5**).

Table 1. ^{1}H NMR Spectroscopic Data for Compounds **2** – **5**.

	2	**3**	**4**	**5**
Position	δ_H[a] (*J* in Hz)	δ_H[a] (*J* in Hz)	δ_H[b] (*J* in Hz)	δ_H[b] (*J* in Hz)
1	2.58, br d (11.4)	2.58, br d (10.2)	2.54, br d (10.6)	2.43, br d (10.6)
2	a: 1.99, m	a: 1.91, m	a: 1.89, m	a: 1.93, m
	b: 1.37, qd (11.4, 5.4)	b: 1.42, qd (11.7, 5.4)	b: 1.50, qd (11.7, 5.5)	b: 1.45, qd (11.7, 5.4)
3	2.08, m	a: 2.06, m	a: 1.98, m	a: 2.08, m
		b: 1.88, m	b: 1.95, m	b: 1.93, m
5	5.79, d (4.1)	5.52, br s	5.71, br d (5.1)	5.57, br d (4.4)
6	2.04, m	2.10, m	2.11, m	2.10, m
7	1.53, tt (10.2, 5.1)	1.65, tt (10.2, 5.1)	1.68, td (10.3, 5.1)	1.52, ddd (3.2, 8.7, 10.7)
8	a: 2.15, dt (19.8, 5.1)	a: 2.27, dt (19.8, 5.1)	a: 2.38, dt (19.6, 5.1)	4.13, br d (8.7)
	b: 1.97, m	b: 2.02, m	b: 2.01, m	
9	7.14, br s	7.10, br s	6.95, br t (3.9)	6.79, d (1.8)
11	2.03, m	2.05, m		2.25, m
12	0.83, d (6.8)	3.77 (dd, 4.8, 10.6)	1.23, s	1.00, d (7.1)
13	0.90, d (6.8)	1.03, d (7.0)	1.18, s	1.10, d (7.1)
14				
15	4.03, br s	1.68, br s	1.66, br s	1.68, br s

[a]$CDCl_3$, 300 MHz. [b]Acetone-d_6, 300 MHz.

Table 2. ^{13}C NMR Spectroscopic Data for Compounds **2** – **5**.

	2	**3**	**4**	**5**
Position	δ_C, mult.[a,c]	δ_C, mult.[a, c]	δ_C, mult.[b, c]	δ_C, mult.[b, c]
1	34.0, CH	33.8, CH	35.6, CH	35.2, CH
2	25.1, CH_2	25.4, CH_2	26.2, CH_2	26.0, CH_2
3	26.2, CH_2	30.3, CH_2	30.8, CH_2	31.5, CH_2
4	138.3, qC	135.6, qC	133.7, qC	134.9, qC
5	124.3, CH	123.0, CH	126.6, CH	125.1, CH
6	35.5, CH	35.8, CH	36.9, CH	36.2, CH
7	40.0, CH	38.6, CH	47.2, CH	48.8, CH
8	25.4, CH_2	28.0, CH_2	29.7, CH_2	68.7, CH
9	142.6, CH	142.1, CH	140.2, CH	143.7, CH
10	132.9, qC	133.1, qC	134.3, qC	134.3, qC
11	26.4, CH	35.3, CH	72.6, qC	27.3, CH
12	15.0, CH_3	64.9, CH_2	27.4, CH_3	18.9, CH_3
13	21.3, CH_3	15.4, CH_3	28.7, CH_3	21.1, CH_3
14	172.2, qC	172.0, qC	168.0, qC	168.0, qC
15	67.3, CH_2	23.9, CH_3	23.9, CH_3	23.9, CH_3

[a]$CDCl_3$, 75.5 MHz. [b]Acetone-d_6, 75.5 MHz.
[d] Implied multiplicities determined by DEPT.

Stereochemistry

The Cotton effect in the CD spectrum of (+)-sclerosporin (**1)** was similar to that reported in the literature (Kitahara *et al.*, 1985), confirming the absolute configuration of **1** to be that of (+)-sclerosporin (see Table 3). The absolute configurations of compounds **2** - **5** were established by analyses of CD and NOESY spectra. The CD spectra of the hydroxylated compounds **2** - **5** were closely similar to that of (+)-sclerosporin (**1**), thus the identical absolute configuration can be proposed for compounds **2** – **4** (see Table 3). However, the configuration at position C-11 in **3** remains unresolved. Interestingly, **5** was the only one with a negative specific rotation (see Table 3). This change on specific rotation was most probably caused by the additional stereogenic center at C-8. The configuration at C-8 was established making use of NOESY correlations and ^{1}H-^{1}H coupling constants. A NOESY correlation between H-1 and H-6 is in agreement with the configuration of the other sclerosporin derivatives, and further correlations between H-8 and H-6, H-11, H_3-12, H_3-13 indicate these protons to be in the same spatial orientation. Furthermore, a ^{1}H-^{1}H coupling constant of 8.7 Hz between H-7 and H-8 indicated a *trans*-type spatial arrangement. Knowing the absolute configuration of H-1, H-6 and H-7 from CD spectroscopic data, we can thus assign the configuration of **5** to be 1*R*, 6*S*, 7*R*, 8*S*.

We propose the trivial names (+)-15-hydroxysclerosporin, (+)-12-hydroxysclerosporin, (+)-11-hydroxysclerosporin and (-)-8-hydroxysclerosporin for compounds **2**, **3**, **4** and **5**, respectively.

Table 3. Comparison of the CD Spectra and Specific Rotation Values for the Reported Sclerosporins (+ and -) and Compounds **1** - **5**.

	Compound	Δε Maxima and Minima in the CD Spectra (*c* 1.6 × 10^{-6} mol/L, MeOH)	Optical Rotation
(+)	(+)-sclerosporin[7]	$\Delta\varepsilon_{196}$ + 11.0[a]	$[\alpha]^{20}_{D}$ + 11.4 (*c* 0.035, MeOH)
(-)	(-)-sclerosporin[5]	$\Delta\varepsilon_{214}$ + 17.0[a]	$[\alpha]^{20}_{D}$ - 11.1 (*c* 0.090, MeOH)
(1)	(+)-sclerosporin	$\Delta\varepsilon_{196}$ + 10.1, $\Delta\varepsilon_{215}$ - 12.4	$[\alpha]^{23}_{D}$ + 14 (*c* 0.033, MeOH)
(1)	(+)-sclerosporin		$[\alpha]^{23}_{D}$ + 57 (*c* 0.033, $CHCl_3$)
(2)	(+)-15-hydroxy	$\Delta\varepsilon_{197}$ + 5.2, $\Delta\varepsilon_{214}$ - 14.8	$[\alpha]^{23}_{D}$ + 64 (*c* 0.033, $CHCl_3$)
(3)	(+)-12-hydroxy	$\Delta\varepsilon_{195}$ + 6.1, $\Delta\varepsilon_{214}$ - 6.2	$[\alpha]^{23}_{D}$ + 69 (*c* 0.033, $CHCl_3$)
(4)	(+)-11-hydroxy	$\Delta\varepsilon_{198}$ + 3.2, $\Delta\varepsilon_{213}$ - 16.3	$[\alpha]^{23}_{D}$ + 73 (*c* 0.033, $CHCl_3$)
(5)	(-)-8-hydroxy	$\Delta\varepsilon_{193}$ + 8.2, $\Delta\varepsilon_{215}$ - 8.0	$[\alpha]^{23}_{D}$ - 62 (*c* 0.033, $CHCl_3$)

[a]Δε minima for + and – sclerosporin not reported in the literature

Bioactivity assays

Compound **2** was evaluated in the protease elastase (HLE) inhibition assay (tested at 100 μM), in the cytotoxic activity assay against a panel of three cancer cell lines (NCI-H460, MCF7 and SF268, tested at 100 μM), in the protein kinases DYRK1A and CDK5 inhibition activity assay (tested at 10 mM), for inhibition of the viral HIV-1 and HIV-2 induced cytopathogenic effect in MT-4 cells (tested at 50 μg/mL), in the Epstein-Barr virus (EBV) assay (tested at 100 μg/mL), and in the antiplasmodial activity assay against *Plasmodium berghei* (tested at 25 μM), but did not show any activity. Compound **2** was further tested against a pannel of three respiratory viruses, the severe acute respiratory syndrome coronavirus (SARS) assay, Flu A (H5N1) and Flu B (tested at 100 μg/mL in the three tests), bud did not show any significant activity. Compound **3** was evaluated against two influenza viruses, Flu A (H5N1) and Flu B (tested at 100 μg/mL), but did not show any activity. Compound **5** was evaluated against 3-T3-L1 murine adipocytes assay and showed weak inhibitory activity with an IC_{50} of 212 μM for triglyceride accumulation inhibition along with an IC_{50} cytotoxic effect value of 304 μM (see Appendix – bioactivity results). All compounds were tested for sporogenic activity (concentrations from 0.005 μg/mL to 5 μg/mL in BMS-agar plates) but the results were inconclusive, i.e. sporogenesis activity was observed but not with direct correlation with increasing quantity, probably due to compound unstability. All compounds were evaluated in antibacterial (*Escherichia coli*, *Bacillus megaterium*),

antifungal (*Mycotypha microspora*, *Eurotium rubrum*, and *Microbotryum violaceum*), and antialgal (*Chlorella fusca*) assays but did not showed activity at 50 µg/disc dose.

Experimental Section

General Experimental Procedures See chapter 3 - General methodology.

Fungal material. See chapter 3 - General methodology.

Culture, extraction and isolation. A sporous culture of *Cadophora malorum* on a 10 L solid biomalt medium (biomalt 20 g/L, 15 g/L agar) supplemented with sea salt was performed during 3 months. An extraction with 5 L EtOAc yielded 890 mg of extract which was subjected to a VLC fractionation in a silica open column using a gradient solvent system from PE to acetone, namely 10:1, 5:1, 2:1, 1:1, 100 % acetone and 100 % MeOH, yielded a total of 6 fractions. Compounds **1** to **5** were isolated from VLC fraction 2 (112 mg) by HPLC fractionation using PE-acetone 5:1.
Sclerosporin (**1**) was collected in fraction 1 of 7 (2.7 mg, RT 6 min); (+)-15-hydroxysclerosporin (**2**) was collected in fraction 7 of 7 (14.0 mg, RT 22 min); (+)-12-hydroxysclerosporin (**3**) was collected in fraction 6 of 7 (7.1 mg) which was further purified by HPLC fractionation with PE-acetone 26:5 (fraction 1 of 2; 4.5 mg, RT 31 min); (+)-11-hydroxysclerosporin (**4**) was collected in fraction 3 of 7 (2.2 mg, RT 13 min); (-)-8-hydroxysclerosporin (**5**) was collected in fraction 2 of 7 (3.5 mg, RT 11 min).

(1*R*, 6*S*, 7*R*)-(+)-sclerosporin (1): $[\alpha]^{23}_{D}$ + 57 (*c* 0.033, $CHCl_3$); CD (see Table 3); HREIMS *m/z* 234.1623 (calcd for $C_{15}H_{22}O_2$, 234.1620); spectroscopic data were identical with the previously reported data.[4,5,7]

(1*R*, 6*S*, 7*R*)-(+)-15-hydroxysclerosporin (2): yellow amorphous solid (1.4 mg/L, 1.57 %); $[\alpha]^{23}_{D}$ + 64 (*c* 0.033, $CHCl_3$); UV (MeOH) λ_{max} (log ε) 217 nm (3.8); CD (see Table 3); IR (ATR) ν_{max} 3397, 2927, 1682 cm^{-1}; ^{1}H NMR and ^{13}C NMR (see Tables 1 and 2); LREIMS *m/z* 250.1; HREIMS *m/z* 232.1457 $[M\text{-}H_2O]^+$ (calcd for $C_{15}H_{20}O_2$, 232.1463).

(1*R*, 6*S*, 7*S*)-(+)-12-hydroxysclerosporin (3): yellow amorphous solid (0.71 mg/L, 0.81 %); $[\alpha]^{23}_{D}$ + 69 (*c* 0.033, $CHCl_3$); UV (MeOH) λ_{max} (log ε) 218 nm (3.9); CD (see Table 3). IR (ATR) ν_{max} 3397, 2923, 1682 cm^{-1}; ^{1}H NMR and ^{13}C NMR (see Tables 1 and 2); LREIMS *m/z* 250.1; HREIMS *m/z* 232.1463 $[M - H_2O]^+$ (calcd for $C_{15}H_{20}O_2$, *m/z* 232.1463).

(1*R*, 6*S*, 7*S*)-(+)-11-hydroxysclerosporin (4): yellow amorphous solid (0.22 mg/L, 0.25 %); $[\alpha]^{23}_{D}$ + 73 (*c* 0.033, $CHCl_3$); UV (MeOH) λ_{max} (log ε) 219 nm (3.8); CD (see Table 3); IR (ATR) ν_{max} 3277, 2928, 1681 cm^{-1}; ^{1}H NMR and ^{13}C NMR (see Tables 1 and 2); LREIMS *m/z* 250.1; HREIMS *m/z* 232.1464 $[M - H_2O]^+$ (calcd for $C_{15}H_{20}O_2$, *m/z* 232.1463).

(1*R*, 6*S*, 7*R*, 8*S*)-(-)-8-hydroxysclerosporin (5): yellow amorphous solid (0.35 mg/L, 0.39 %); $[\alpha]^{23}_{D}$ - 62 (*c* 0.033, $CHCl_3$); UV (MeOH) λ_{max} (log ε) 220 nm (3.7); CD (see Table 3); IR (ATR) ν_{max} 3397, 2928, 1688 cm^{-1};^{1}H NMR and ^{13}C NMR (see Tables 1 and 2); LREIMS *m/z* 250.1; HREIMS *m/z* 232.1458 $[M - H_2O]^+$ (calcd for $C_{15}H_{20}O_2$, *m/z* 232.1463).

Biological Assays. See chapter 3 - General methodology.

10. Novel Bisabolane Sesquiterpenes from the Marine-derived Fungus *Verticillium tenerum*

Abstract

Chemical investigations of the marine-derived fungus *Verticillium tenerum* yielded two new hydroxylated bisabolane-type sesquiterpenes verticinol A (**1**) and B (**2**). The planar structures of the new compounds were elucidated by employing spectroscopic (NMR, UV, and IR) and mass spectrometric techniques. The absolute configuration of the cyclohexenyl moiety was deduced by a combination of CD spectroscopy and NOESY measurements.

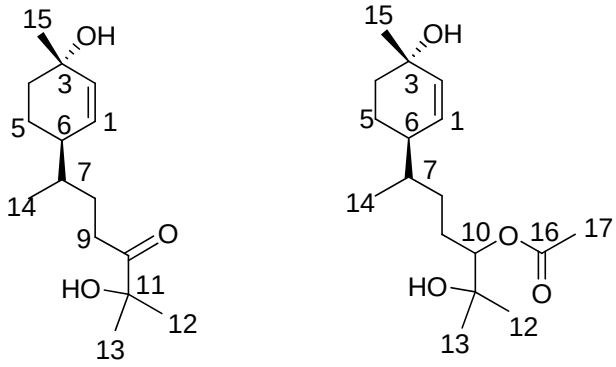

Figure 1. Structures of compounds **1** and **2**

Introduction

Fungi are an extremely valuable source of novel natural products with a wide array of biological activities (König and Wright, 1996). Polyketides are the dominant class of fungal secondary metabolites, however, peptides and heteroaromatic compounds are found in these microorganisms as well (Schneider *et al.*, 2008). Fungal terpenes are known as potent toxins, for example trichothecenes and botrydials, and as plant growth hormones, for example gibberellins and abscisic acid (Pinedo *et al.*, 2008).
To date, bisabolane-type sesquiterpenes have been rarely found in fungi. One report refers to α-bisabolol produced by a mangrove-derived ascomycete (Laurent *et al.*, 2002), and a second one describes highly oxygenated bicylic bisabolanes from the basidiomycete *Cheimonophyllum candidissimum* (Stadler *et al.*, 1994). Basidiomycetes of the genus *Lepista* were found to contain the volatile α- and ß-bisabolenes as well as the bicyclic tetrahydrofuran-containing lepistirone (Abraham *et al.*, 1991). Aromatic bisabolanes include curcutetraol, sydonol and waraterpol (Muelhaupt *et al.*, 2005).

In a project focusing on new and bioactive natural products from the marine-derived fungus *Verticillium tenerum*, which was isolated from an unknown alga and cultivated in a medium supplemented with sea salt, two new bisabolane sesquiterpenes (**1**, **2**) were obtained (Figure 1).

Results and Discussion

The molecular formula of **1** was deduced from accurate MS measurements (HRESIMS) to be $C_{15}H_{26}O_3$, implying three degrees of unsaturation. The IR spectrum showed characteristic absorption bands at 3376 and 1706 cm $^{-1}$, which indicated the presence of both hydroxy and carbonyl groups. NMR spectra (Table 1) confirmed the presence of 15 carbon atoms with 24 carbon-attached protons, indicating that two protons are associated with hydroxy groups. A more detailed analysis of NMR chemical shifts indicated the presence of one sp^3 secondary methyl (H_3-14, δ_H = 0.82) and three sp^3 tertiary methyl groups (H_3-12, H_3-13 and H_3-15 with δ_H = 1.37, 1.37 and 1.27). Furthermore, ^{1}H NMR signals for four sp^3 methylene groups, two of them aliphatic

(CH_2-8 and CH_2-9) and a further two alicyclic (CH_2-4 and CH_2-5), are present, as well as two sp^3 quaternary carbons (C-3, C-11), and the carbonyl carbon C-10 (δ_C = 214.5). There are two downfield shifted ^{1}H NMR signals for methine protons, i.e. the olefinic protons H-1 (δ_H = 5.49) and H-2 (δ_H = 5.63). Two further ^{1}H NMR signals are slightly downfield shifted and attached to sp^3 hybridized carbons (H-6, δ_H = 2.11 and H-7, δ_H = 1.46). Moreover, the ^{13}C NMR chemical shifts suggested the presence of two tertiary hydroxy groups (C-3, δ_C = 69.7 and C-11, δ_C = 76.1). A significant structural fragment of **1** (fragment A) could be deduced from the ^{1}H-^{1}H COSY spectrum, whereas

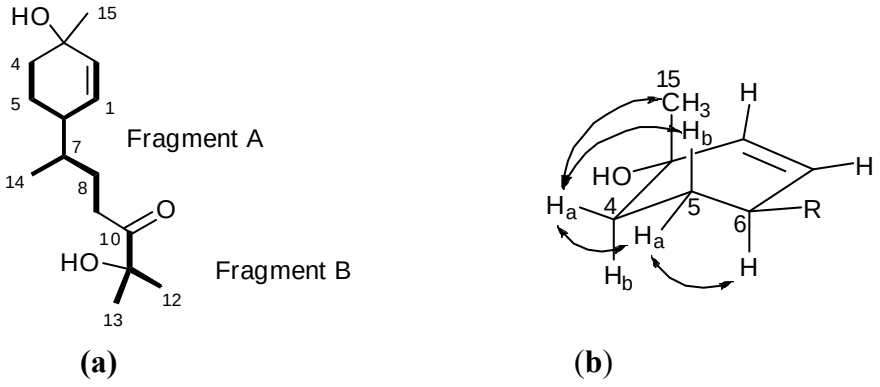

Figure 2: (**a**) Fragments of compound **1** as deduced from ^{1}H-^{1}H COSY and ^{1}H-^{13}C HMBC correlations; (**b**) Key NOESY correlations for compounds **1** and **2**

fragment B was delineated from heteronuclear couplings in the ^{1}H-^{13}C HMBC spectrum (Figure 2a). Thus, mutual correlations in the ^{1}H-^{1}H COSY spectrum between the resonances for H-2, H-1, H-6, H_2-5 and H_2-4 indicated these protons and their respective carbons to be adjacent. In addition, the ^{1}H-^{1}H COSY spectrum revealed a continuous chain of couplings from H_3-14 to H-6 and H-9 through H-7 and H-8. The correlations between H_3-12/H_3-13 and both C-10 and C-11 in the ^{1}H-^{13}C HMBC spectrum indicated that methyl groups CH_3-12 and CH_3-13 are bonded to C-11, which is further connected to C-10 giving rise to fragment B. The connection of fragments A and B was evidenced by an HMBC correlation between H-9 and C-10. Finally, HMBC correlations between H_3-15 and C-2, C-3 and C-4 completed the cyclohexenyl ring and thus the planar structure of **1**.

Table 1: 1D and 2D NMR spectroscopic data for compound **1.**

No.	δ_c[a,b,e]	δ_H[a,b] (mult., *J* in	COSY[a,b,c]	HMBC[a,d]	NOESY[a,b,c]
1	131.3, CH	5.49, br d (10.3)	2, 5a, 6	2, 3, 5, 6, 7	2, 6, 8a, 8b, 14
2	135.1, CH	5.63, br d (10.3)	1, 4a, 6	1, 4, 6	1, 15
3	69.7, qC				
4	38.1, CH_2	a: 1.86, m	2, 4b, 5a, 5b	2, 3, 5, 6	4b, 5a, 5b, 15
		b: 1.65, m	4a, 5a, 5b	3, 5, 6	4a
5	22.3, CH_2	a: 1.67, m	4a, 4b, 5b, 6	4, 6	4a, 5b, 6
		b: 1.39, m	4a, 4b,5a, 6	4, 6	4a, 5a
6	40.1, CH	2.11, m	1, 2, 5a, 5b, 7	7	1, 5a, 7, 8a, 9, 14
7	36.3, CH	1.46, m	6, 8a, 8b, 14	14	6, 9, 14
8	27.9, CH_2	a: 1.71, m	7, 8b, 9	6, 7	1, 8b, 9
		b: 1.44, m	7, 8a, 9	6, 7	8a, 9
9	33.6, CH_2	2.55, m	8a, 8b	7, 8, 10	6, 7, 8a, 8b, 12, 13, 14
10	214.5, qC				
11	76.1, qC				
12	26.5, CH_3	1.37, s		10, 11, 13	9
13	26.5, CH_3	1.37, s		10, 11, 12	9
14	15.5, CH_3	0.82, d (6.6)	7, 8a	6, 7, 8	1, 6, 7, 9
15	28.4, CH_3	1.27, s		2, 3, 4	2, 4a

[a]Chloroform-d_1, 300/75 MHz. [b]Assignments are based on extensive 1D and 2D NMR measurements (HMBC, HSQC, COSY). [c]Numbers refer to proton resonances. [d]Numbers refer to carbon resonances. [e]Implied multiplicities determined by DEPT.

The molecular formula of **2** was found to be $C_{17}H_{30}O_4$, as deduced from HRMS and NMR data, implying three degrees of unsaturation. The ^{13}C NMR spectrum showed 17 carbon signals attributed to five methyls, four methylenes, five methines and three quaternary carbons (Table 2). Considering the molecular formula and according to the IR data (3390 cm^{-1}), it was evident that the two remaining protons had to be part of hydroxy groups. The marked similarities in the NMR spectra of **1** and **2** (Tables 1 and 2) suggested that their structures are closely related. Compound **2** is a reduced and acetylated derivative of **1**, i.e. the only difference between the molecules is the acetylated hydroxy group at C-10 in **2**, compared with the carbonyl group in **1**. The connection of the acetyl group (C-16 with δ_C=172.9 and C-17 with δ_C=21.0) to C-10 is supported by a ^1H-^{13}C HMBC long range correlation between H-10 and C-16.

Table 2: 1D and 2D NMR spectroscopic data for compound **2**.

No.	δ_c [a,b,e]	δ_H [a,b] (mult., *J* in	COSY[a,b,c]	HMBC[a,d]	NOESY[a,b,c]
1	132.2, CH	5.50, br d (10.3)	2, 5a, 6	2, 3, 5, 6	2, 6, 7, 8a, 8b[w], 14
2	136.1, CH	5.62, br d (10.3)	1, 4a, 6	6	1, 15
3	70.2, qC				
4	38.7, CH_2	a: 1.84, m	5a, 5b	3	4b, 5b, 15
		b: 1.70, m	5a, 5b	3	4a
5	23.0, CH_2	a: 1.69, m	4a, 4b, 5b, 6		5b, 6
		b: 1.43, m	4a, 4b, 5a, 6		4a, 5a
6	41.0, CH	2.17, m	1, 2, 5a, 5b, 7		1, 5a, 7, 14
7	37.9, CH	1.53, m	6, 14		1, 6, 14
8	31.8, CH_2	a: 1.39, m	8b, 9a, 9b	7	8b
		b: 1.17, m	8a, 9a, 9b	7	8a
9	28.5, CH_2	a: 1.81, m	8a, 8b, 9b, 10		9b, 10, 12, 13
		b: 1.50, m	8a, 8b, 9a, 10		9a
10	81.3, CH	4.81, dd (1.8, 10.3)	9a, 9b	8, 9, 11, 16	9a, 9b, 12, 13, 17
11	72.7, qC				
12	25.5, CH_3	1.20, s		10, 11, 13	9a, 10, 17
13	26.0, CH_3	1.20, s		10, 11, 12	9a, 10, 17
14	16.3, CH_3	0.87, d (6.6)	7	6, 7, 8	1, 7, 8a, 8b, 9a
15	28.7, CH_3	1.25, s		2, 3, 4	2, 4a, 5b
16	172.9, qC				
17	21.0, CH_3	2.11, s		16	12, 13

[a]Methanol-d_4, 300/75 MHz. [b]Assignments are based on extensive 1D and 2D NMR measurements (HMBC, HSQC, COSY). [c]Numbers refer to proton resonances. [d]Numbers refer to carbon resonances. [e]Implied multiplicities determined by DEPT. [w]weak signal.

Figure 2. HMBC correlations of compound **1** and **2**

Stereochemistry

The relative configuration at C-3 and C-6 for compounds **1** and **2** was established by means of a NOESY measurement. NOESY correlations were observed between H_3-15 and H_a-4, between H_a-4 and both H_a-5 and H_b-5, and between H_a-5 and H-6 (Tables 1 and 2, Figure 2b) indicating methyl group CH_3-15 and proton H-6 to be on opposite sides of the molecule.

To determine the absolute configuration at C-3 and C-6 of compounds **1** and **2**, CD spectra were measured. Compounds **1** and **2** both revealed a negative Cotton effect at around 195 nm. This effect was compared with the Cotton effects of two reference compounds of known configuration, as seen in Figure 3 (spectroscopic description for reference compounds in Mori, 2006) which possess the same cyclohexene ring as compounds **1** and **2**, but without the extended side chain (C-7 to C-13). Comparing the CD effects, the absolute configuration of **1** and **2** has to be *S* at C-3, and hence *R* at C-6, as it was evident in a relative sense from the NOESY data. The configuration at C-7 for compounds **1** and **2** and at C-10 for compound **2** remains unresolved. Compounds **1** and **2** are new natural products for which the trivial names verticinol A (**1**) and B (**2**) are proposed.

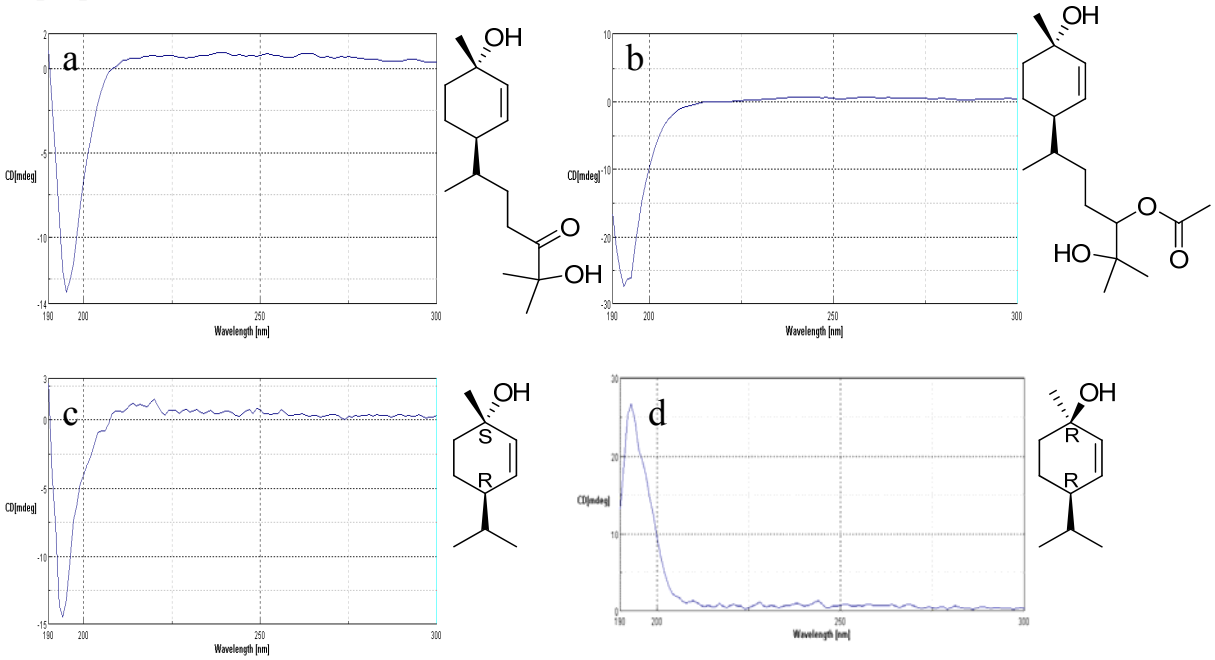

Figure 3: CD spectra of compound **1** (a), compound **2** (b), reference compounds (c) and (d). CD values for (c) (*c* 1.07 x 10^{-3} mol/L, MeOH) λ nm (Δε): 194 (-4.1); CD values for (d) (*c* 1.07 x 10^{-3} mol/L, MeOH) λ nm (Δε): 193 (+7.5).

Biological activity

Verticinol A was evaluated for cytotoxic activity against three cancer cell lines (NCI-H460, MCF7 and SF268, tested at 100 μM), two bacterial species (*Escherichia coli*, *Bacillus megaterium*) and three fungi (*Mycotypha microspora*, *Eurotium rubrum*, and *Microbotryum violaceum*), and the alga *Chlorella fusca* (at a dose of 50 μg/disc), but did not show any activity. Verticinol A was further evaluated for inhibition of HIV-1 and HIV-2 induced cytopathogenic effects in MT-4 cells (tested at 50 μg/mL), antiplasmodial activity against *Plasmodium berghei* (tested at 25 μM), and activity against both the Respiratory Syncytial virus (RSV) and the Influenza virus B (Flu B; tested at 100 μg/mL in both assays). However, no activity in any of the assays was found. Verticinol B was evaluated for cytotoxic activity against three cancer cell lines (NCI-H460, MCF7 and SF268, tested at 100 μM), two protein kinases DYRK1A and CDK5 inhibition activity assay (tested at 10 mM), and in the 3T3-L1 murine adipocytes assay (tested at 100 μg/mL). There was no activity in any of these assays.

Experimental section

General experimental procedures: See chapter 3 - General methodology.

Fungal material : See chapter 3 - General methodology.

Culture, extraction and isolation*:* A 10 L culture of *Verticillium tenerum* grown on solid biomalt medium (biomalt 20 g/L, 15 g/L agar) supplemented with sea salt was maintained during 2 months. An extraction with 5 L EtOAc yielded 980 mg extract which was subjected to a VLC fractionation in a silica open column using a gradient solvent system from PE to acetone, namely 10:1, 5:1, 2:1, 1:1, 100 % acetone and 100 % MeOH, in a total of six fractions. Fraction 3 was separated in a first step by using NP-HPLC with PE – acetone 7:2 to yield 10 subfractions. Subfraction 5 was purified utilizing RP-HPLC with MeOH-H_2O 70:30, which afforded the new compound **1** (3.0 mg, R.T. 9 min). Subfraction 9 was purified utilizing RP-HPLC with MeOH-H_2O (70:30) yielding subfraction 2, that required further purification utilizing RP-HPLC with MeOH-H_2O (80:20) to yield the new compound **2** (1.6 mg, R.T. 7 min.).

Verticinol A (1): Yellowish white oil (0.3 mg/L, 0.31 %); $[\alpha]^{23}_{D}$ -74.3 (c 0.23, acetone); UV (MeOH) λ_{max} (log ε): 204 (3.4); IR (ATR): 3376, 2931, 1706 cm^{-1}; CD (*c* 1.97 x 10^{-3} mol/L, MeOH) λ nm (Δε): 194 (-2.0); ^{1}H and ^{13}C NMR data: Table 1; EIMS: *m/z* 236 (6), 221 (3), 59 (100); HRMS (ESI, positive mode): *m/z* $(M\text{-}H_2O)^+$ calcd for $C_{15}H_{24}O_2$: 236.1776; found: 236.1776.

Verticinol B (2): Light yellow (0.16 mg/L, 0.16 %); $[\alpha]^{23}_{D}$ +32.6 (c 0.15, MeOH); UV (MeOH) λ_{max} (log ε): 204 (3.25); IR (ATR): 3390, 2928, 1716 cm^{-1}; CD (*c* 1.68 x 10^{-3} mol/L, MeOH) λ nm (Δε): 194 (-4.9); ^{1}H and ^{13}C NMR data: Table 2; EIMS: *m/z* 280 (10), 265 (5), 262 (2), 223 (7), 93 (44), 91 (18), 59 (42), 42 (100); HRMS (ESI, positive mode): *m/z* $(M\text{-}H_2O)^+$ calcd for $C_{17}H_{28}O_3$: 280.2038; found: 280.2040.

Biological activity: See chapter 3 - General methodology.

11. Discussion

The marine environment is a tremendous source of natural products. Moreover, many of the new compounds isolated from marine micro- and macroorganisms showed prominent biological effects, and some turned out to be valuable sources of lead structures for the development of promising anticancer drug candidates, e.g., the marine-fungal derived lead halimide (Kanoh *et al.*, 1997) or the tunicate-derived compound trabectedin (Rinehart, *et al.* 1990, Wright, *et al.* 1990).
The main goal of this study was the isolation, identification and biological evaluation of new marine-derived fungal natural products as potential drug leads, from which we report the isolation of 57 secondary metabolites. From these, 25 are new natural products and were isolated from three different fungal strains (further 10 novel N-methylated cyclic peptides are in structure elucidation procedures), confirming once more that endophytic marine-derived fungi are a valuable source of new and interesting secondary natural products.

Considerations on the present future of natural products research

Since the major pharmaceutical companies have terminated or considerably scaled down their natural product drug discovery projects in the 1990s and early 2000s, the academic research in this field is indispensable (Baker et al., 2007). The decline of natural product research in the pharmaceutical industry can be explained by an incompatibility of automated high throughput screening (HTS) programs and the time-consuming work on natural products extract libraries on the one hand, and on the other hand the development of combinatorial chemistry, which generates large so-called screen-friendly synthetic chemical libraries for supporting the HTS efforts (Koehn & Carter, 2005).

The interest of the pharmaceutical industry in some areas of natural products research have been kept or renewed, mainly on cancer research, which still cannot be effectively treated (Hill and Fenical, 2010). The natural products leadfinding success in this area is shown by the fact that 60% of all anticancer agents in clinical use are natural products

or derivatives thereof (Jacob, 2010; Newman and Cragg, 2007; Buttler, 2004). There is currently also a renewed interest from pharmaceutical companies in leadfinding new classes of antibiotics to overcome the growing problem of antibiotic resistance in many bacterial pathogens (Hill and Fenical, 2010; Jacob, 2010). The incredible potential of natural products as leads for new antibiotics is shown by the fact that for bacterial infections, about 80% of the medicines in clinical use are either natural products or derivatives thereof (Jacob, 2010; Newman and Cragg, 2007; Buttler, 2004).

Although we see nowadays a revival of leadfinding marine natural antibiotics, as observed in international natural products conferences, the major research in leadfinding new bioactive natural products is almost reduced to three countries USA, Germany and Japan, and only some isolated institutes spread worldwide. This means that natural products research is still performed by a low number of researchers, taking in consideration the size of pharmaceutical industry and the importance of natural products in society.

A low point in the worldwide research is the low cooperation between institutes isolating new natural products and institutes providing bioassays, as well as the motivation of a natural products chemist in finding bioassays for bioactivity attribution, after the demanding chemical work necessary. This work was heavily complemented with a worldwide cooperation with non-profit institutes and universities for bioassay experiments with agreements performed during research. If it is essential to know where to find valuable natural products, it is equally essential to have bioassays available. An organization connecting bioassay providers and natural product laboratories, where economic interests should be equally distributed according to the amount of work would be thus a solution.

Traditional cultivation and isolation of fungal-derived natural products is indeed time consuming, compound availability is very low and structural complexity can be very high, amongst other disadvantages (intellectual property issues, access to natural chemistry diversity, supply issues, methodological issues, dereplication, etc.) that make it unattractive for pharmaceutical industries, even if the starting biological material has great value. We believe that the rise of natural products research will not depend on funding, but in understanding the biology of microorganisms, which can increase the

rate of isolated new molecules derived from microorganisms, for which a multidisciplinary approach is needed (better than having a chemist, an ecologist, a microbiologist and a pharmacist working together, would be to have one single person with the basic knowledge in all these areas, creating thus a unique vision of nature). This, along with the development of low cost methods will attract funds and researchers to the field.

Furthermore it is necessary to focus on research areas applicable in a short/medium term to the generality of natural product research laboratories worldwide. There has been a great deal of efforts in developing tools for over expressing and discovering bioactive secondary metabolites, heterologous expression in microbial and plant cell cultures, metagenomics or new spectroscopic analytic methods. But low cost methods for the discovery of valuable natural products would lead to the integration of low funded laboratories worldwide in major pharmaceutical discoveries. For example metagenomics is nowadays a hot topic in the field. Its application in cases such as the chemical analysis of gene clusters isolated from unculturable bacteria is indeed state of the art and of unvaluable scientific interest. But these research areas are still (and will be on the next decades) too expensive, time consuming, uncertain regarding success of finding new natural products or in over-expressing pharmaceutically valuable natural products, hence it is promising but far from being a massive tool for academic/industrial natural products discovery. A more interesting approach would be to understand why the great majority of bacterial species are unculturable to this day, i.e. by discovering the biological needs of these bacterial species, one would create a low cost and probably globally applied methodology for the expression of natural products in culture-independent methods. It is considered obviously a huge barrier, but when overcome it would open a new (and applicable massively) world in natural products research.

Natural products laboratories also possess chemical libraries of known but rare compounds isolated in house. Though, many are kept in the freezer, when they should be tested for bioassays as quick as possible, not only because they may possess bioactivity holding the cure for a disease, but because they lose activity during time. Nowadays the field is focusing in leadfinding cytotoxic or antimicrobial new natural products. Though, if a new natural product does not have these biological properties, it

must be seen not as a dead lead, but as the starting point for the remaining immense biological assays available.

The future of natural products research will be considered again economically valuable when the pharmaceutical industry regains the interest on the field. Fast, low cost, and working on biological samples with high probabilities of finding valuable natural products are in need. The potential of other areas not commonly explored in this area should also be investigated, such as searching bioactive proteins from microorganisms. Another poorly understood world but biotechnologically extremely valuable is the study of bacteria associated with eucariotic organisms, mainly because the secondary metabolites produced by these prokaryotes may be the main reason for association/symbiosis, and these kind of associations work as a nature's pre-clinical trial, having thus these molecules more chances of being used for pharmaceutical applications.

12. Summary

The marine environment is distinguished by unique groups of organisms being the source of a wide array of fascinating structures. Marine microorganisms, such as fungi often occur associated with macroorganisms like algae, sponges or tunicates and produce secondary metabolites with novel structures and potential pharmaceutical significance. The goal of this study was the evaluation of new natural products of marine-derived fungi in order to find novel lead structures for drug development. To achieve this aim seven fungal strains living associated with marine algae and sponges were cultivated during 40 to 60 days, and the extracts tested for bioactivity. Subsequently, the natural products were isolated, their structures determined and their bioactivity established.

From algicolous and sponge-derived fungi, 35 new secondary metabolites were isolated, 14 of which display unprecedented carbon skeletons implying unknown biosynthetic reactions in fungi. All pure compounds were subjected to an extensive panel of bioactivity tests, in a total of around 850 individual biological activity assays against 111 bioactivity targets, from which antiproliferative, antiplasmodial and protease inhibitory properties, as well as affinity to receptors involved in psychoactive activity could be attributed.

The fungus *Stachylidium* sp. was isolated from the tropical marine sponge *Callyspongia* cf. *C. flammea.* This fungus yielded upon cultivation on marine media a plethory of polyketide- (marilines, marilones) and tyrosine-derived metabolites. The skeleton of marilines and marilones is most unusual, and its biosynthesis is suggested to require unusual biochemical reactions in fungal secondary metabolism.

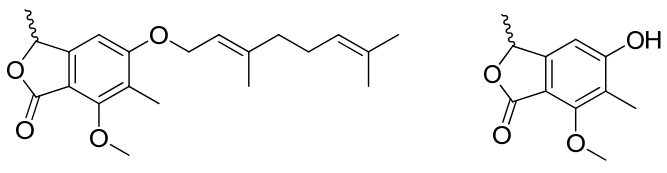

Figure 1. Structure formulae for marilones A and B

Ten new phthalide derivatives with unusual structural motives, i.e. marilones A – J were obtained. In the epimeric compounds marilones I and J the phthalide (=isobenzofuranone) nucleus is modified to an isobenzofuran ring

with ketal and acetal functionality. Marilone A was found to have antiplasmodial activity against *Plasmodium berghei* with an IC_{50} of 12.1 µM. Marilone B showed selective antagonistic activity towards the serotonin receptor 5HT2B with a K_i value of 7.7 µM.

Further chemical investigation of this marine-derived fungus led to the isolation of the novel phthalimidine derivatives marilines A - D. Both enantiomers marilines A and B inhibited human leucocyte elastase (HLE) with an IC_{50} value of 0.86 µM, and acetylcholinesterase (AChE) with IC_{50} values of 0.18 µM (offset = 49 %) and 0.63 µM (offset = 54 %), respectively.

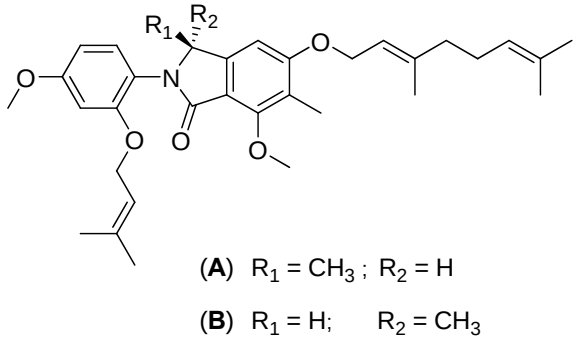

Figure 2. Structure formulae of Marilines A and B.

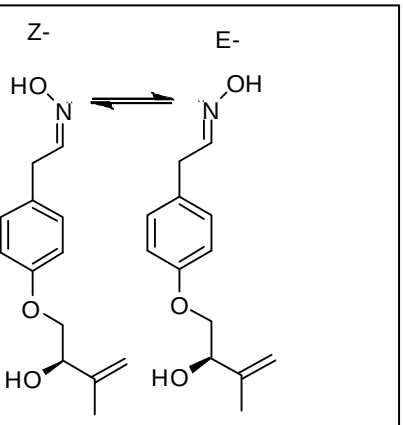

Figure 3. Structure formulae of Stachyline A

The diverse secondary metabolism of this fungal strain was additionally demonstrated by the identification of yet four further new, putatively tyrosine-derived natural products, i.e. stachylines A – D. The absolute configuration of these novel compounds was established by Mosher's method. Stachyline A possesses a rare terminal oxime group and occurs as an interchangeable mixture of *E*/*Z*-isomers.

In the more hydrophilic fractions of the fungal extract, ten N-methylated cyclic peptides, endolides A-J, could be found. The absolute configuration of these compounds and biological activity is currently under investigation.

Further novel compounds, to date with no pharmacological activity attributed, were retrieved from the fungus *Cadophora malorum*. This green alga derived fungus yielded four new hydroxylated sclerosporin derivatives, namely 15-hydroxysclerosporin, 12-hydroxysclerosporin, 11-hydroxysclerosporin and 8-hydroxysclerosporin, the absolute configuration of which was established by CD spectroscopy. Furthermore, the chemical investigation of *Verticillium tenerum* yielded the two new hydroxylated bisabolane-type sesquiterpenes verticinol A and B. The absolute configuration of the cyclohexenyl moiety within these metabolites was deduced by a combination of CD spectroscopy and NOESY measurements.

In conclusion, the chemical investigation of marine fungi living associated with algae and sponges led to new natural products, of which the marilines A and B represent the most unusual and unprecedented structural type. Also, this study identified molecules with potent bioactivity, e.g. the HLE and AChE inhibiting activity of marilines A and B.

The results of this study demonstrate that endophytic marine-derived fungi are producers of novel and pharmacologically relevant compounds.

References

Abbenante G. and Fairlie D.P., *Med. Chem.*, **2005**, 1, 71-104.

Abraham W.R., Hanssen H.P. and Urbasch I., *Z. Naturforsch. C*, **1991**, 46, 169-171.

Absalon M.J. and Smith F.O., *Expert Opin. Pharmacother.*, **2009**, 10, 1, 57-79.

Achenbach H., Mühlenfeld A. and Brillinger G.U., *Liebigs Ann. Chem.*, **1985**, 1596-1628.

Achilles K. and Bednarski P.J., *Biol. Chem.*, **2003**, 384, 817-824.

Akazawa T., Miljanich P. and Conn E.E., *Plant Physiol.*, **1960**, 35, 535-538.

Alvarado J.J., Nemkal A., Sauder J.M., Russell M., Akiyoshi D.E., Shi W., Almo S.C. and Weiss L.M., *Mol. Biochem. Parasit*., **2009**, 168, 2, 158-167.

Alves A., Junior J., Slana G., Cardoso J., Wang Q., Lopes R. and Lopes C., *Synthetic Comm.*, **2009**, 39, 3693-3709.

Amade P., Mallea M. and Bouaïcha, N., *J. Antibiot.*, **1993**, 47, 201-207.

Anchel M., Hervey A. and Robbins W.J., *Proc. Natl. Acad. Sci. U.S.A.*, **1950**, 36, 300-305.

Andersen J., *Agric. Food Chem.*, **1987**, 35, 1, 60-62.

Andersson R.J. and Williams D.E. In *Chemistry in Marine Environment*; Hester R.E., Harrison R.M. Eds.; The Royal Society of Chemistry: Cambridge, **2000**, 55.

Andreae M.O., *Mar. Chem.*, **1990**, 30, 1-29.

Arai K., Yasuji A. and Yamamoto Y., *Chem. Pharm. Bull.*, **1989**, 37, 3, 621-625.

Aronson J.K., An Account of the Foxglove and Its Medical Uses, 1785-1985, *London, New York, Oxford University Press*, *Oxford* 1985.

Asami Y., Kakeya H., Okada G., Toi M. and Osada, H., *J. Antibiotics.*, **2006**, 59, 724-728.

Awad G., Mathieu F., Coppel Y. and Lebrihi A., *Can. J. Microbiol.*, **2005**, 51, 59-67.

Ayer W.A. and Racok J.S., *Can. J. Chem.*, **1990**, 68, 2095-2101.

Ayer W.A., Lu P. and Orszanzka H., *J. Nat. Prod.*, **1993**, 56, 10, 1835-1838.

Baekelandt M., *Curr. Opin. Investig. Drugs*, **2002**, 3, 1517-1526.

Baker D.D., Chu M., Oza U. and Rajgarhia V., *Nat. Prod. Rep.*, **2007**, 24, 1225-1244.

Barnard D.L., Hill C.L., Gage T., Matheson J.E., Huffman J.H., Sidwell R.W., Otto M.I. and Schinazi R.F., *Antiviral Res.*, **1997**, 34, 27-37.

Barnard D.L., Huffman J.H., Meyerson L.R. and Sidwell R.W., *Chemotherapy*, **1993**, 39, 212-217.

Barrero A.F., Oltra J.E. and Poyatos J.A., *Phytochem.*, **1996**, 42, 5, 1427-1433.

Bauer A.W., Kirby W.M., Sherris J.C. and Turck M., *Am. J. Clin. Pathol.*, **1966**, 45, 4, 493-496.

Bedford C.T., Knittel P., Money T., Phillips G.T and Salisbur P., *Can. J. Chem.*, **1973**, 51, 694-697.

Bennett J.W. and Chung K-T., *Adv. Appl. Microbiol.*, **2001**, 49, 163-184.

Bérdy J., *J. Antibiotics*, **2005**, 58, 1-26.

Bernier S.G., Westlin W.F. and Hannig, G., *Drugs Future*, **2005**, 30, 497-508.

Bettayeb K., Oumata N., Echalier A., Ferandin Y., Endicott J.A., Galons H. and Meijer L., *Oncogene*, **2008**, 27, 5797-5807.

Bhadury P., Mohammad B.T. and Wright P.C., *J. Ind. Microbiol. Biotechnol*., **2006**, 33, 325-337.

Bieth J.G. In: Barrett A.J., Rawlings N.D. and Woessner J.F., *Handbook of Proteolytic Enzymes*, **1998**, Academic Press, San Diego Chapter 15.

Bingham J.P., Mitsunaga E. and Bergeron Z.L., *Chem. Biol. Interact.*, **2010**, 183, 1-18.

Birch A.J. and Hussain S.F., *J. Chem. Soc.*, **1969**, 1473-1474.

Bjarnholt N. and MØller B.L., *Phytochemistry*, **2008**, 69, 1947-1961.

Boesenken J., *Rec.Trav.Chim* (J.R.Neth Chem.Soc), **1939**, 53, 528.

Bosch F. and Banos J-E., *AINE*, **1998**, 2, 108-117.

Bouchillon S., Hoban D., Jordan A., Johnson B., Scangarella N., Shawar R and Johnson J., Retapamulin (SB-275833), a novel pleuromutilin–a multi-center global surveillance of activity against 3,797 beta and alpha hemolytic streptococci isolated from skin and skin structure infections (SSSIs). In: Abstracts and Proceedings of the 45th Interscience Conference on Antimicrobial Agents and Chemotherapy (ICAAC), Washington (DC), December 16-19, 2005. Washington (DC): American Society for Microbiology; 2005. p. 109. Abstract F-2061.

Brooks G., Burgess W., Colthurst D., Hinks J.D., Hunt E., Pearson M.J., Shea B., Takle A.K., Wilson J.M. and Woodnutt G., *Bioorg. Med. Chem.*, **2001**, 9, 1221-1231.

Bugni T.S. and Ireland C.M., *Nat. Prod. Rep*., **2004**, 21, 143-163.

Bull S.D., Davies S.G., Parkin R.M. and Sánchez-Sancho F.**,** *J. Chem. Soc.*, **1998**, 1, 2313-2320.

Burton A., *The Lancet Infect. Diseas.*, **2002**, 2, 9, 513.

Butler M.S., *J. Nat. Prod*., **2004**, 67, 12, 2141-2153

Buttler M.S., *Nat. Prod. Rep*., **2005**, 22, 162-195.

Buttler M.S., *Nat. Prod. Rep*., **2008**, 25, 475-516.

Calcul L., Inman W.D., Morris A.A., Tenney K., Ratnam J., McKerrow J.H., Valeriote F.A. and Crews P., *J. Nat. Prod*., **2010**, 73, 365-72.

Canel C., Moraes R.M., Dayan F.E. and Ferreira D., *Phytochemistry*, **2000**, 54, 115-120.

Chen Y.S., *Bull. Agr. Chem. Soc. Japan*, **1958**, 22, 136-142.

Chua F. and Laurent G.J., *Proc. Am. Thorac. Soc*., **2006**, 3, 424-427.

Chun E., Han C.K., Yoon J.H., Sim T.B., Kim Y.K. and Lee K.Y., *Int. J. Cancer.*, **2005**, 114, 124-130.

Cimino G., de Stefano S. and Minale L., *Experientia*, **1975**, 31, 756-757.

Crowden R.K. and Ralph B.J., *Aust. J. Chem*., **1961**, 14, 475-478.

Cuevas C., Perez M., Martin M.J., Chicharro J.L., Fernandez-Rivas C., Flores M., Francesch A., Gallego P., Zarzuelo M., de la Calle F., Garcia J., Polanco C., Rodriguez I. and Manzanares I., *Org. Lett.*, **2000**, 2, 2545-2548.

Datta B.K., Rahman M.M., Gray A.I., Nahar L., Hossein S.A., Auzi, A.A., Sarker S.D., *J. Nat. Med.* **2007**, 61, 391-396.

Daum R.S., Kar S. and Kirkpatrick P., *Nat. Rev. Drug Discov.*, **2007**, 6, 865-866.

Deng W-W., Ogita S. and Ashihara H., *Phytochem. Lett.*, **2008,** 1, 115-119.

Dewick P.M., *Medicinal Natural Products: A biosynthetic approach;* 3rd ed., John Wiley & Sons Ltd, Chichester, England, **2009**, 110-111.

Dey D., Pal B.C., Biswas T., Roy S.S., Bandyopadhyay A., Mandal S.K., Giri B.B. and Bhattacharya S., *Mol. Cell. Biochem.*, **2007**, 300, 1-2, 149-157.

Dickschat J.S., Bode H.B., Wenzel S.C., Müller R. and Schulz S., *ChemBioChem*, **2005a**, 6, 2023-2033.

Dickschat J.S., Helmke E. and Schulz S., *Chem. Biodiversity*, **2005b**, 2, 318-353.

Dickschat J.S., Wagner-Döbler I. and Schulz S., *J. Chem. Ecol.*, **2005**, 31, 925-947.

Dickschat J.S., Wenzel S.C., Bode H.B., Müller R. and Schulz S., *ChemBioChem*, **2004**, 5, 778-787.

Didier P.J., Phillips J.N., Kuebler D.J., Nasr M., Brindley P.J., Stovall M.E., Bowers L.C. and Didier, E.S., *Antimicrob. Agents Chemother.*, **2006**, 50, 2146-2155.

Dudler R. and Eberl L., *Curr. Opin. Biotech.*, **2006**, 17, 268-273.

El-Beih A.A., Kato H., Tsukamoto S. and Ohta T., *J. Nat. Med.*, **2007**, 61, 2, 175-177.

Engels F.K., Sparreboom A., Mathot R.A. and Verweij J., *Br. J. Cancer*, **2005**, 93, 2, 173-177.

Esper A.M. and Martin G.S., *Expert Opin. Investig. Drugs*, **2005**, 14, 633-645.

Eyberger A.L., Dondapati R. and Porter J.R., *J. Nat. Prod.*, **2006**, 69, 1121-1124.

Findlay J.A., Li G., Miller J.D. and Womiloju T.O., *Can. J. Chem.*, **2003**, 81, 284-292.

Flemning, F.F., *Nat. Prod. Rep.*, **1999**, 16, 597-606.

Fujii I., Ebizuka Y., *Chem. Rev.*, **1997**, 97, 2511-2523.

Fujita M., Yamada M., Nakajima S., Kawai K.I. and Nagai M., *Chem. Pharm. Bull.*, **1984**, 32, 2622-2627.

Fumoleau P., Trigo J., Campone M., Baselga J., Sistac F., Gimenez P., Manos L., Fontaine H., Semiond D., Sanderink G., Perard D. and Besenval M., Phase I and pharmacokinetics (PK) study of RPR 116258A given as a weekly 1-hour infusion at day 1, day 8, day 15, day 22 every 5 weeks in patients (pts) with advanced solid tumors.AACR-NCI-EORTC International Conference; October 29-November 2, **2001**; Miami Beach, FL. Abstract 282 and poster.

Ganesan A., *Curr. Opin. Chem. Biol.*, **2008**, 12, 306-317.

Garson M.J., Staunton J. and Jones P.G., *J. Chem. Soc.*, **1984**, 1021-1026.

Gaudilliere J-P., *Stud. Hist. Philos. Biol. Biomed. Sci.*, **2005**, 36, 612-644.

Gaur S., Newcomb R., Rivnay B., Bell J.R., Yamashiro D., Ramahandran J. and Miljanich, G.P., *Neuropharmacol.*, **1994**, 33, 1211-1219.

Gelmon K.A., Latreille J., Tolcher A., Génier L., Fisher B., Forand D., D'Aloisio S., Vernillet

L., Daigneault L., Lebecq A., Besenval M. and Eisenhauer E., *J. Clin. Oncol.*, **2000**, 18, 24, 4098-4108.

Geris R. and Simpson T. J., *Nat. Prod. Rep*. **2009,** 26, 1063-1094.

Ghuysen J-M., *Int. J. Antimicrob. Agents*, **1997**, 8, 45-60.

Glaser K.B. and Mayer A.M.S., *Biochem. Pharmacol*., **2009**, 78, 440-448.

Grimm A., Madduri K., Ali A. and Hutchinson C. R., *Gene*, **1994**, 151, 1-10.

Gurib-Fakim A., *Mol. Aspects Med.*, **2006**, 27, 1-93.

Gyimesi J., *Acta Chim. Hung. Tomus*, **1965**, 45, 323-328.

Haefner B., *Drug Discov. Today*, **2003***,* 8, 536-544.

Hamilton-Miller J.M.T., *Int. J. Antimicrob. Agents*, **2008**, 31, 189-192.

Harden E.A., Falshaw R., Carnachan S.M., Kern E.R. and Prichard M.N., *Antiviral Res.*, **2009**, 83, 282-289.

Harper K., Arif A., Ford E., Strobel G., Porco J., Tomer P., Oneill K., Heidere E. and Grant D., *Tetrahedron*, **2003,** 59, 2471-2476.

Hashimoto M., Komori T., Kamiya T., *J. Antibiot*., **1976**, 29, 890-901.

Herrero A.B., Martin-Castellanos C., Marco E., Gago F. and Moreno S., *Cancer Res.*, **2006**, 66, 8155-8162.

Hong, S.W., Han, H.E. and Chae, K.S., *J. Liq. Chrom.*, **1981**, 4, 285-292.

Horiuchi M., Maoka T., Iwase N. and Ohnishi K., *J. Nat. Prod.*, **2002**, 65, 8, 1204-1205.

Horiuchi M., Ohnishi K., Iwase N., Nakajima Y., Tounai K., Yamashita M. and Yamada Y., *Biosci. Biotechnol. Biochem*., **2003**, 67, 7, 1580-1583.

Hunt E., *Drugs Future*, **2000**, 25, 1163-1168.

Hutchinson C.R., *Chem. Rev*., **1997**, 97, 2525.

Ignelzi R.J. and Atkinson J.H., *Neurosurgery*, **1980**, 6, 584-590.

Ingavat N., Dobereiner J., Wiyakrutta S., Mahidol C., Ruchirawat S. and Kittakoop P., *J. Nat. Prod.*, **2009**, 72, 2049-2052.

Ingber D., Fujita T., Kishimoto S., Sudo K., Kanamaru T., Brem H. and Folkman J., *Nature*, **1990**, 348, 555-557.

Isaaki Y., Matsunaga S., Fusetani, N., *Tetrahedron*, **1993**, 49, 3749-3754.

Jacob E.J., *Drug Discov. Today*, **2010**, 15, 11-12, 409-410.

Jacobs M.R., Future Microbiol., 2007, 2, 591-600.

Ji Y., Bi J-N., Yan B. and Zhu X-D*., Chinese Journal of Biotechnology*, **2006**, 22, 1, 1-6.

Jinming G., Lin H. and Jikai L., *Steroids*, **2001**, 66, 771-775.

Kanoh K., Kohno S., Asari T., Harada T., Katada J., Muramatsu M., Kawashima H., Sekiya H. and Uno I., *Bioorg. Med. Chem. Lett.*, **1997**, 7, 2847-2852.

Kanoh K., Kohno S., Katada J., Hayashi Y., Muramatsu M. and Uno I., *Biosci. Biotechnol. Biochem.*, **1999a**, 63, 1130-1133.

Kanoh K., Kohno S., Katada J., Takahashi J. and Uno I., *J. Antibiot.*, **1999b**, 52, 134-141.

Kassianidis E., Pearson R.J., Philp D., *Org. Lett.*, **2005**, 7, 18, 3833-3836.

Katayama M., Marumo S. and Hattori H., *Tetrahedron Lett.*, **1983***,* 24, 1703-1706.

Kawagishi H., Ando M. and Mizuno T., *Tetrahedron Lett.*, **1990**, 31, 373-376.

Kawahara N., Nozawa K., Nakajima S., Udagawa S. and Kawai K., *Chem. Pharm. Bull.*, **1988**, 36, 398-400.

Kelly W.L. and Townsend C.A., *J. Am. Chem. Soc.*, **2002**, 124, 8186-8187.

Kelly W.L. and Townsend C.A., *J. Bacteriol.*, **2005**, 187, 739-746.

Kerr L.M. and Yoshikami D., *Nature*, **1984**, 308, 282-284.

Kim S.-K. and Wijesekara I., *J. of Functional Foods*, **2010**, 2, 1, 1-9.

Kim Y.M., An J.J., Jin Y.J., Rhee Y., Cha B.S., Lee H.C. and Lim S.K., *J. Mol. Endocrinol.*, **2007**, 38, 455-465.

Kitahara T., Kurata H., Matsuoka T., Mori K., *Tetrahedron*, **1985**, 41, 5475-5485.

Kitahara T., Matsuoka T., Katayama M., Marumo S. and Mori K., *Tetrahedron Lett.*, **1984**, 25, 4685-4688.

Klemke C., Kehraus S., Wright A.D. and König G.M., *J. Nat. Prod.*, **2004,** 67, 1058-1063.

Koehn F.E. and Carter G.T., *Nat. Rev. Drug Discov.*, **2005**, 4, 206-220.

König G.M. and Wright A.D., *Planta Medica*, **1996**, 62, 193-211.

Korba B.E. and Gerin J.L., *Antiviral Res*. **1992**, 19, 55-70.

Kruger E.A. and Figg W.D., *Expert Opin. Investig. Drugs.*, **2000**, 9, 1383-1396.

Kumaki Y., Day C.W., Wandersee M.K., Schow B.P., Madsen J.S., Grant D., Roth J. P., Smee D.F., Blatt L.M. and Barnard D.L., *Biochem. Biophys. Res. Commun.*, **2008**, 371, 110-113.

Laurent D., Guella G., Mancini I., Roquebert M.F., Farinole F., Pietra F., *Tetrahedron*, **2002**, 58, 9163-9167.

Laustsen G., Shaul M. and Short G., Retapamulin (altabax), *Nurse Pract.*, **2008**, 33, 15.

Laws P.E., Spark J.I., Cowled P.A. and Fitridge R.A., *Eur. J.Vasc. Endovasc*, **2004**, 27, 1, 6-16.

Lee H.S., Choi W.K., Son H.J., Lee S.S., Kim J.K., Ahn S.K., Hong C.I., Min H.K., Kim M. and Myung S.W., *Arch. Pharm. Res.*, **2004**, 27, 265-272.

Li E., Jiang L., Guo L., Zhang H. and Che Y., *Bioorg. & Med. Chem.*, **2008**, 16, 1, 7894-7899.

Lin G., Chan S. S-K., Chung H-S. and Li S-L., *Studies in Natural Products Chemistry Bioactive Natural Products (Part L)*, **2005**, 32, 12, 2005, 611-669.

Lu C., Bai L., Shen Y., *Chem. Nat. Compd.*, **2008**, 44, 5, 594-597.

Lu H.W., Chong C.R., Hu X. and Liu J.O., *J. Med. Chem.*, **2006**, 49, 5645-5648.

Marrapodi M. and Chiang J.Y.L., *J. Lipid Res*., **2000**, 41, 514-520.

MARTINDALE (database on the internet, www.micromedex.com). Cytarabine, Accessed December 1, **2009**. Micromedex Health Care, Martindale-The Complete Drug Reference.

MARTINDALE (database on the internet, www.micromedex.com). Vidarabine,. Accessed December 1, **2009**. Micromedex Health Care, Martindale-The Complete Drug Reference.

Matsumoto K., Nagashima K., Kamigauchi T., Kawamura Y., Yasuda Y., Ishii K., Uotani N., Sato T., Nakai H., Terui Y., Kikuchi J., Ikenisi Y., Yoshida T., Kato T. and Itayaki H., *J. Antibiot.*, **1995**, 48, 6, 439-446.

Mayer A.M.S., Glaser K.B., Cuevas C., Jacobs R.S., Kem W., Little R.D., McIntosh J.M., Newman D.J., Potts B. C. and Shuster D.E., *Trends Pharmacol. Sci*., **2010**, 31, 6, 255-265.

Mccloskey L., Zonis R., Broskey J., Biswas S., Pizzollo J., Jakielaszek C., Payne D. and Rittenhouse S., In-vitro spectrum of retapamulin activity against organisms associated with skin structure and community acquired infections. In: Abstracts and Proceedings of the 45th Interscience Conference on Antimicrobial Agents and Chemotherapy (ICAAC), Washington (DC), December 16-19, 2005. Washington (DC): American Society for Microbiology; **2005**. p. 109. Abstract F-2055.

McGivern J.G., *Drug Discov. Today*, **2006**, 11, 245-253.

McMorris T.C. and Anchel, M., *J. Am. Chem. Soc.*, **1965**, 87, 1594-1600.

McMorris T.C., Kelner M.J., Wang W., Yu J., Estes L.A. and Taetle R., *J. Nat. Prod.*, **1996**, 59, 896-899.

McMorris T.C., Yu J., Lira R., Dawe R., MacDonald J.R., Waters S.J. and Kelner M.J., *J. Org. Chem.*, **2001**, 66, 6158-6163.

Melnikova I. and Golden J., *Nat. Rev. Drug Discov.*, **2004,** 3, 993-994.

Miljanich G. P., *Curr. Med. Chem*., **2004,** 11, 3029-3040.

Monks A., Scudiero D., Skehan P., Shomaker R., Paull K., Vistica D. and Hose C., *J. Natl. Cancer Inst.*, **1991**, 83, 661-757.

Moreau A., Lorion M., Couture A., Deniau E. and Grandclaudon P., **2006**, *J. Org. Chem.*, 71, 8, 3303-3305.

Mori K., *Tetrahedron Asymmetry*, **2006**, 17, 2133-2142.

Moulton K.S., Heller E., Konerding, M.A., Flynn E., Palinski W. and Folkman J., *Circulation*, **1999**, 99, 1726-1732.

Moya P., Castillo M., Primo-Yúfera E., Couillaud F., Martínez-Máñez R., Garcerá M.-D., Miranda M.A., Primo J. and Martínez-Pardo R., *J. Org. Chem.*, **1997**, 62, 8544-8545.

Muelhaupt T., Kaspar H., Otto S., Reichert M., Bringmann G. and Lindel T., *Eur. J. Org. Chem.*, **2005**, 334-341.

Mutschler E., Geisslinger G., Kroemer H.K., Ruth P. and Schäfer-Korting M., Wissenschaftliche Verlagsgesellschaft, Stuttgart, **2008**, 419.

Nair M.G. and Burke B.A., *Phytochem*., **1988**, 27, 10, 3169-3173.

Nair M.G., Burke B.A., *Phytochemistry*, **1988**, 27, 3169-3173.

Namikoshi M., Murakami T., Fujiwara T., Nagai H., Niki T., Harigaya E., Watanabe M.F., Oda T., Yamada J. and Tsujimura S., *Chem. Res. Toxicol*., **2004**, 17,12, 1692-1696.

Neumann K., Kehraus S., Gütschow M. and König G.M., *Nat. Prod. Commun.* **2009**, 4, 347-354.

Newman D.J. and Cragg G.M., *J. Nat. Prod.*, **2007**, 70, 461-477.

Newman D.J., Cragg G.M. and Battershill C.N., *Diving Hyperb. Med.*, **2009**, 39, 216-225.

Newman D.J., Cragg G.M. and Snader K.M., *Nat. Prod. Rep.*, **2000**, 17, 215-234.

Nicholson B., Lloyd G.K., Miller B.R., Palladino M.A., Kiso Y., Hayashi Y. and Neuteboom S.T.C., *Anticancer drugs*, **2006**, 17, 25-31.

Nozawa Y., Ito M., Sugawara K., Kazunori H., Mizoue K., *J. Antib.*, **1997**, 50, 8, 641-645.

Ogawa K., Nakamura M., Hayashi M., Yaginuma S., Yamamoto S., Furihata K., Shin-Ya K. and Seto H., *J. Antibiot.*, **1995**, 48, 12, 1396-1400.

Olivera B.M., *Fusetani, N., ed.*, Basel, Karger, **2000**, 75-85.

Pannecouque C., Daelemans D., De Clercq E., *Nat. Protocols*, **2008**, 3, 427-434.

Paolucci C. and Rosini G., *Tetrahedron: Asymmetry*, **2007**, 18, 2923-2946.

Pham C.T., *Nat. Rev. Immunol*., **2006**, 6, 541.

Pinedo C., Wang C-M., Pradier J-M., Dalmais B., Choquer M., Le Pecheur P., Morgant G., Collado I.G., Cane D.E., Viaud M., *ACS Chemical Biology*, **2008**, 3, 791-801.

Pollak F.C. and Berger R.G., *Appl. Environ. Microbiol.*, **1996**, 62, 1295-1299.

Pommier Y., Kohlhagen G., Bailly C., Waring M., Mazumber A. and Kohn K.W., *Biochemistry*, **1996**, 35, 13303-13309.

Prudêncio M., Rodrigues C.D., Ataide R. and Mota M.M., *Cell Microbiol.*, **2008**, 10, 218-224.

Psychoactive receptors: For experimental details see http://pdsp.med.unc.edu/UNC-CH%20Protocol%20Book.pdf

Puri S.C., Verma V., Amna T., Qazi G.N. and Spiteller M., *J. Nat. Prod.*, **2005**, 68, 1717-1719.

Rauck R.L., Wallace M.S., Burton A.W., Kapural L. and North J.M., *Pain Pract.*, **2009**, 9, 327-337.

Rinehart K.L., Holt T.G., Fregeau N.L., Stroh J.G., Kieffer P.A., Sun F., Li L.H. and Martin D.G., *J. Org. Chem.*, **1990**, 55, 4512-4515, (Original isolation); (Erratum): Rinehart K.L., Holt T.G., Fregeau N.L., Stroh J.G., Kieffer P.A., Sun F., Li L.H. and Martin D.G., *J. Org. Chem.*, **1991**, 56, 1676.

Roggo B.E., Petersen F., Sills M., Roesel J.L., Moerker T. and Peter H.H., **1996**, *J. Antibiot (Tokyo)*, 49, 1, 13-19.

Saroglou V., Karioti A., Demetzos C., Dimas K. and Skaltsa H., *J. Nat. Prod.*, **2005**, 68, 1404-1407.

Sasaoka K., Ogawa T., Tsuji H. and Bando N., *Biochi. Biophys. Acta,* **1980**, 630, 137-140.

Sashidhara K.V., White K.N. and Crews, P., *J. Nat. Prod.*, **2009**, 72, 588-603.

Sawai K., Okuno T. and Yoshkawa E., *Agric. Biol. Chem.*, **1985**, 49, 2501-2503.

Schmitz R. F., *Pharm. Hist.*, **1985**, 27, 61-74.

Schneider G., Anke H. and Sterner O., *Z. Naturforsch C*, **1996**, 51, 11-12, 802-806.

Schneider P., Misiek M. and Hoffmeister D., *Mol. Pharm.,* **2008**, 5, 234-242.

Schöller E.G., Gürtler H., Pedersen R., Molin S. and Wilkins K., *J. Agric. Food Chem.*, **2002**, 50, 2615-2621

Schuh, H., *Die Zeit*, **2008**, 34, 31.

Schulte K.E., Ruccker G. and Fachmann H., *Tetrahedron Lett*., **1968**, 4763-4764.

Schulz S. and Dickschat J.S., *Nat. Prod. Rep.*, **2007**, 24, 814-842.

Schulz B., Boyle C., Draeger S., Rommert A.K. and Krohn K., *Mycol. Res.*, **2002**, 106, 996-1004.

Schulz B., Sucker J., Aust H.-J., Krohn K., Ludewig K., Jones P.G. and Döring D., *Mycol. Res.*, **1995**, 99, 1007-1015.

Schumacher M., Cerella C., Eifes C., Chateauvieux S., Morceau F., Jaspars M., Dicato M. and Diederich M., *Biochem. Pharmacol.*, **2010**, 79, 4, 2010, 610-622.

Seale A.P., de Jesus L.A., Kim Se-Y. , Choi Y-H. , Lim H.B., Hwang C-S. and Kim Y-S., *Biotechnol*. *Lett*., **2005**, 27, 4, 221-225.

Seibert S.F., Eguereva E., Krick A., Kehraus S., Voloshina E., Raabe G., Fleischhauer J., Leistner E., Wiese M., Prinz H., Alexandrov K., Janning P., Waldmann H. and König G.M*., Org. Biomol. Chem.*, **2006**, 4, 2233-2240.

Seiden M.V., Gordon A.N., Bodurka D.C., Matulonis U.A., Penson R.T., Reed E., Alberts D.S., Weems G., Cullen M. and McGuire W.P., *Gynecol. Oncol.*, **2006**, 101, 55-61.

Sells M.A., Zelent A.Z., Shvartsman M. and Acs G., *J. Virol*., **1988**, 62, 2836-2844.

Sessa C., Cuvier C., Caldiera S., Bauer J., Van den Bosch S., Monnerat C., Semiond D., Pérard D., Lebecq A., Besennval M. and Marty M., *Ann Oncol*., **2002**, 13, 7, 1140-1150.

Shimokawa K., Iwase Y., Miwa R., Yamada K. and Uemura D., *J. Med. Chem.*, **2008,** 51, 5912-5914.

Shindo K., Yiuji Y., Yukiko O. and Kawai H., *J. Antibiot.* **1994**, 48, 1072-1074.

Shiner E.K., Rumbaugh K.P. and Williams S.C*., FEMS Microbiol. Rev.*, **2005**, 29, 935-947.

Sibbesen O., Koch B., Halkier B.A. and Moller B.L., *J. Biol. Chem.*, **1995**, 270, 3506-3511.

Sidwell R.W. and Smee D.F., *Antiviral Res*., **2000**, 48, 1-16.

Simunovic V., Zapp J., Rachid S., Krug D., Meiser P. and Müller R., **2006**, *Chembiochem.*, 7, 8, 1206-1220.

Smee D.F., Burger R.A., Warren R.P., Bailey K.W. and Sidwell, R.W., *Antiviral Chem. Chemother.*, **1997**, 8, 573-581.

Smith G., *Biochem. J.*, **1952**, 50, 629.

Smith S., *J. Chem. Soc.*, **1930**, 508-510.

Sperandio V., *Trends Immunol*., **2004**, 25, 505-507.

Staats P.S., Yearwood T., Charapata S.G., Presley R.W., Wallace M.S., Byas-Smith M., Fisher R., Bryce D.A., Mangieri E.A., Luther R.R., Mayo M., McGuire D. and Ellis D., *J. Am. Med. Assoc*., **2004**, 291, 63-70.

Stadler M., Anke H., Sterner O., *Tetrahedron*, **1994**, 50, 12649-12654.

Stevens T., Johnson B., Bouchillon S., Hoban D., Scangarella N., Shawar R., Johnson J. and Badal, R., A multi-center global surveillance study of the in vitro activity of retapamulin (SB-275833), a novel topical pleuromutilin against 2,939 clinical isolates of S. aureus and coagulase negative staphylococci from uncomplicated skin and skin structure infections (SSSIs). In: Abstracts and Proceedings of the 45th Interscience Conference on Antimicrobial Agents and Chemotherapy (ICAAC), Washington (DC), December 16-19, **2005**. Washington DC: American Society for Microbiology; 2005. p. 109. Abstract F-2062

Stierle A., Hershenhorn J. and Strobel G., *Phytochemistry*, **1993**, 32, 5, 1145-1149.

Stierle A., Strobel G. and Stierle D., *Science*, **1993**, 260, 214-216.

Stierle A.A., Stierle D.B., Goldstein E., Parker K., Bugni T., Baarson C., Gress J. and Blake D., *J. Nat. Prod.* **2003**, 66, 1097-1100.

Strobel G. and Daisy B., *Microbiol. Mol. Biol. Rev.*, **2003**, 67, 491-502.

Strobel G., Daisy B., Castillo U. and Harper J., *J. Nat. Prod.*, **2004**, 67, 257-268.

Strobel G.A., Ford E., Worapong J., Harper J.K., Arif A.M., Grant D.M., Fung P. and Chau R.M.W., *Phytochemistry*, **2002**, 60, 179-183.

Stuck T.L., Assink B.K., Bates R.C., Erman D.T., Fedij V., Jennings S.M., Lassig J.A., Smith R.J. and Smith T.L., *Org. Proc. Res. Dev.,* **2003**, 7, 6, 851-855.

Suemitsu R., Ohnishi K., Horiuchi M., Kitaguchi A. and Odamura K., *Phytochemistry*, **1992**, 31, 7, 2325-2326.

Suemitsu R., Ohnishi K., Morikawa Y. and Nagamoto S., *Phytochemistry*, **1995**, 38, 495-497.

Suzuki E., Sekizaki H. and Inoue S., *J. Chem. Soc. Chem. Comm.*, **1973**, 16, 568.

Taggart C.C., Greene C.M., Carroll T.P., O'Neill S.J. and McElvaney N.G., *Am. J. Respir. Crit. Care Med.*, **2005**, 171, 1070-1076.

Takeo T., *Phytochemistry*, **1974**, 13, 1401-1406

Tanaka Y., Sato H., Kageyu A. and Tomita T., *J. Chromatogr.*, **1985**, 347, 275-283.

Tennant, G. *Comprehensive Organic Chemistry, The Synthesis and Reaction of Organic Compounds*; Barton, D.; Ollis, W. D.; Eds. Pergamon Press: Oxford, **1979**, Vol 2, Chapter 8, 383-590.

Thomas X., *Expert Opin. Pharmacother.*, **2009**, 10, 221-237.

Tsuji H., Bando N., Tadashi O. and Sasaoka K., *Biochi. Biophys. Acta*, **1981**, 677, 326-329

Tsuji H., Ogawa T., Bando N. and Sasaoka K., *Biochem Biophys. Res. Comm.*, **1985b**, 130, 2, 633-639.

Tsuji H., Ogawa T., Bando N. and Sasaoka K., *Biochi. Biophys. Acta*, **1985a**, 840, 287-290.

Turner W.B., Polyketides In Fungal Metabolites, Academic press, London, **1971**, 38, 173-175.

Tziveleka L-A., Constantinos V. and Vassilios R., *Curr. Top. Med. Chem.*, **2003**, 3, 1512-1535.

Vane J.R., *Nat. New Biol.*, **1971**, 231, 232-235.

Vender R.L., *J. Invest. Med*, **1996**, 44, 531-539.

Venkateswarlu Y., Reddy N.S., Ramesh P. and Rao J.V., *Biochem. Syst. Ecol.*, **1999**, 27, 519-520.

Verweij J., *J. Clin. Oncol.*, **2009**, 27, 3085-3087.

Vrignaud P., Chiron M., Stackhouse M.A., Zuany-Amorim C., Goulaouic H. and Bissery M-C, In vivo synergy between trastuzumab (Herceptin®) and larotaxel (RPR 109881A), a new taxoid. Presented at 98th Annual AACR meeting; April 14-18, **2007**; Los Angeles, CA. Abstract 1432.

Vrignaud P., Lejeune P. and Bissery M-C, In vivo synergy between doxorubicin, cisplatin or vinorelbine and RPR 109881A, a new taxoid. Poster presented at 96th Annual AACR meeting; April 16-20, **2005**; Anaheim, CA. Abstract 3414.

Wang J., Li G., Lu H., Zheng Z., Huang Y. and Su W., *FEMS Microbiology Letters*, **2000**, 193, 2, 249-253.

Wang Y.X., Gao D., Pettus M., Phillips C. and Bowersox S. S., *Pain*, **2000**, 84, 271-281.

Weissman K.J., Bycroft M., Staunton J. and Leadlay P.F., *Biochem*., **1998**, 37, 11012-11017.

Wilkins K., *Chemosphere*, **1996**, 32, 1427-1434.

Wolfgang K. and Kund K., *J. Org. Chem*., **1990**, 55, 2325-2332.

Woynarowska B.A., Woynarowski J.M., Herzig M.C.S., Roberts K., Higdon A.L. and MacDonald J.R., *Biochem. Pharmacol.*, **2000**, 59, 1217-1226.

Wright A.E., Forleo D.A., Gunawardana G.P., Gunasekera S.P., Koehn F.E. and McConnell O.J., *J. Org. Chem.*, **1990**, 55, 4508-4512.

Yang X., Strobel G., Stierle A., Hess W.M., Lee J. and Clardy J., *Plant Sci.*, **1994**, 102, 1, 1-9.

Yap T.A., Carden C.P. and Kaye S.B., *Nat. Rev. Cancer*, **2009**, 9, 167-181.

Yoshimoto A., Matzuzawa T., Oki T., Takeuchi T. and Umezawa H., *J. Antibiot.*, **1981**, 34, 951.

Yue J-M., Chen S-N., Lin Z-W. and Sun H-D., *Phytochemistry*, **2001**, 56, 8, 801-806.

Zhan P., Liu X., Fang Z., Pannecouque C. and De Clercq E., *Bioorg. Med. Chem.*, **2009**, 17, 6374-6379.

Zhang Y., Yeh J.R., Mara A., Ju R., Hines J.F., Cirone P., Griesbach H.L., Schneider I., Slusarski D.C., Holley S.A. and Crews C.M., *Chem. Biol.*, **2006**, 13, 1001-1009.

Zikmundova M., Drandarov K., Hesse M., Werner C., *Z Naturforsch.*, **2002**, 57C, 660-665.

13. APPENDIX

13.1. Bioactivity data

Marilines

Figure 1. HLE protease inhibition activity assay results for mariline A (W223_A) and mariline B (W223_B). Calculated IC_{50}values in table 7.

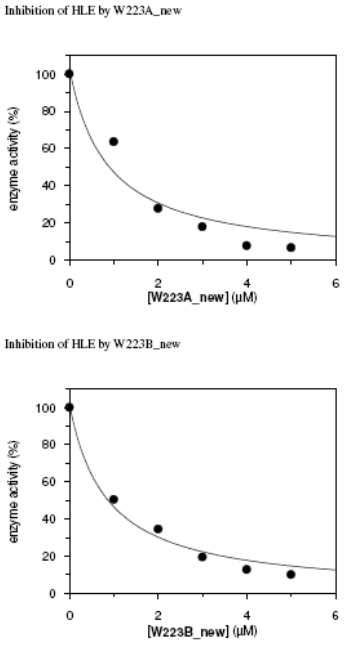

Figure 2. ACEase protease inhibition activity assay results for mariline A (W223_A) and mariline B (W223_B). Calculated IC_{50} values in table 7.

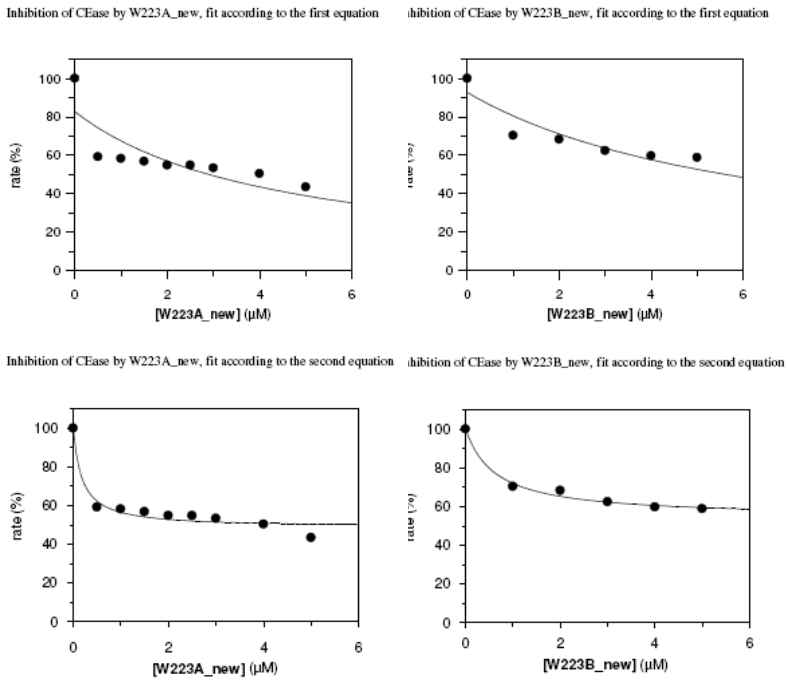

Table 1. Antiproliferative activity results of mariline A against 5 cancer cell lines

Growth delaying activity (represented by GI_{50}), cytostatic activity (represented by TGI) and cytotoxic activity (represented by LC_{50}) were observed. GI_{50} is different than the IC_{50} in that it contains a correction for the starting population. Results in μM.

CEL LINES		Mariline A
NCI-H460	*GI50*	29,6
	TGI	60,1
	LC5	90,7
MCF7	*GI50*	6,9
	TGI	33,5
	LC5	81,0
SF268	*GI50*	25,3
	TGI	56,0
	LC5	86,6
A549	*GI50*	30,8
	TGI	73,4
	LC5	>100
PC3	*GI50*	29,6
	TGI	80,7
	LC5	<100

cancer cell lines: NCI-H460/lung, A549/lung, MCF7/breast and SF268/CNS and CAKI/renal. Averge values in Table 6.

Figure 3. Mean graph for antiproliferative activity against 19 cancer cells of mariline B

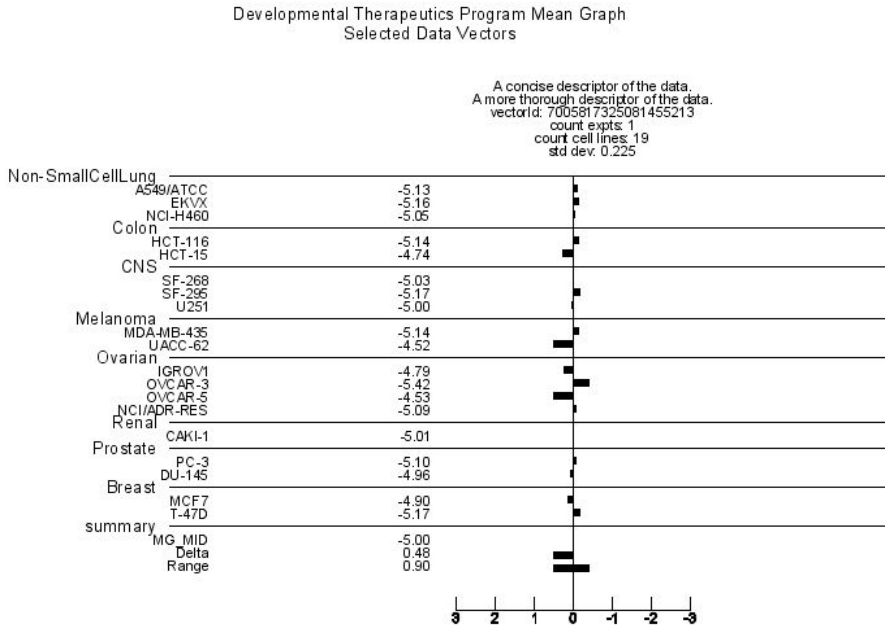

(GI50s of cell lines are represented as bars vs. the mean of all GI50s (average of all GI50s). Bars to the left denote the sensitive cell lines, those to the right the resistant.)

Table 2. Pairwise coefficient correlations (PCC) of the COMPARE data analysis of mariline B with the synthetic compounds database.

Rank	Correlation	namecode	Seed Vector Ident For Display	Seed Vector descriptor For Display	Target Vector Ident For Display	Target Vector descriptor For Display	Count Common Cell Lines	Seed Standard Deviation	Target Standard Deviation
1	0.807	PUBLIC	A concise descriptor of the data.	A more thorough descriptor of the data.	NSC:S717844 Endpt:GI50 ExpId:AVGDATA hiConc:-4.0		19	0.219	0.17
2	0.801	PUBLIC	A concise descriptor of the data.	A more thorough descriptor of the data.	NSC:S736281 Endpt:GI50 ExpId:AVGDATA hiConc:-4.0		18	0.225	0.121
3	0.785	PUBLIC	A concise descriptor of the data.	A more thorough descriptor of the data.	NSC:S710284 Endpt:GI50 ExpId:AVGDATA hiConc:-4.0		19	0.219	0.204
4	0.777	PUBLIC	A concise descriptor of the data.	A more thorough descriptor of the data.	NSC:S720423 Endpt:GI50 ExpId:AVGDATA hiConc:-4.0		19	0.219	0.159
5	0.771	PUBLIC	A concise descriptor of the data.	A more thorough descriptor of the data.	NSC:S720458 Endpt:GI50 ExpId:AVGDATA hiConc:-4.0		19	0.219	0.161
6	0.743	PUBLIC	A concise descriptor of the data.	A more thorough descriptor of the data.	NSC:S683691 Endpt:GI50 ExpId:AVGDATA hiConc:-4.0		18	0.225	0.313
7	0.727	PUBLIC	A concise descriptor of the data.	A more thorough descriptor of the data.	NSC:S690404 Endpt:GI50 ExpId:AVGDATA hiConc:-4.0		17	0.23	0.178
8	0.724	PUBLIC	A concise descriptor of the data.	A more thorough descriptor of the data.	NSC:S715368 Endpt:GI50 ExpId:AVGDATA hiConc:-4.0		19	0.219	0.176
9	0.724	PUBLIC	A concise descriptor of the data.	A more thorough descriptor of the data.	NSC:S666234 Endpt:GI50 ExpId:AVGDATA hiConc:-4.0		16	0.229	0.203
10	0.723	PUBLIC	A concise descriptor of the data.	A more thorough descriptor of the data.	NSC:S638478 Endpt:GI50 ExpId:AVGDATA hiConc:-4.0	INOSTAMYCIN	18	0.221	0.437
1	-0.783	PUBLIC	A concise descriptor of the data.	A more thorough descriptor of the data.	NSC:S117199 Endpt:GI50 ExpId:AVGDATA hiConc:-4.0		19	0.219	0.127
2	-0.759	PUBLIC	A concise descriptor of the data.	A more thorough descriptor of the data.	NSC:S730139 Endpt:GI50 ExpId:AVGDATA hiConc:-4.0		19	0.219	0.178
3	-0.747	PUBLIC	A concise descriptor of the data.	A more thorough descriptor of the data.	NSC:S676886 Endpt:GI50 ExpId:AVGDATA hiConc:-4.0		19	0.219	0.131

Table 3. Pairwise coefficient correlations (PCC) of the COMPARE data analysis of mariline B with the diversity set database.

Rank	Correlation	namecode	Seed Vector Ident For Display	Seed Vector descriptor For Display	Target Vector Ident For Display	Target Vector descriptor For Display	Count Common Cell Lines	Seed Standard Deviation	Target Standard Deviation
1	0.69	PUBLIC	A concise descriptor of the data.	A more thorough descriptor of the data.	NSC:S120672 Endpt:GI50 Expid:AVGDATA hiConc:-4.0		19	0.219	0.132
2	0.676	PUBLIC	A concise descriptor of the data.	A more thorough descriptor of the data.	NSC:S320852 Endpt:GI50 Expid:AVGDATA hiConc:-4.0		19	0.219	0.212
3	0.613	PUBLIC	A concise descriptor of the data.	A more thorough descriptor of the data.	NSC:S629659 Endpt:GI50 Expid:AVGDATA hiConc:-4.0		19	0.219	0.135
4	0.61	PUBLIC	A concise descriptor of the data.	A more thorough descriptor of the data.	NSC:S128166 Endpt:GI50 Expid:AVGDATA hiConc:-4.0		19	0.219	0.219
5	0.599	PUBLIC	A concise descriptor of the data.	A more thorough descriptor of the data.	NSC:S118836 Endpt:GI50 Expid:AVGDATA hiConc:-4.0		19	0.219	0.193
6	0.597	PUBLIC	A concise descriptor of the data.	A more thorough descriptor of the data.	NSC:S73109 Endpt:GI50 Expid:AVGDATA hiConc:-4.0		19	0.219	0.157
7	0.574	PUBLIC	A concise descriptor of the data.	A more thorough descriptor of the data.	NSC:S17776 Endpt:GI50 Expid:AVGDATA hiConc:-4.0		19	0.219	0.15
8	0.571	PUBLIC	A concise descriptor of the data.	A more thorough descriptor of the data.	NSC:S3753 Endpt:GI50 Expid:AVGDATA hiConc:-4.0		19	0.219	0.137
9	0.569	PUBLIC	A concise descriptor of the data.	A more thorough descriptor of the data.	NSC:S309881 Endpt:GI50 Expid:AVGDATA hiConc:-4.0		19	0.219	0.221
10	0.567	PUBLIC	A concise descriptor of the data.	A more thorough descriptor of the data.	NSC:S56452 Endpt:GI50 Expid:AVGDATA hiConc:-4.0		19	0.219	0.341
1	-0.783	PUBLIC	A concise descriptor of the data.	A more thorough descriptor of the data.	NSC:S117199 Endpt:GI50 Expid:AVGDATA hiConc:-4.0		19	0.219	0.127
2	-0.668	PUBLIC	A concise descriptor of the data.	A more thorough descriptor of the data.	NSC:S44677 Endpt:GI50 Expid:AVGDATA hiConc:-4.0	1H-INDAZOL-3-AMINE (9CI)	19	0.219	0.08
3	-0.595	PUBLIC	A concise descriptor of the data.	A more thorough descriptor of the data.	NSC:S90630 Endpt:GI50 Expid:AVGDATA hiConc:-4.0		19	0.219	0.18

Table 4. Pairwise coefficient correlations (PCC) of the COMPARE data analysis of mariline B with the marketed drugs database.

Rank	Correlation	namecode	Seed Vector Ident For Display	Seed Vector descriptor For Display	Target Vector Ident For Display	Target Vector descriptor For Display	Count Common Cell Lines	Seed Standard Deviation	Target Standard Deviation
1	0.284	PUBLIC	A concise descriptor of the data.	A more thorough descriptor of the data.	NSC:S256942 Endpt:GI50 Expid:AVGDATA hiConc:-4.0	EPIRUBICIN HCL	17	0.229	0.476
2	0.266	PUBLIC	A concise descriptor of the data.	A more thorough descriptor of the data.	NSC:S122758 Endpt:GI50 Expid:AVGDATA hiConc:-4.0	RETINOIC ACID (9CI)	19	0.219	0.502
3	0.243	PUBLIC	A concise descriptor of the data.	A more thorough descriptor of the data.	NSC:S123127 Endpt:GI50 Expid:AVGDATA hiConc:-4.0	doxorubicin (Adriamycin)	19	0.219	0.869
4	0.225	PUBLIC	A concise descriptor of the data.	A more thorough descriptor of the data.	NSC:S19893 Endpt:GI50 Expid:AVGDATA hiConc:-4.0	5-fluorouracil	19	0.219	0.877
5	0.224	PUBLIC	A concise descriptor of the data.	A more thorough descriptor of the data.	NSC:S628503 Endpt:GI50 Expid:AVGDATA hiConc:-6.0	TAXOTERE	17	0.228	0.921
1	-0.301	PUBLIC	A concise descriptor of the data.	A more thorough descriptor of the data.	NSC:S409962 Endpt:GI50 Expid:AVGDATA hiConc:-3.3	BCNU	19	0.219	0.188
2	-0.229	PUBLIC	A concise descriptor of the data.	A more thorough descriptor of the data.	NSC:S123127 Endpt:GI50 Expid:AVGDATA hiConc:-5.6	doxorubicin (Adriamycin)	19	0.219	0.907
3	-0.223	PUBLIC	A concise descriptor of the data.	A more thorough descriptor of the data.	NSC:S613327 Endpt:GI50 Expid:AVGDATA hiConc:-4.0	GEMZAR (LILLY)	19	0.219	1.336
4	-0.218	PUBLIC	A concise descriptor of the data.	A more thorough descriptor of the data.	NSC:S25154 Endpt:GI50 Expid:AVGDATA hiConc:-3.3	pipobroman	18	0.221	0.229
5	-0.207	PUBLIC	A concise descriptor of the data.	A more thorough descriptor of the data.	NSC:S3088 Endpt:GI50 Expid:AVGDATA hiConc:-3.1	chlorambucil	19	0.219	0.286

Table 5. Pairwise coefficient correlations (PCC) of the COMPARE data analysis of mariline B with the standard agents database

(Standard agents represent a set of compounds with known mechanism of action. PCC>0.6 gives a first prediction for a putative mechanism of action. PCC is used to measure the similarity degree of the experimental drug (=seed) vs. those of the databases used. Any PCC greater or equal to 0.6 is considered as positive match. The closer to 1 the PCC the greatest the similarity).

Rank	Correlation	namecode	Seed Vector Ident For Display	Seed Vector descriptor For Display	Target Vector Ident For Display	Target Vector descriptor For Display	Count Common Cell Lines	Seed Standard Deviation	Target Standard Deviation
1	0.427	PUBLIC	A concise descriptor of the data.	A more thorough descriptor of the data.	NSC:S332598 Endpt:GI50 Expid:AVGDATA nlConc:-4.0	rhizoxin	18	0.221	0.545
2	0.422	PUBLIC	A concise descriptor of the data.	A more thorough descriptor of the data.	NSC:S332598 Endpt:GI50 Expid:AVGDATA nlConc:-9.0	rhizoxin	17	0.225	0.843
3	0.388	PUBLIC	A concise descriptor of the data.	A more thorough descriptor of the data.	NSC:S32946 Endpt:GI50 Expid:AVGDATA nlConc:-4.0	methyl-GAG	19	0.219	0.304
4	0.368	PUBLIC	A concise descriptor of the data.	A more thorough descriptor of the data.	NSC:S7365 Endpt:GI50 Expid:AVGDATA nlConc:-3.6	DON	18	0.221	0.345
5	0.353	PUBLIC	A concise descriptor of the data.	A more thorough descriptor of the data.	NSC:S133100 Endpt:GI50 Expid:AVGDATA nlConc:-4.0	rifamycin SV	19	0.219	0.292
6	0.334	PUBLIC	A concise descriptor of the data.	A more thorough descriptor of the data.	NSC:S349438 Endpt:GI50 Expid:AVGDATA nlConc:-2.0	4-Ipomeanol	19	0.219	0.134
7	0.311	PUBLIC	A concise descriptor of the data.	A more thorough descriptor of the data.	NSC:S77037 Endpt:GI50 Expid:AVGDATA nlConc:-4.3	D-tetrandrine	18	0.221	0.141
8	0.307	PUBLIC	A concise descriptor of the data.	A more thorough descriptor of the data.	NSC:S77037 Endpt:GI50 Expid:AVGDATA nlConc:-4.0	D-tetrandrine	18	0.225	0.273
9	0.291	PUBLIC	A concise descriptor of the data.	A more thorough descriptor of the data.	NSC:S322921 Endpt:GI50 Expid:AVGDATA nlConc:-2.7	pibenzimol hydrochloride	18	0.223	0.906
10	0.281	PUBLIC	A concise descriptor of the data.	A more thorough descriptor of the data.	NSC:S32946 Endpt:GI50 Expid:AVGDATA nlConc:-2.6	methyl-GAG	18	0.221	0.493
1	-0.601	PUBLIC	A concise descriptor of the data.	A more thorough descriptor of the data.	NSC:S37364 Endpt:GI50 Expid:AVGDATA nlConc:-3.3	O6-methylguanine	18	0.221	0.261
2	-0.496	PUBLIC	A concise descriptor of the data.	A more thorough descriptor of the data.	NSC:S284356 Endpt:GI50 Expid:AVGDATA nlConc:-3.6	miltindomide	18	0.223	0.331
3	-0.441	PUBLIC	A concise descriptor of the data.	A more thorough descriptor of the data.	NSC:S237020 Endpt:GI50 Expid:AVGDATA nlConc:2.6	largomycin	18	0.219	0.337

Figure 4 a-c. Antiplasmodial activity data for marilines A and B

Bioactivity test relates to the inhibition of the infection of *Plasmodium berghey* on the liver stage. The parasite expresses luciferase, thus the infection is measured by luminescence (Bars); the cellular density (i.e. the non-toxicity of the compounds) is measured by fluorescence. The tests were performed in quadruplicate measurements per compound. Samples were dissolved in acetone which was also tested alone. Results show that the solvent has a low effect on the cells of the infection (the X axis of the acetone graphic shows not the concentration of the solvent but the highest quantity of acetone present in the corresponding compound concentrations. Grey bars indicate the non-treated cells results

Figure 4a. Acetone measurements (control)

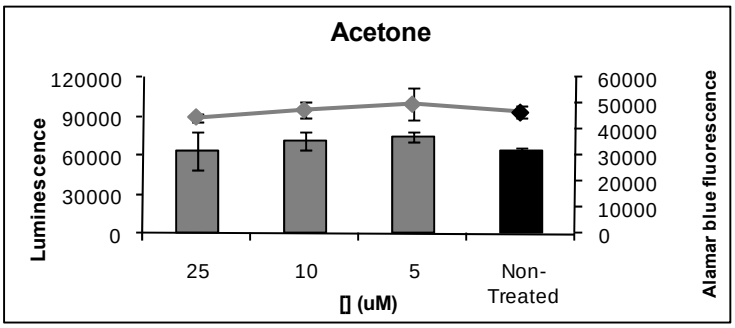

Figure 4b. Mariline A measurements

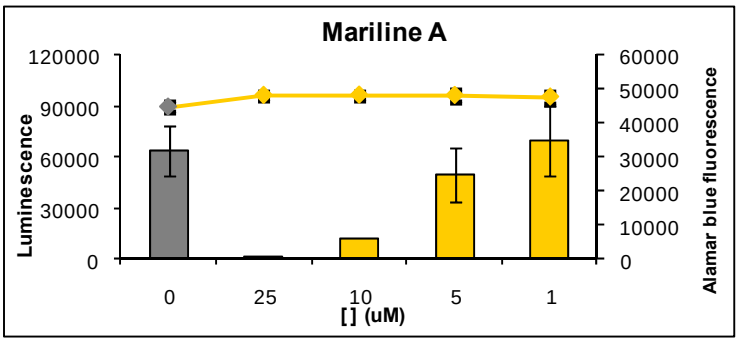

Figure 4c. Mariline B measurements

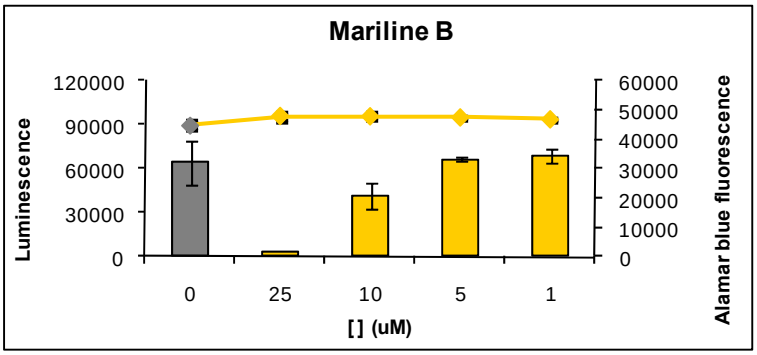

Figure 5. Ki determination of mariline B (compound 16587) against the receptor dopamine transporter DAT

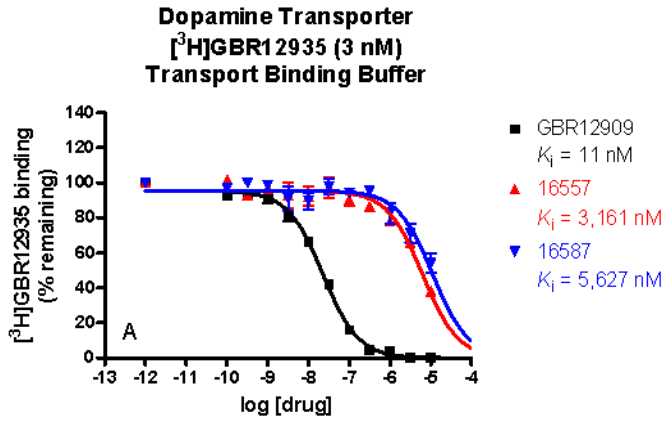

(Erratum, value is 5627 nM)

Figure 6. Ki determination of mariline B (compound 16587) against the adregenic receptors Beta 3

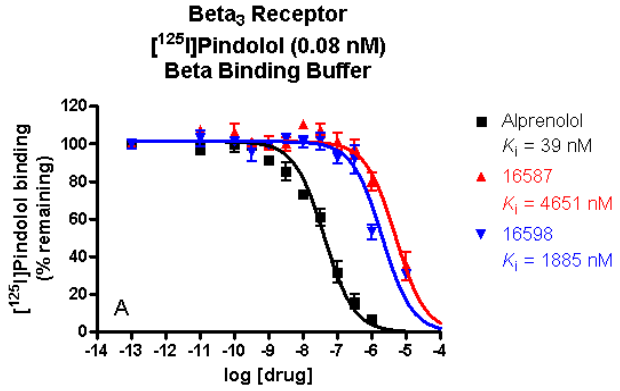

Figure 7. Ki determination of mariline B (compound 16587) against the histamine receptor H2.

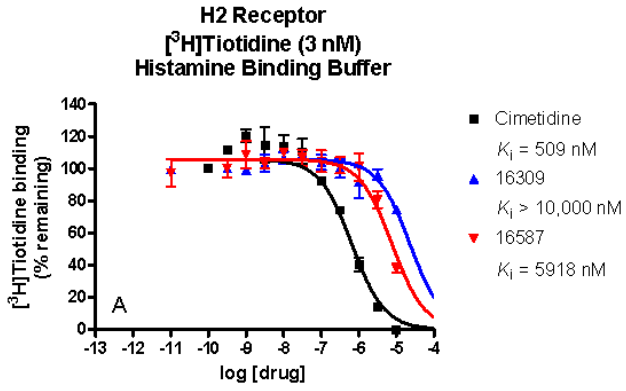

Figure 8. Ki determination for the ligands Mariline C (compound 16594) and D (compound 16595) against the cannabinoid receptor CB_2.

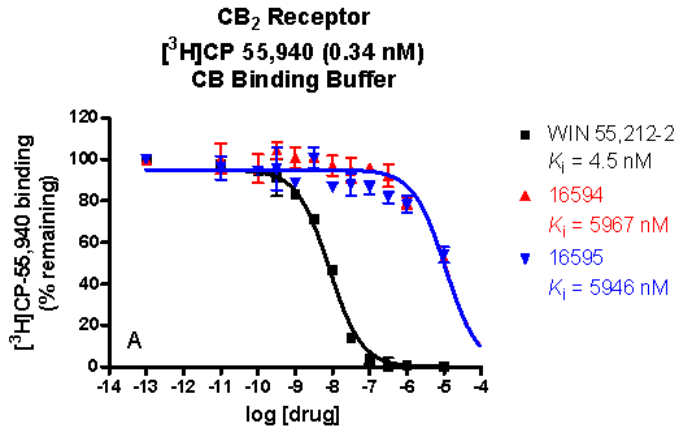

Table 6. Antiproliferative and antiplasmodial biological activity data for marilines A - D

	Antiproliferative activity against cancer cell lines (GI50)*	**Antiplasmodial activity (IC50)****
Mariline A	24.44 µM	6.68 µM
Mariline B	5.00 µM	11.61 µM
Mariline C	48.32 µM	13.84 µM
Mariline D	> 100 µM	> 25 µM

*Growth delaying activity represented by GI50 is the average value registered for the tested cell lines; mariline A was tested against 10 cancer cell lines, mariline B against 19 cell lines, marilines C and D against 5 cancer cell lines. All compounds were tested in two independent experiments, each one run in triplicate. Growth rates are the mean of the two experiments. As positive control it was used etoposide treated in the same way.

**Antiplasmodial activity test relate to the inhibition of the infection of *Plasmodium berghey* on the liver stage. The parasite expresses luciferase, thus the infection is measured by luminescence. The tests were performed in quadruplicate measurements per compound.

Table 7. Protease HLE and cease inhibition data review for marilines A and B

	HLE	**Porcine Cease**	
		equation used for analysis $v = v_0/(1+[I]/IC_{50})$	**equation used for analysis** $v = (v_0\text{-offset})/(1+[I]/IC_{50})+\text{offset}$
Mariline A	IC_{50} = 0.86 ± 0.26 μM	IC_{50} = 4.4 ± 1.6 μM	IC_{50} = 0.18 ± 0.08 μM, offset = 49 ± 3%
Mariline B	IC_{50} = 0.86 ± 0.12 μM	IC_{50} = 6.6 ± 1.8 μM	IC_{50} = 0.63 ± 0.20 μM, offset = 54 ± 3%
Mariline C	> 10 μM	> 10 μM	> 10 μM
Mariline D	-	-	-

IC_{50} values obtained from quadruplicate measurements at five different inhibitor concentrations.

Bioactivity data - Marilones

Figure 9. Antiproliferative activity data for marilones A and C

Growth delaying activity (represented by GI_{50}), cytostatic activity (represented by TGI) and cytotoxic activity (represented by LC_{50}) were observed. GI_{50} is different than the IC_{50} in that it contains a correction for the starting population. Results in μM.

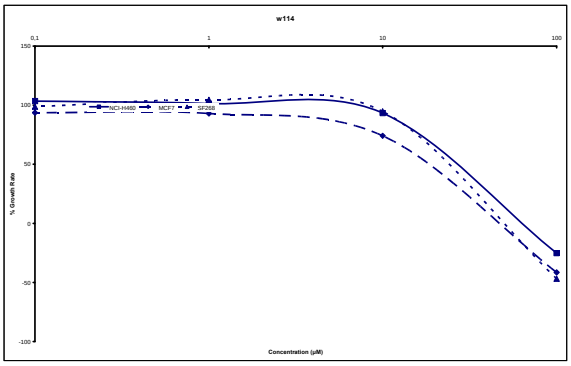

GI_{50} marilone A

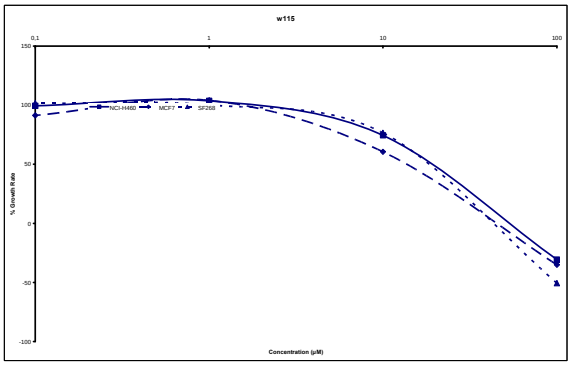

GI_{50} marilone C

CELL LINES		(A)	(C)	Etoposide
NCI-H460	GI_{50}	42,9	31,0	0,4
	TGI	80,9	73,8	22,4
	LC_{50}	>100	>100	124,2
MCF7	GI_{50}	28,8	20,0	22,8
	TGI	67,7	67,0	118,0
	LC_{50}	>100	>100	213,1
SF268	GI_{50}	38,4	28,9	7,7
	TGI	70,2	64,2	90,4
	LC_{50}	>100	99,6	201,4

Cancer cell lines: NCI-H460/lung, MCF7/breast and SF268/CNS

Average values in chapter 4.

Figure 10a-c. Antiplasmodial activity data for marilones A and C

Bioactivity test relates to the inhibition of the infection of *Plasmodium berghey* on the liver stage. The parasite expresses luciferase, thus the infection is measured by luminescence (Bars); the cellular density (i.e. the non-toxiciy of the compounds) is measured by fluorescence. The tests were performed in quadruplicate measurements per compound. Samples were dissolved in acetone which was also tested alone. Results show that the solvent has a low effect on the cells of the infection (the X axis of the acetone graphic shows not the concentration of the solvent but the highest quantity of acetone present in the corresponding compound concentrations. Grey bars indicate the non-treated cells results

Figure 10 a. Acetone measurements (control)

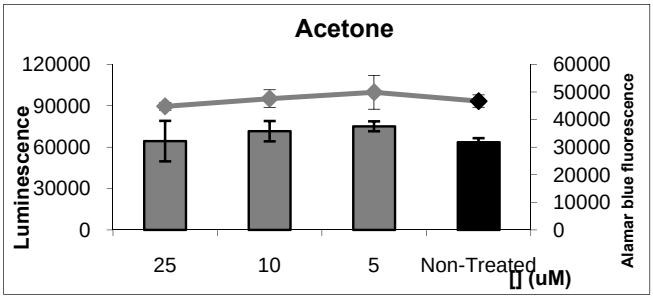

Figure 10b. Marilone A

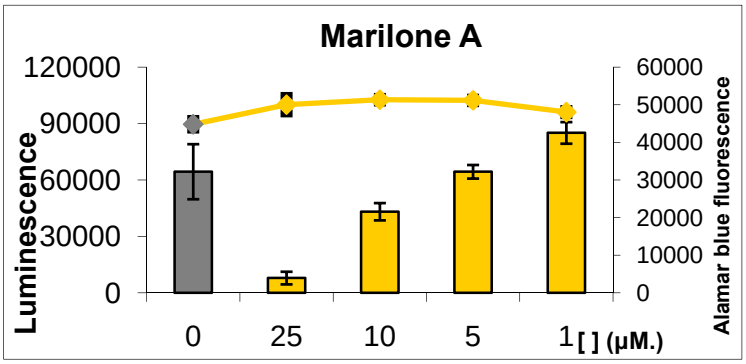

Figure 10c. Marilone C

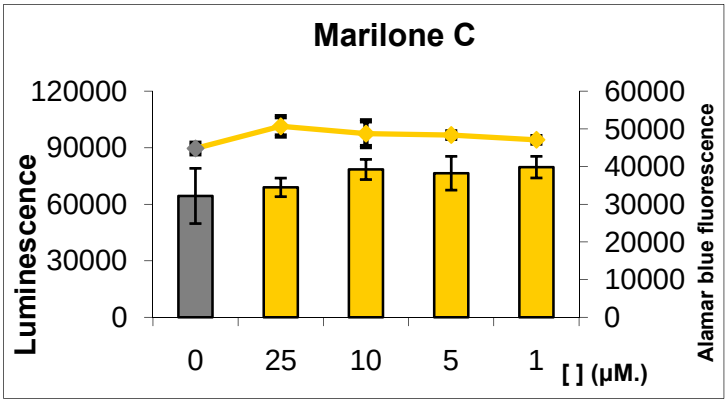

Figure 11. Ki value determination of the antagonistic effect of Marilone B (compound 16591) against the serotonin receptor 5HT2B.

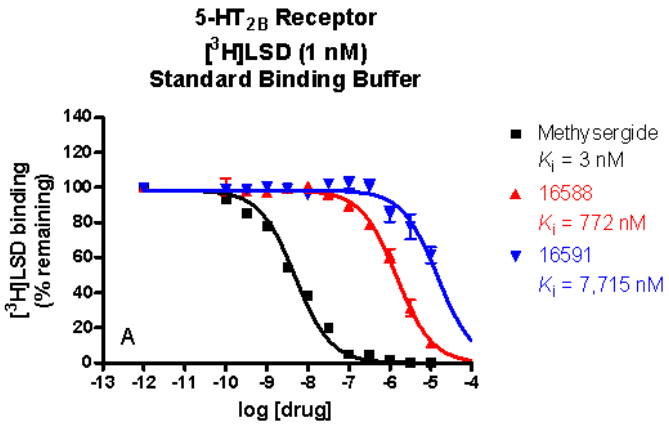

13.2. Appendix - Protocols and media

Protocol for Laser Microscopy Sample Preparation

Take a small piece of fungi from a petri dish into an eppendorf

Take care not to take media

I

Add 200-400 µL 0.85% NaCl

Mix with pipette

I

Take 10 µL sample and place in PCR-eppendorf

I

Add 0.5 µL stain solution stock

Mix, and incubate in dark for 15 min

I

Place 5 – 10 µL sample in microscope glass slide

I

Add 5 µL slow fade reagent enhancer

I

Check in laser microscope

Material

Eppendorfs (normal and PCR-small)

Live-dead bac viability kit

Slowfade fluorescence enhancer

0.85% NaCl

Protocol Advanced Marfey's Method

(Peptide hydrolysis)

1. Take a minimum of 0.5 mg of peptide in a small glass vial with metal screw-top
2. Add 0.5 mL of 6 N HCl
3. Incubate for 16 hours at 110 ºC
4. Dry hydrolysed peptide in a N_2 flow until dryness

(Marfey reaction)

5. Add 50 µL pure water.
6. Add 40 µL of 1 M $NaHCO_3$
7. Add 100 µl of 1% L-FDLA (or L-FDAA, both are Marfey reagent) (stock solution, 1 mg/100 µL of acetone)
8. Incubate at 70 ºC for 40 minutes (reaction of Marfey reagent and amino acid residues)
9. Cool at room temperature and add 20 µL 2N HCl in order to stop the reaction
10. Dry in N_2 flow and add 250 µL ACN for LC-MS analysis (method "Christian 1"; see solvent system in the peptides articles)

Standard amino acids preparation

Measure 1 mg of the L-amino acid and in a second vial 0.5 mg of the L-amino acid and 0.5 mg of the D- amino acid.

With both vials perform the Marfey reaction above described (point 5. until 10., final concentration for LC-MS 1 mg/ml)

Repeat this with every standard amino acids present in the peptide for comparison.

Notes:

Hydrolysis is performed to break the peptidic bonds between the amino acid residues. In Marfey's reaction, the L-L configuration (e. g. L-Phe-L-FDLA) usually comes first as the D-L (e.g. D-Phe-L-FDLA). With both reactions of the standard amino acids we establish first in the mixture of D/L residues the retention time of both D- and L- amino acid configurations reacting with the L-Marfey reagent. Then the vial with only the L-amino acid configuration is basically to confirm which one is the peak corresponding to the product of the reaction L-amino acid with the L-FDLA. You establish then unambiguously the configuration of the residues present in each peak. Then analyse the extracted ion of the same amino acid in your peptide and compare the retention time, it should be the same as L-residue/L-FDLA or D-residue/L-FDLA and you can assign the configuration.

Protocol Mosher's Method for Configurational Determination of Chiral Centers with a Hydroxyl Group/Proton (Secondary and Tertiary alcohols)

(a) - Calculations of the mol of Stachymide A in 1 mg

236.26 g ------- 1 mol

0.001 g ----- X X = 4.233 x 10^{-6} mol

(b) - Calculation of the mg and final volume of MTPA-Cl (M.W 252.62) corresponding to 10 eq (normally reaction is made with 3 eq).

10 eq = 4.223 x 10^{-5} mol

252.62 g ----- 1 mol

X g ------ 4.223 x 10^{-5} mol X = 10.6 mg

MTPA-Cl density (ρ) = 1.6, (ρ = m/v) thus vol. of MTPA-Cl to insert is 6.625 µL.

(c) **- (*R*)- and (*S*)-MTPA esters reaction**. Dissolve the secondary alcohol (1 eq, 1 mg, 4.23 x 10^{-6} µmol) with the corresponding MTPA-Cl (10 eq) in an adequate quantity of deuterated pyridine and DMAP (1 eq) in an NMR tube. The reaction is followed by ^{1}H-NMR to observe the downfield proton shift of H-2'. After 1 hour reaction time (or more if needed), record the final ^{1}H-NMR, dry the sample and re-dissolve in D-acetone for ^{1}H-^{13}C HSQC measurements if necessary.

(d) **The $\Delta^{(S-R)}$** values between (*S*)- and (*R*)- MTPA esters can be recorded with ^{1}H-NMR and/or ^{1}H-^{13}C HSQC and they correspond to the difference of the proton shifts near the chiral carbon between the (*S*)- and (*R*)- MTPA esters. Normally the reaction is confirmed as successful if both sides have opposite (+ and -) values of $\Delta^{(S-R)}$.

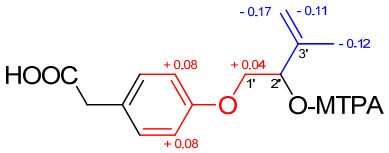

Use the general formula in this described figure (positive side in the back, negative in the front, rotate molecule (proton on back side) and determine the R/S configuration.

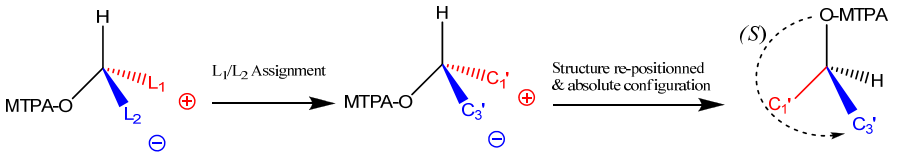

NOTE: Not even one molecule of water should be present in flasks/pipets/reagents!

The 3D model for MPA is the REVERSE of the MTPA, i.e. $\Delta^{(R-S)}$, negative Δ in the back, and positive Δ in the front of the model.

UV Spectra Calculations

UV spectra were recorded on a Perkin-Elmer Lambda 40 with UV WinLab Version 2.80.03 software, using 1.0 cm quartz cells. The molar absorption coefficient ε was determined in accordance with the Lambert-Beer-Law:

$$\varepsilon = A / C.D$$

A = Absorption at peak maximum (U.A.)

C = concentration used in the cuvette (mol/L)

D = length of the measurement (normally 1 cm)

Results presented as the logarithm of the molar absorption coefficient (log ε) e.g. "UV (MeOH) λ_{max} (log ϵ) 219 nm (log ε 4.11)"

Protocols and Calculations for Circular Dichroism Spectra

CD spectra were recorded in MeOH at room temperature using a JASCO J-810-150S spectropolarimeter. The CD (circular dichroism) is measured as ellipticity Θ (in mdeg, millidegrees) and subsequently converted into the molar ellipticity $[\Theta]_M$ and finally into $\Delta\varepsilon$ in accordance to the following equation:

$$[\theta] = \theta \, . \, M / 10 \, . \, C \, . \, d$$

[Θ] = molar ellipticity [degrees x cm^2/dmol]

θ = ellipticity (values in mdegrees, which are the Y axis values taken from the CD measurement)

M = molecular weight (g/mol)

C = concentration in the cuvette (mg/ml)

D = measurement distance, or path lenght (normally 0.1 cm)

Results presented as $\Delta\varepsilon = [\theta] / 3300$, and written with the molar concentration, *c*, in the cuvette, e.g. "CD (*c* 2.8×10^{-4} mol/L, MeOH) λ (Δε) = 202 (-9.0), 218 (+12.4), 248 (+6.1)".

Protocol for the effect of (+) sclerosporin and 4 hydroxylated derivatives on <u>sporulation</u> and growth of *Cadophora malorum.*

5 compounds tested, all under LIGHT conditions

Protocol *per* compound, made in triplicate.

sporogenic activity

compound concentration (µg/mL medium)	**concentration to use in 20 ml BMS media from STOCK***	**growth area (cm^2) = A**	**Spore number/growth area (1 cm^2) =B**	**total spore number (AxB)**
0	0			
0.005	1 µL			
0.5	10 µL			
5	100 µL			

*Stock solution: dissolve compounds in acetone (500 µg samples in 500 µL)

9 cm radium petri dish, 20 mL media

1 week waiting time.

Spore number count: take 1 cm^2 medium, place in a small quantity of water (e.g. 2 mL) and analyze in the microscope with a microscope slide counting chamber. Determine the number of spores and multiply the microscopic volume for the total water volume and subsequently for the total growth area.

Media preparations

Artificial Sea Water (ASW), 1L

KBr	1.0 g
NaCl	234.8 g
$MgCl_2x6H_2O$	106.1 g
$CaCl_2x2H_2O$	14.7 g
KCl	6.6 g
$SrCl_2x6H_2O$	0.4 g
Na_2SO4	39.2 g
$NaHCO_3$	1.9 g
$H3BO_3$ (boric acid)	0.3 g

Biomalt medium (BM), 1L

Biomalt 20 g

- For BMS, dissolve in ASW
- For BMS-agar, add 15g/L agar

MYA, 1L

East extract 4 g

Malt extract 10 g

Glucose 4 g

1L Dist. water and adjust to pH 7.3

- For MYA-ASW dissolve in ASW
- For MYA-agar, add 15g/L agar

Czapek medium, 1L

Dissolve 35 g Difco™ Czapek-dox Broth in 1L distilled water.

MPY medium, 1L

Yeast extract 5 g

Peptone from Fish 3 g

Mannitol 25 g

1L Distilled water

Minimal Peptone Basal medium

Difco™ Minimal Broth Davis without Dextrose 10.6 g

Peptone from meat 3 g

1L Distilled water

Several carbon sources added from 3g/L to 10 g/L, insoluble carbon sources inoculated with 1% DMSO.

Peptone medium

Peptone 10 g

NaCl 5 g

1L Distilled water and adjust pH to 7.2

-For solid-medium add agar 20 g/L

Trypticase Soy medium

Pancreatic digest of casein 15 g

Enzymatic digest of soy bean 5 g

NaCl 5g

1L Distilled water and adjust pH to 7.3

- For solid-medium, agar 15 g/L

PDA medium, 1L

Dissolve 24 g Difco™ Potato Dextrose Broth in 1L distilled water.

13.3. Appendix - Complete 2D NMR spectroscopic tables

Marilines

Table 1. 1D and 2D NMR spectroscopic data for marilines A/B

position	δ_N, δ_C, mult.[a, b, e]	δ_H[a, b] (*J* in Hz)	COSY[a, c]	HMBC[a,b, d]	NOESY[a, c]
N	132.4, N				
1	166.2, qC				
2	116.4, qC				
3	157.2, qC				
4	119.4, qC				
5	161.9, qC				
6	101.8, CH	6.95, s		2, 4, 5, 7, 8	8, 9, 1'
7	150.0, qC				
8	57.5, CH	4.97, q (6.8)	6, 9	1, 7, 9	6, 9
9	19.4, CH_3	1.27, d (6.8)	8	7, 8, N	6, 8
10	62.1, CH_3	3.99, s		3	11
11	8.8, CH_3	2.12, s		3, 4, 5	10, 9'
12	120.1, qC				
13	156.8, qC				
14	101.2, CH	6.67, d (2.6)	16	12, 13, 15, 16	18, 1"
15	160.8, qC				
16	105.5, CH	6.56, dd (2.6, 8.6)	14, 17	12, 14, 15	17, 18
17	131.9, CH	7.19, d (8.6)	16	12, 13, 15, N	8, 9, 16
18	55.7, CH_3	3.81, brs		15	14, 16
1'	66.2, CH_2	a: 4.68, dd (6.6, 12.3)	1'b, 2'	5, 2', 3'	6, 2', 9'
		b: 4.72, dd (6.6, 12.3)	1'a, 2'	5, 2', 3'	
2'	120.6, CH	5.53, t (6.6)	1'a, 1b, 9'	4', 9'	1', 4'
3'	141.5, qC				
4'	40.1, CH_2	2.12, m	5'	5'	2'
5'	27.0, CH_2	2.14, m	4', 6'	4'	6'
6'	124.6, CH	5.10, t (6.6)	5', 8'	5', 8',10'	5', 8'
7'	132.0, qC				
8'	25.8, CH_3	1.63, brs	6'	6', 7', 10'	6'
9'	16.7, CH_3	1.77, brs	2'	2', 3', 4'	1'
10'	17.7, CH_3	1.59, brs	6'	6', 7', 8'	
1"	66.1, CH_2	a: 4.54, dd (6.6, 12.0)	1"b, 2", 4", 5"	11, 2", 3"	12, 2", 4", 5"
		b: 4.58, dd (6.6, 12.0)	1"a, 2", 4", 5"	11, 2", 3"	
2"	120.8, CH	5.35, t (6.6)	1"a, 1"b, 4", 5"	4", 5"	1", 5"
3"	137.9, qC				
4"	18.2, CH_3	1.68, brs	2"	2", 3", 5"	1"
5"	25.7, CH_3	1.67, brs	2"	2", 3", 4"	2"

[a]acetone-d_6, 300/75.5 MHz. [b] Assignments are based on extensive 1D and 2D NMR experiments (^{1}H-^{13}C, ^{1}H-^{15}N HMBC, HSQC, COSY). [c] Numbers refer to proton resonances. [d] Numbers refer to carbon resonances. [e] Implied multiplicities determined by DEPT.

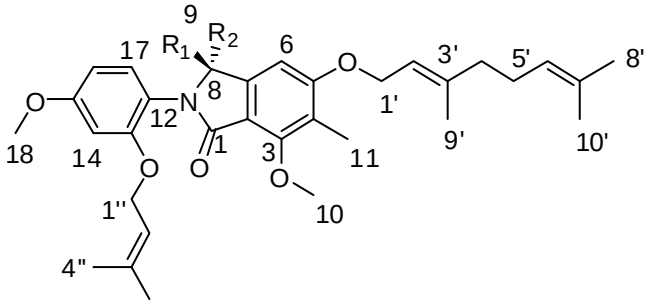

Table 2. 1D and 2D NMR spectroscopic data for mariline C

position	δ_C, mult.[a, b, e]	δ_H[a, b] (*J* in Hz)	COSY[a, c]	HMBC[a, d]
1	167.3, qC			
2	116.3, qC			
3	156.9, qC			
4	119.3, qC			
5	161.7, qC			
6	101.8, CH	6.92, s	8	2, 3, 4, 5, 7, 8
7	150.0, qC			
8	56.9, CH	4.62, q (6.8)	6, 9	1, 2, 6, 7, 9
9	18.9, CH_3	1.44, d (6.8)	8	7, 8
10	62.1, CH_3	3.98, s		3
11	8.8, CH_3	2.09, s		3, 4, 5
12	43.6, CH_2	a 3.85, dt (14.0, 5.5)	12b, 13	1, 8, 13
		b: 3.33, dt (14.0, 5.5)	12a, 13	1, 8, 13
13	61.7, CH_2	3.71, m	12a, 12b	12
1'	66.2, CH_2	a: 4.65, dd (6.6, 12.3)	2', 9'	5, 2', 3'
		b: 4.71, dd (6.6, 12.3)		
2'	120.6, CH	5.51, t (6.6)	1', 4', 9'	4'
3'	141.5, qC			
4'	40.1, CH_2	2.12, m	2',	3', 5', 6'
5'	27.0, CH_2	2.14, m	6', 8'	3', 4', 6', 7'
6'	124.6, CH	5.10, t (6.6)	5', 8', 10'	
7'	132.1, qC			
8'	25.8, CH_3	1.63, brs	5', 6'	6', 7', 10'
9'	16.7, CH_3	1.76, brs	1', 2'	2', 3', 4'
10'	17.7, CH_3	1.58, brs	6'	6', 7', 8'

[a]acetone-d_6, 300/75.5 MHz. [b] Assignments are based on extensive 1D and 2D NMR experiments (^{1}H-^{13}C, ^{1}H-^{15}N HMBC, HSQC, COSY). [c] Numbers refer to proton resonances. [d] Numbers refer to carbon resonances. [e] Implied multiplicities determined by DEPT. * Weak correlation.

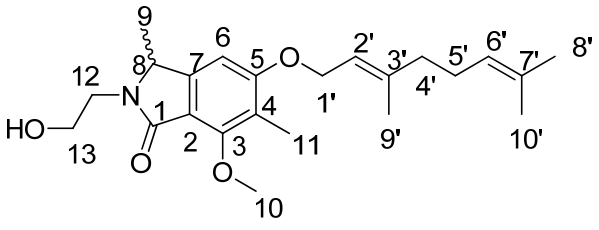

Table 3. 1D and 2D NMR spectroscopic data for mariline D

position	δ_C, mult.[a, b, e]	δ_H[a, b] (*J* in Hz)	COSY[a, c]	HMBC[a, d]
1	171.7, qC			
2	114.5, qC			
3	158.4, qC			
4	118.9, qC			
5	162.3, qC			
6	105.0, CH	6.68, s		2, 3, 4, 5, 8
7	152.1, qC			
8	53.2, CH	4.53, q (6.8)	9	1, 2, 6, 7, 9
9	20.8, CH_3	1.42, d (6.8)	8	7, 8
10	62.5, CH_3	3.95, s		3
11	8.6, CH_3	2.15, s		3, 4, 5

[a]MeOD, 300/75.5 MHz. [b] Assignments are based on extensive 1D and 2D NMR experiments (HMBC, HSQC, COSY). [c] Numbers refer to proton resonances. [d] Numbers refer to carbon resonances. [e] Implied multiplicities determined by DEPT.

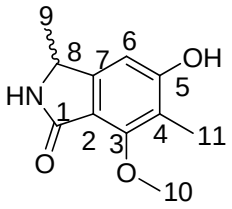

Marilones

Table 4. 1D and 2D NMR spectroscopic data for marilone A

position	δ_C, mult.[a, b, e]	δ_H[a, b] (*J* in Hz)	COSY[a, c]	HMBC[a, d]
1	168.2, qC			
2	110.0, qC			
3	158.0, qC			
4	120.4, qC			
5	164.2, qC			
6	100.8, CH	6.95, s		2, 3, 4, 5, 7, 8
7	154.2, qC			
8	77.0, CH	5.43, q (6.6)	11	1, 2, 6, 7, 11
9	62.1, CH_3	3.98, s		3
10	8.8, CH_3	2.09, s		3, 4, 5
11	20.9, CH_3	1.54, d (6.6)	8	7, 8
1'	66.5, CH_2	a: 4.69, dd (6.6, 12.1)	1'b, 2'	5, 2', 3'
		b: 4.74, dd (6.6, 12.1)	1'a, 2'	5, 2', 3'
2'	120.1, CH	5.52, t (6.6)	1'a, 1'b, 9'	1', 4', 9'
3'	142.1, qC			
4'	40.1, CH_2	2.10, m	5'	2', 6'
5'	26.9, CH_2	2.13, m	4', 6'	3', 4', 6', 7'
6'	124.64, CH	5.09, m	4', 5', 8', 10'	4', 5'; 8'
7'	132.1, qC			
8'	25.8, CH_3	1.63, br s	6'	6', 7'
9'	16.7, CH_3	1.76, br s	2'	2', 3', 4'
10'	17.7, CH_3	1.58, br s	6'	6', 7'

[a] CD_3COCD_3, 300/75.5 MHz. [b] Assignments are based on extensive 1D and 2D NMR experiments (HMBC, HSQC, COSY). [c] Numbers refer to proton resonances. [d] Numbers refer to carbon resonances. [e] Implied multiplicities determined by DEPT.

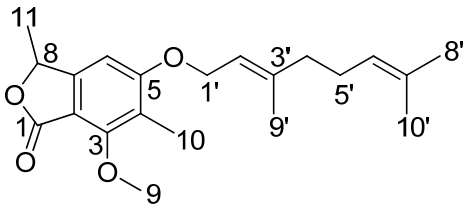

Table 5. 1D and 2D NMR spectroscopic data for marilone B

position	δ_C, mult.[a, b, e]	δ_H[a, b] (*J* in Hz)	COSY[a, c]	HMBC[a, d]
1	168.2, qC			
2	109.1, qC			
3	158.9, qC			
4	118.8, qC			
5	163.2, qC			
6	103.6, CH	6.73, s		2, 3, 4, 5, 8
7	153.9, qC			
8	76.6, CH	5.43, q (6.6)	11	1, 2, 6, 7, 11
9	62.0, CH_3	3.89, s		3
10	8.6, CH_3	2.02, s		3, 4, 5
11	21.0, CH_3	1.44, d (6.6)	8	7, 8

[a] MeOD, 300/75.5 MHz. [b] Assignments are based on extensive 1D and 2D NMR experiments (HMBC, HSQC, COSY). [c] Numbers refer to proton resonances. [d] Numbers refer to carbon resonances. [e] Implied multiplicities determined by DEPT.

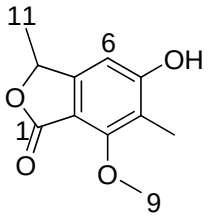

Table 6. 1D and 2D NMR spectroscopic data for marilone C

position	δ_C, mult.[a, b, e]	δ_H[a, b] (*J* in Hz)	COSY[a, c]	HMBC[a, d]
1	68.9, CH_2	5.50, s		2, 3, 5, 7, 8
2	128.4, qC			
3	153.9, qC			
4	124.8, qC			
5	159.7, qC			
6	102.0, CH	7.03, s		2, 3, 4, 5, 7, 8
7	125.8, qC			
8	171.1, qC			
9	59.3, CH_3	3.96, s		3
10	9.8, CH_3	2.15, s		3, 4, 5
1'	66.4, CH_2	4.7, d (6.6)	2'	5, 2', 3'
2'	120.5, CH	5.51, t (6.6)	1', 9'	4', 9'
3'	141.6, qC			
4'	40.1, CH_2	2.10, m		2', 3', 6'
5'	26.9, CH_2	2.14, m	4', 6'	3', 4', 6', 7'
6'	124.6, CH	5.10, m	4', 5', 8', 10'	4', 8', 10'
7'	132.05, qC			
8'	25.8, CH_3	1.63, s (br)	6'	6', 7', 10'
9'	16.7, CH_3	1.78, s (br)	2'	2', 3', 4'
10'	17.7, CH_3	1.58, s (br)	6'	6', 7', 8'

[a] CD_3COCD_3, 300/75.5 MHz. [b] Assignments are based on extensive 1D and 2D NMR experiments (HMBC, HSQC, COSY). [c] Numbers refer to proton resonances. [d] Numbers refer to carbon resonances. [e] Implied multiplicities determined by DEPT.

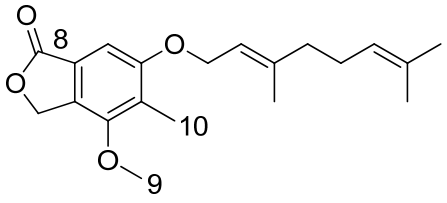

Table 7. 1D and 2D NMR spectroscopic data for marilone D

position	δ_C, mult.[a, b, e]	δ_H[a, b] (*J* in Hz)	COSY[a, c]	HMBC[a, d]
1	66.1, CH_2	a: 4.39, d (9.9)	1b	2, 3, 7, 9
		b: 4.41, d (9.9)	1a	2, 3, 7, 9
2	119.6, qC			
3	159.3, qC			
4	116.1, qC			
5	157.1, qC			
6	108.5, CH	6.91, s		2, 3, 5, 7, 8, 11
7	147.2, qC			
8	65.9, CH	5.06, q (6.3)	12	2, 6, 7, 12
9	61.8, CH_3	3.67, s		3
10	9.1, CH_3	2.09, s		3, 4, 5
11	57.8, CH_3	3.32, s		1a, 1b
12	25.4, CH_3	1.33, d (6.3)	8	7, 8

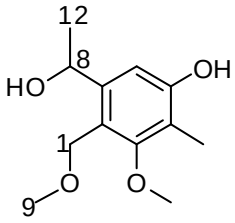

[a] CD_3COCD_3, 300/75.5 MHz. [b] Assignments are based on extensive 1D and 2D NMR experiments (HMBC, HSQC, COSY). [c] Numbers refer to proton resonances. [d] Numbers refer to carbon resonances. [e] Implied multiplicities determined by DEPT.

Table 8. 1D and 2D NMR spectroscopic data for mariline E

position	δ_C, mult.[a, b, e]	δ_H[a, b] (*J* in Hz)	COSY[a, c]	HMBC[a, d]
1	66.9, CH_2	4.53, s		2, 3, 7, 9
2	120.3, qC			
3	160.0, qC			
4	117.5, qC			
5	157.9, qC			
6	111.6, CH	6.77, s		2, 3, 4, 5, 7, 8
7	141.4, qC			
8	62.6, CH_2	4.64, s		2, 3, 4, 6, 7
9	62.2, CH_3	3.74, s		3
10	9.2, CH_3	2.15, s		3, 4, 5
11	58.1, CH_3	3.42, s		1

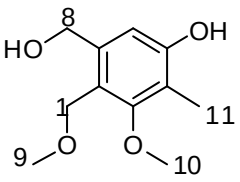

[a] CD_3COCD_3, 300/75.5 MHz. [b] Assignments are based on extensive 1D and 2D NMR experiments (HMBC, HSQC, COSY). [c] Numbers refer to proton resonances. [d] Numbers refer to carbon resonances. [e] Implied multiplicities determined by DEPT.

Table 9. 1D and 2D NMR spectroscopic data for marilone F

position	δ_C, mult.[a, b, e]	δ_H[a, b] (*J* in Hz)	COSY[a, c]	HMBC[a, d]
1	10.1, CH_3	0.85, t (7.3)	2	2, 3
2	30.6, CH_2	1.35, m	1, 3	1, 3
3	69.4, CH	3.85, m	2, 4	1
4	49.5, CH_2	a: 2.41, dd (4.4, 16.5)	3, 4b	2, 3, 5
		b: 2.51, m	4a	2, 3, 5
5	214.8, qC			
6	48.1, CH	2.87, m	7a, 7b, 16	5, 7, 8, 16
7	29.8, CH_2	a: 2.81, m	6, 7b	5, 6, 8, 9, 13, 16
		b: 2.53, m	6, 7a	5, 6, 8, 9, 13, 16
8	122.1, qC			
9	159.2, qC			
10	115.6, qC			
11	155.6, qC			
12	111.5, CH	6.51, s		8, 10, 11, 14
13	141.9, qC			
14	26.3, CH_2	2.52, m	15	8, 12, 13, 15
15	15.8, CH_3	1.10, t (7.5)	14	13, 14
16	15.9, CH_3	0.94, d (6.7)	6	5, 6, 7
17	60.4, CH_3	3.65, s		9
18	9.4, CH_3	2.08, s		9, 10, 11

[a] CD_3COCD_3, 300/75.5 MHz. [b] Assignments are based on extensive 1D and 2D NMR experiments (HMBC, HSQC, COSY). [c] Numbers refer to proton resonances. [d] Numbers refer to carbon resonances. [e] Implied multiplicities determined by DEPT.

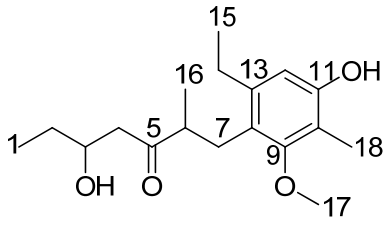

Table 10. 1D and 2D NMR spectroscopic data for marilone G

position	δ_C, mult.[a, b, e]	δ_H[a, b] (*J* in Hz)	COSY[a, c]	HMBC[a, d]
1	67.1, CH	5.54, dd (1.6, 6.5)	9	2, 3, 7, 8
2	139.4, qC			
3	158.4, qC			
4	128.1, qC			
5	159.8, qC			
6	103.3, CH	6.87, s		2, 4, 5, 8
7	137.2, qC			
8	206.4, qC			
9	48.4, CH_2	a: 3.08, dd (6.5, 19.1)	1, 9b	1, 2, 8
		b: 2.50, dd (1.6, 19.1)	1, 9a	1, 2, 8
10	61.1, CH_3	4.01, s		3
11	10.0, CH_3	2.23, s		3, 4, 5, 6

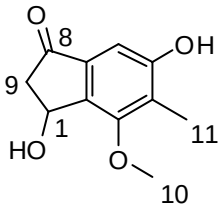

[a]MeOD, 300/75.5 MHz. [b] Assignments are based on extensive 1D and 2D NMR experiments (HMBC, HSQC, COSY). [c] Numbers refer to proton resonances. [d] Numbers refer to carbon resonances. [e] Implied multiplicities determined by DEPT.

Table 11. 1D and 2D NMR spectroscopic data for marilone H

position	δ_C, mult.[a, b, e]	δ_H[a, b] (*J* in Hz)	COSY[a, c]	HMBC[a, d]
1	166.0, qC			
2	98.2, qC			
3	165.6, qC			
4	99.1, CH	6.02, s		2, 3, 5, 6
5	164.9, qC			
6	27.1, CH_2	2.42, q (7.5)	7	4, 5, 7
7	11.3, CH_3	1.13, t (7.5)	6	5, 6
8	8.5, CH_3	1.81, s		1, 2, 3

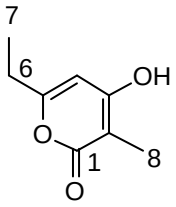

[a]CD_3COCD_3, 300/75.5 MHz. [b] Assignments are based on extensive 1D and 2D NMR experiments (HMBC, HSQC, COSY). [c] Numbers refer to proton resonances. [d] Numbers refer to carbon resonances. [e] Implied multiplicities determined by DEPT.

Table 12. 1D and 2D NMR spectroscopic data for marilone I

position	δ_C, mult.[a, b, e]	δ_H[a, b] (*J* in Hz)	COSY[a, c]	HMBC[a, d]	NOE[a, d]
1	105.4, CH	6.32, s		2, 3, 6, 7, 8, 13	9, 12, 13
2	121.4, qC				
3	154.8, qC				
4	119.0, qC				
5	160.4, qC				
6	100.2, CH	6.60, s		1, 2, 3, 4, 5, 7, 8, 10	10, 11, 12, 1'
7	141.7, qC				
8	111.4, qC				
9	59.8, CH_3	3.90, s		3	1
10	9.3, CH_3	2.07, s		2, 3, 4, 5, 6	6
11	28.1, CH_3	1.62, s		7, 8	6, 13
12	49.7, CH_3	2.85, s		8	1, 6
13	54.2, CH_3	3.38, s		1	1, 11
1'	66.1, CH_2	4.64, d (6.6)	2', 9'	2', 3', 5'	6, 9'
2'	120.8, CH	5.48, t (6.6)	1', 9'	4', 9'	
3'	141.1, qC				
4'	40.1, CH_2	2.08, m	5'	2', 3', 5', 6', 9'	6'
5'	27.0, CH_2	2.11, m	6', 4'	3', 4', 6'	6'
6'	124.6, CH	5.11, m	5', 8', 10'		4', 5', 8'
7'	132.0, qC				
8'	25.8, CH_3	1.64, br s	6'	6', 7', 10'	6'
9'	16.6, CH_3	1.75, br s	2', 1'	2', 3', 4'	1'
10'	17.7, CH_3	1.59, br s	6'	6', 7', 8'	

[a] CD_3COCD_3, 300/75.5 MHz. [b] Assignments are based on extensive 1D and 2D NMR experiments (HMBC, HSQC, COSY). [c] Numbers refer to proton resonances. [d] Numbers refer to carbon resonances. [e] Implied multiplicities determined by DEPT.

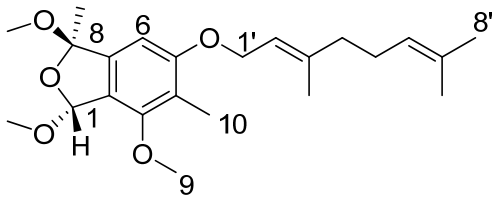

Table 13. 1D and 2D NMR spectroscopic data for marilone J

position	δ_C, mult.[a, b, e]	δ_H[a, b] (*J* in Hz)	COSY[a, c]	HMBC[a, d]	NOE[a, d]
1	104.8, CH	6.02, s		7, 8, 13	9, 11, 13
2	121.5, qC				
3	154.9, qC				
4	119.2, qC				
5	160.4, qC				
6	100.2, CH	6.59, s		2, 3, 5, 4, 7, 8, 10	10, 11, 12, 1'
7	141.3, qC				
8	110.8, qC				
9	59.8, CH_3	3.89, s		3	1, 13
10	9.3, CH_3	2.06, s		2, 3, 4, 5, 6	6
11	27.8, CH_3	1.55, s		7, 8	1, 6, 12
12	50.5, CH_3	2.94, s		8	6, 11, 13
13	55.5, CH_3	3.50, s		1	1, 9, 12
1'	66.2, CH_2	4.63, d (6.6)	2', 9'	5, 2', 3'	6, 9'
2'	120.9, CH	5.48, t (6.6)	1', 9'	4', 9'	
3'	141.1, qC				
4'	40.1, CH_2	2.07, m	5'	2', 3', 5', 6', 9'	6'
5'	27.0, CH_2	2.11, m	4', 6'	3', 4', 6'	6'
6'	124.7, CH	5.10, m	5', 8', 10'		4', 5', 8'
7'	132.0, qC				
8'	25.8, CH_3	1.64, br s	6'	6', 7', 10'	6'
9'	16.7, CH_3	1.75, br s	1', 6'	2', 3', 4'	1'
10'	17.7, CH_3	1.58, br s	6'	6', 7', 8	

[a] CD_3COCD_3, 300/75.5 MHz. [b] Assignments are based on extensive 1D and 2D NMR experiments (HMBC, HSQC, COSY). [c] Numbers refer to proton resonances. [d] Numbers refer to carbon resonances. [e] Implied multiplicities determined by DEPT.

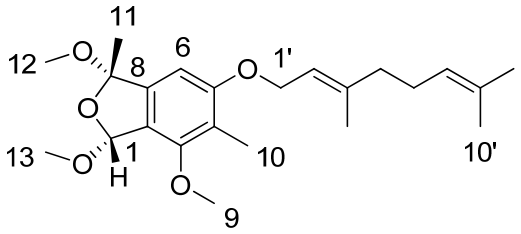

Stachylines

Table 14. 1D and 2D NMR spectroscopic data for stachyline A **(*Z*-)**.

Position	δ_c, mult. [a,b,e]	δ_H [a,b] (*J* in Hz)	COSY[a,b,c]	HMBC[a,d]	NOESY[a,b,c]
1	130.1. qC				
2	130.5, CH	7.17, d (8.4)	3	4, 6	3, 7
3	115.5, CH	6.88, d (8.4)	2	1, 5	1'a, 1'b, 2
4	158.5, qC				
5	115.5, CH	6.88, d (8.4)	6	1, 3	1'a, 1'b, 6
6	130.5, CH	7.17, d (8.4)	5	2, 4	5, 7
7	31.0, CH_2	3.60, d (5.5)	8	6, 8	2, 6, 8
8	150.0, CH	6.73, t (5.5)	7	1, 7	7
1'	72.1, CH_2	a: 3.90, dd (7.3, 9.5)	1'b, 2'	2', 3', 4	1'b, 2', 3, 5
		b: 4.01, dd (3.7, 9.5)	1'a, 2'	2', 3', 4	1'a, 2', 3, 5
2'	73.9, CH	4.39, m	1'a, 1'b		
3'	146.1, qC				
4'	112.1, CH_2	a: 4.89, br s	4'b, 5'	2'	4'b
		b: 5.08, br s	4'a, 5'	2', 3'	4'a
5'	18.7, CH_3	1.78, s	4'a, 4' b	2', 3', 4'	1'a, 1'b, 2', 4'a

[a] CD_3COCD_3, 300/75.5 MHz. [b] Assignments are based on extensive 1D and 2D NMR experiments (HMBC, HSQC, COSY). [c] Numbers refer to proton resonances. [d] Numbers refer to carbon resonances. [e] Implied multiplicities determined by DEPT.

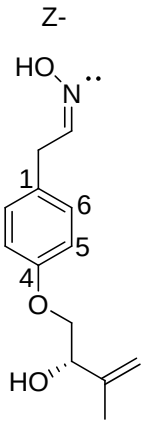

Table 15. 1D and 2D NMR spectroscopic data for stachyline A **(*E*-)**

Position	δ_c, mult. [a,b,e]	δ_H [a,b] (*J* in Hz)	COSY[a,b,c]	HMBC[a,d]	NOESY[a,b,c]
1	130.1. qC				
2	130.5, CH	7.13, d (8.4)	3	4, 6	3, 7
3	115.5, CH	6.88, d (8.4)	2	1, 5	1'a, 1'b, 2
4	158.7, qC				
5	115.5, CH	6.88, d (8.4)	6	1, 3	1'a, 1'b, 6
6	130.5, CH	7.13, d (8.4)	5	2, 4	5, 7
7	35.4, CH_2	3.39, d (6.2)	8	6, 8	2, 6, 8
8	149.7, CH	7.40, t (6.2)	7	1, 7	7
1'	72.1, CH_2	a: 3.90, dd (7.3, 9.5)	1'b, 2'	2', 3', 4	1'b, 2', 3, 5
		b: 4.01, dd (3.7, 9.5)	1'a, 2'	2', 3', 4	1'a, 2', 3, 5
2'	73.9, CH	4.39, m	1'a, 1'b		
3'	146.1, qC				
4'	112.1, CH_2	a: 4.89, br s	4'b, 5'	2'	4'b
		b: 5.08, br s	4'a, 5'	2', 3'	4'a
5'	18.7, CH_3	1.78, s	4'a, 4' b		1'a, 1'b, 2', 4'a

[a] CD_3COCD_3, 300/75.5 MHz. [b] Assignments are based on extensive 1D and 2D NMR experiments (HMBC, HSQC, COSY). [c] Numbers refer to proton resonances. [d] Numbers refer to carbon resonances. [e] Implied multiplicities determined by DEPT.

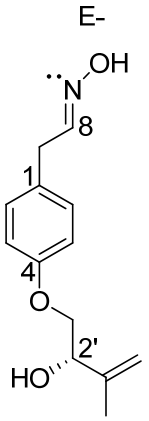

Table 16. 1D and 2D NMR spectroscopic data for stachyline B.

Position	δ_C, mult.[a, b, e]	δ_H[a, b] (*J* in Hz)	COSY[a, c]	HMBC[a, d]
1	128.0, qC			
2	131.2, CH	7.20, d (8.4)	3	3, 4, 7
3	115.3, CH	6.87, d (8.4)	2	1, 2, 4
4	158.8, qC			
5	115.3, CH	6.87, d (8.4)	6	1, 4, 6
6	131.2, CH	7.20, d (8.4)	5	4, 5, 7
7	40.5, CH_2	3.51, s		1, 2, 6, 8
8	173.0, qC			
1’	72.1, CH_2	a: 4.01, dd (4.0, 9.8)	1’b, 2’	4, 2’, 3’
		b: 3.90, dd (7.2, 9.8)	1’a, 2’	
2’	73.9, CH	4.40, dd (4.0, 7.2)	1’a, 1’b	1’, 3’, 4’, 5’
3’	146.1, qC			
4’	112.1, CH_2	a: 4.88, br s	4’a, 5’	2’, 3’, 5’
		b: 5.08, br s	4’b, 5’	
5’	18.8, CH_3	1.79, br s	4’a, 4’b	2’, 3’, 4’

[a] CD_3COCD_3, 300/75.5 MHz. [b] Assignments are based on extensive 1D and 2D NMR experiments (HMBC, HSQC, COSY). [c] Numbers refer to proton resonances. [d] Numbers refer to carbon resonances. [e] Implied multiplicities determined by DEPT.

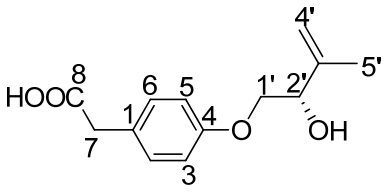

Table 17. 1D and 2D NMR spectroscopic data for stachyline C

Position	δ_C, mult.[a, b, e]	δ_H[a, b] (*J* in Hz)	COSY[a, c]	HMBC[a, d]
1	132.5, qC			
2	130.7, CH	7.13, d (8.4)	3	4, 6, 7
3	115.2, CH	6.84, d (8.4)	2	1, 2, 4, 5
4	158.3, qC			
5	115.2, CH	6.84, d (8.4)	6	1, 3, 4, 6
6	130.7, CH	7.13, d (8.4)	5	2, 4, 7
7	39.4, CH_2	2.72, t (7.1)	8	1, 2, 6, 8
8	64.1, CH_2	3.68, t (7.1)	7	1, 7
1’	72.1, CH_2	a: 4.00, dd (4.3, 9.8)	1’b, 2’	4, 2’, 3’
		b: 3.89, dd (7.2, 9.8)	1’a, 2’	
2’	74.0, CH	4.39, dd (4.3, 7.2)	1’a, 1’b	1’, 3’, 4’, 5’
3’	146.2, qC			
4’	112.0, CH_2	a: 4.89, br s	4’b, 5’	2’, 3’, 5’
		b: 5.09, br s	4’a. 5’	
5’	18.8, CH_3	1.79, br s	4’a, 4’b	2’, 3’, 4’

[a] CD_3COCD_3, 300/75.5 MHz. [b] Assignments are based on extensive 1D and 2D NMR experiments (HMBC, HSQC, COSY). [c] Numbers refer to proton resonances. [d] Numbers refer to carbon resonances. [e] Implied multiplicities determined by DEPT.

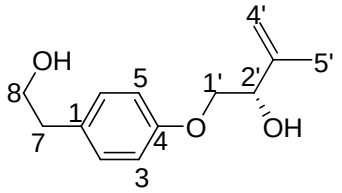

Table 18 .1D and 2D NMR spectroscopic data for stachyline D

Position	δ_C, mult.[a, b, e]	δ_H[a, b] (*J* in Hz)	COSY[a, c]	HMBC[a, d]
1	127.9, qC			
2	131.2, CH	7.19, d (8.4)	3	3, 4, 6, 7
3	115.2, CH	6.87, d (8.4)	2	1, 4, 5
4	159.0, qC			
5	115.2, CH	6.87, d (8.4)	6	1, 3, 4
6	131.2, CH	7.19, d (8.4)	5	2, 4, 5, 7
7	40.4, CH_2	3.52, br s		1, 2, 6
8	173.2, qC			
1’	71.6, CH_2	a: 4.00, dd (4.0, 9.8)	1’b, 2'	4, 2', 3'
		b: 3.89, dd (6.6, 9.8)	1’b, 2’	
2’	74.6, CH	3.68, m	1'a, 1’b, 3'	1', 3', 4', 5'
3’	31.6, CH	1.86, m	2', 4', 5'	1', 2', 5', 4'
4’	19.4, CH_3	0.97, d (6.8)	3'	2', 3', 5'
5’	17.7, CH_3	0.97, d (6.8)	3'	2', 3', 4'

[a] CD_3COCD_3, 300/75.5 MHz. [b] Assignments are based on extensive 1D and 2D NMR experiments (HMBC, HSQC, COSY). [c] Numbers refer to proton resonances. [d] Numbers refer to carbon resonances. [e] Implied multiplicities determined by DEPT.

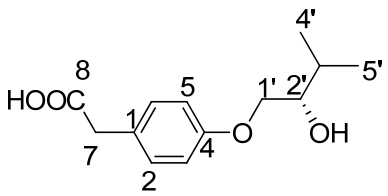

Sclerosporins

Table 19. 1D and 2D NMR Spectroscopic Data for [(+)-15-hydroxysclerosporin]

Position	δ_C, mult.[a, b, e]	δ_H[a, b] (*J* in Hz)	COSY[a, c]	HMBC[a, d]	NOESY[a, c]
1	34.0, CH	2.58, br d (11.4)	2a, 2b, 6	6, 7, 9, 10	6
2	25.1, CH_2	a: 1.99, m	1, 2b, 3	1, 3, 6	2b
		b: 1.37, qd (11.4, 5.4)	1, 2a, 3	1, 3, 6	2a, 7
3	26.2, CH_2	2.08, m	2a, 2b	4, 5	
4	138.3, qC				
5	124.3, CH	5.79, d (4.1)	6, 15	1, 3, 6, 15	6, 12, 15
6	35.5, CH	2.04, m	1, 5, 7	1	1, 8a, 12
7	40.0, CH	1.53, tt (10.2, 5.1)	6, 8a, 8b	6, 11, 12, 13	2b, 11
8	25.4, CH_2	a: 2.15, dt (19.8, 5.1)	7, 8b, 9	6, 7, 9, 10, 14	8b, 9
		b: 1.97, m	7, 8a, 9	6, 7, 9, 10, 14	8a, 9
9	142.6, CH	7.14, br s	8a, 8b	1, 7, 8, 10, 14	8a, 8b
10	132.9, qC				
11	26.4, CH	2.03, m	7, 12, 13	12, 13	12, 13
12	15.0, CH_3	0.83, d (6.8)	11	7, 11, 13	5, 11
13	21.3, CH_3	0.90, d (6.8)	11	7, 11, 12	11
14	172.2, qC				
15	67.3, CH_2	4.03, br s	5	3, 4, 5	5

[a] $CDCl_3$, 300/75.5 MHz. [b] Assignments are based on extensive 1D and 2D NMR experiments (HMBC, HSQC, COSY). [c] Numbers refer to proton resonances. [d] Numbers refer to carbon resonances. [e] Implied multiplicities determined by DEPT.

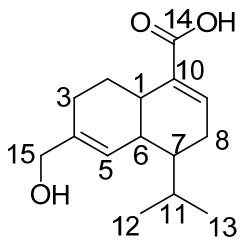

Table 20. 1D and 2D NMR Spectroscopic Data for [(+)-12-hydroxysclerosporin]

Position	δ_C, mult [a, b, e]	δ_H [a, b] (*J* in Hz)	COSY [a, c]	HMBC [a, d]	NOESY [a, c]
1	33.8, CH	2.58, br d (10.2)	2a, 2b, 6	3	6
2	25.4, CH_2	a: 1.91, m	1, 2b, 3a, 3b	1, 6	2b
		b: 1.42, qd (11.7, 5.4)	1, 2a, 3a, 3b	1,6	2a, 7
3	30.3, CH_2	a: 2.06, m	2a, 2b, 3b		3b
		b: 1.88, m	2a, 2b, 3a		2b, 3a
4	135.6, qC				
5	123.0, CH	5.52, br s	6, 15	1, 3, 6, 15	6, 12a, 12b, 15
6	35.8, CH	2.10, m	1, 5	8	1, 5
7	38.6, CH	1.65, tt (10.2, 5.1)	6, 8a, 8b	11, 12	2b, 11
8	28.0, CH_2	a: 2.27, dt (19.8, 5.1)	7, 8b	6, 7, 9, 10	8b, 9
		b: 2.02, m	7, 8a, 9	6, 7, 9, 10	8a, 9
9	142.1, CH	7.10, br s	8a, 8b	1, 7, 8, 10, 14	8a, 8b
10	133.1, qC				
11	35.3, CH	2.05, m	7, 12a, 12b, 13		7
12	64.9, CH_2	a: 3.77 (dd, 4.8, 10.6)	11, 12b	7, 11, 13	5, 6, 12b
		b: 3.52, t (10.6)	11, 12a	7, 11, 13	5, 6, 12a
13	15.4, CH_3	1.03, d (7.0)	11	7, 11, 12	11
14	172.0, qC				
15	23.9, CH_3	1.68, br s	5	3, 4, 5	5

[a] $CDCl_3$, 300/75.5 MHz. [b] Assignments are based on extensive 1D and 2D NMR experiments (HMBC, HSQC, COSY). [c] Numbers refer to proton resonances. [d] Numbers refer to carbon resonances. [e] Implied multiplicities determined by DEPT.

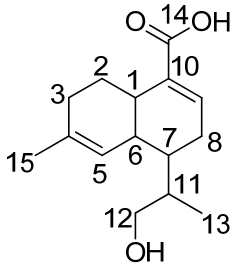

Table 21. 1D and 2D NMR Spectroscopic Data for [(+)-11-hydroxysclerosporin]

Position	δ_C, mult. [a, b, e]	δ_H [a, b] (*J* in Hz)	COSY[a, c]	HMBC[a, d]	NOESY[a, c]
1	35.6, CH	2.54, br d (10.6)	2a, 2b, 6		6
2	26.2, CH_2	a: 1.89, m	1, 2b, 3a, 3b	1, 6	2b
		b: 1.50, qd (11.7, 5.5)	1, 2a, 3a, 3b		2a, 7
3	30.8, CH_2	a: 1.98, m	2a, 2b		
		b: 1.95, m	2a, 2b		
4	133.7, qC				
5	126.6, CH	5.71, br d (5.1)	6, 15	1, 3, 6, 15	6, 12, 15
6	36.9, CH	2.11, m	1, 5	5, 7, 8	1, 5, 12
7	47.2, CH	1.68, td (10.3, 5.1)	8a, 8b	6, 11	2b, 8a, 12, 13
8	29.7, CH_2	a: 2.38, dt (19.6, 5.1)	7, 8b, 9	6, 7, 9, 10, 11	7, 8b, 9, 13
		b: 2.01, m	7, 8a, 9		8a, 9
9	140.2, CH	6.95, br t (3.9)	8a, 8b	1, 7, 8, 10, 14	8a, 8b
10	134.3, qC				
11	72.6, qC				
12	27.4, CH_3	1.23, s		7, 11, 13	5
13	28.7, CH_3	1.18, s		7, 11, 12	
14	168.0, qC				
15	23.9, CH_3	1.66, br s	5	3, 4, 5	5

[a]Acetone-d_6, 300/75.5 MHz. [b] Assignments are based on extensive 1D and 2D NMR experiments (HMBC, HSQC, COSY). [c] Numbers refer to proton resonances. [d] Numbers refer to carbon resonances. [e] Implied multiplicities determined by DEPT.

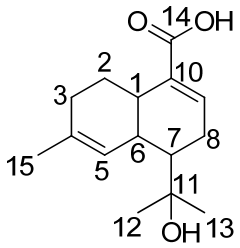

Table 22. 1D and 2D NMR Spectroscopic Data for [(-)-8-hydroxysclerosporin]

Position	δ_C, mult. [a, b, e]	δ_H [a, b] (*J* in Hz)	COSY[a, c]	HMBC[a, d]	NOESY[a, c]
1	35.2, CH	2.43, br d (10.6)	2a, 2b, 6	7	6
2	26.0, CH_2	a: 1.93, m	1, 2b, 3a, 3b		2b
		b: 1.45, qd (11.7, 5.4)	1, 2a, 3a, 3b		2a
3	31.5, CH_2	a: 2.08, m	2a, 2b, 3b		3b
		b: 1.93, m	2a, 2b, 3a		3a
4	134.9, qC				
5	125.1, CH	5.57, br d (4.4)	6, 15	1, 3, 6, 15	6, 11, 12, 13, 15
6	36.2, CH	2.10, m	1, 5, 7	1, 7, 11	1
7	48.8, CH	1.52, ddd (3.2, 8.7, 10.7)	6, 8, 11	1, 6, 8	12, 13
8	68.7, CH	4.13, br d (8.7)	7, 9	7, 9, 10, 11	6, 9, 11, 12, 13
9	143.7, CH	6.79, d (1.8)	8	1, 7, 10, 14	8
10	134.3, qC				
11	27.3, CH	2.25, m	7, 12, 13	7, 8	7, 8, 9, 12, 13
12	18.9, CH_3	1.00, d (7.1)	11	7, 11, 13	5, 7, 8, 11
13	21.1, CH_3	1.10, d (7.1)	11	7, 11, 12	5, 7, 8, 11
14	168.0, qC				
15	23.9, CH_3	1.68, br s	5	3, 4, 5	5

[a]Acetone-d_6, 300/75.5 MHz. [b] Assignments are based on extensive 1D and 2D NMR experiments (HMBC, HSQC, COSY). [c] Numbers refer to proton resonances. [d] Numbers refer to carbon resonances. [e] Implied multiplicities determined by DEPT.

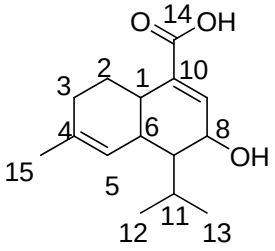

2D NMR tables for Verticinols in the main text
2D NMR tables for the novel furyl derivative in the main text

13.4. Appendix - Spectroscopic data Supporting Information

Note: Supporting information of verticinols A and B, and the furyl derivative 2-(furan-3-yl)acetic acid were integrated in the respective chapters

Supporting Information for Marilines A – D (*Stachylidium* sp.)

Figure 1. Key HMBC and NOE correlations of marilines A – D

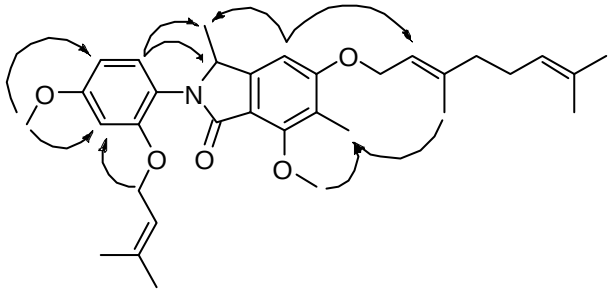

NOE Correlations (marilines A and B)

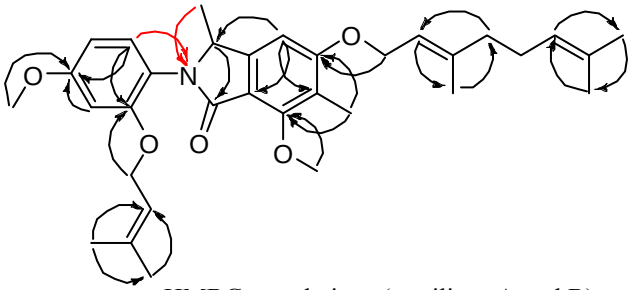

HMBC correlations (marilines A and B)
(^{15}N HMBC correlations in red arrows)

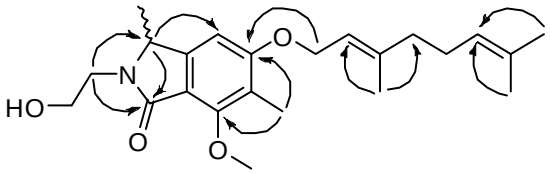

HMBC correlations (marilines C)

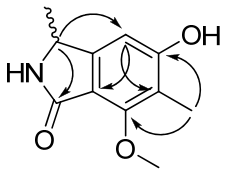

HMBC correlations (marilines D)

Figure 2. HMBC NMR data for marilines A and B

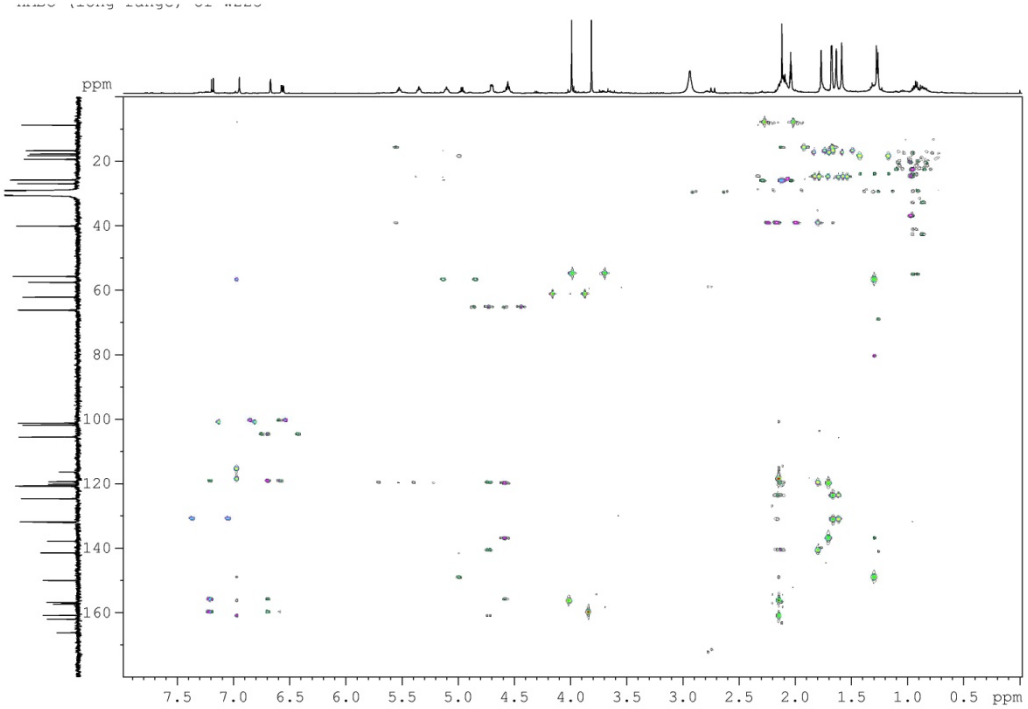

Figure 3. NOE NMR data for marilines A and B

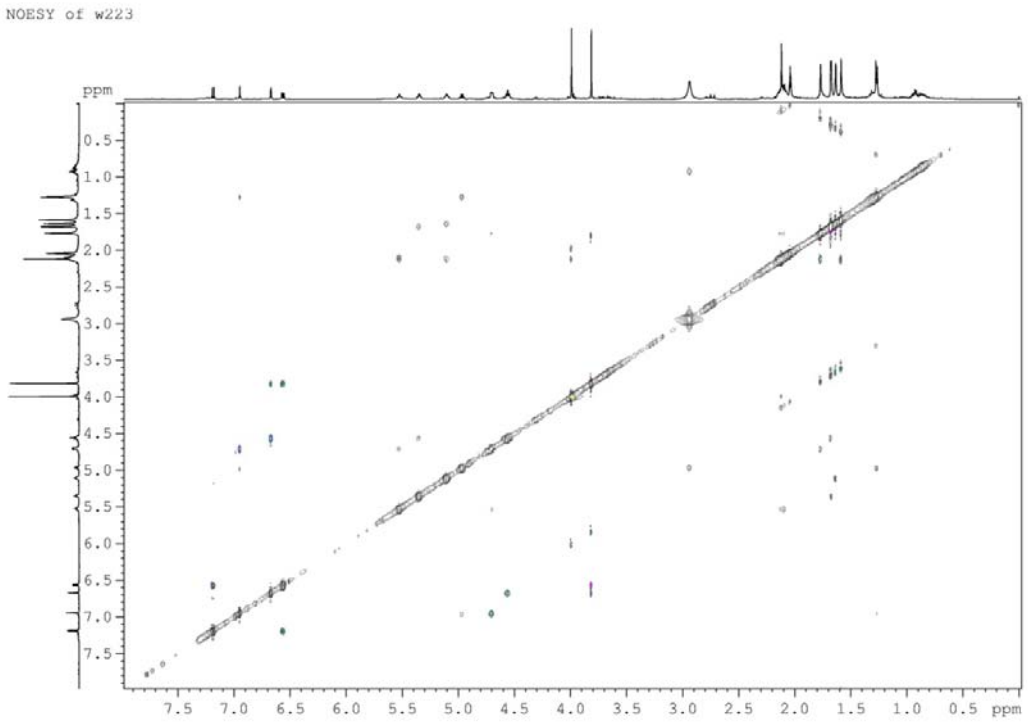

Figure 4. Separation chromatogram for marilines A (compound 1) and B (compound 2)

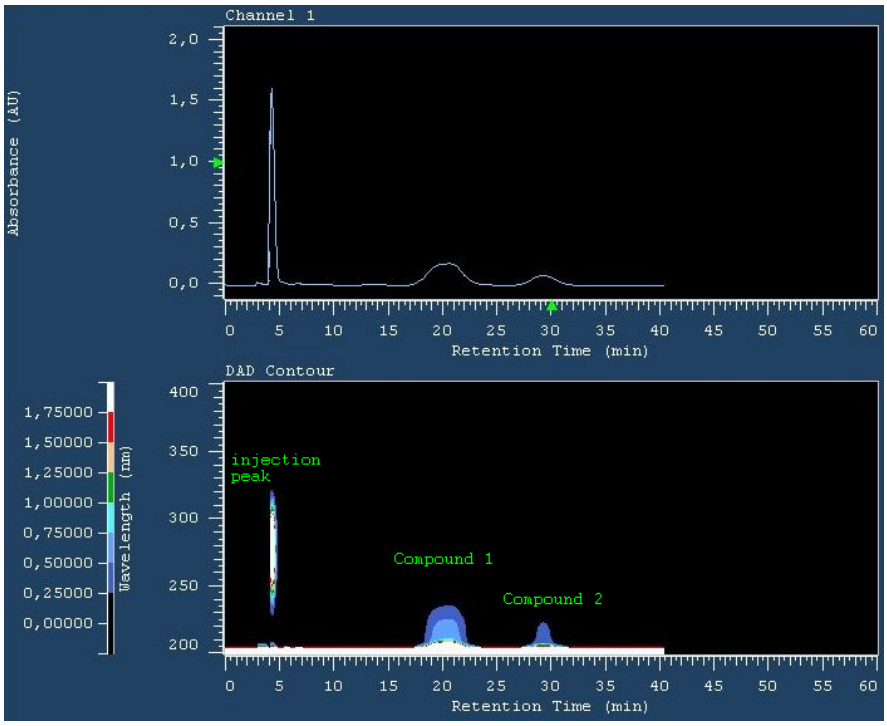

Figure 5. Formation of 2, 4-dihydroxyaniline, putative precursor of marilines A/B

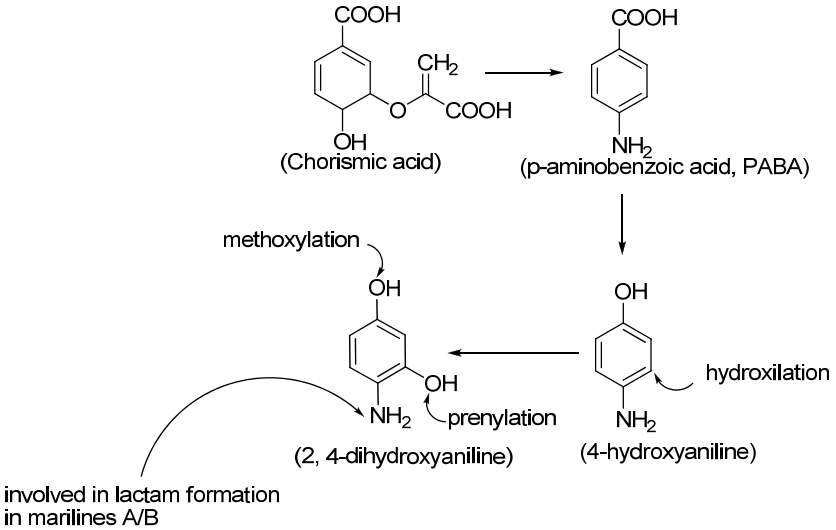

Figure 6. Reported structures similar to marilines A-D referred in the marilines chapter

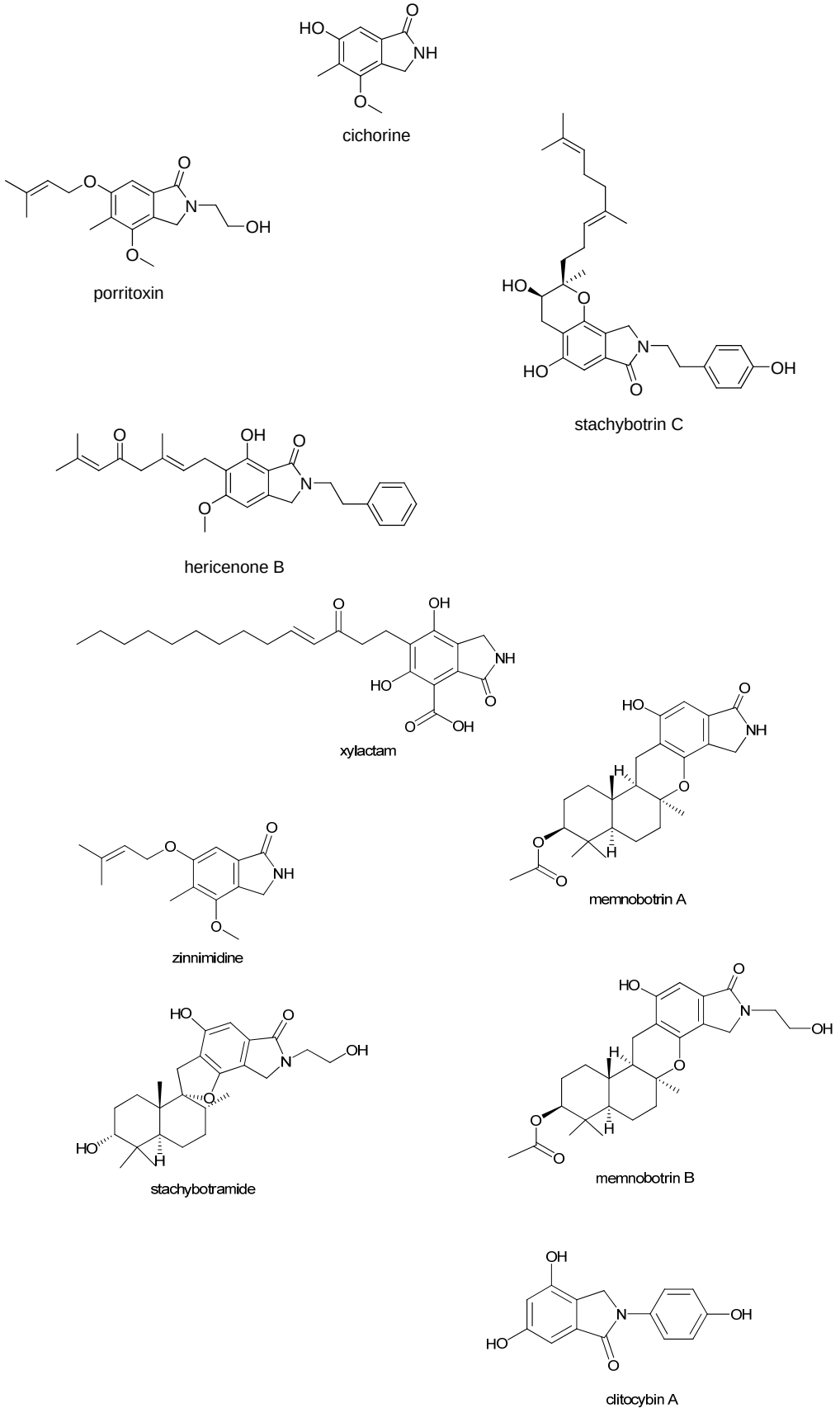

Figure 7. Reported natural products with similar backbones related to 2,4-dihydroxyaniline

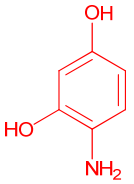

2, 4-dihydroxyaniline

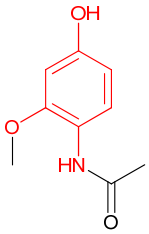

4-hydroxy-2-methoxyacetanilide

Fungal endophyte DAOM 221611 from spruce needles:
(Findlay *et al*., 2003)
and from *Penicillium* sp.:
(El-Beih *et al*., 2007)

Porifera *Oceanapia* sp.:
(Venkateswarlu *et al*., 1999)

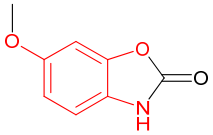

coixol

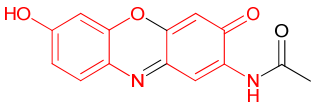

2-Acetylamino-7-hydroxy-3H-phenoxazin-3-one

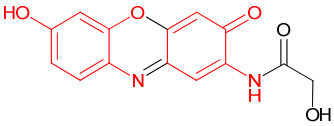

7-Hydroxy-2-(2-hydroxyacetyl)-amino-3H-phenoxazin-3-one

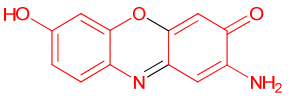

2-Amino-7-hydroxy-3H-phenoxazin-3-one

Fungus *Chaetosphaeria* sp.:
(Zikmundova *et al*., 2002)

Figure 8. Key HMBC correlations for marilones A - J

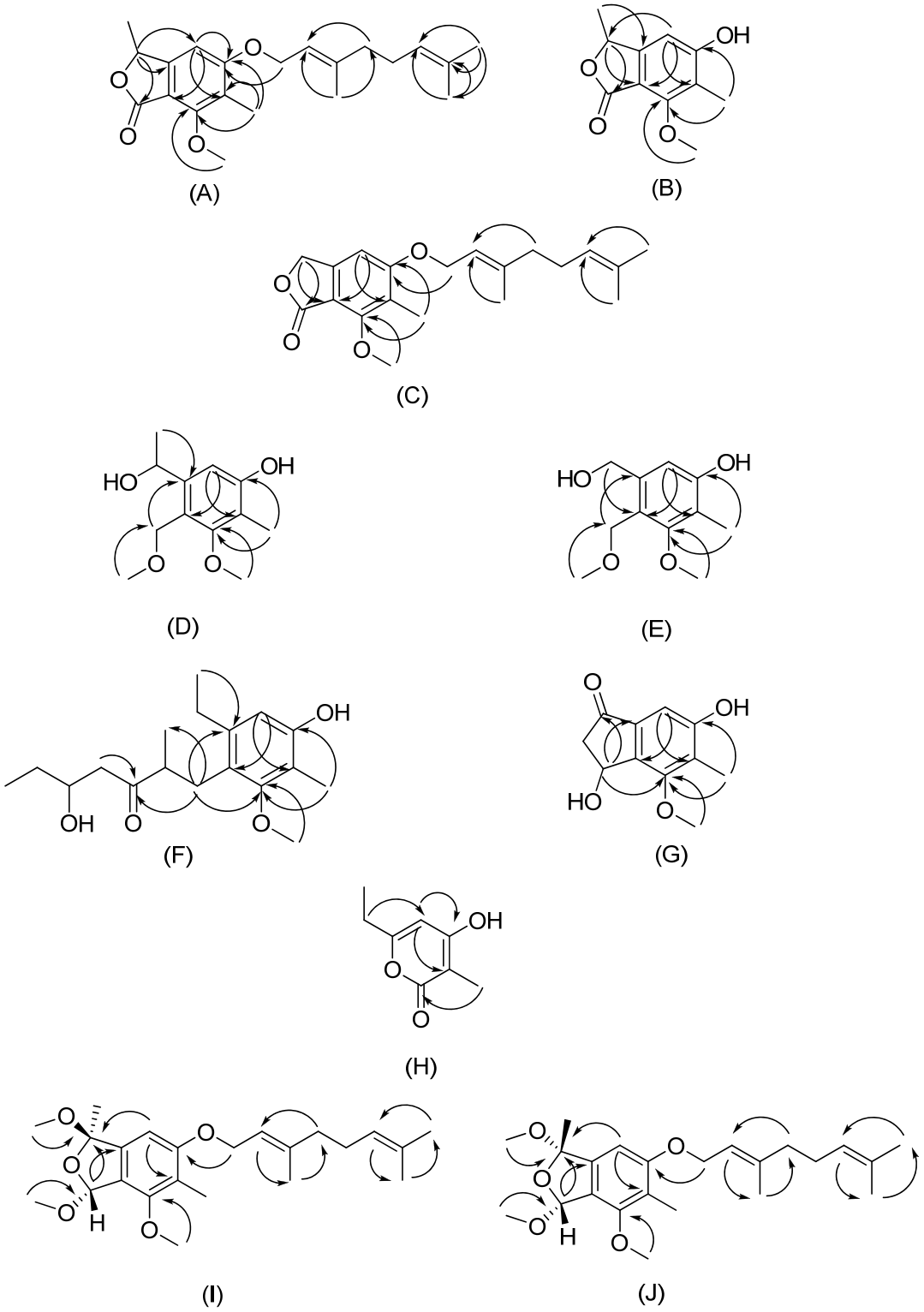

Table 1. ^{1}H-NMR spectroscopic data comparison of reported values for silvaticol and nidulol with compound 9 (marilones chapter) for the conclusive elucidation as silvaticol

	^{1}H NMR ($CDCl_3$)		
Position	Compound **9**	Silvaticol*	Nidulol*
1			
2			
3			
4			
5			
6	**7.05**	**7.04**	**6.59**
7			
8	5.39	5.39	5.15
9	3.90	3.91	4.08
10	2.23	2.23	2.19

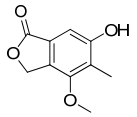

Silvaticol

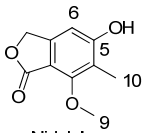

Nidulol

* (Kawahara *et al*, **1988**)

Table 2. ^{1}H-NMR spectroscopic data comparison of compounds **1** and **3** with silvaticol and nidulol derivatives

			^{1}H NMR ($CDCl_3$)	
position	**Marilone A**	**Marilone C**	6-(3',3'-dimethylallyloxy-4-methoxy-5-methylphthalide**	5-(3',3'-dimethylallyloxy-7-methoxy-6-methylphthalide**
1				
2				
3				
4				
5				
6	**6.54**	**7.05**	**7.08**	**6.62**
7				
Protons at C-1/C8	5.39	5.39	5.38	5.18
9	4.04	3.90	3.89	4.03
10	2.18	2.23	2.21	2.15
			silvaticol derivative	nidulol derivative

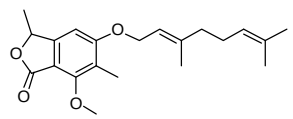

marilone A

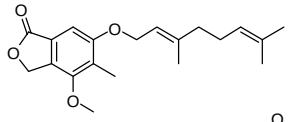

marilone C

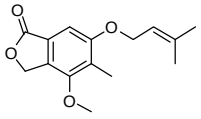

silvaticol derivative

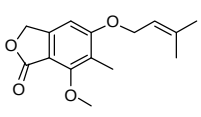

nidulol derivative

** (Suemitsu *et al.*, **1995**)

Figure 9a and b. CD spectra of stachylines B and C

a) CD spectra of stachyline B

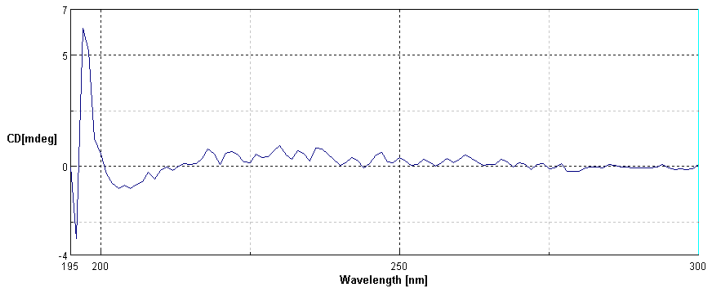

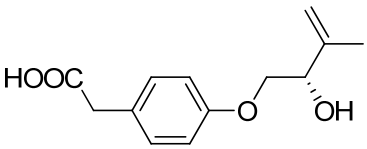

b) CD spectra of stachyline C

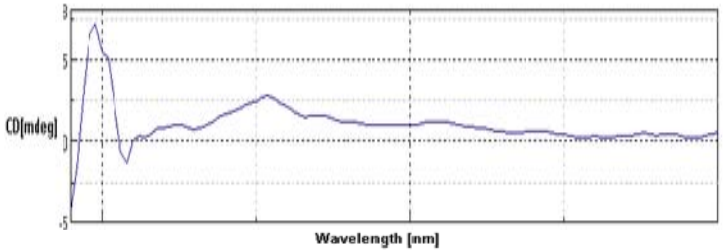

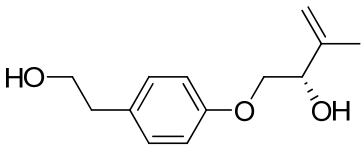

Figure 10. Key HMBC correlations of stachylines A - D

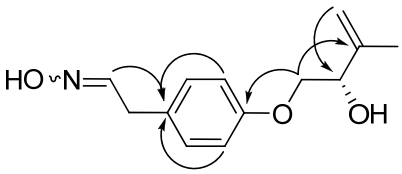

(**A**)

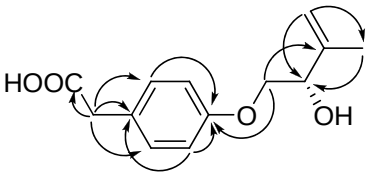

(**B**)

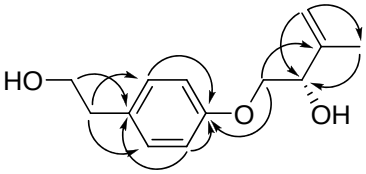

(**C**)

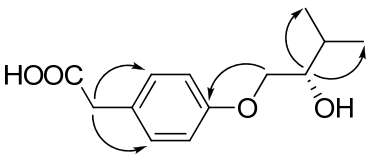

(**D**)

Figure 11. ^{1}H NMR spectroscopic data of the respective (*R*)- and (*S*)-MTPA esters of stachyline B.

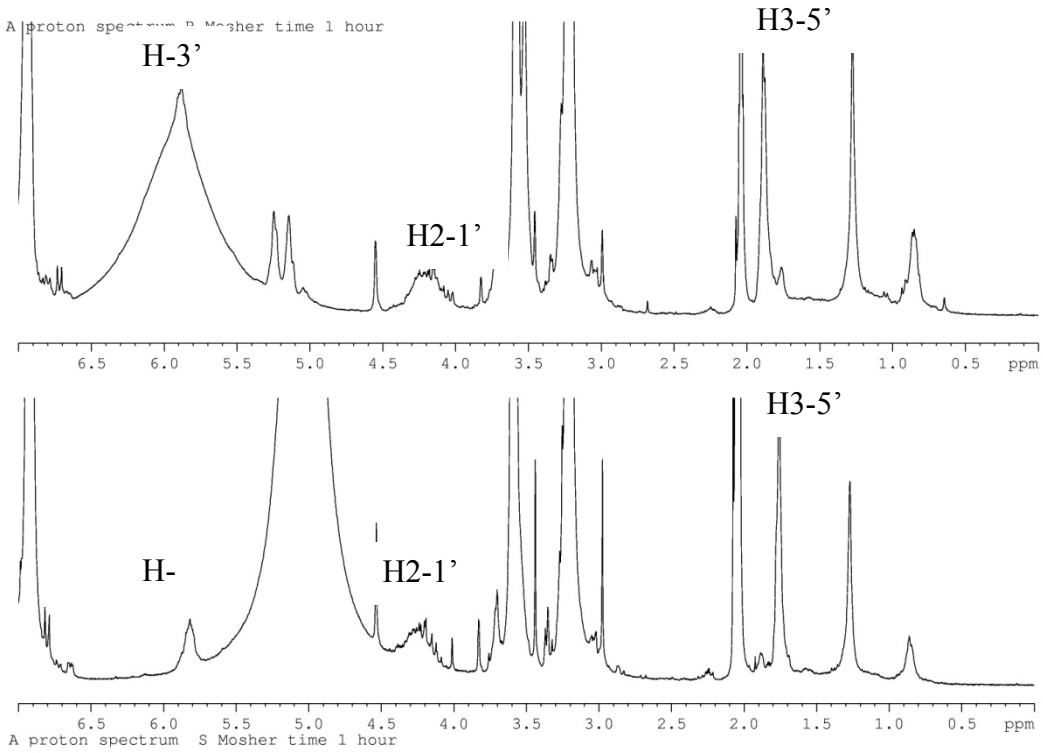

Figure 12 (a-c). ^{1}H-^{13}C HSQC spectroscopic data of stachyline B and the respective (*R*)- and (*S*)-MPTA esters.

a) HSQC spectrum of stachyline B:

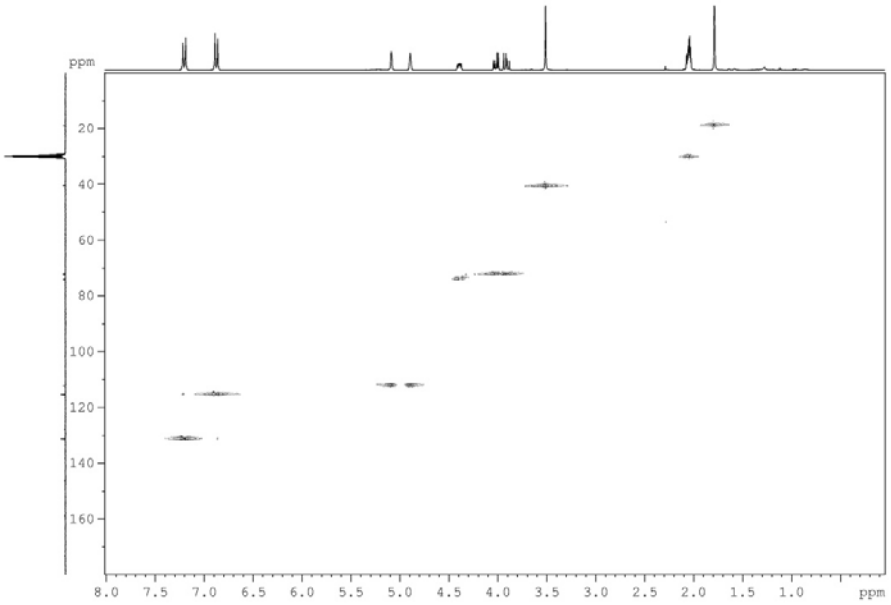

b) HSQC spectrum of *S*- Mosher

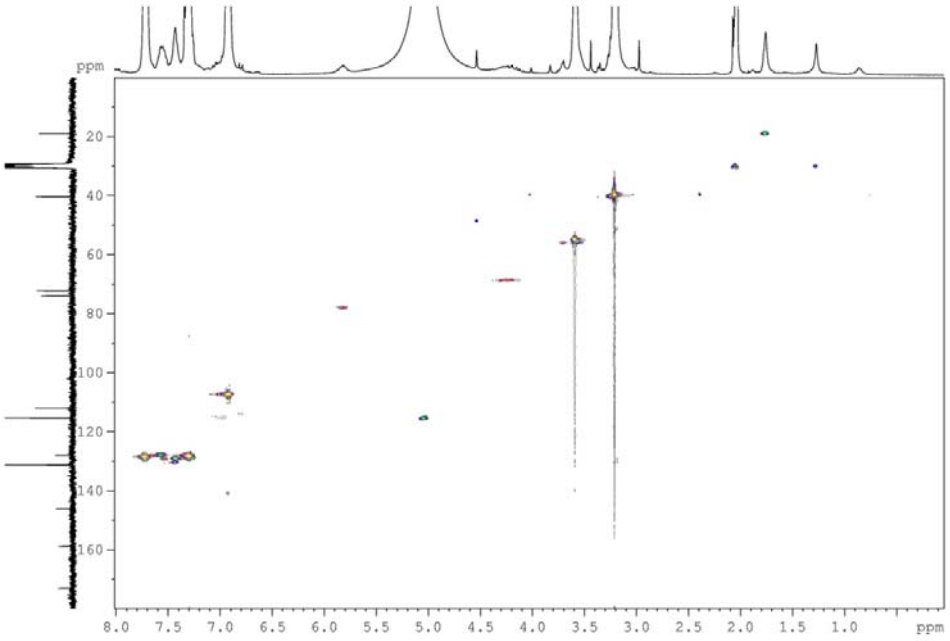

c) HSQC spectrum of *R*- Mosher

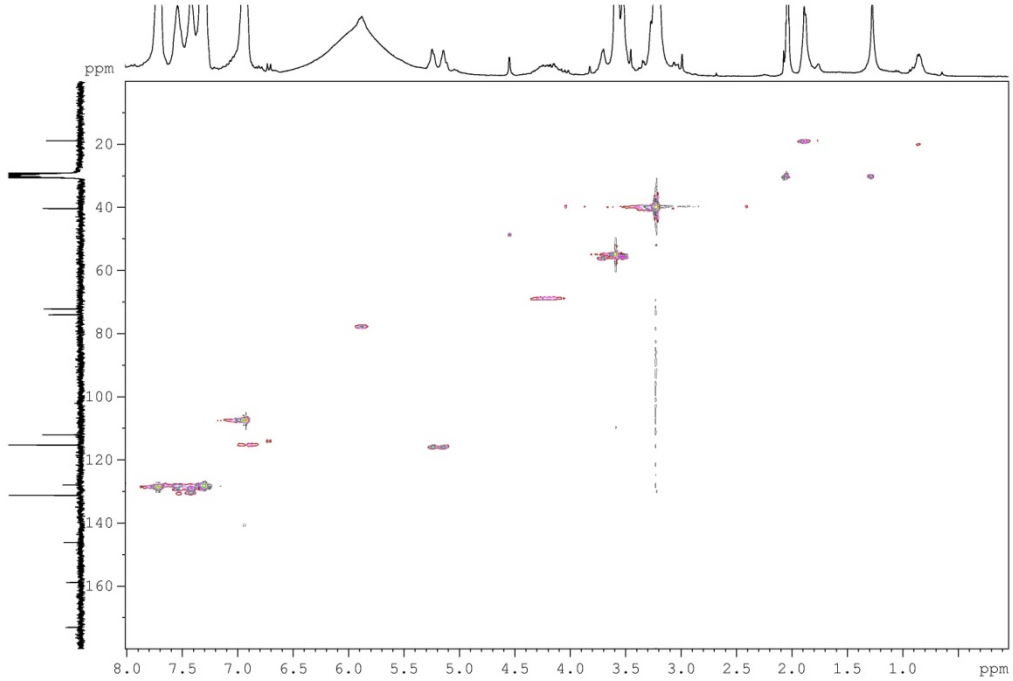

Figure 13. LC-MS (ESI, 2 experiments in + mode) data for stachyline A (*E*- and *Z*-)

Peak 16.05 min., 236.4 and 236.3 $(M+H)^+$

Peak 16.61 min., 236.1 and 236.3 $(M+H)^+$

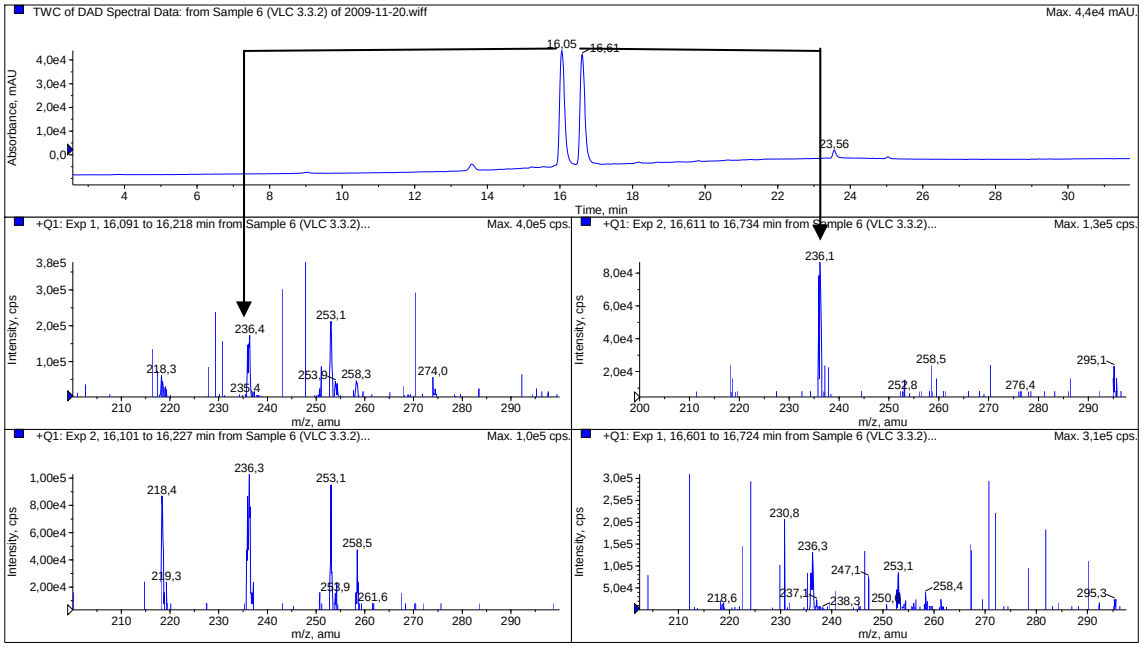

Supporting Information for Hydroxylated Sclerosporin Derivatives (*Cadophora malorum*)

Figure 14. Infra-red spectra of sclerosporin and the four novel hydroxylated sclerosporin derivatives

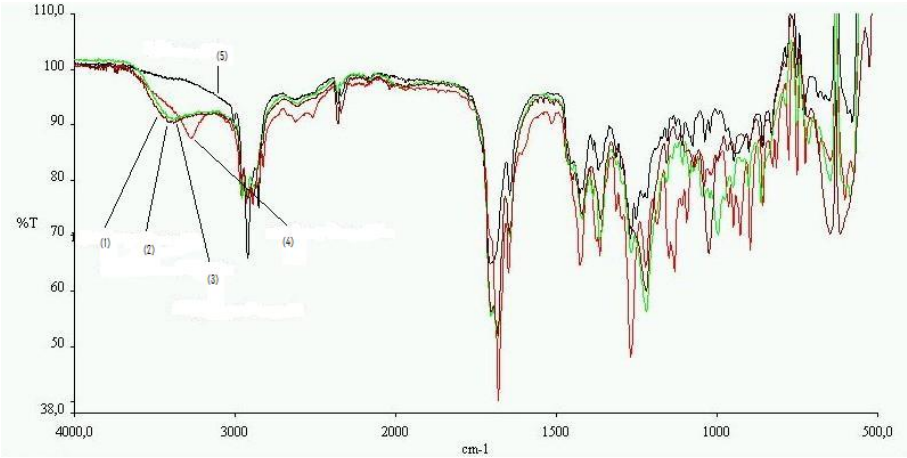

Figure 15. Key HMBC correlations for the four novel hydroxylated sclerosporin derivatives

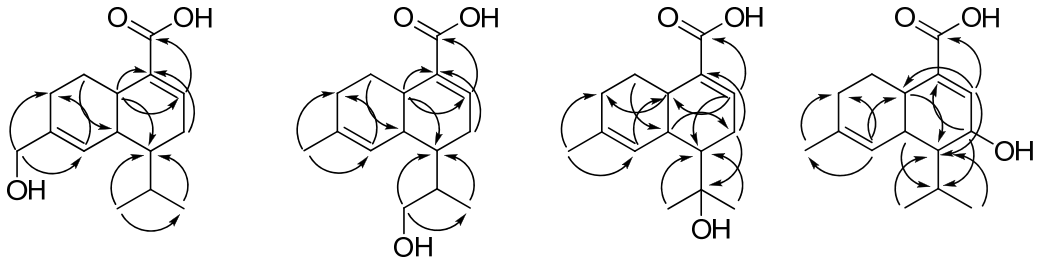

(+)-15-hydroxysclerosporin (2) **(+)-12-hydroxysclerosporin (3)** **(+)-11-hydroxysclerosporin (4)** **(-)-8-hydroxysclerosporin (5)**

Figure 16. Key NOESY correlations for four novel hydroxylated sclerosporin derivatives

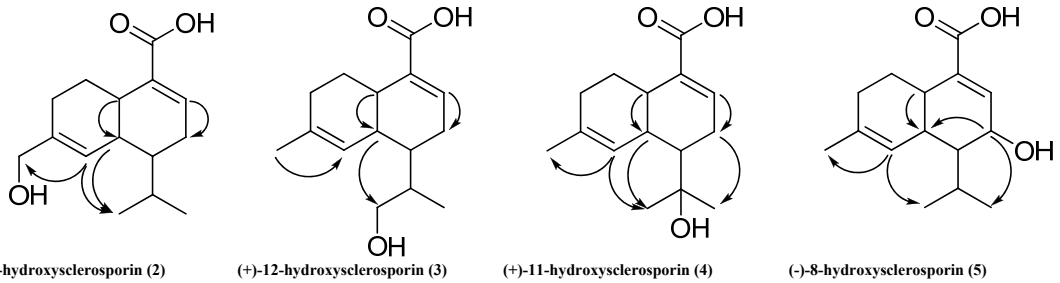

(+)-15-hydroxysclerosporin (2) **(+)-12-hydroxysclerosporin (3)** **(+)-11-hydroxysclerosporin (4)** **(-)-8-hydroxysclerosporin (5)**

Figures 17 a-e. CD spectra for sclerosporin and the hydroxylated sclerosporin derivatives. Respective absolute configuration on the right side.

a) (+)-15-hydroxysclerosporin

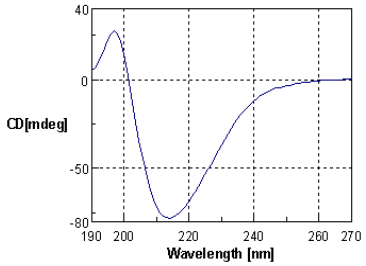

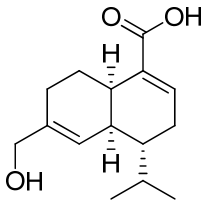

b) (+)-12-hydroxysclerosporin

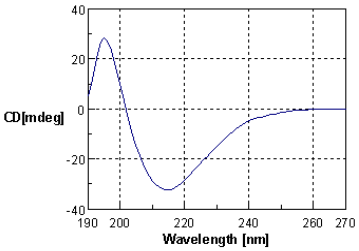

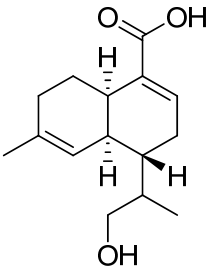

c) (+)-11-hydroxysclerosporin

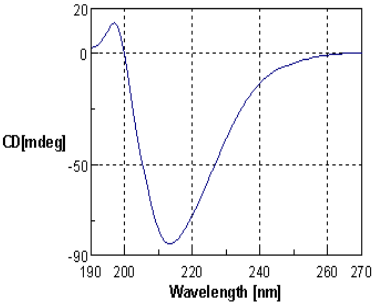

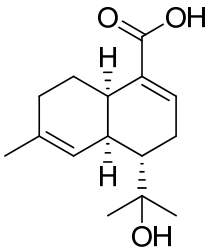

d) (-)-8-hydroxysclerosporin

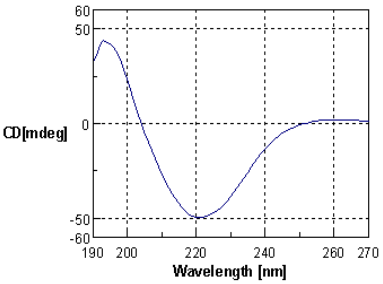

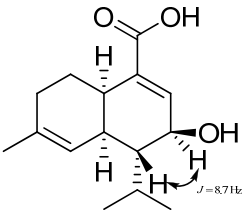

e) (+)-sclerosporin

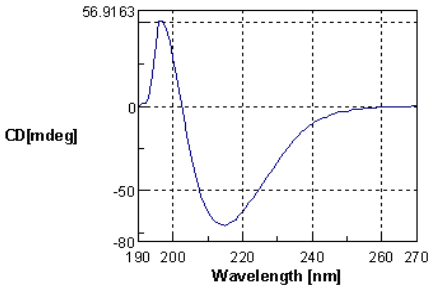

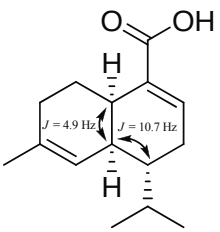

13.5. ^{1}H and ^{13}C NMR spectra

13.5.1. ^{1}H and ^{13}C NMR spectra of new molecules

New molecules from *Stachylidium* sp.

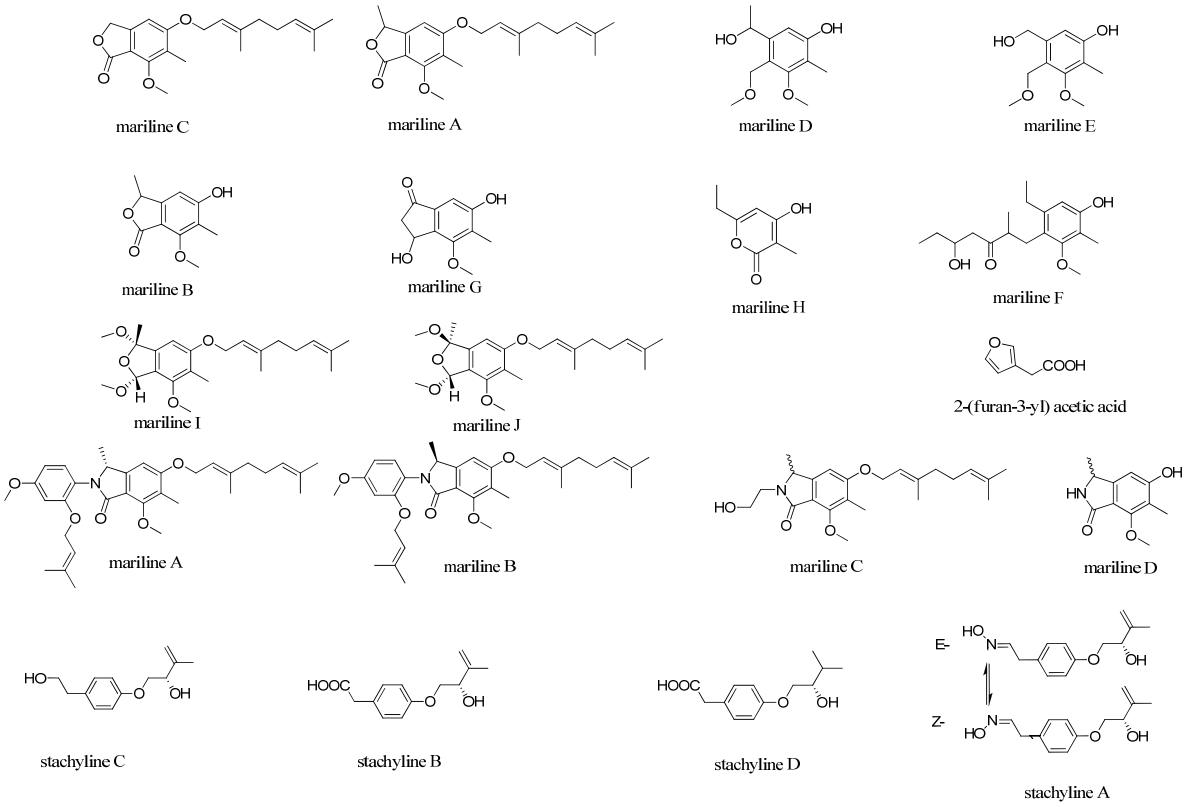

New sclerosporing derivatives from *Cadophora malorum*

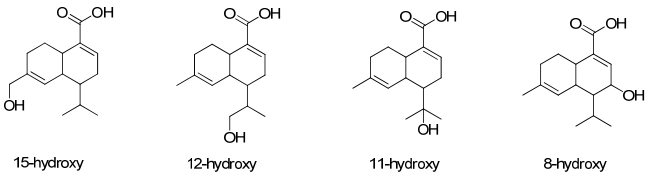

New molecules from *Verticillium tenerum*

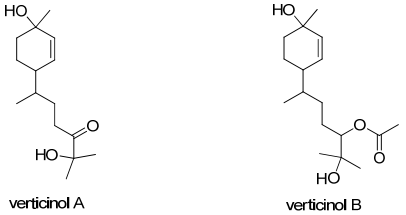

^{1}H NMR spectra (300 MHz, CD_3COCD_3) of marilines A and B

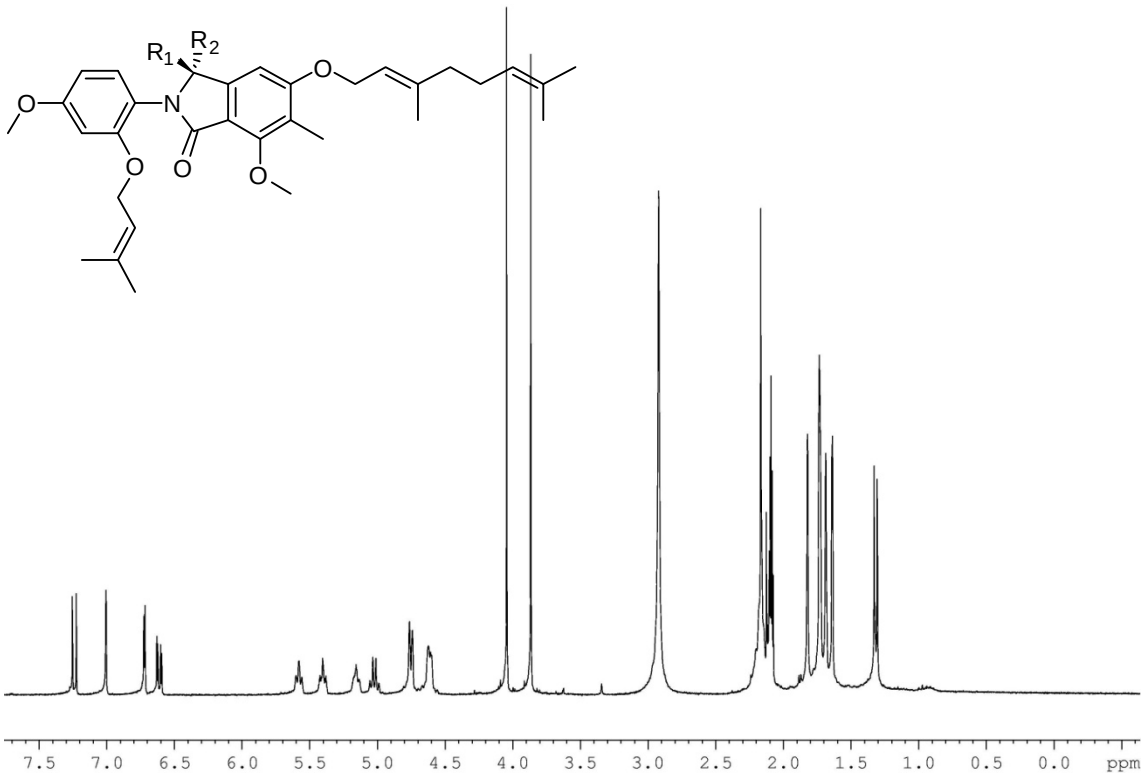

^{13}C NMR spectra (75 MHz, CD_3COCD_3) of marilines A and B

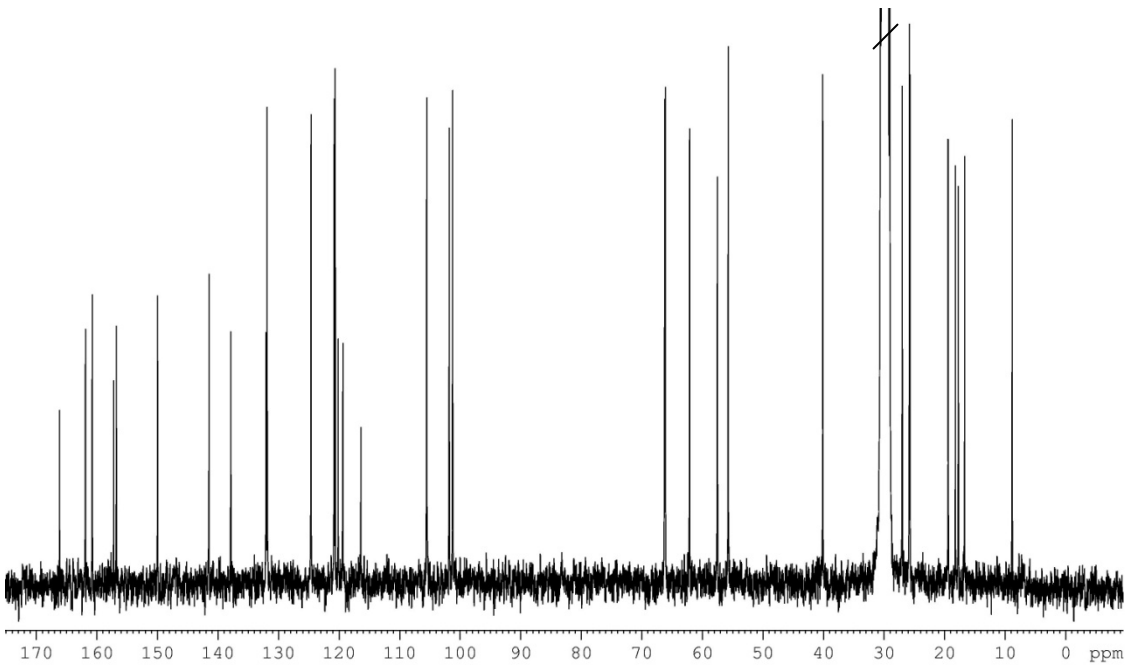

^{1}H NMR spectrum (300 MHz, CD_3COCD_3) of mariline C

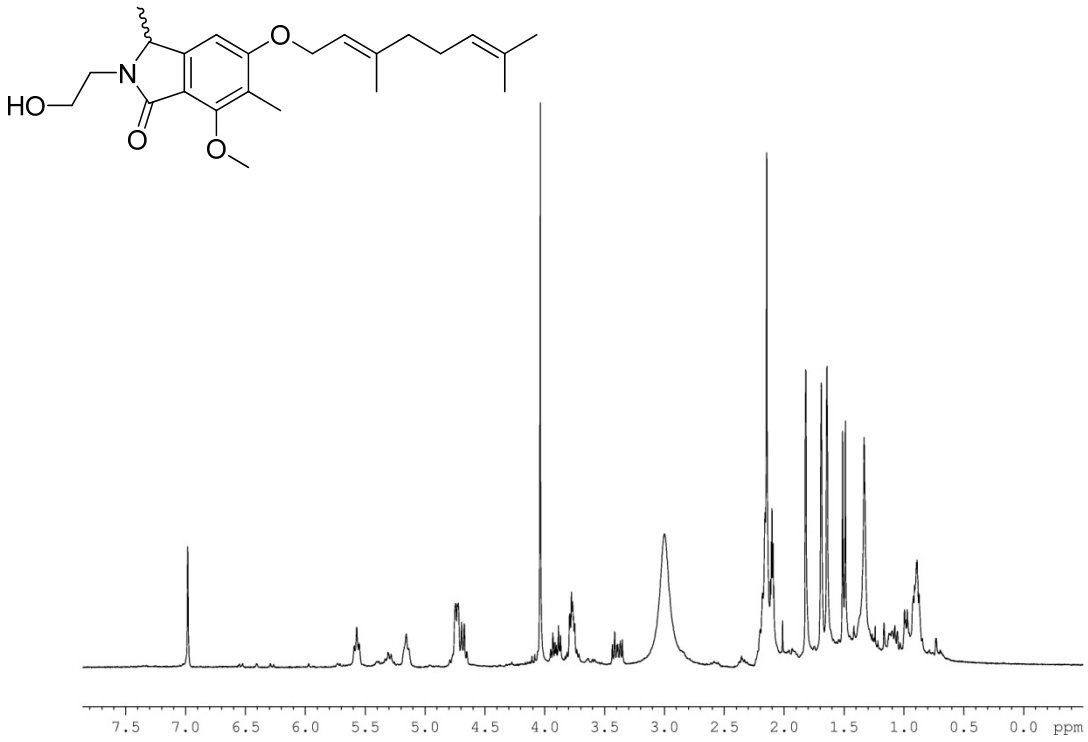

^{13}C NMR spectrum (75 MHz, CD_3COCD_3) of mariline C

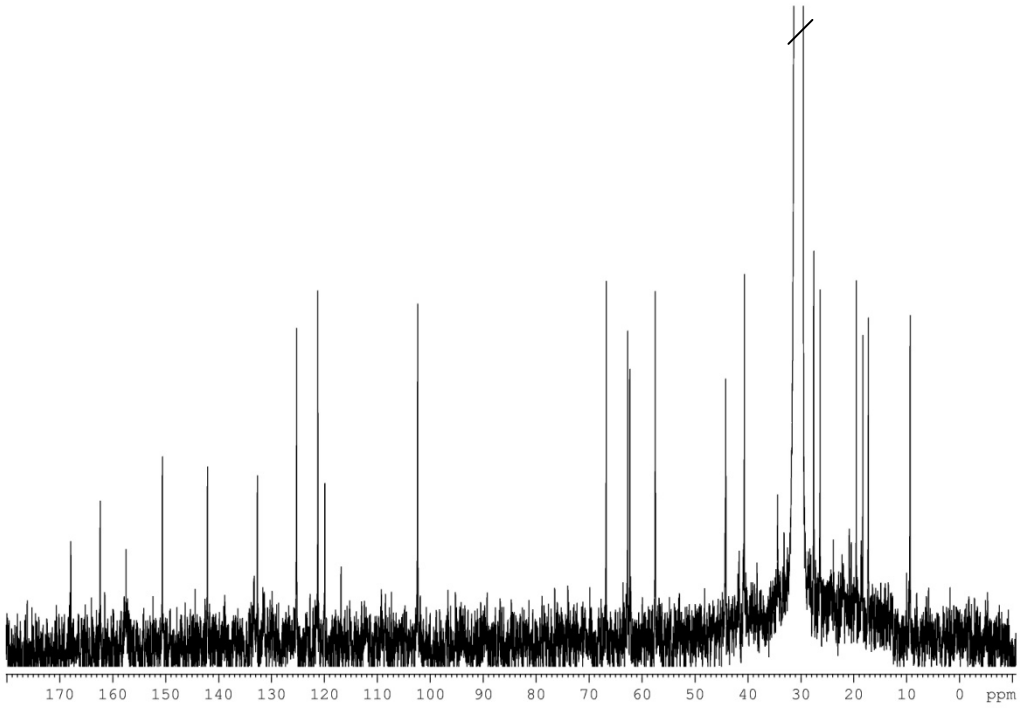

^{1}H NMR spectrum (300 MHz, MeOD) of mariline D

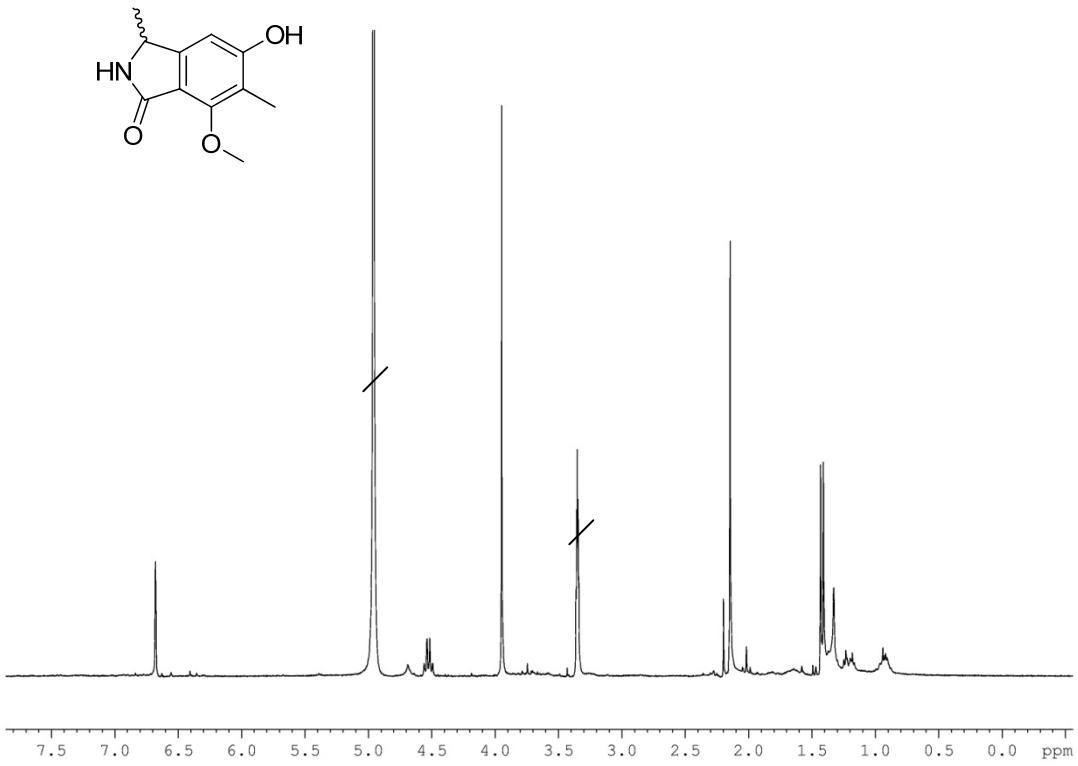

^{13}C NMR spectrum (75 MHz, MeOD) of mariline D

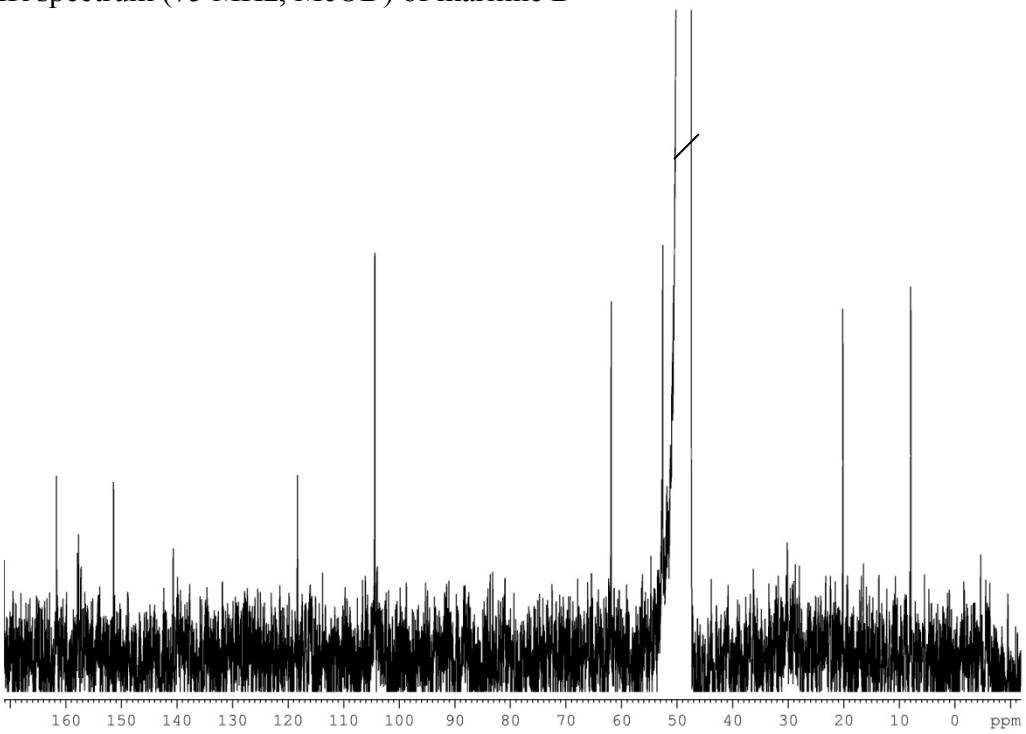

^{1}H NMR (300 MHz, CD_3COCD_3) of marilone A

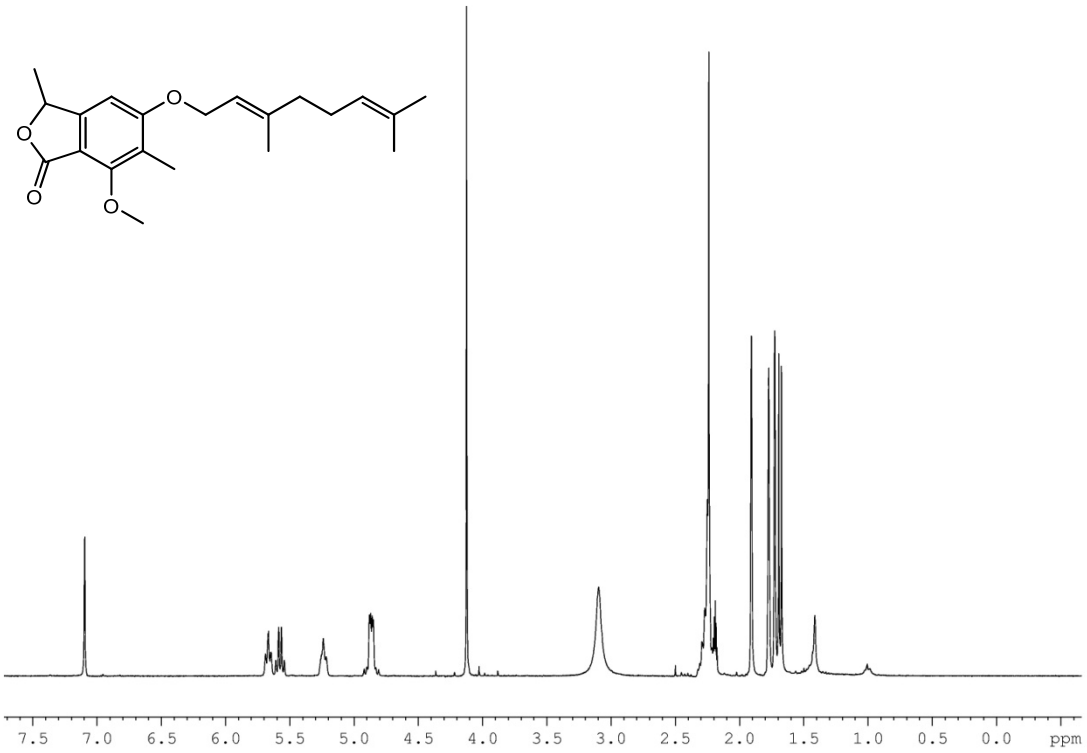

^{13}C NMR (75 MHz, CD_3COCD_3) of marilone A

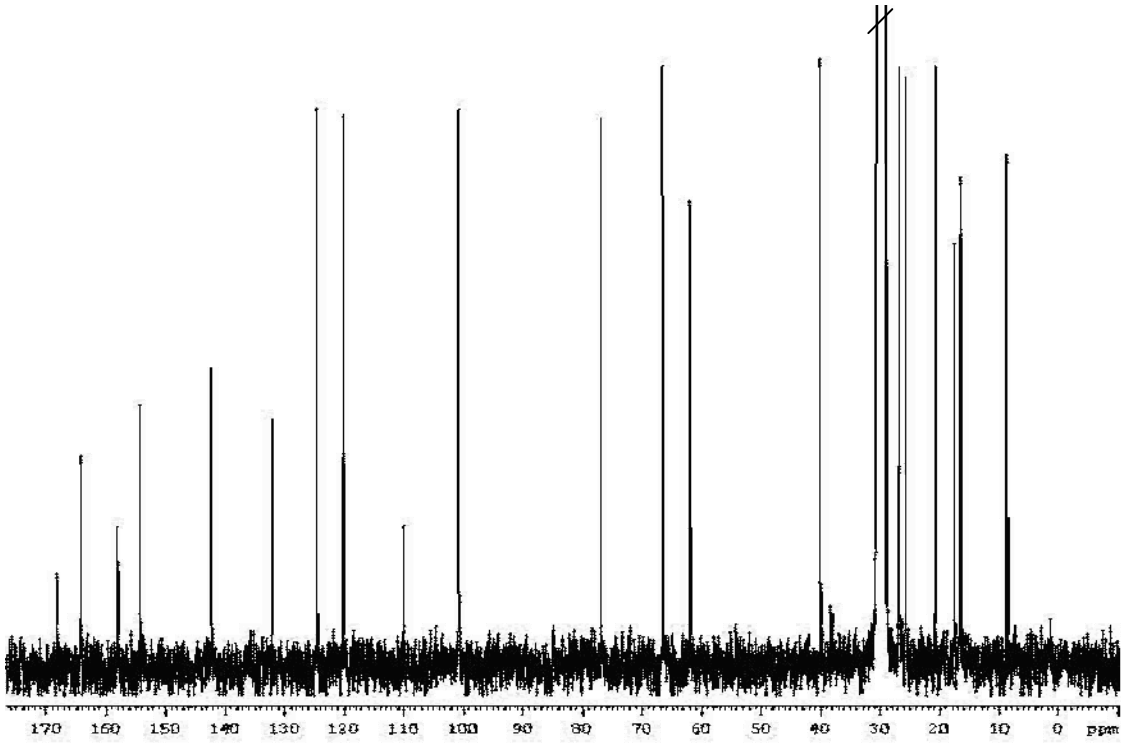

^{1}H NMR (300 MHz, CD_3COCD_3) of marilone B

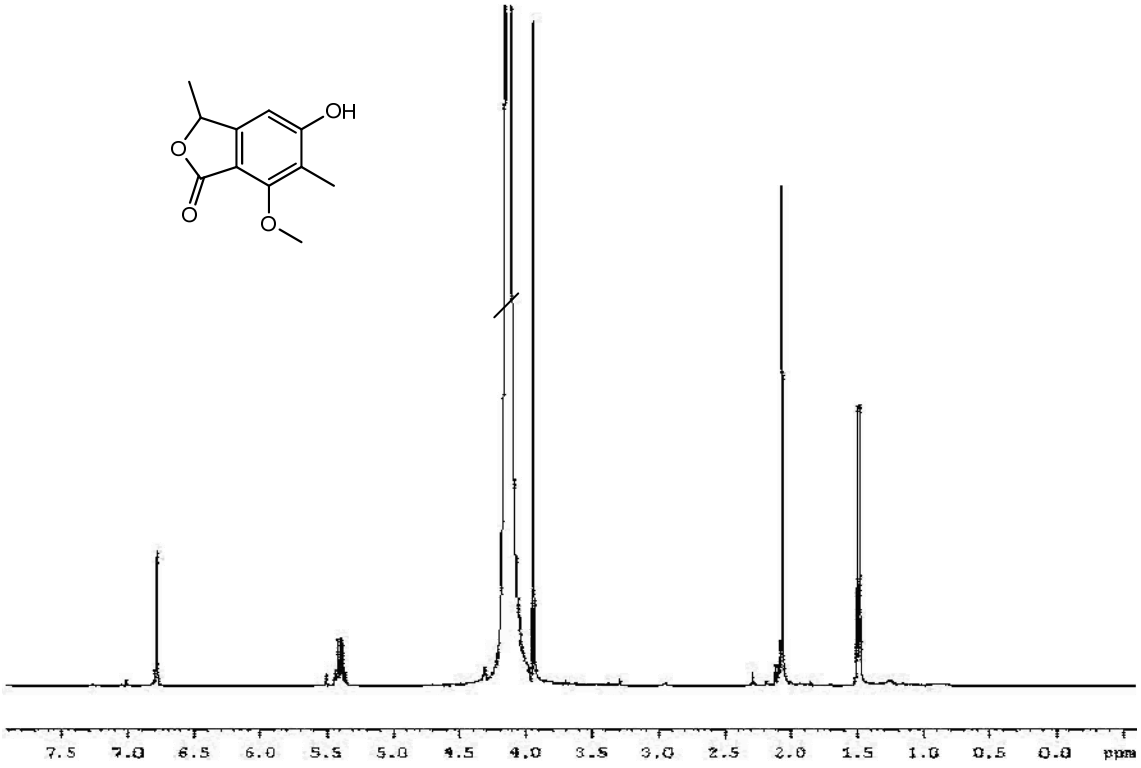

^{13}C NMR (75 MHz, CD_3COCD_3) of marilone B

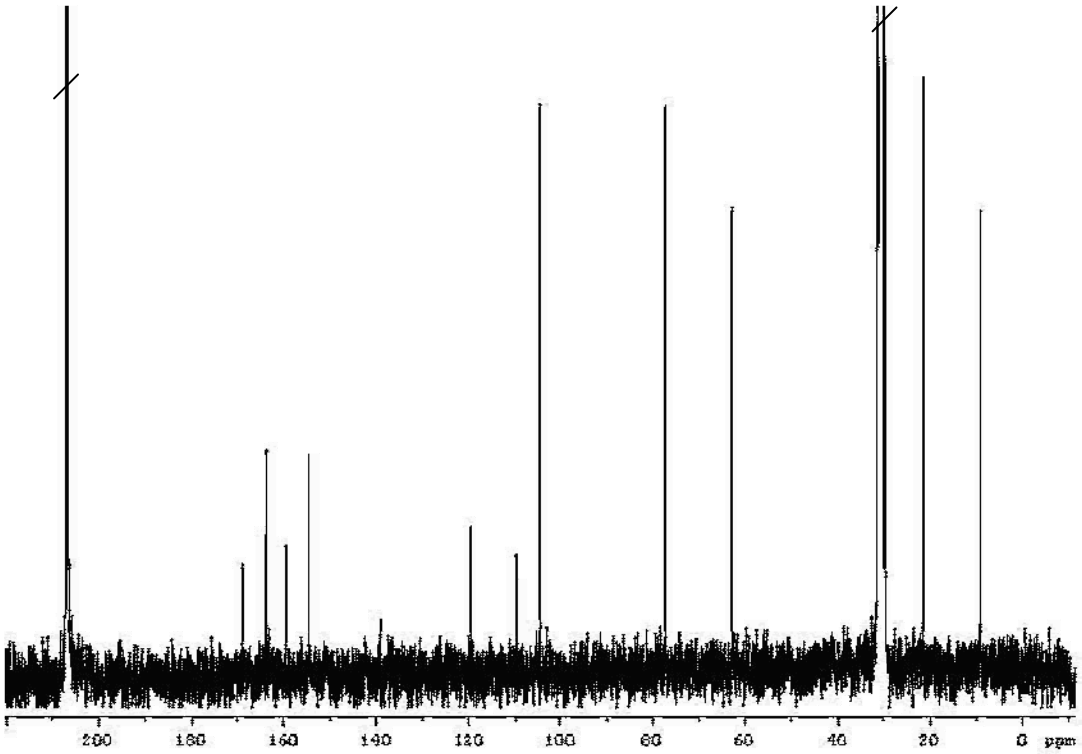

^{1}H NMR (300 MHz, CD_3COCD_3) of marilone C

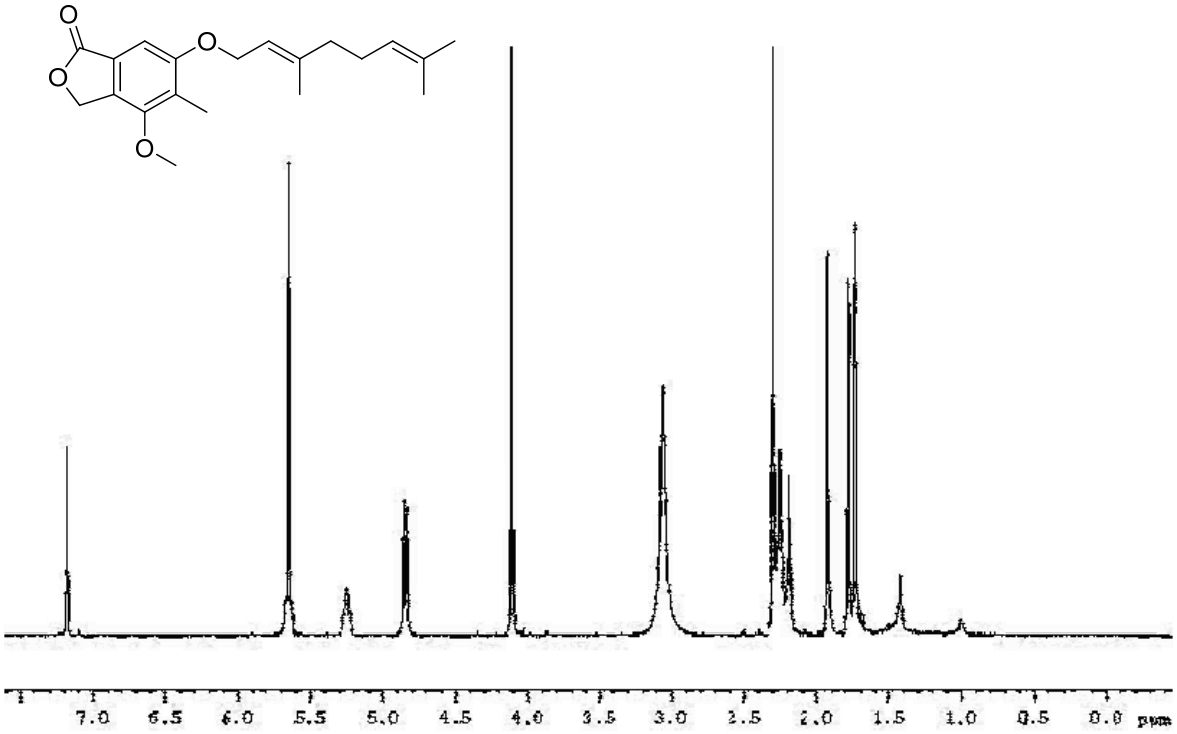

^{13}C NMR (75 MHz, CD_3COCD_3) of marilone C

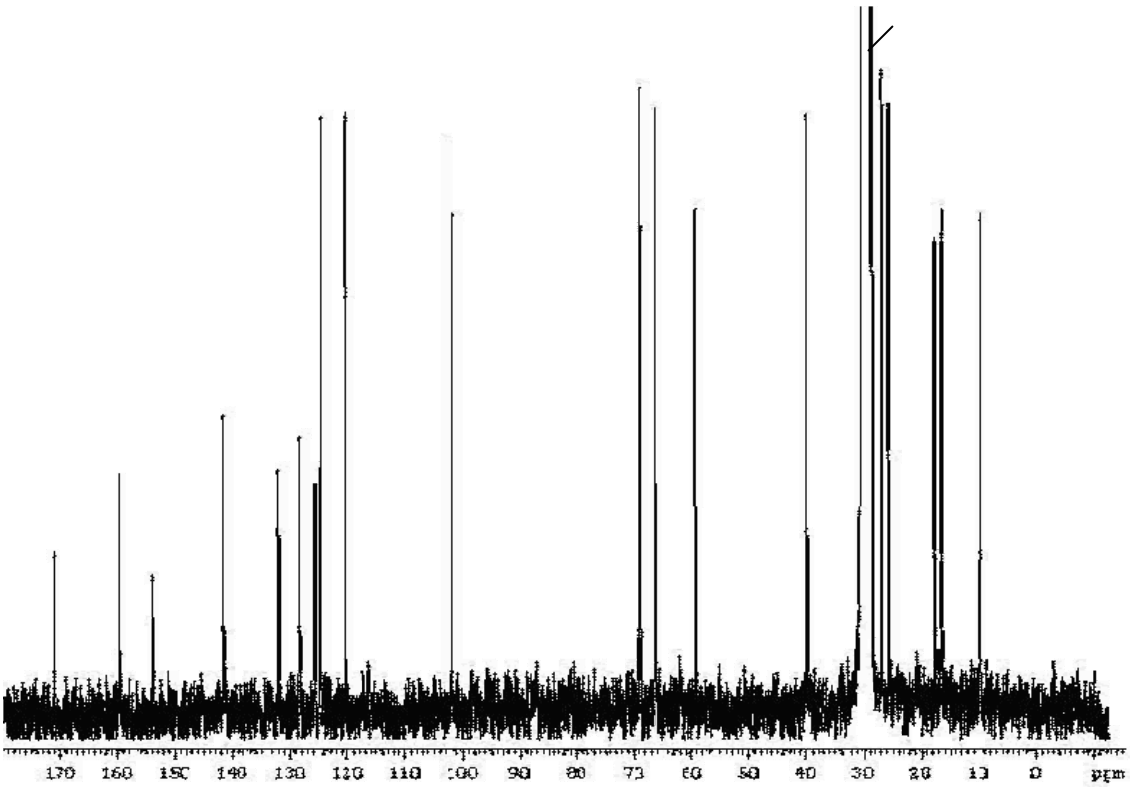

^{1}H NMR (300 MHz, CD_3COCD_3) of marilone D

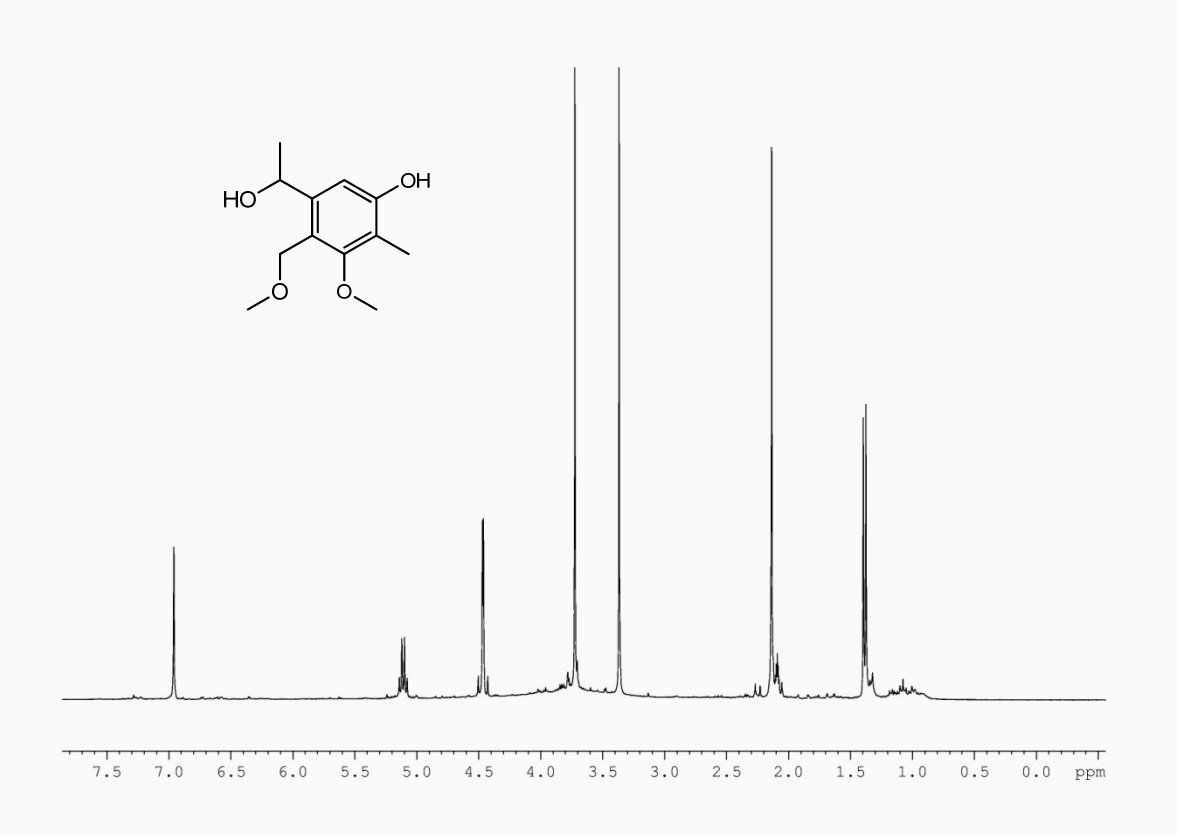

^{13}C NMR (75 MHz, CD_3COCD_3) of marilone D

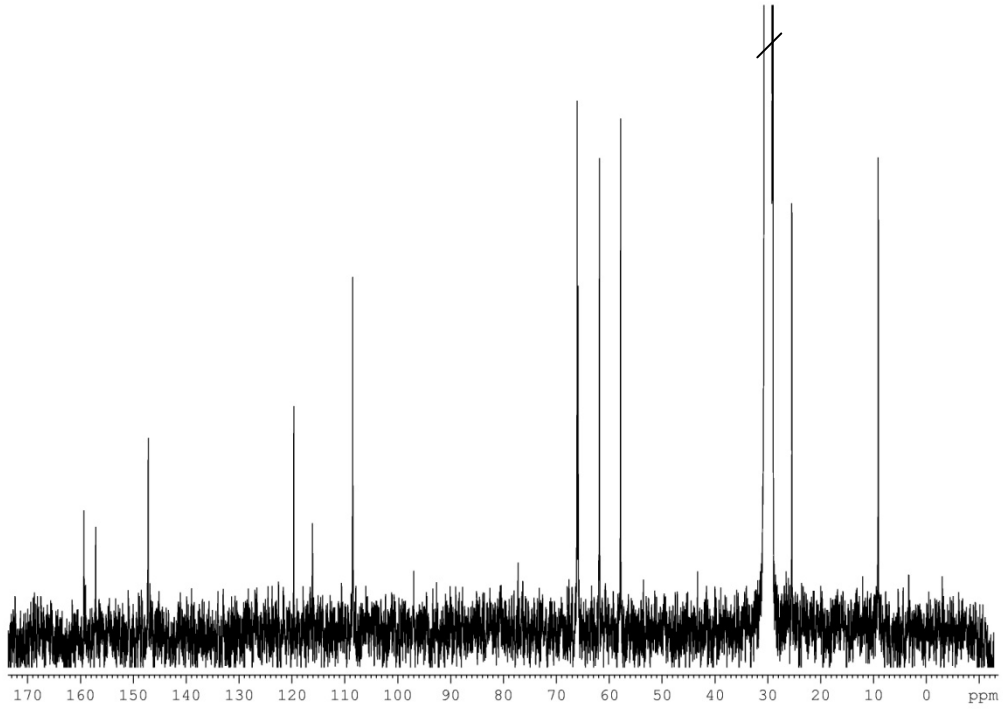

^{1}H NMR (300 MHz, MeOD) of marilone E

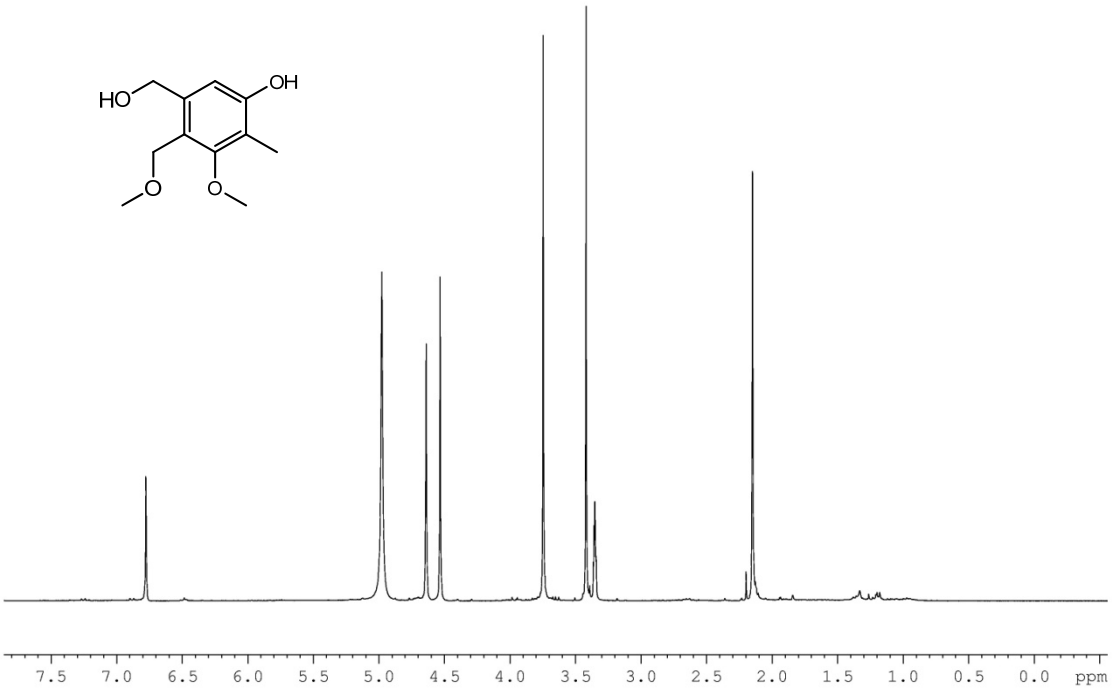

^{13}C NMR (75 MHz, MeOD) of marilone E

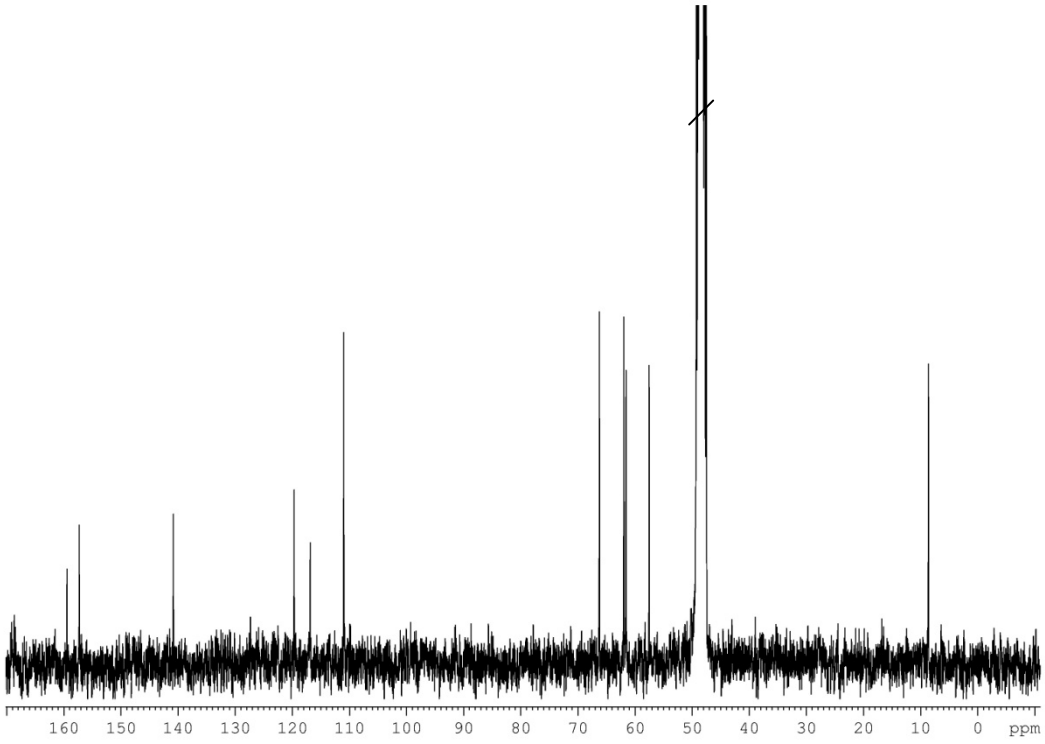

^{1}H NMR (300 MHz, CD_3COCD_3) of marilone F

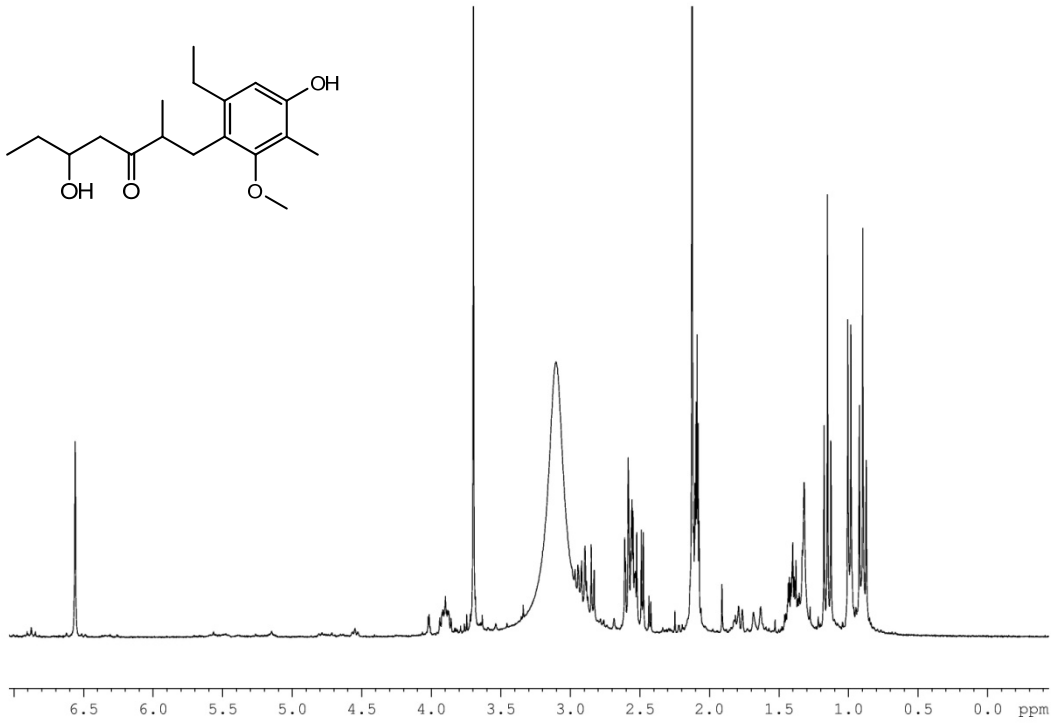

^{13}C NMR (300 MHz, CD_3COCD_3) of marilone F

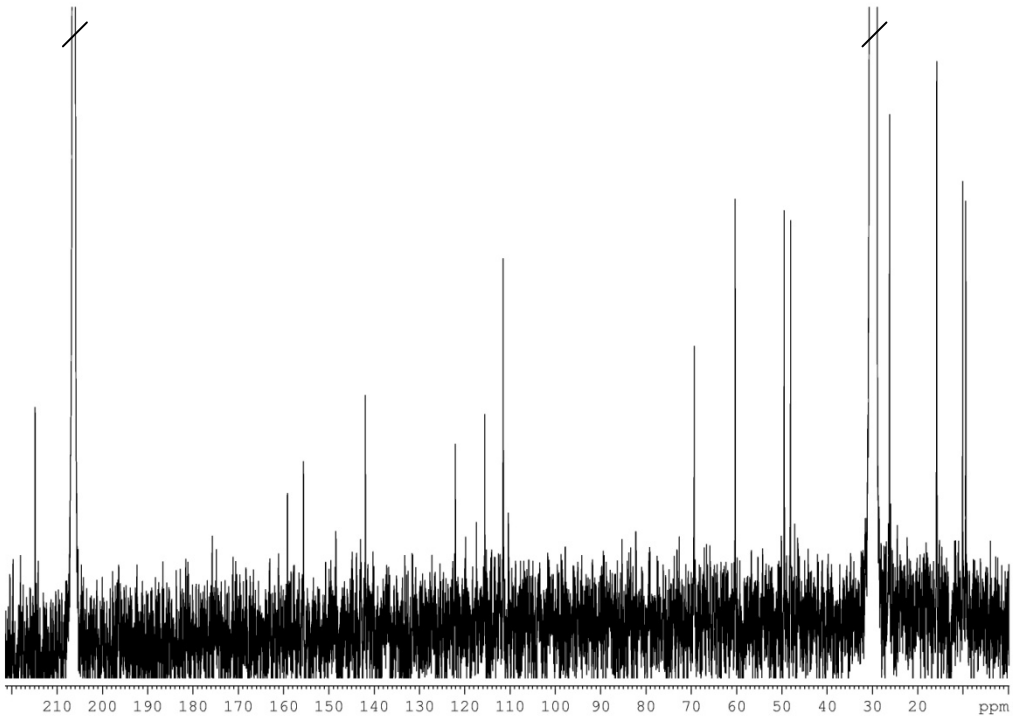

^{1}H NMR (300 MHz, MeOD) of marilone G

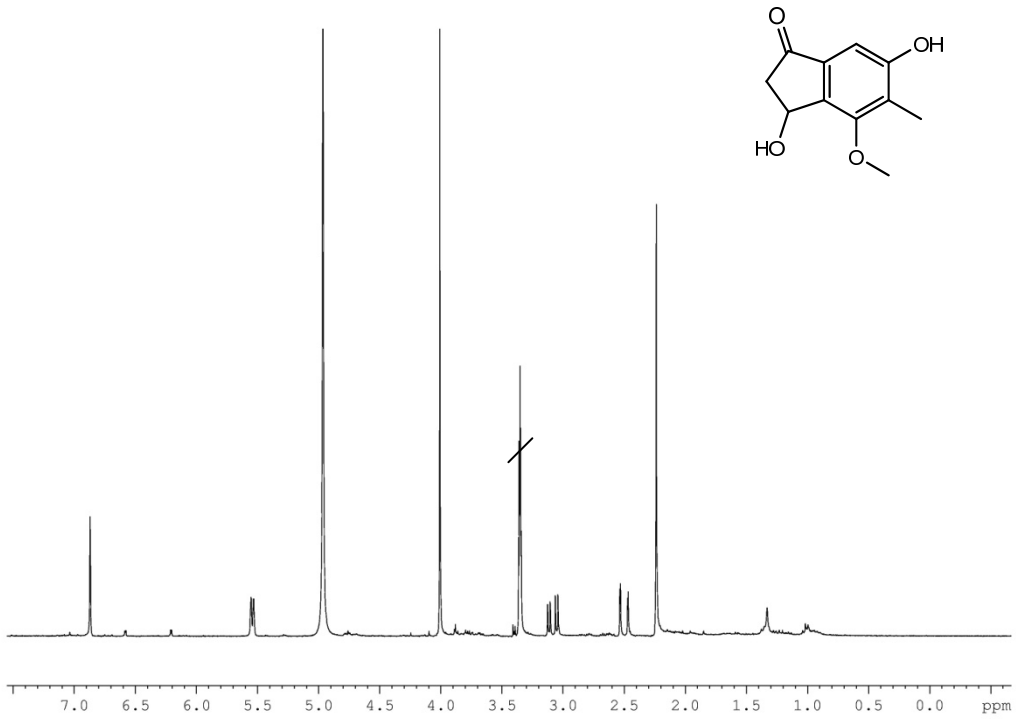

^{13}C NMR (75 MHz, MeOD) of marilone G

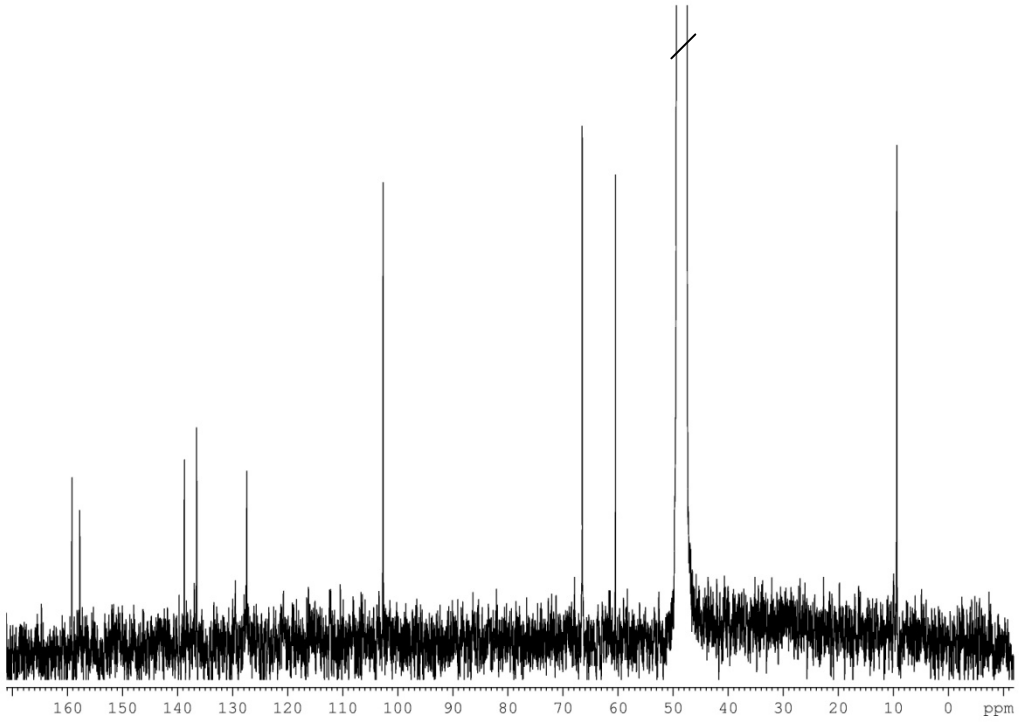

^{1}H NMR (300 MHz, CD_3COCD_3) of marilone H

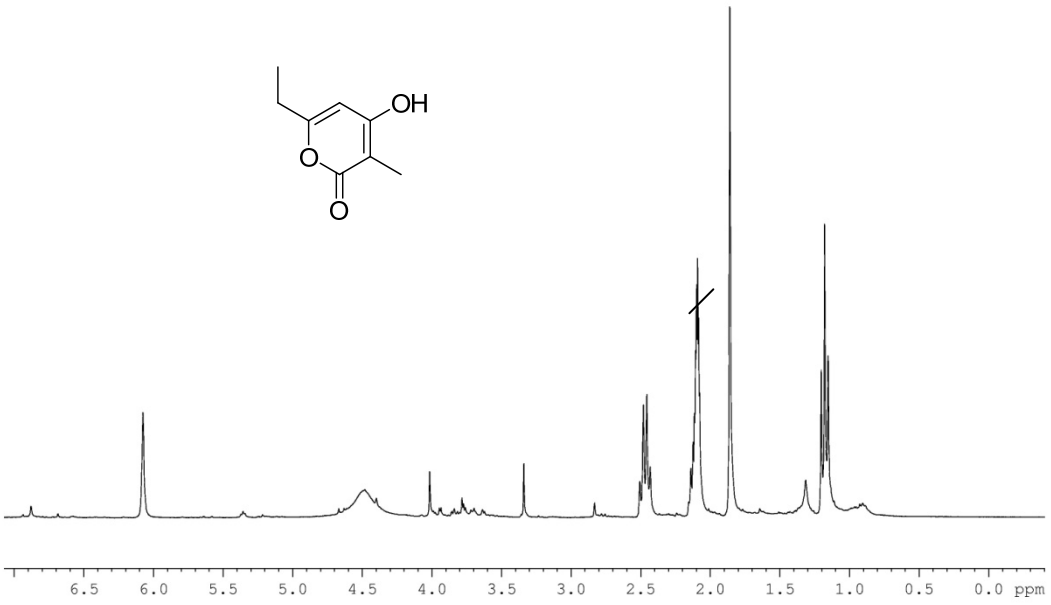

^{13}C NMR (75 MHz, CD_3COCD_3) of marilone H

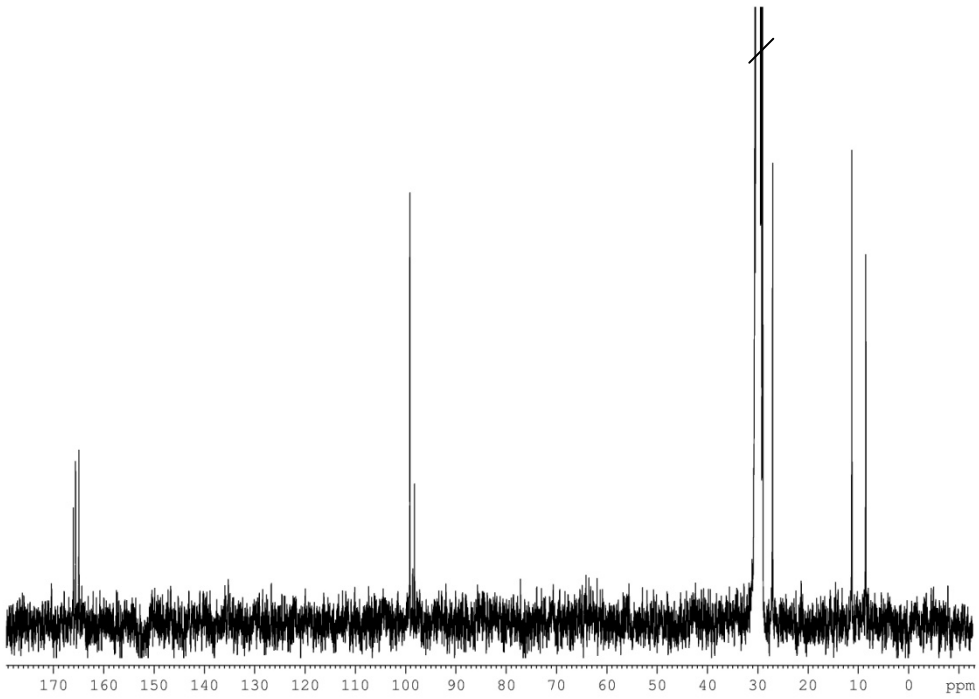

^{1}H NMR (300 MHz, CD_3COCD_3) of marilone I

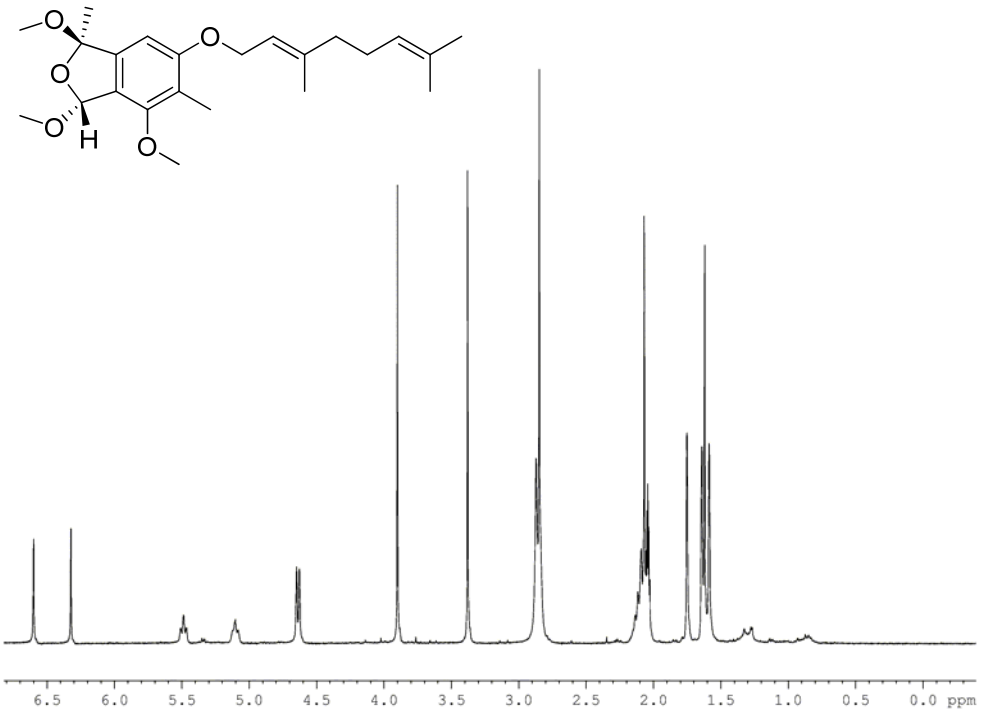

^{13}C NMR (75 MHz, CD_3COCD_3) of marilone I

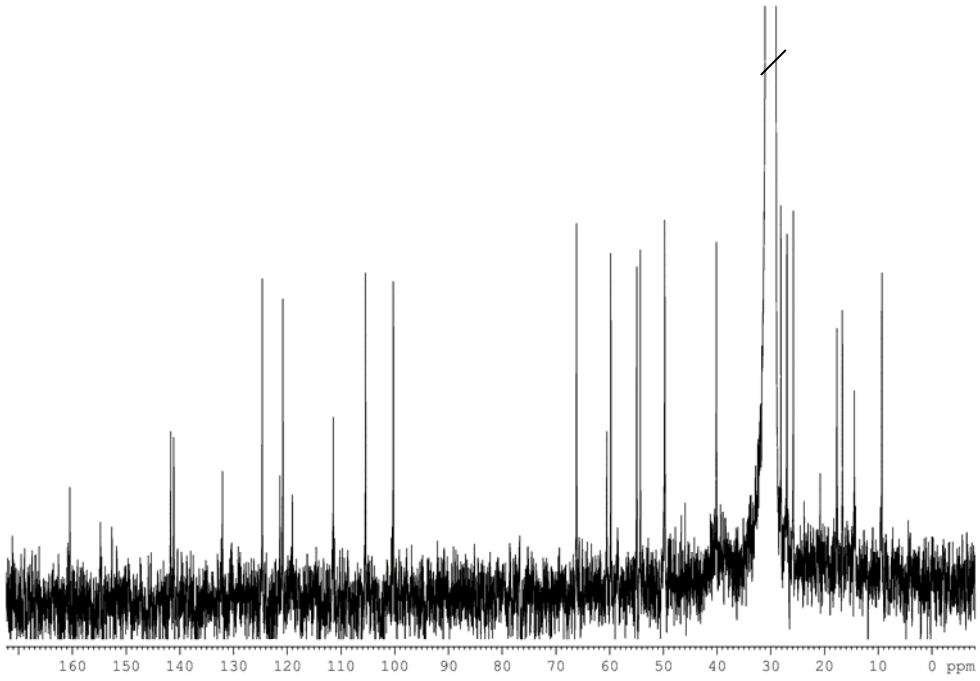

^{1}H NMR (300 MHz, CD_3COCD_3) of marilone J

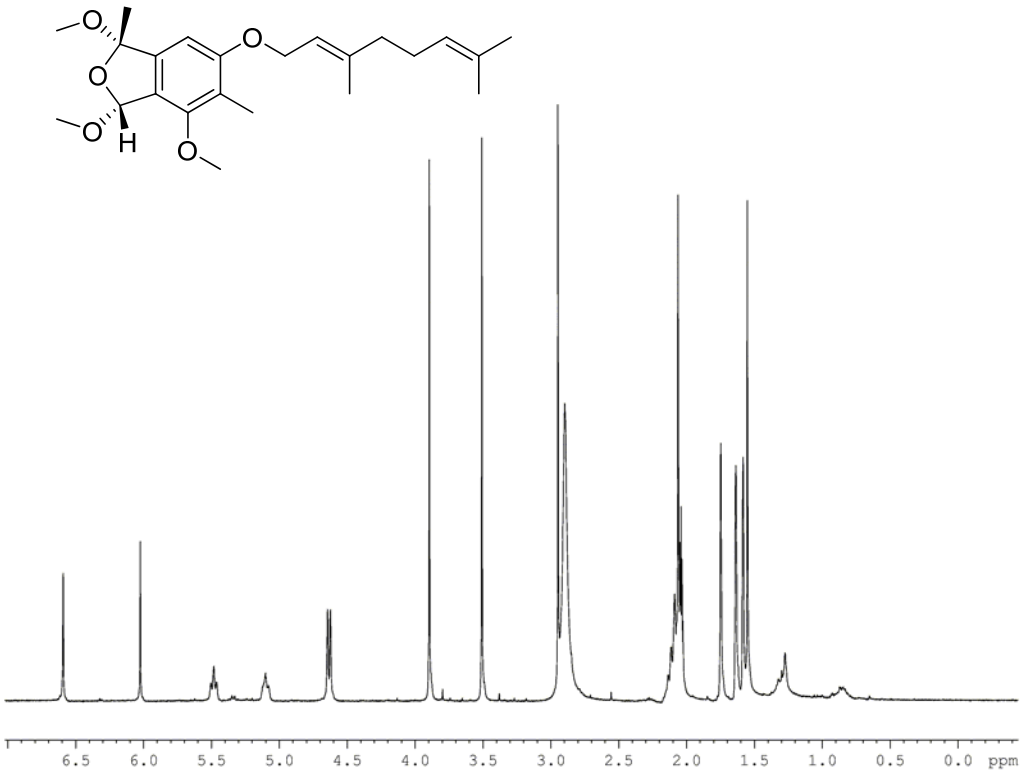

^{13}C NMR (75 MHz, CD_3COCD_3) of marilone J

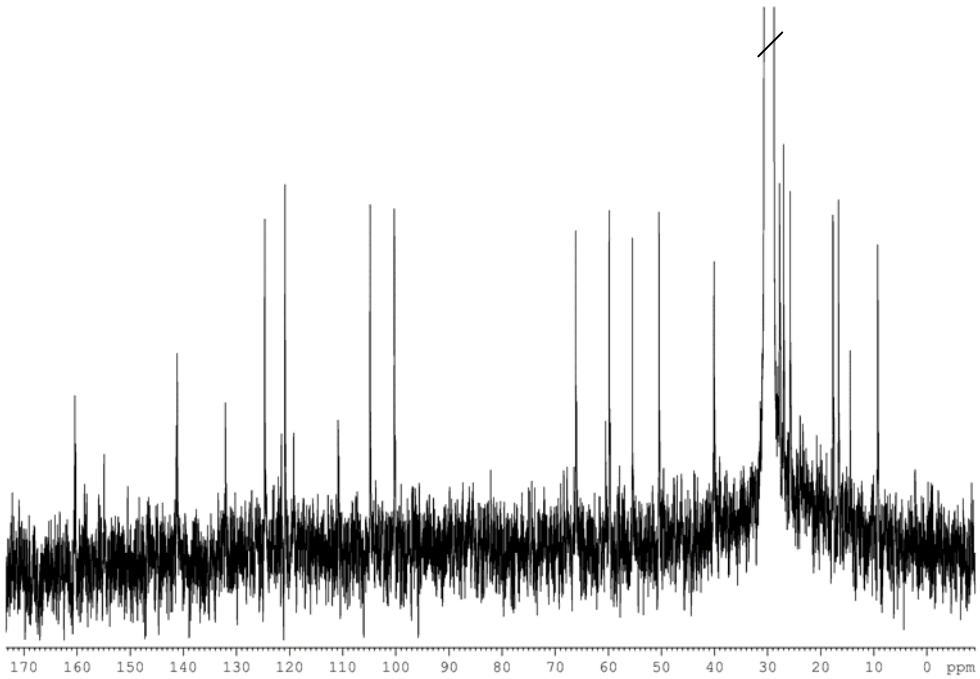

^{1}H NMR (300 MHz, CD_3COCD_3) of stachyline A

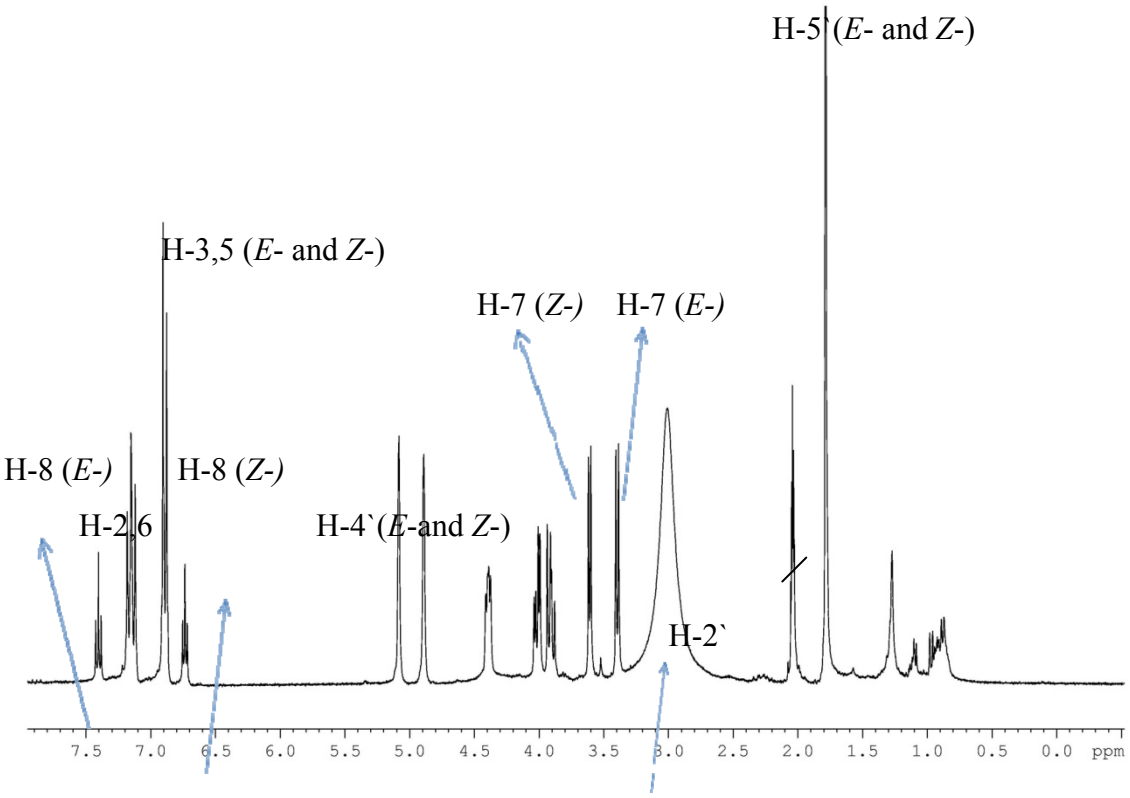

^{13}C NMR (75 MHz, CD_3COCD_3) of stachyline A

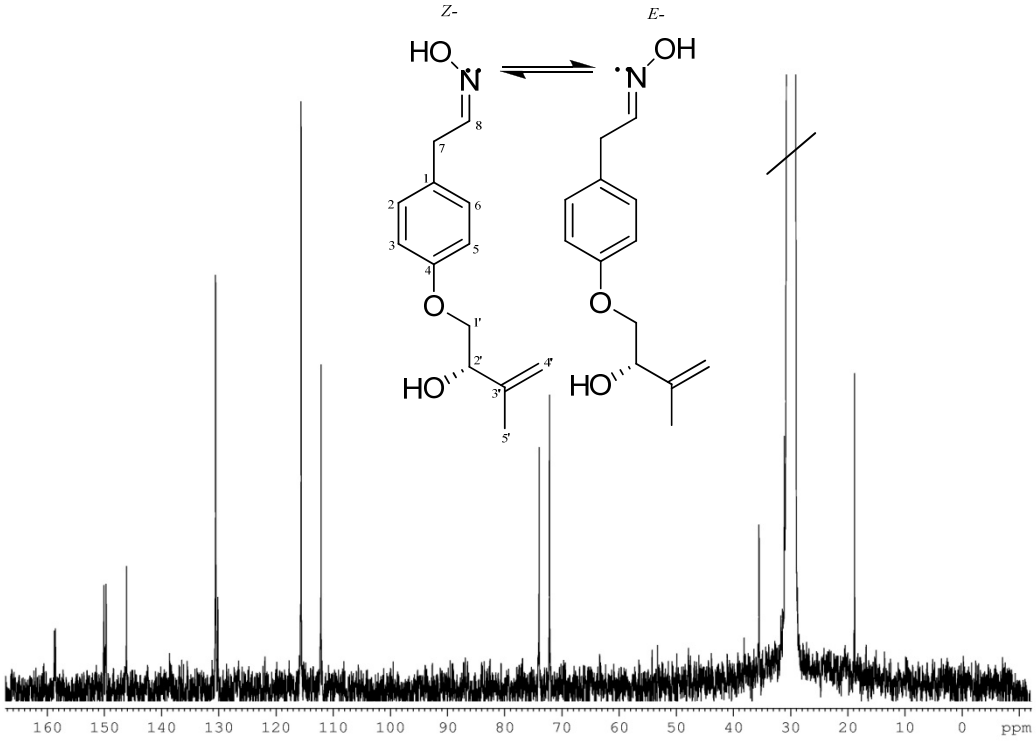

^{1}H NMR (300 MHz, CD_3COCD_3) of stachyline B

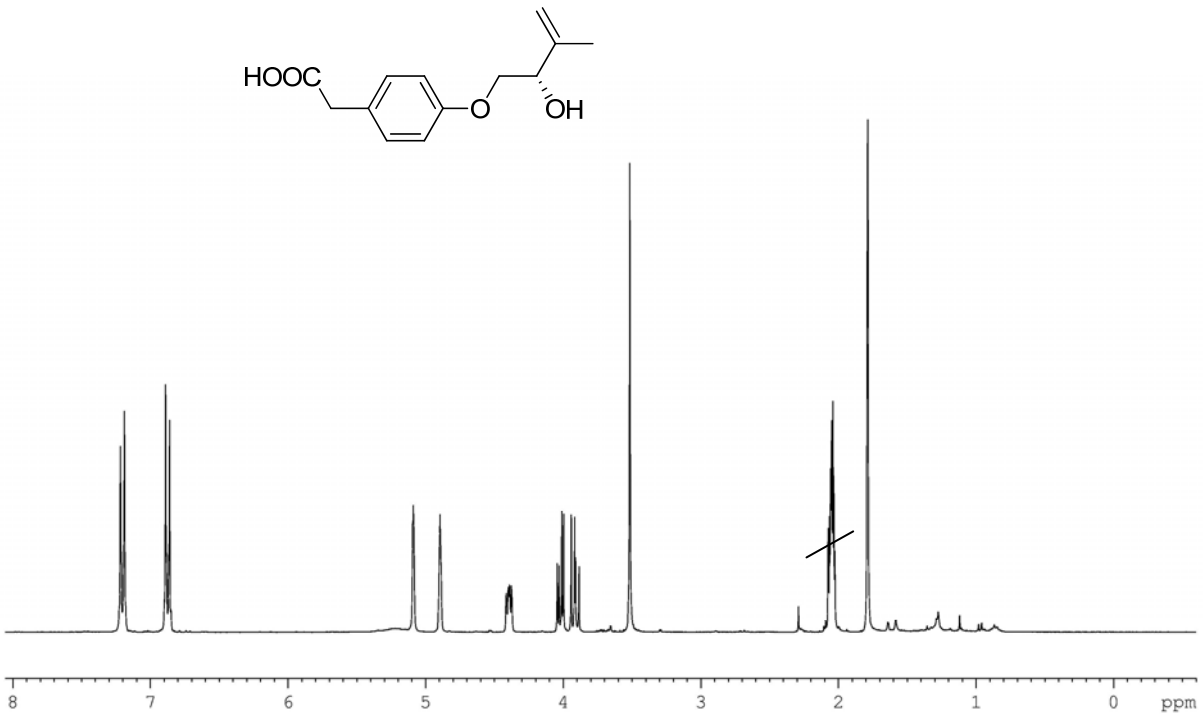

^{13}C NMR (75 MHz, CD_3COCD_3) of stachyline B

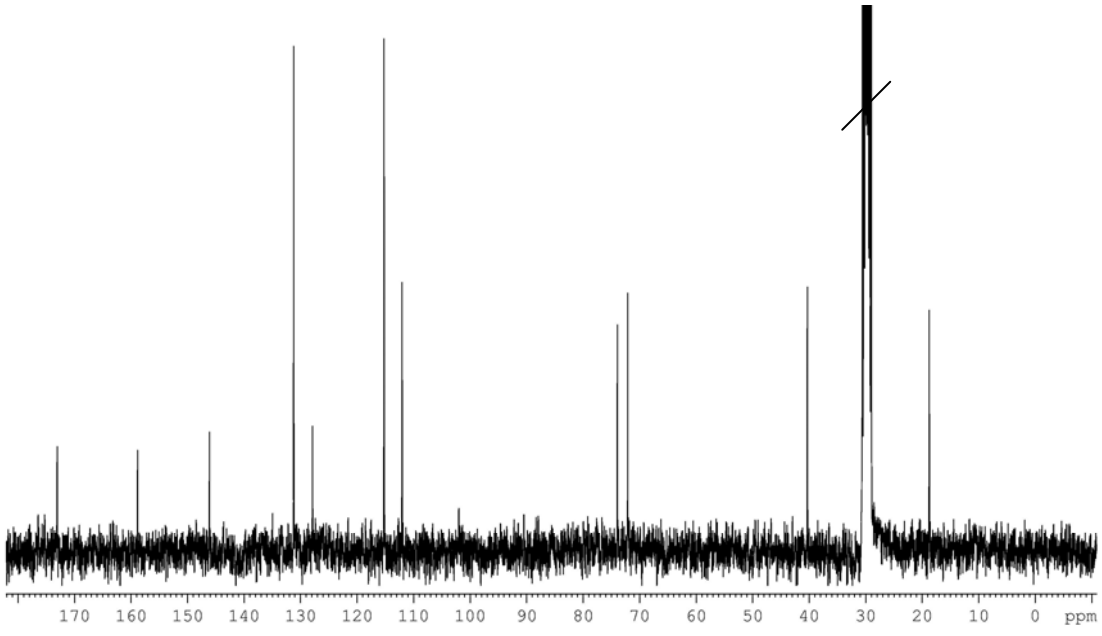

^{1}H NMR (300 MHz, CD_3COCD_3) of stachyline C

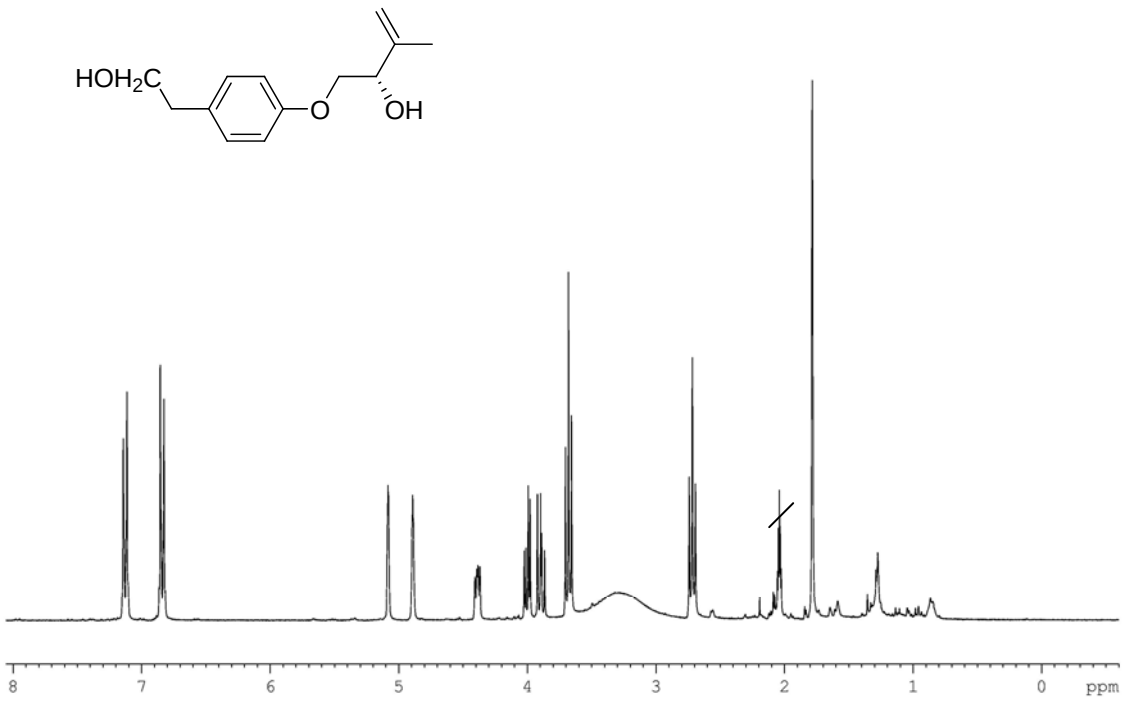

^{13}C NMR (75 MHz, CD_3COCD_3) of stachyline C

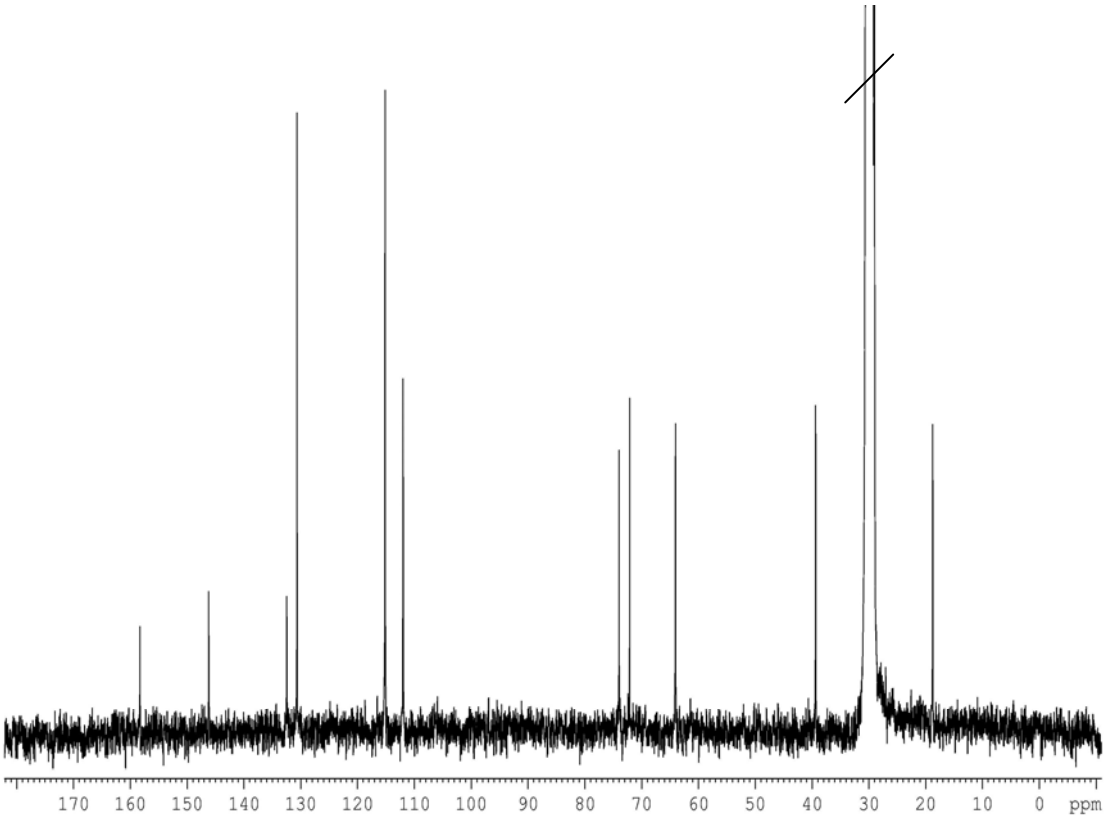

^{1}H NMR (300 MHz, CD_3COCD_3) of stachyline D

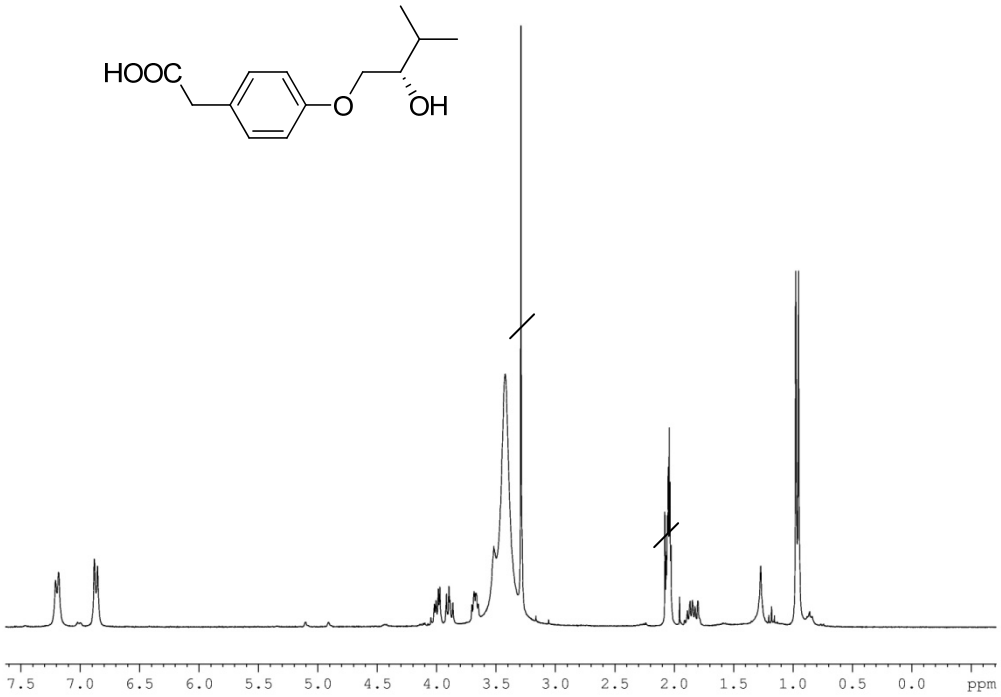

^{13}C NMR (75 MHz, CD_3COCD_3) of stachyline D

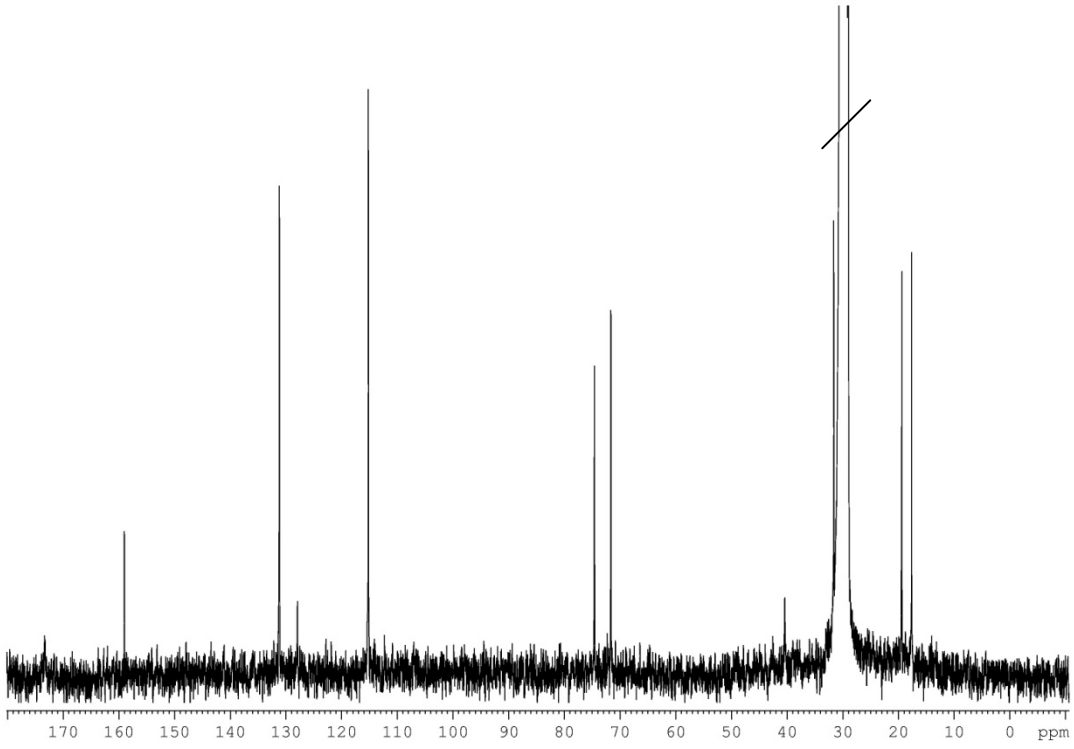

^{1}H NMR (300 MHz, CD_3COCD_3) of 2-(furan-3-yl)acetic acid

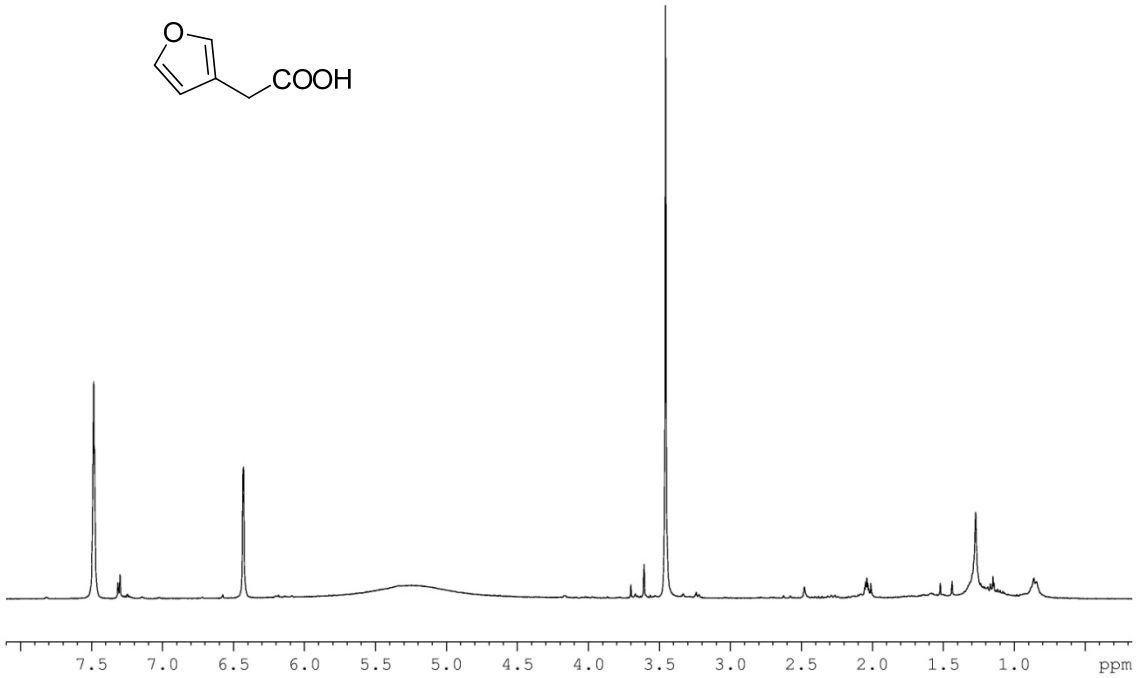

^{13}C NMR (75 MHz, CD_3COCD_3) of 2-(furan-3-yl)acetic acid

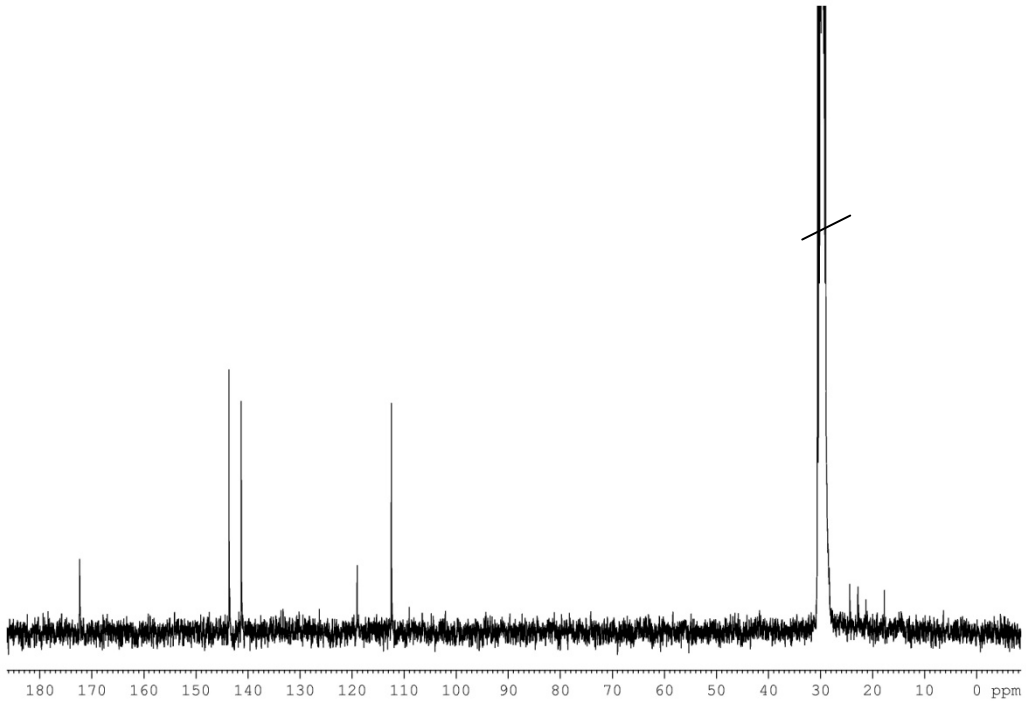

^{1}H NMR spectrum (300 MHz, $CDCl_3$) of 15-hydroxysclerosporin

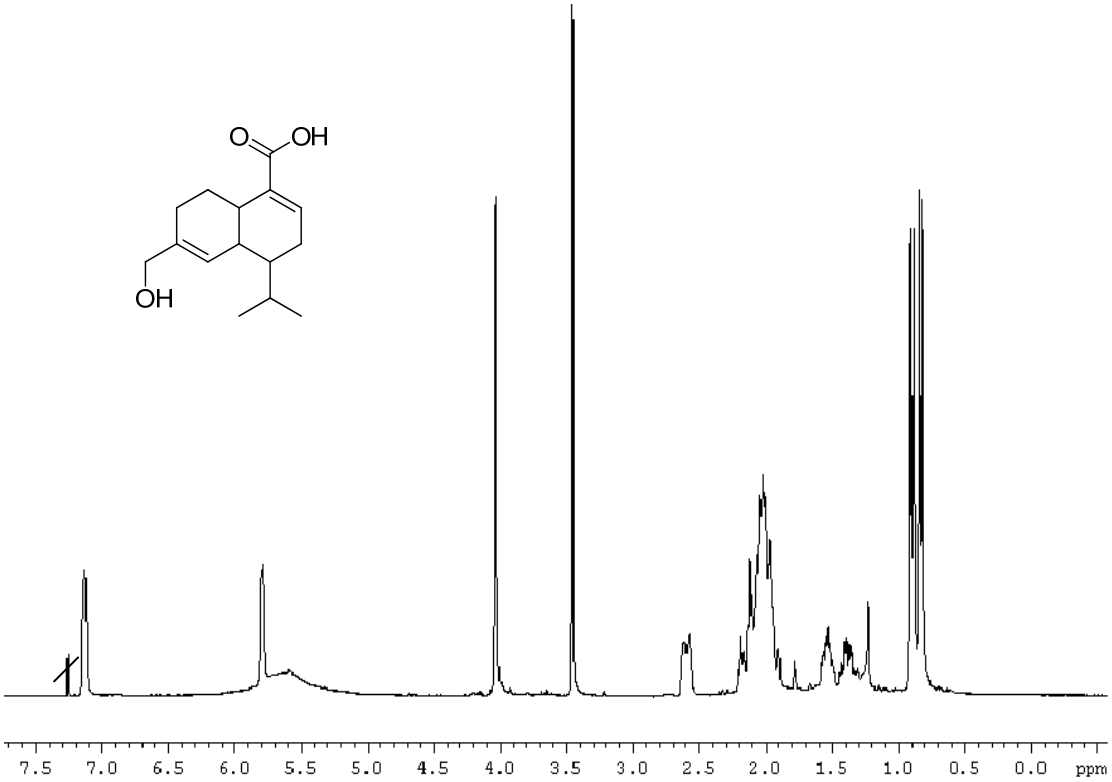

^{13}C NMR spectrum (75 MHz, $CDCl_3$) of 15-hydroxysclerosporin

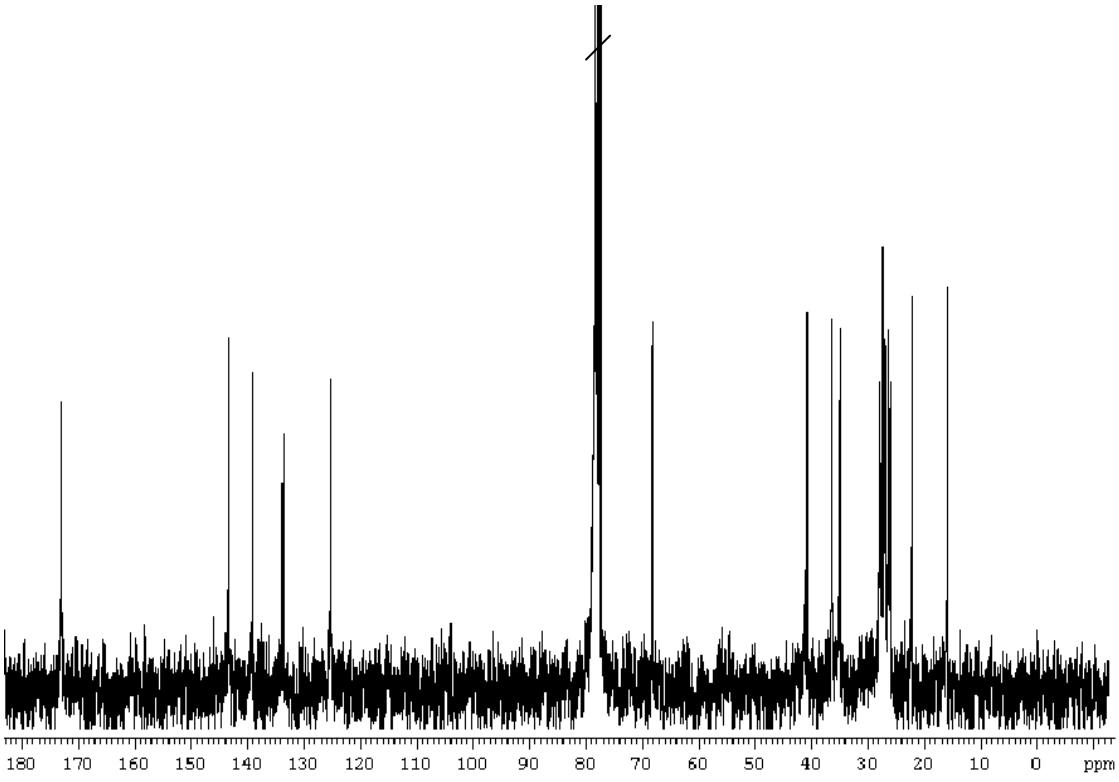

^{1}H NMR spectrum (300 MHz, $CDCl_3$) of 12-hydroxysclerosporin

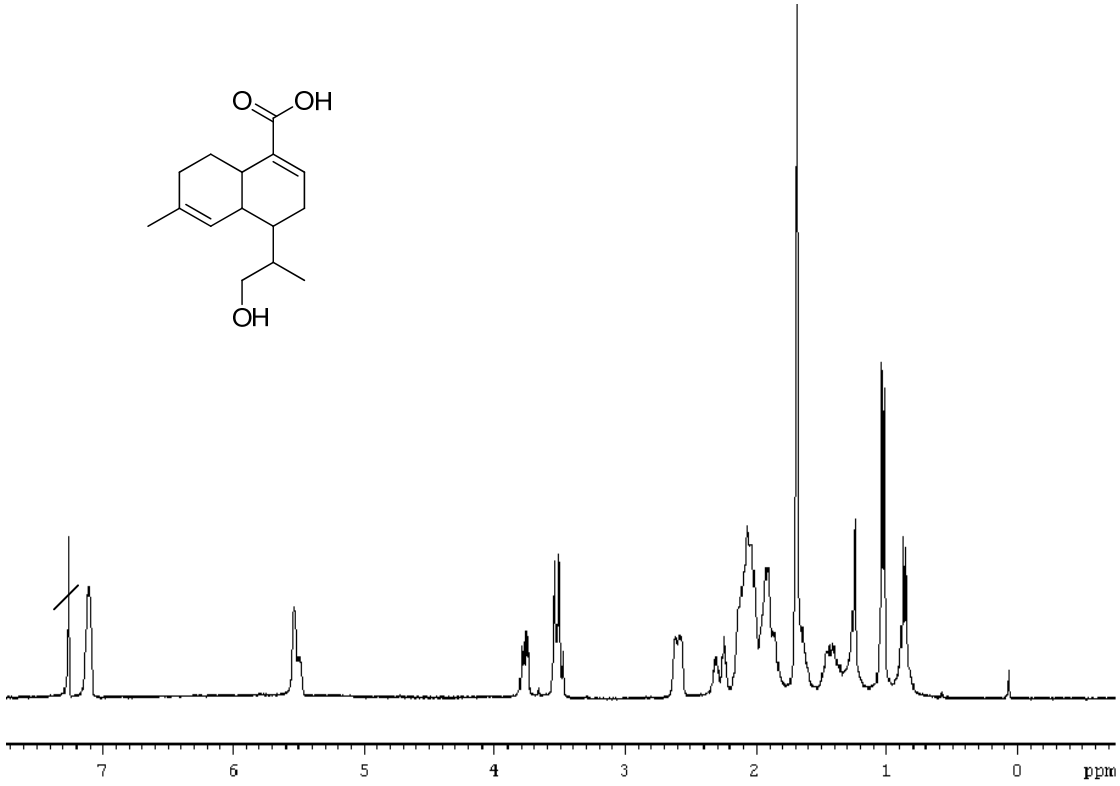

^{13}C NMR spectrum (75 MHz, $CDCl_3$) of 12-hydroxysclerosporin

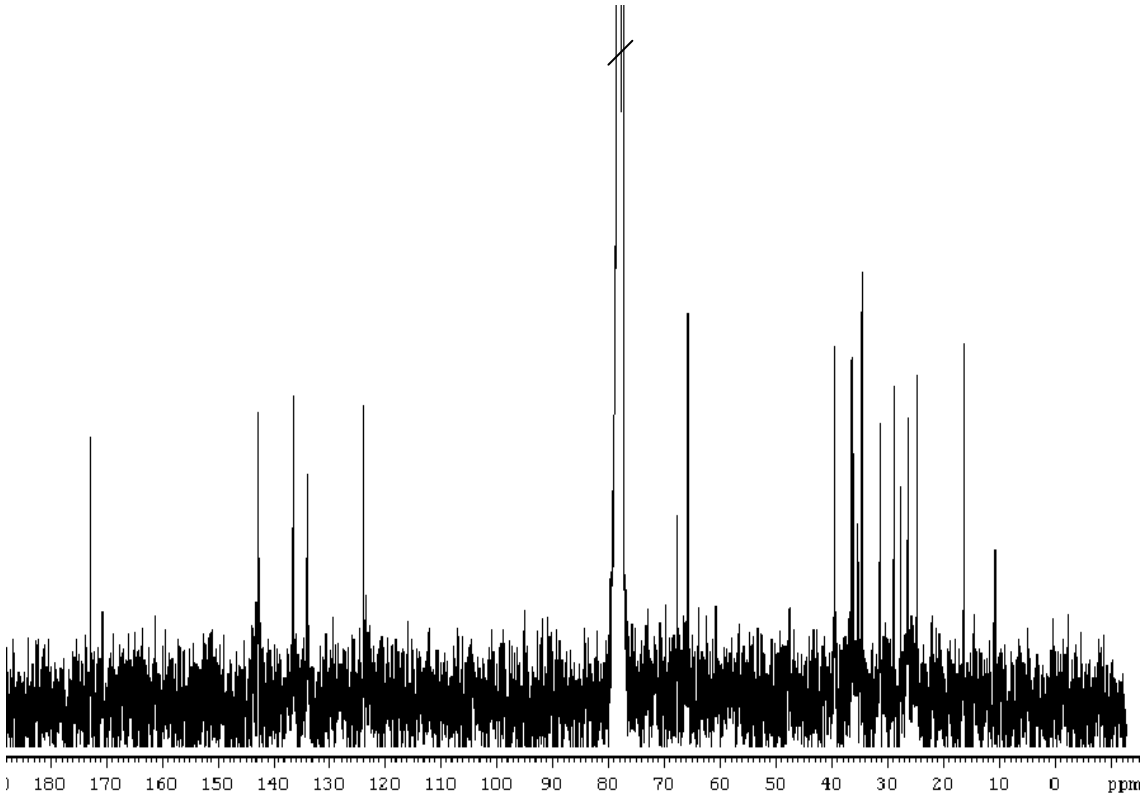

^{1}H NMR spectrum (300 MHz, acetone-d_6) of 11-hydroxysclerosporin

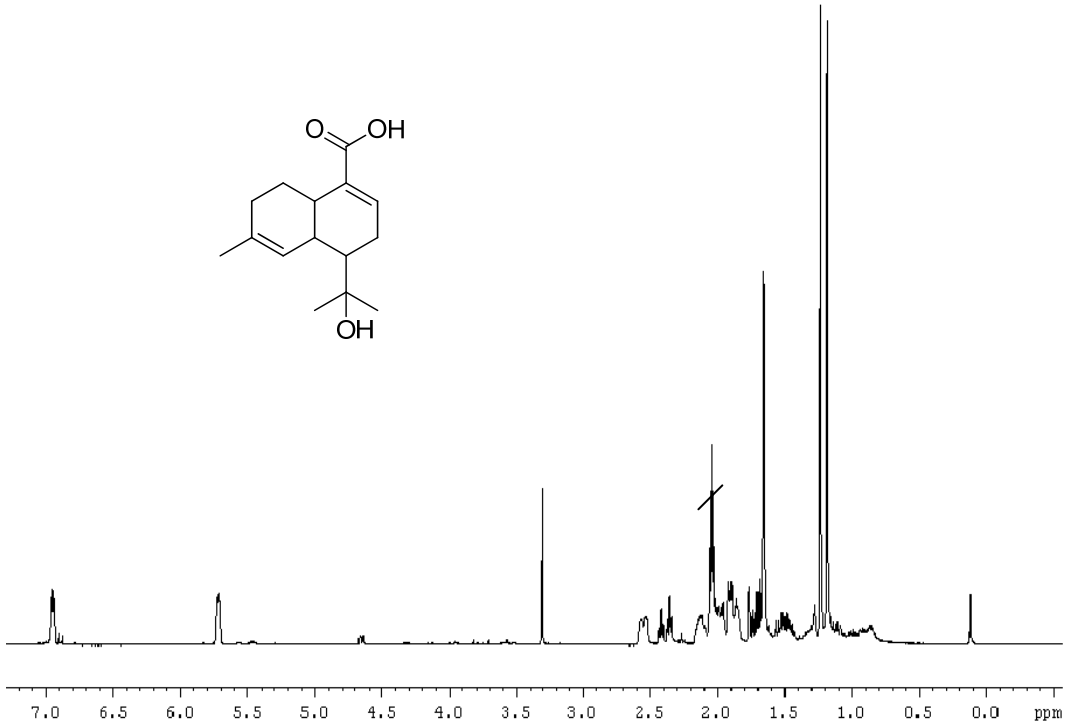

^{13}C NMR spectrum (75 MHz, acetone-*d6*) of 11-hydroxysclerosporin

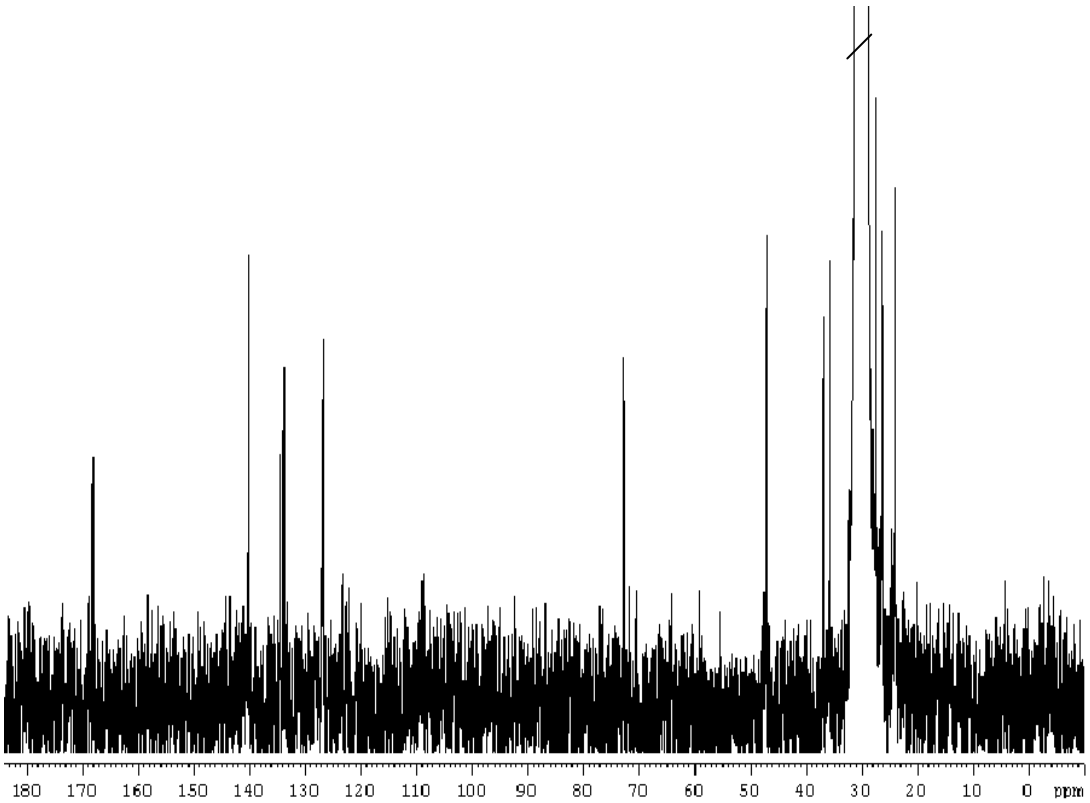

^{1}H NMR spectrum (300 MHz, acetone-d_6) of 8-hydroxysclerosporin

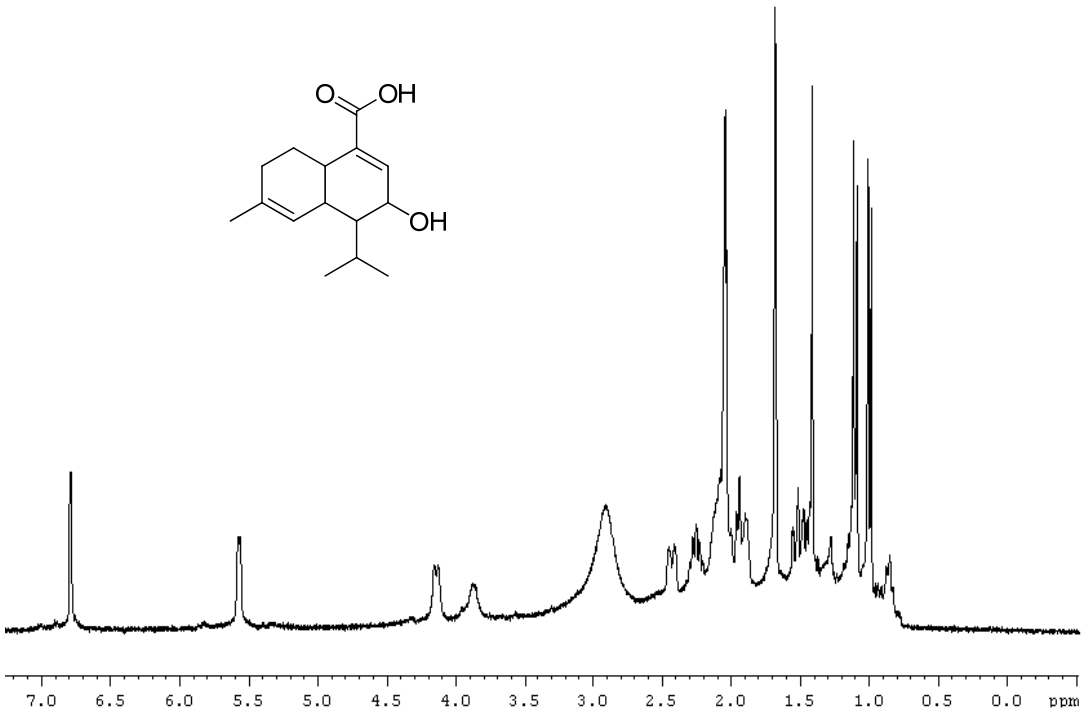

^{13}C NMR spectrum (75 MHz, acetone-d_6) of 8-hydroxysclerosporin

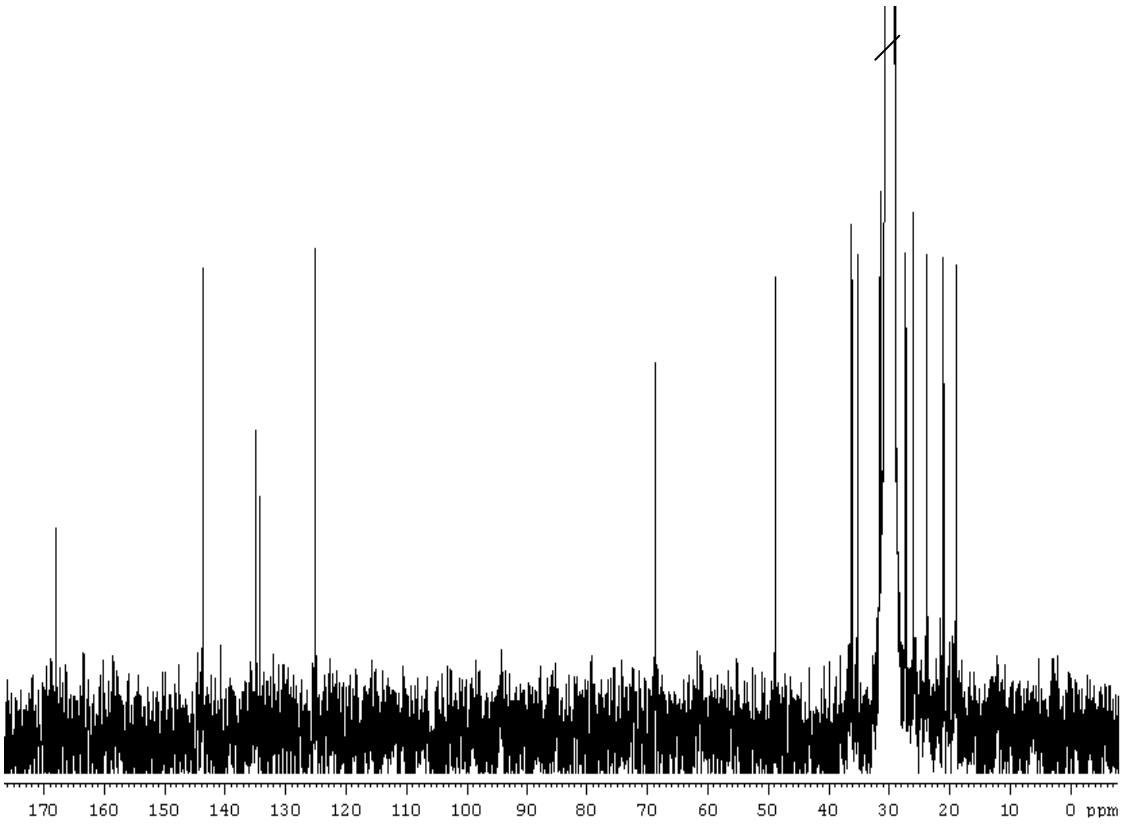

^{1}H NMR (300 MHz, $CDCl_3$) of verticinol A

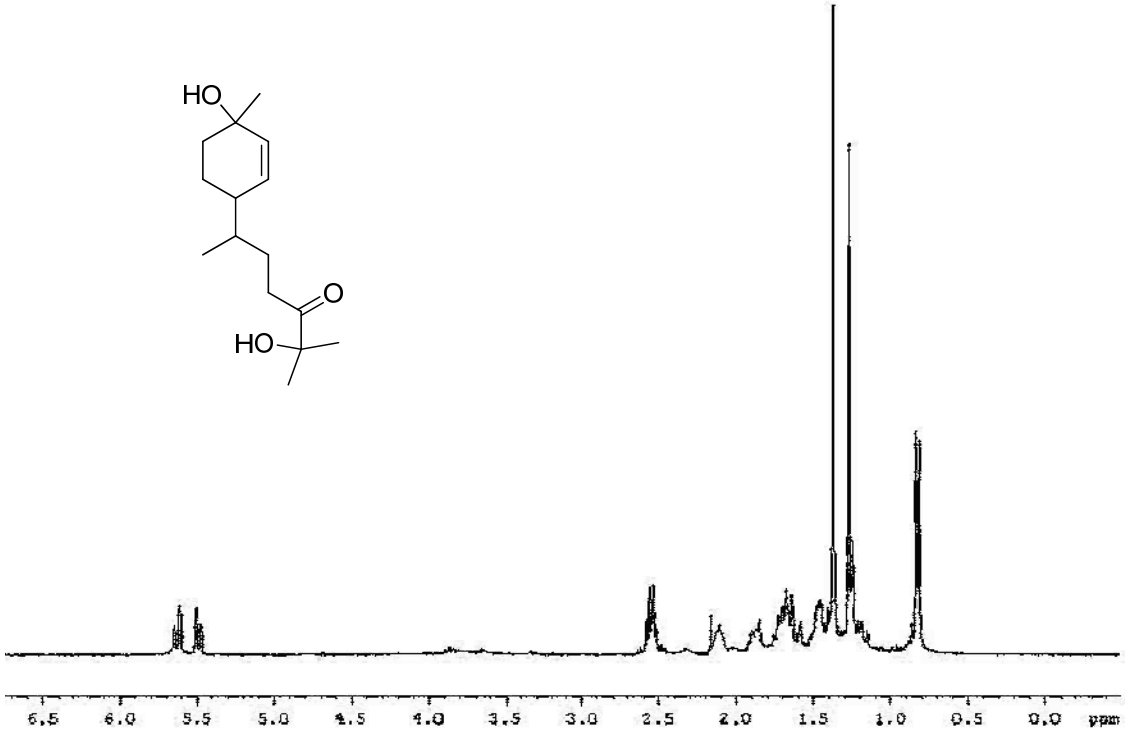

^{13}C NMR (75 MHz, $CDCl_3$) of verticinol A

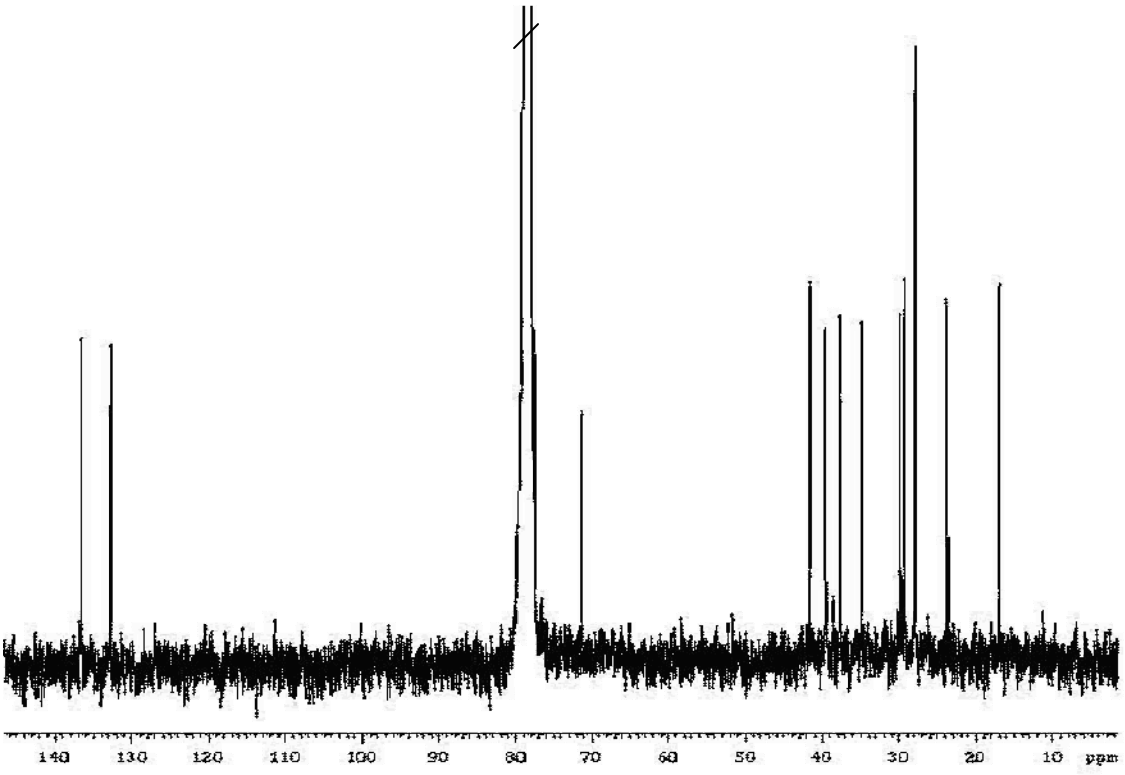

^{1}H NMR (300 MHz, MeOD) of verticinol B

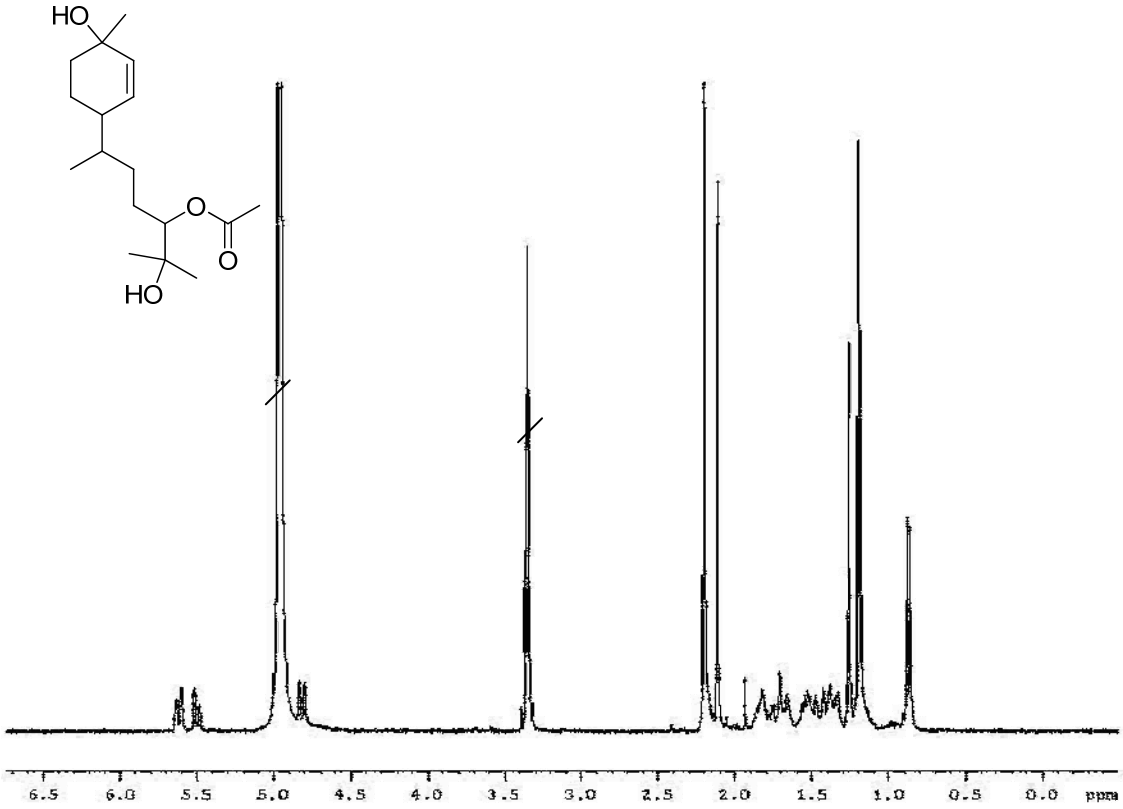

^{13}C NMR (75 MHz, MeOD) of verticinol B

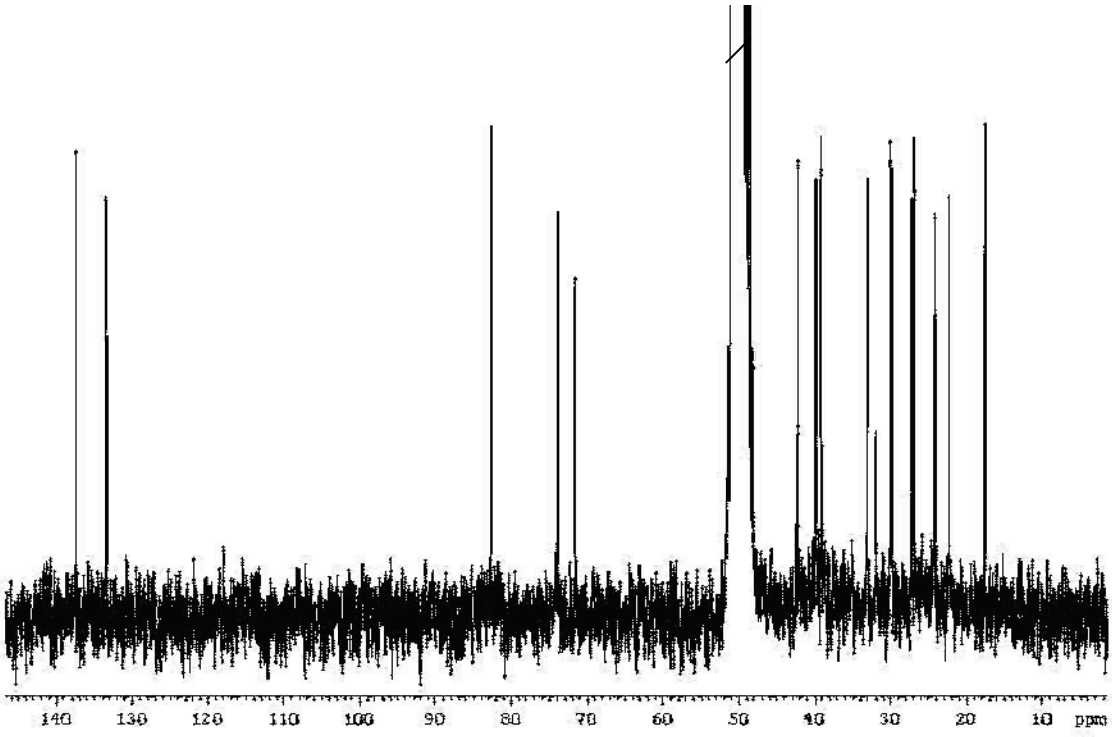

13.5.2. ^{1}H and ^{13}C NMR spectra of known molecules

(trivial names in the 1D NMR spectra)

***Eurotium* sp.**

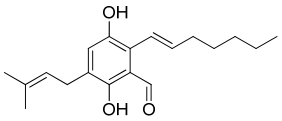

(1)

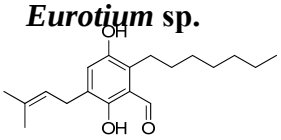

(2)

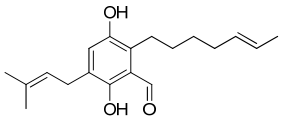

(3)

1 - 3. (Arai *et al.*, **1989**)

Phialophorophoma litoralis

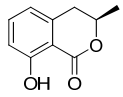

(4)

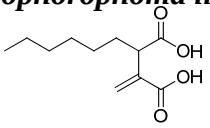

(5)

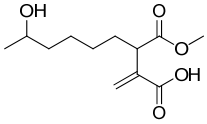

(6)

4. (Garson *et al.*, **1984**)

5 - 6. (Klemke *et al.*, **2004**)

Cadophora Malorum

Verticillium cinnabarinum

Verticillium tenerum

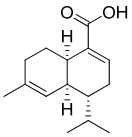

(7)

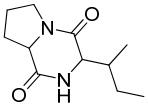

(8)

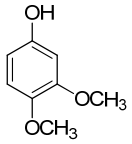

(9)

7. (Kitahara *et al.*, **1984**)

8. (Bull *et al.*, **1998**)

9. (Boeesenken, **1939**)

***Acremonium* sp**

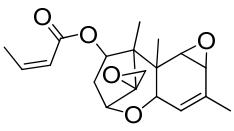

(10)

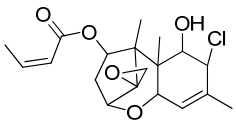

(11)

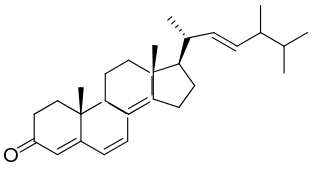

(12)

10. (Gyimesi, **1965**)

11. artefact derived from 10.

12. (Schulte *et al.*, **1968**; Jinming *et al.*, **2001**)

***Stachyllidium* sp.**

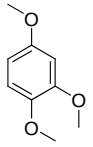

(13)

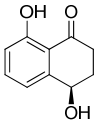

(14)

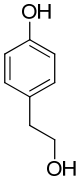

(15)

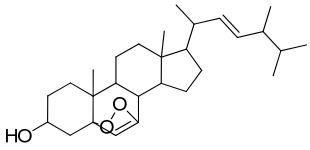

(16)

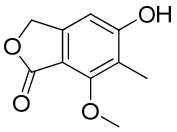

(17)

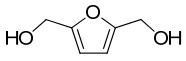

(18)

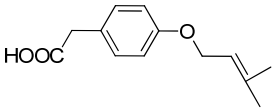

(19)

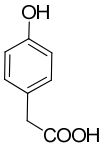

(20)

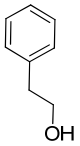

(21)

(22)

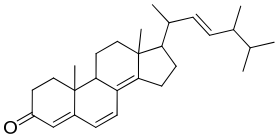

(23)

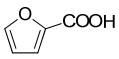

(24)

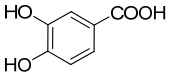

(25)

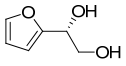

(26)

13. (Andersen, **1987**; Alves *et al.*, **2009**).
14. (Ayer *et al.,* **1993**)
15. (Schneider *et al*., **1996**)
16. (Yue *et al.,* **2001**)
17. (Kawahara *et al.*, **1988**)
18. (Schneider *et al.*, **1996**)
19. (Awad *et al*., **2005**).
20. (Chen, **1958**; Crowden and Ralph, **1961**)
21. (Nair and Burke, **1988**)
22. (Barrero *et al*., **1996**)
23. (Jinming *et al.,* **2001**)
24. (Hong, **1981**)
25. (Turner, **1971**)
26. (Lu *et al.*, **2008**).

Compound 1, (tetrahidroauroglaucin/aspergin), *Eurotium* sp., D-acetone

^{1}H NMR

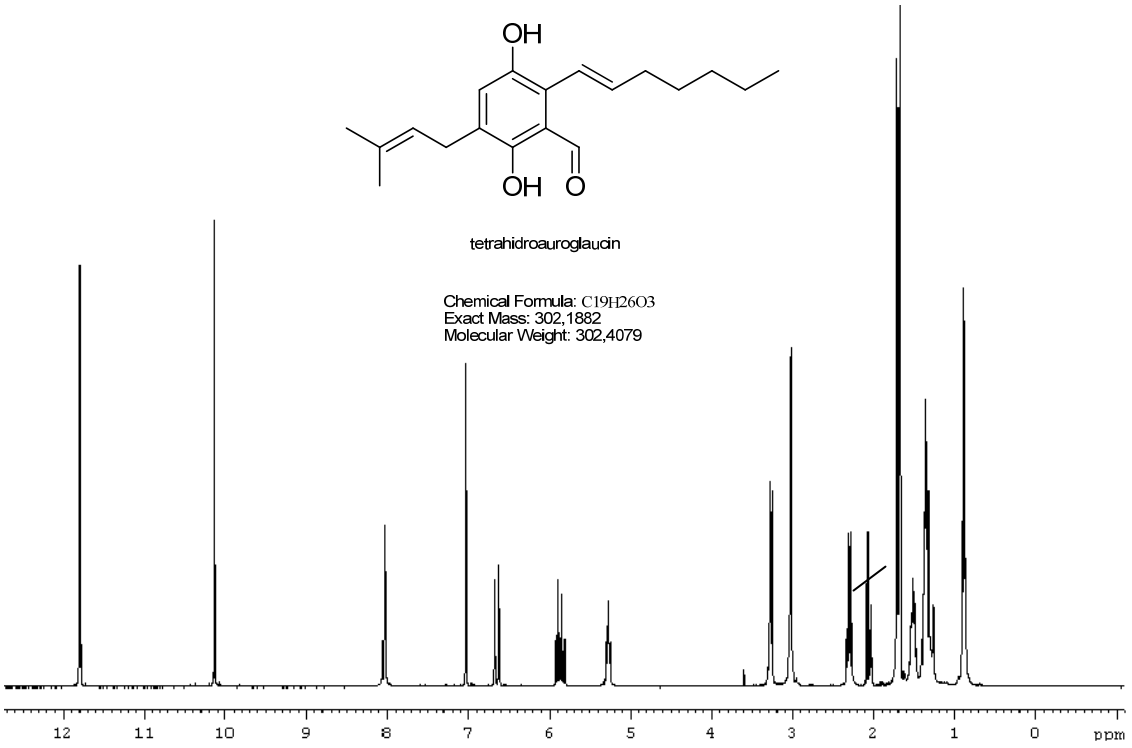

^{13}C NMR

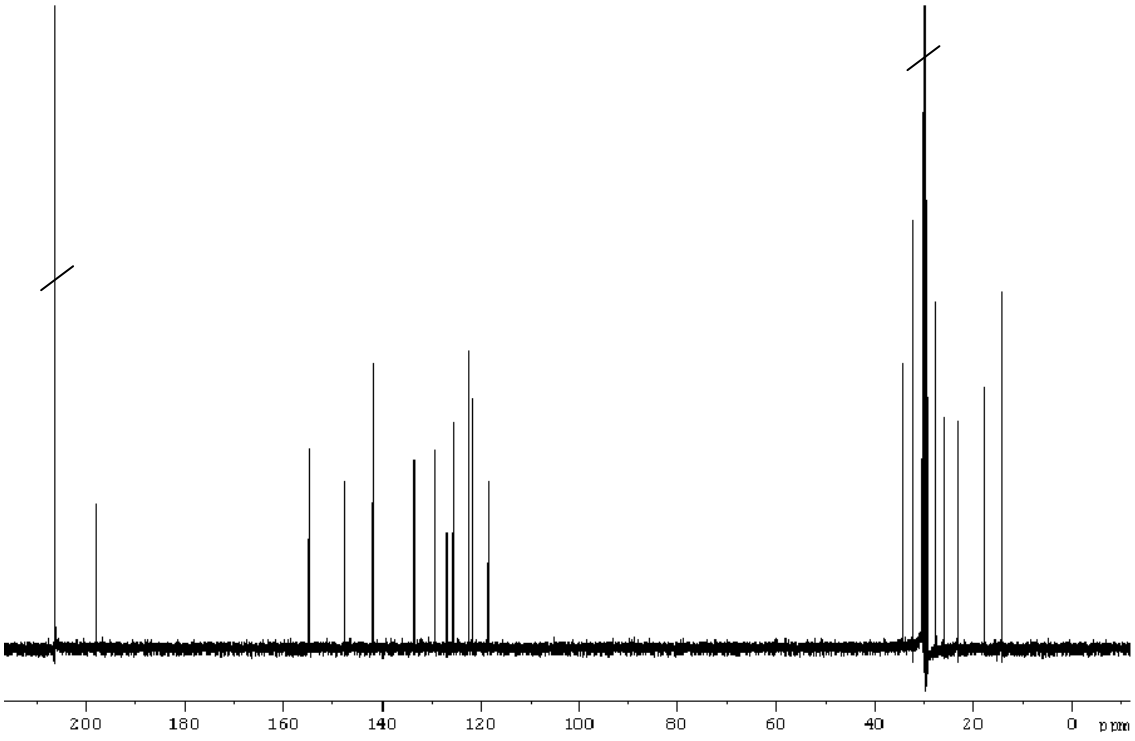

Compound 2, (flavoglaucin), *Eurotium* sp., CD_3COCD_3.

^{1}H NMR

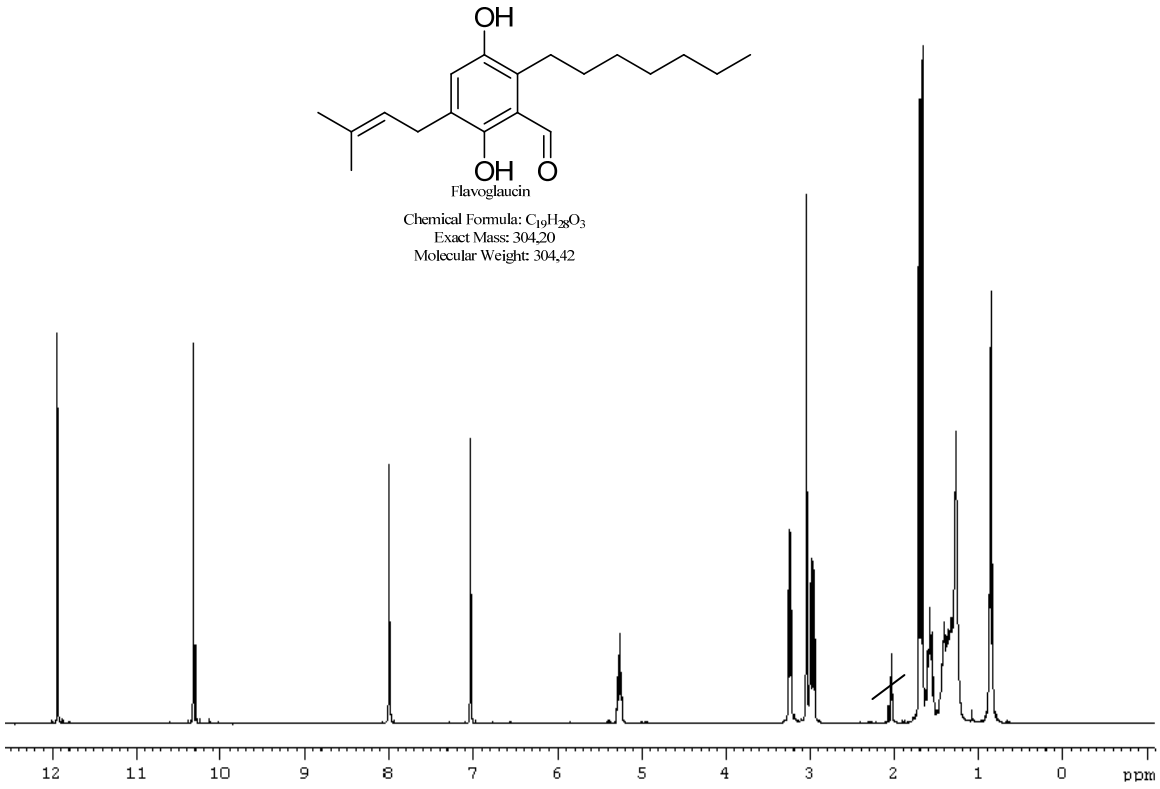

^{13}C NMR

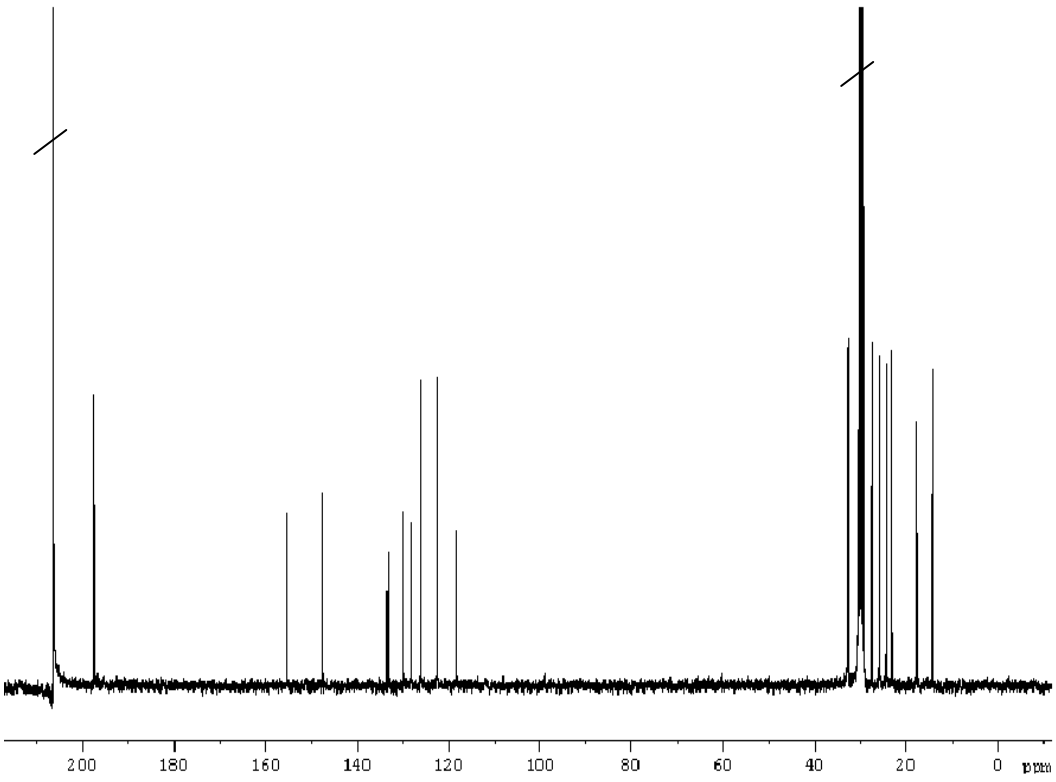

Compound 3, (isotetrahydroauroglaucin), *Eurotium* sp., CD_3COCD_3.

^{1}H NMR

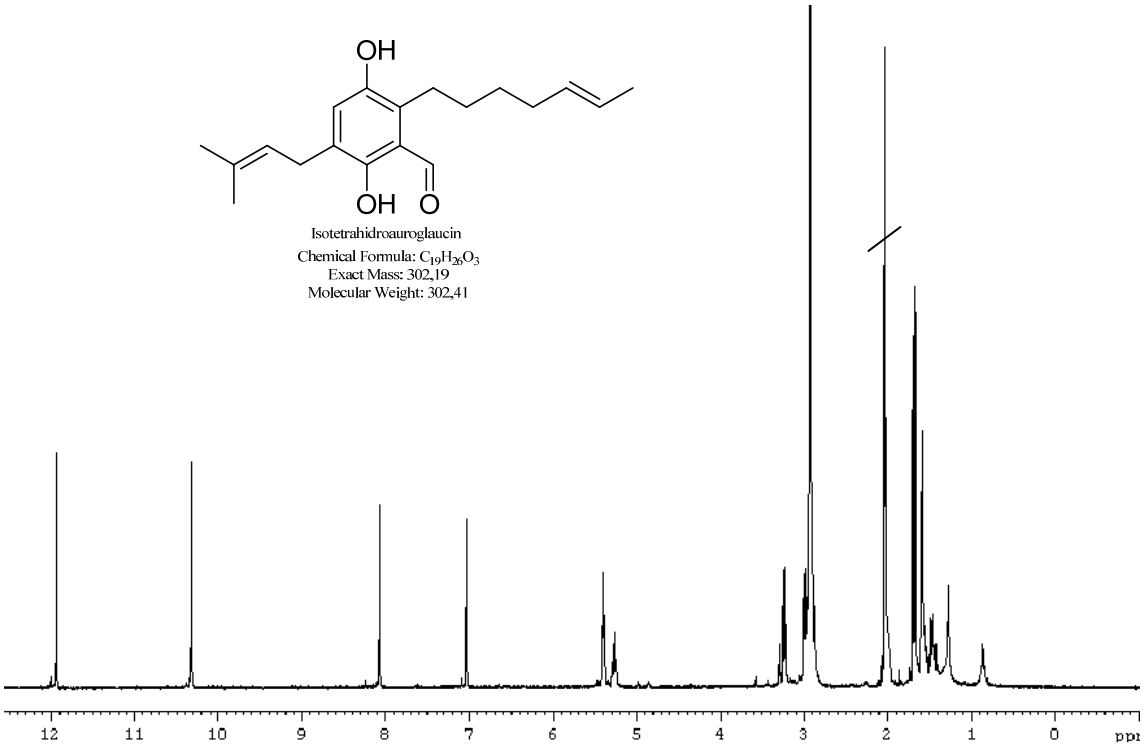

^{13}C NMR

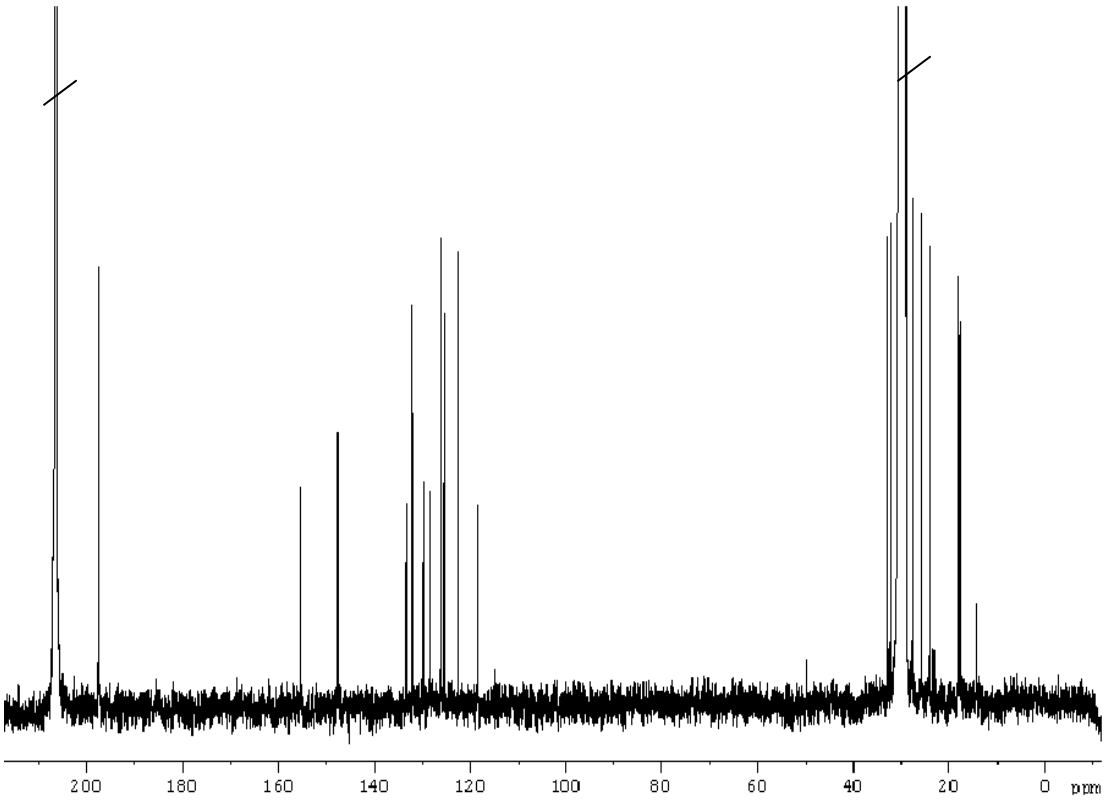

Compound 4, (*R*-mellein), *Phialophorophoma litoralis*, $CDCl_3$.

^{1}H NMR

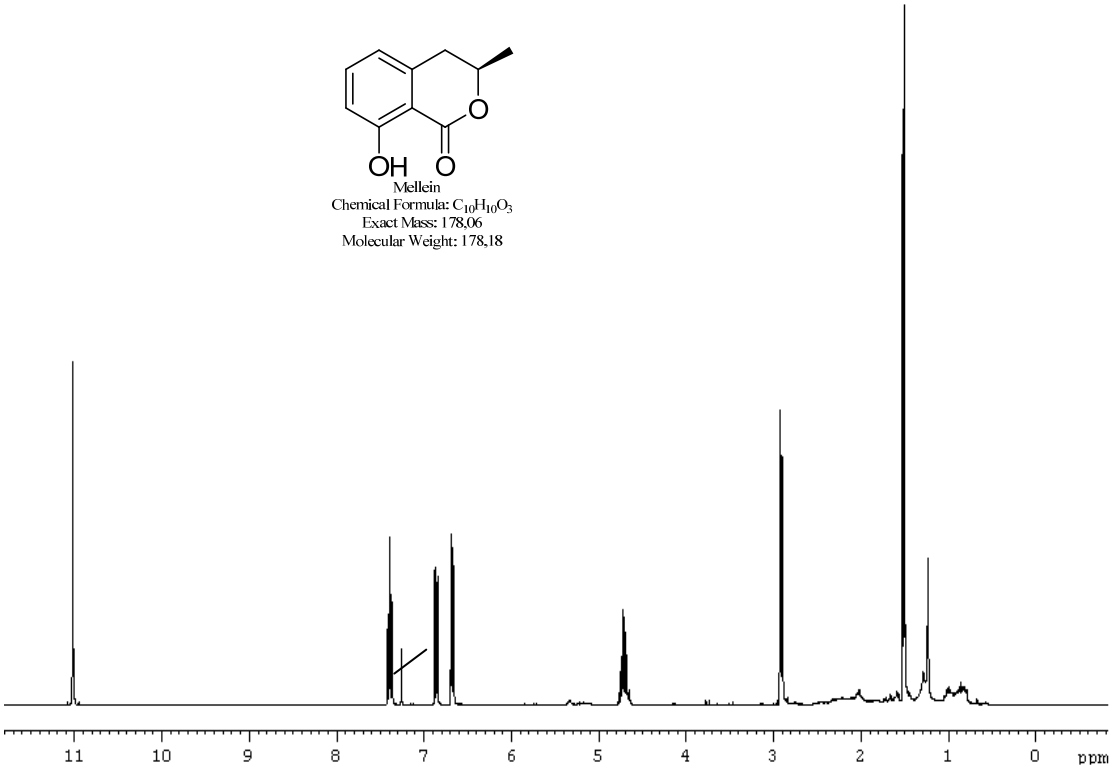

^{13}C NMR

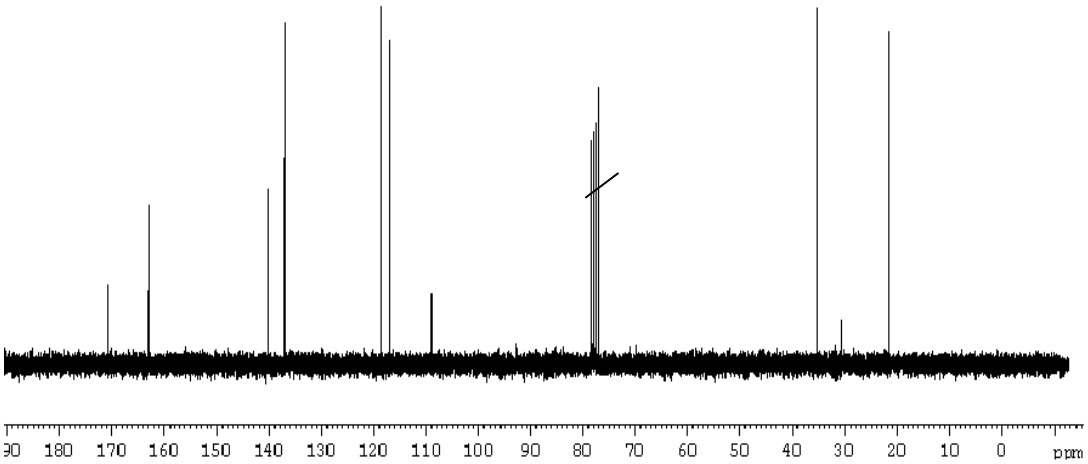

Compound 5, [(-)-hexylitaconic acid], *Phialophorophoma litoralis*, $CDCl_3$.

^{1}H NMR

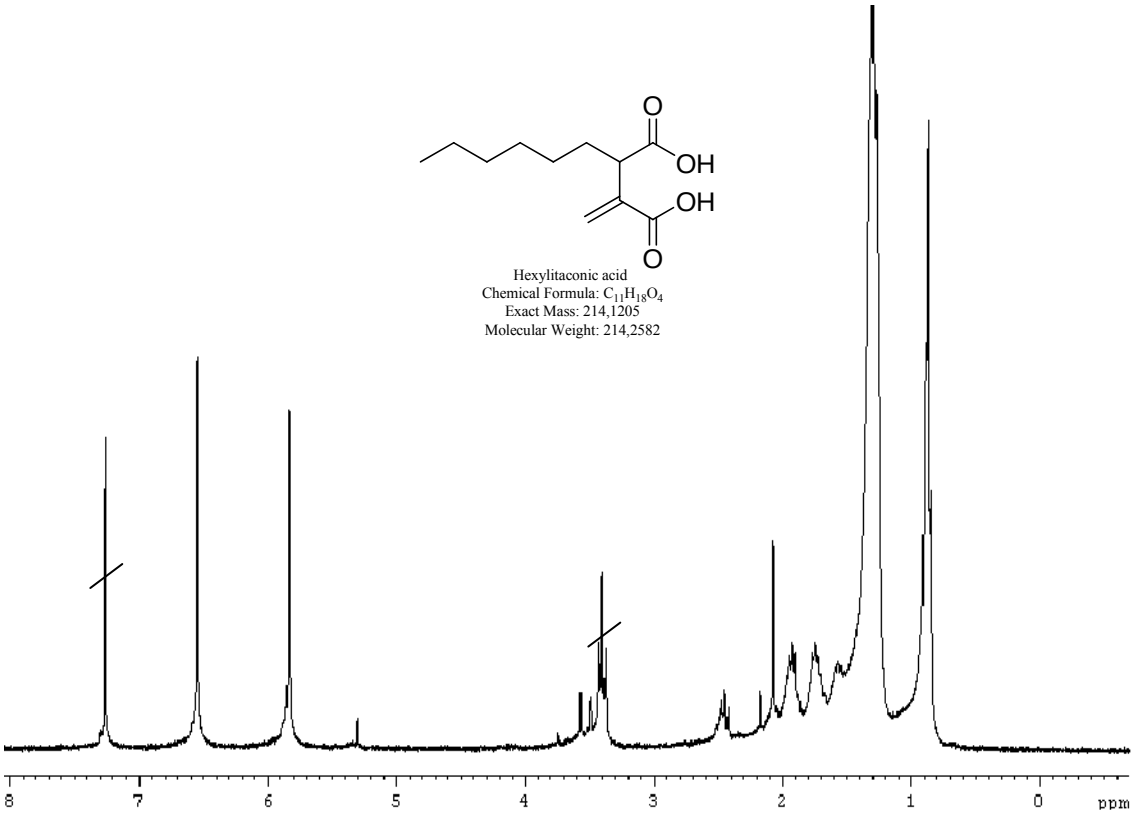

^{13}C NMR

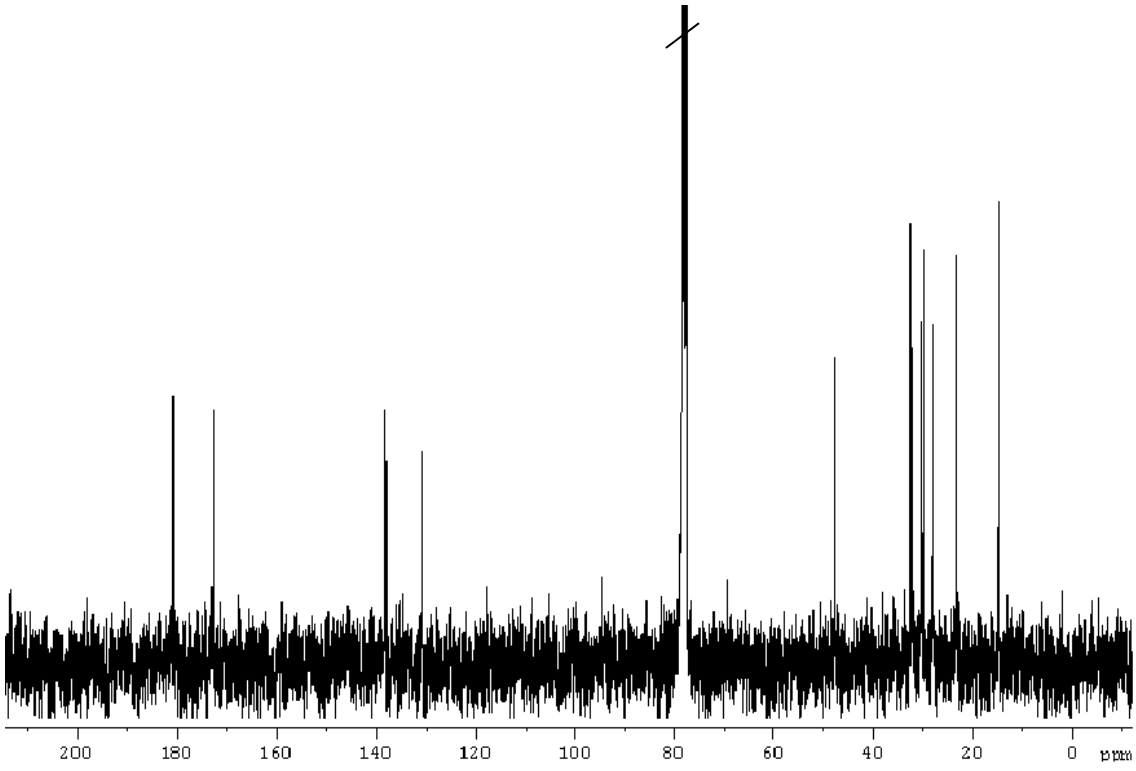

Compound 6, [(-)-9-hydroxy Hexylitaconic acid 1-half-methyl ester], *Phialophorophoma litoralis*, $CDCl_3$.

^{1}H NMR

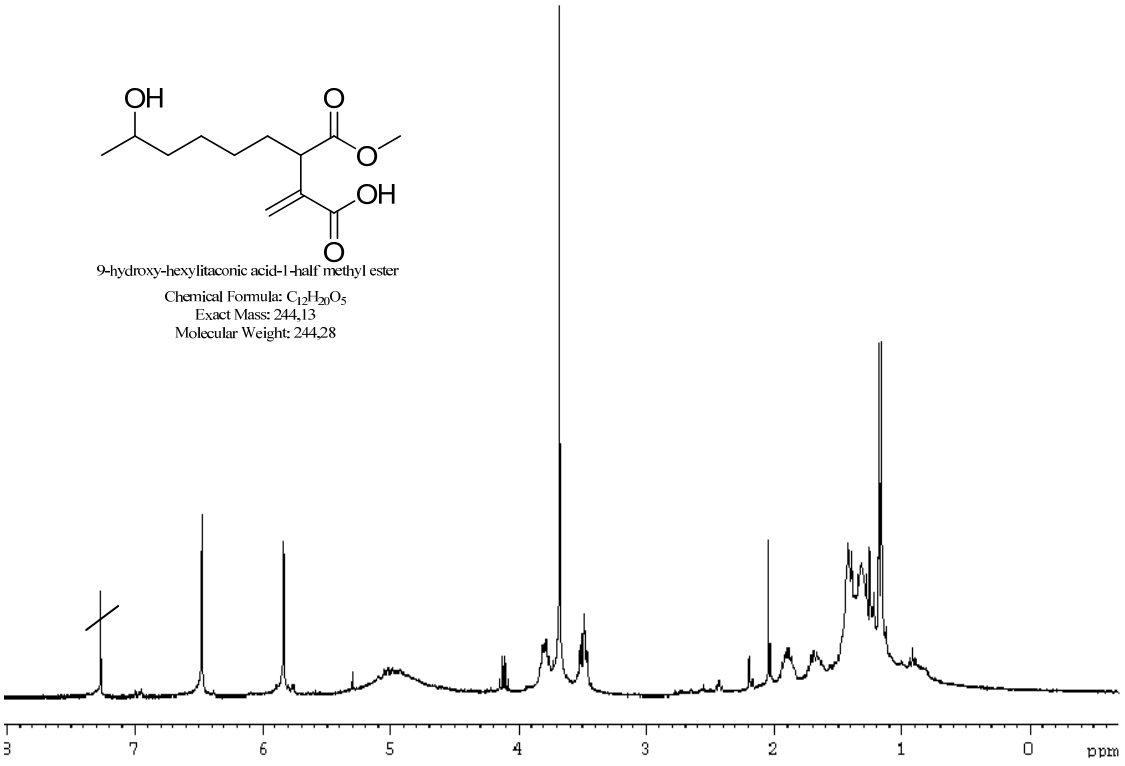

^{13}C NMR

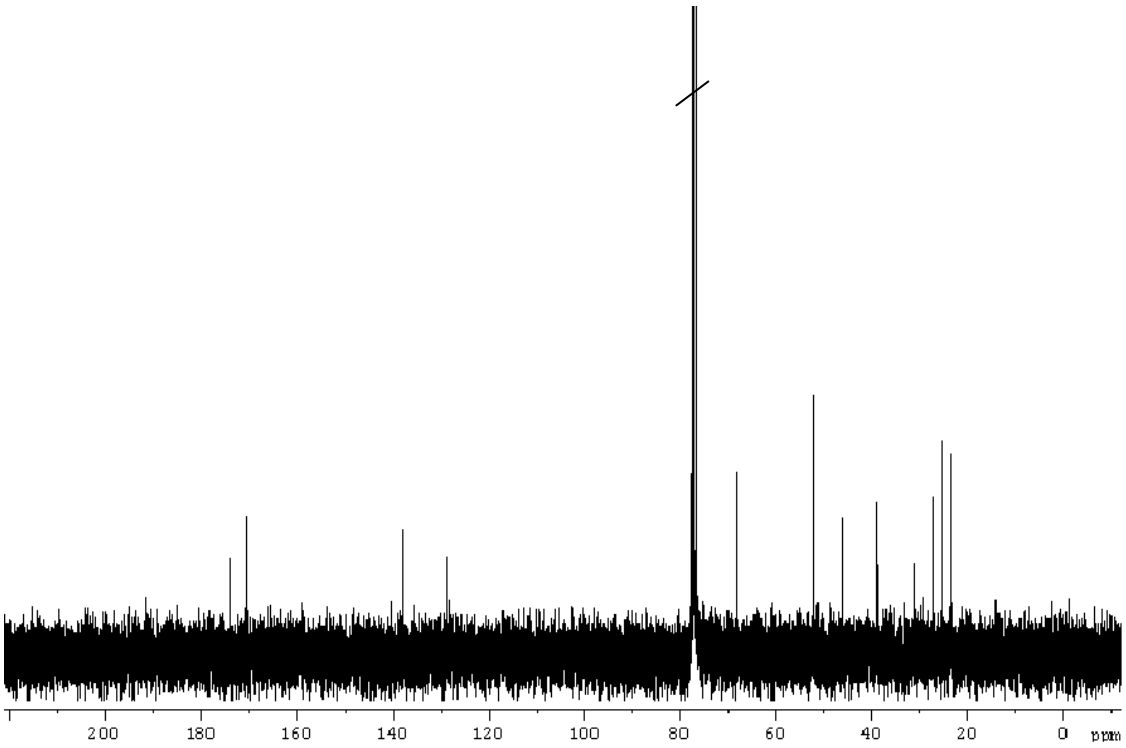

Compound 7, [(+)-sclerosporin], *Cadophora malorum*, $CDCl_3$.

^{1}H NMR

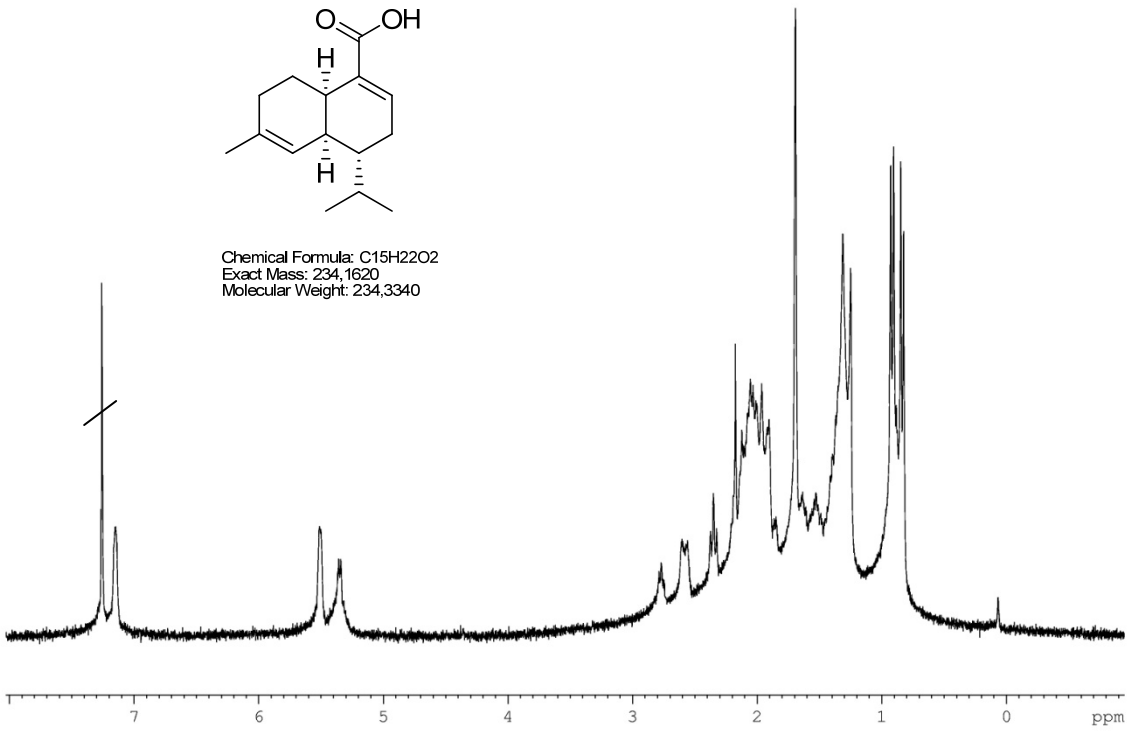

^{13}C NMR

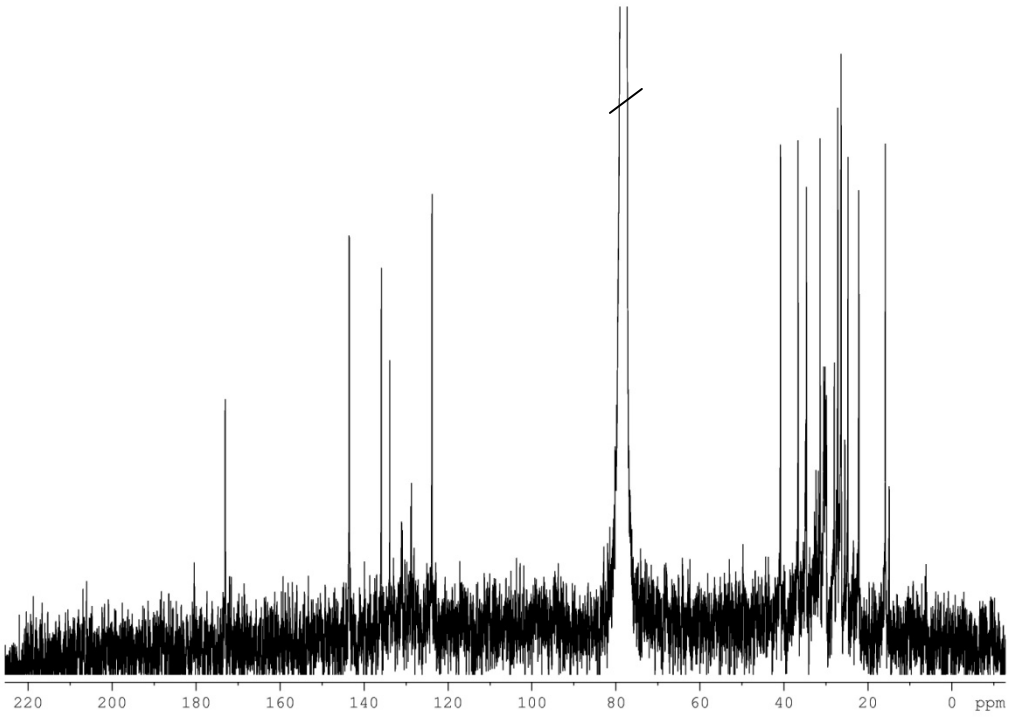

Compound 8, (cyclo-proline-isoleucine), *Verticillium cinnabarinum,* MeOD

^{1}H NMR

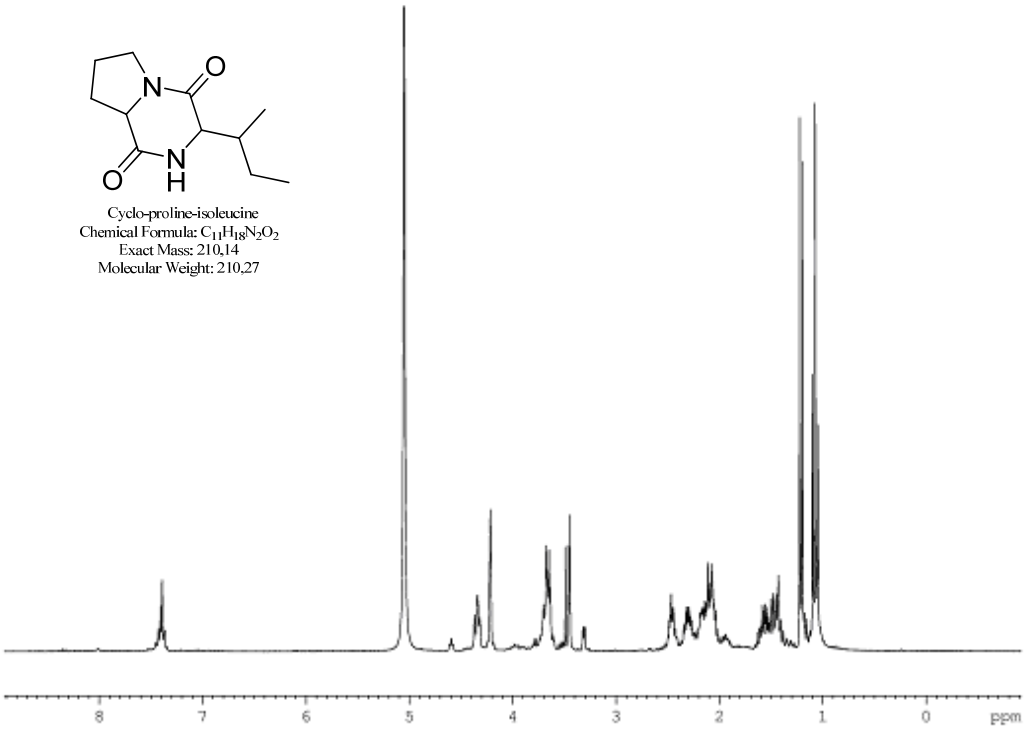

^{13}C NMR

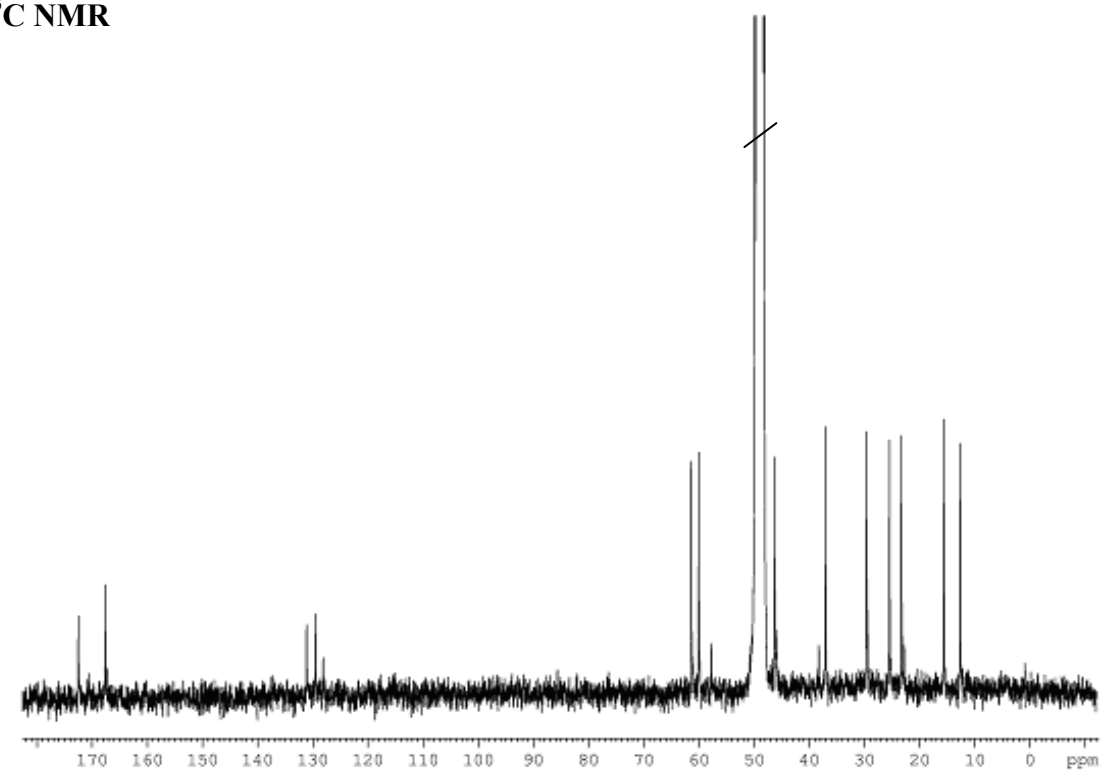

Compound 9, (3, 4-dimethoxy phenol) , *Verticillium tenerum* , $CDCl_3$.

^{1}H NMR

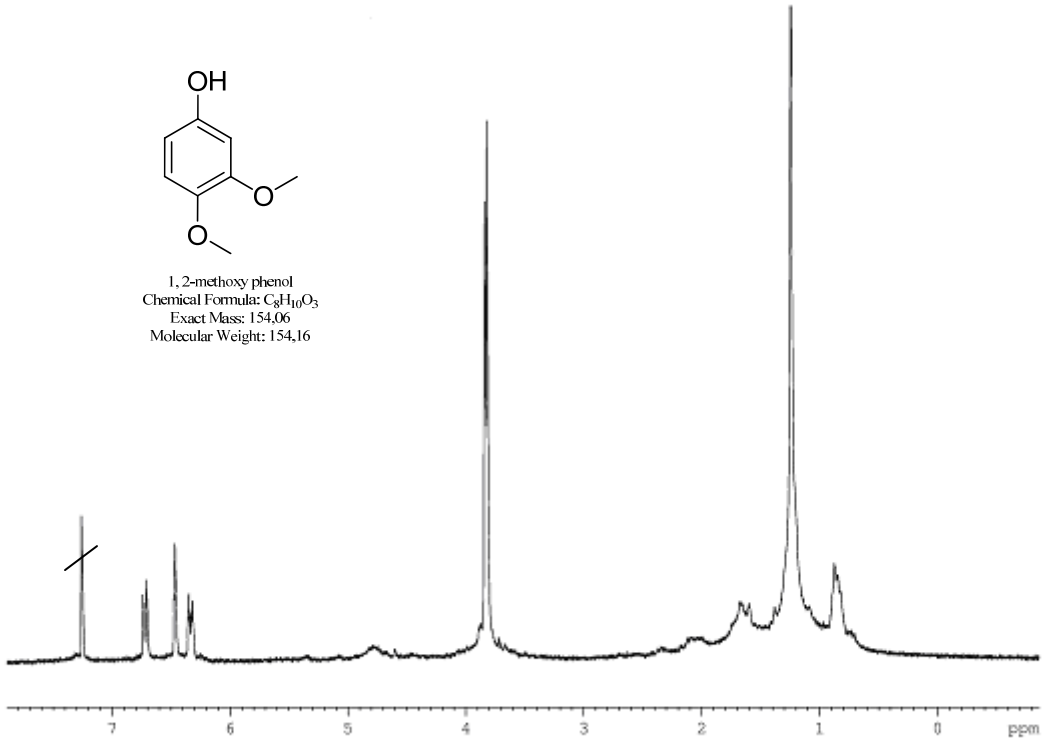

^{13}C NMR

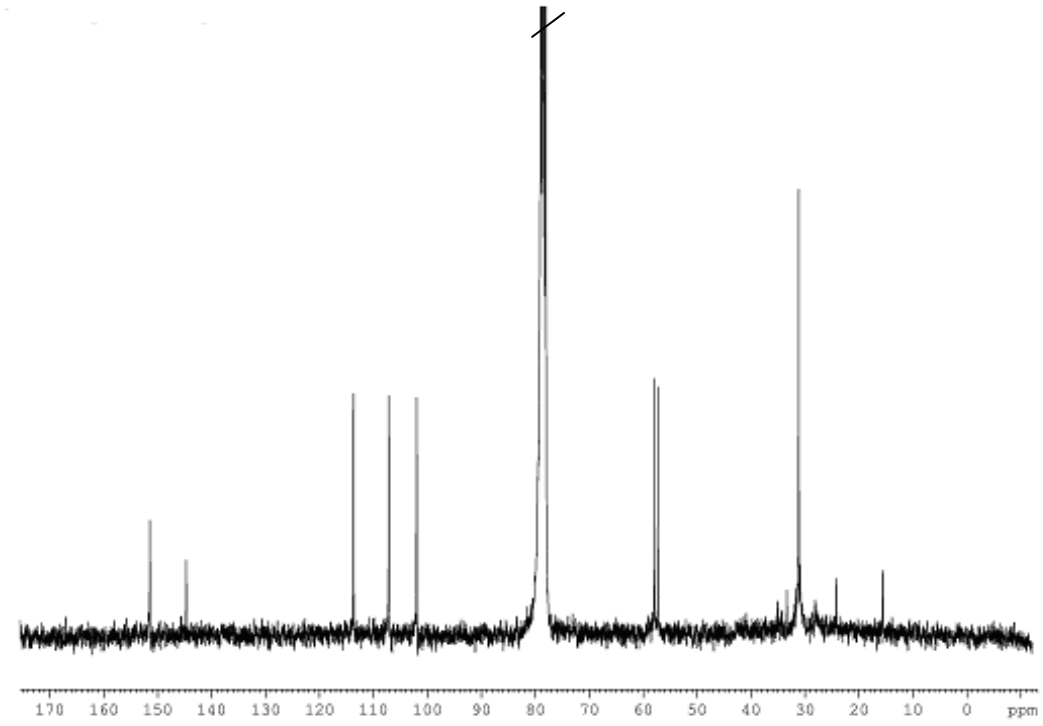

Compound 10, (crotocin), *Acremonium* sp., $CDCl_3$.

^{1}H NMR

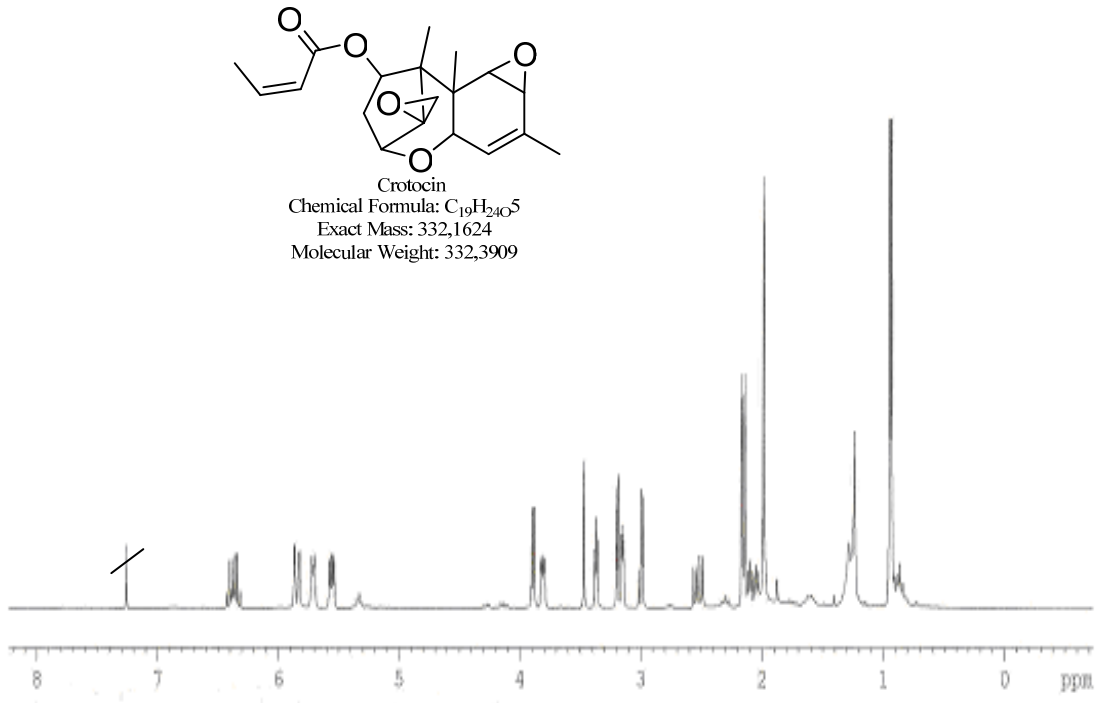

^{13}C NMR

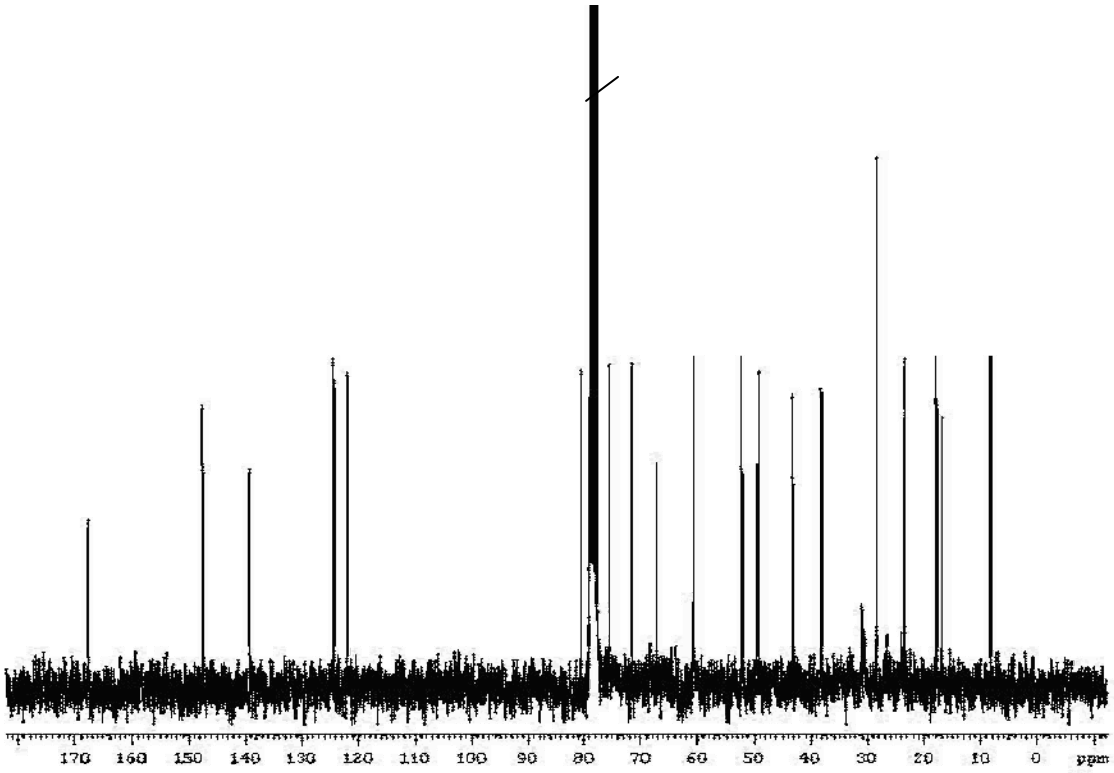

Compound 11, (probable Crotocin artefact - open epoxyde), *Acremonium* sp., MeOD.

^{1}H NMR

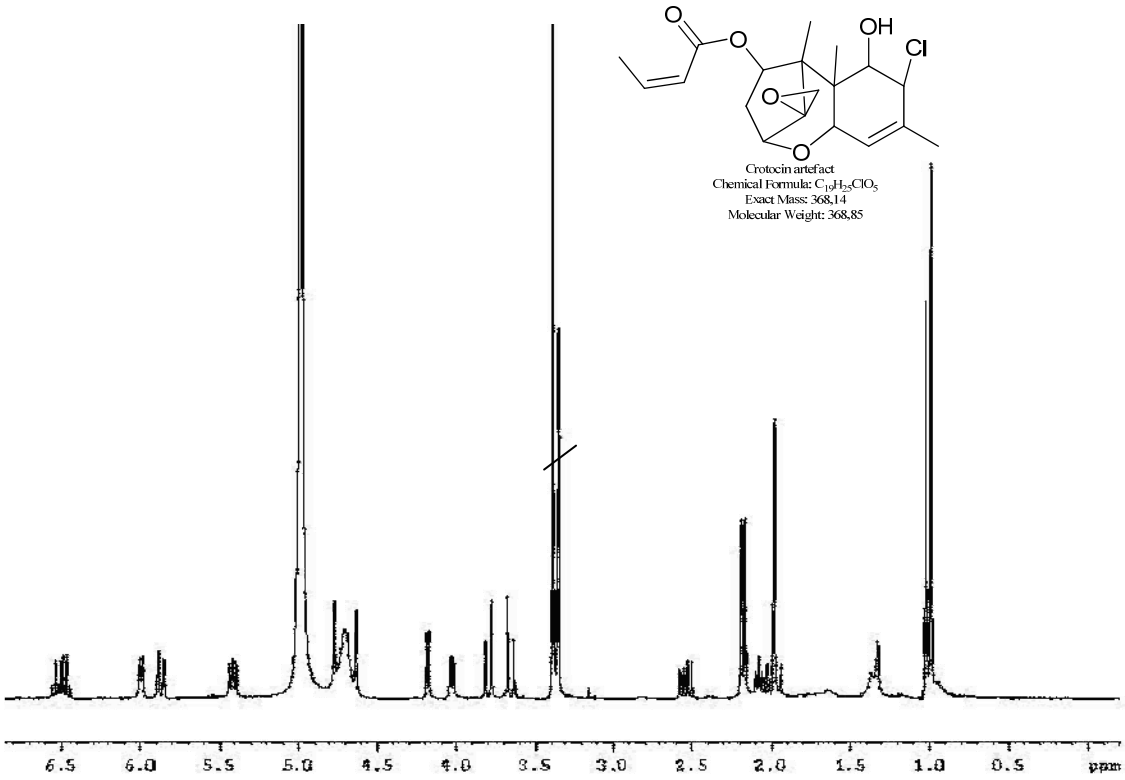

^{13}C NMR

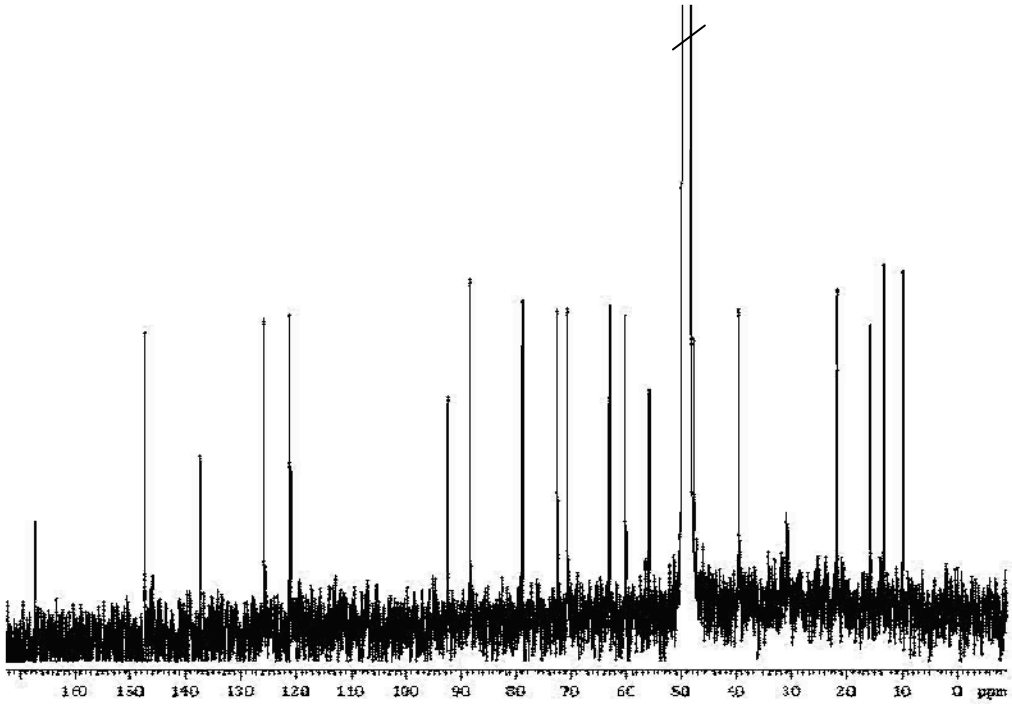

Compound 12, (ergosta-4,6,8 (14), 22-tetraen-3-one, impure sample), *Acremonium* sp., $CDCl_3$.

^{1}H NMR

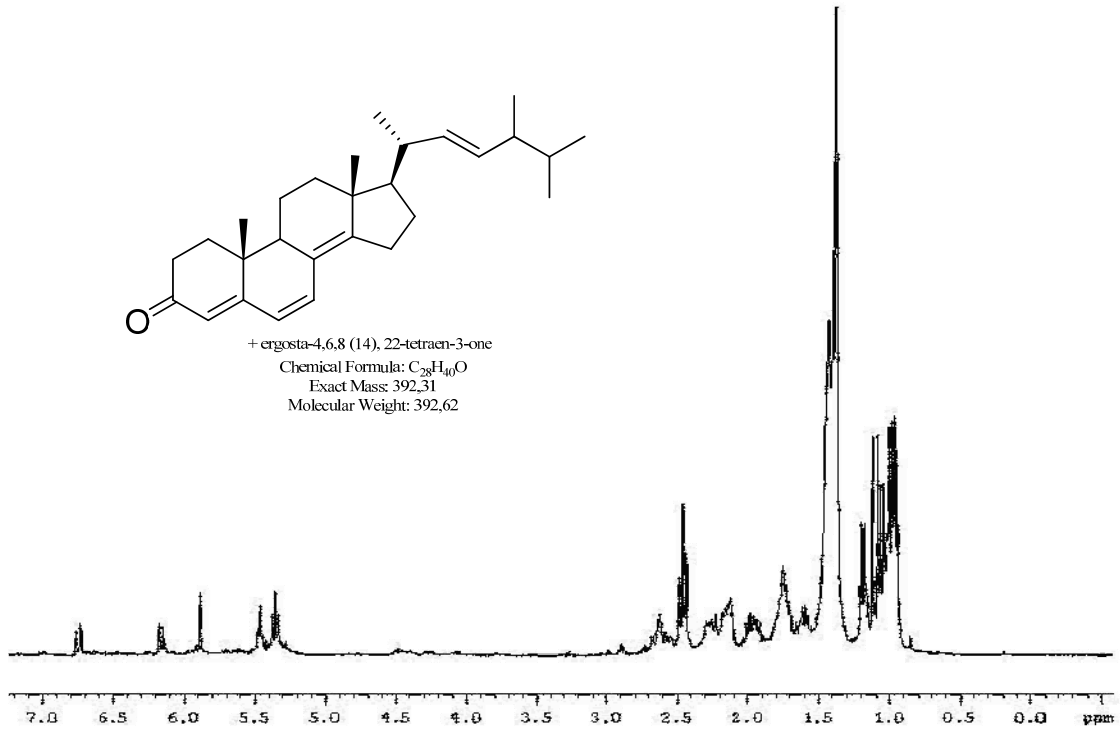

^{13}C NMR

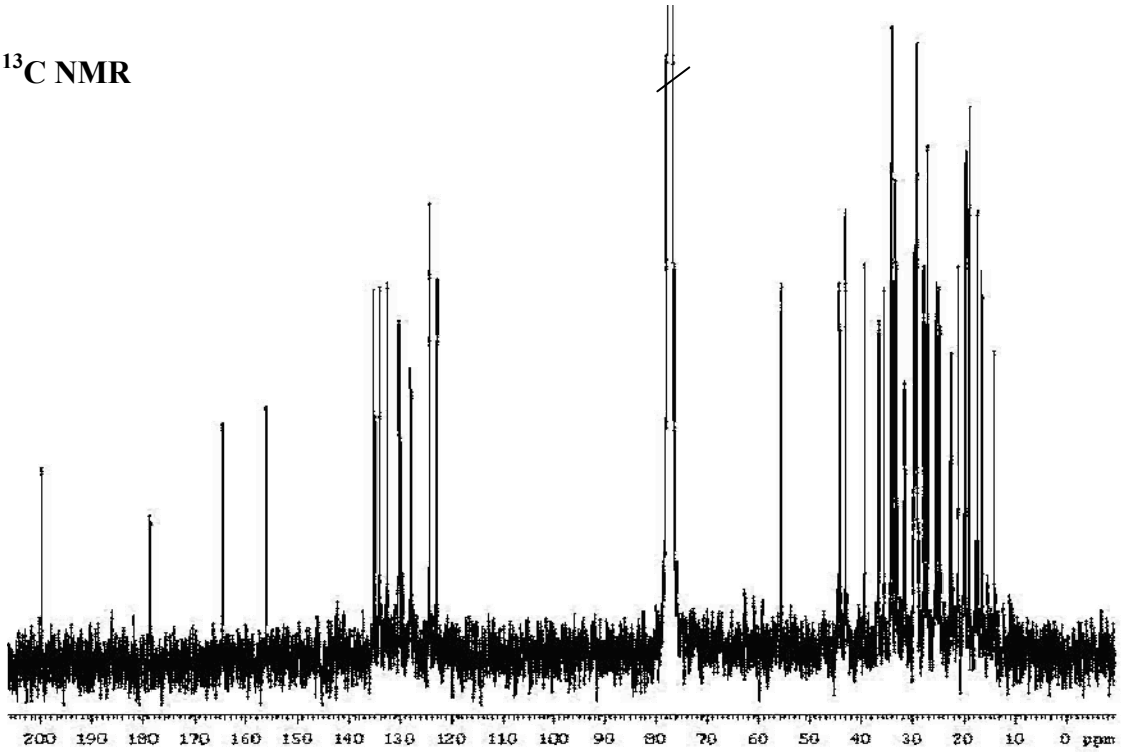

Compound 13,(1, 2, 4-trimethoxy-benzene), *Stachyllidium* sp.,$CDCl_3$.

^{1}H NMR

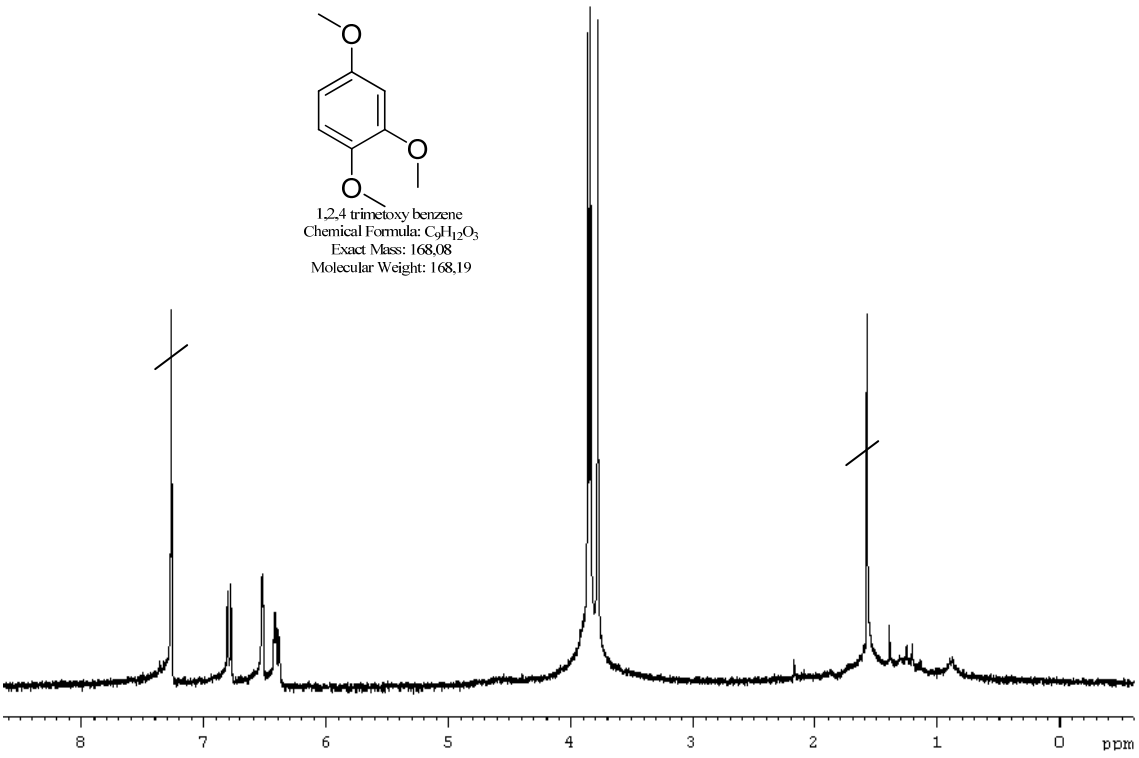

^{13}C NMR

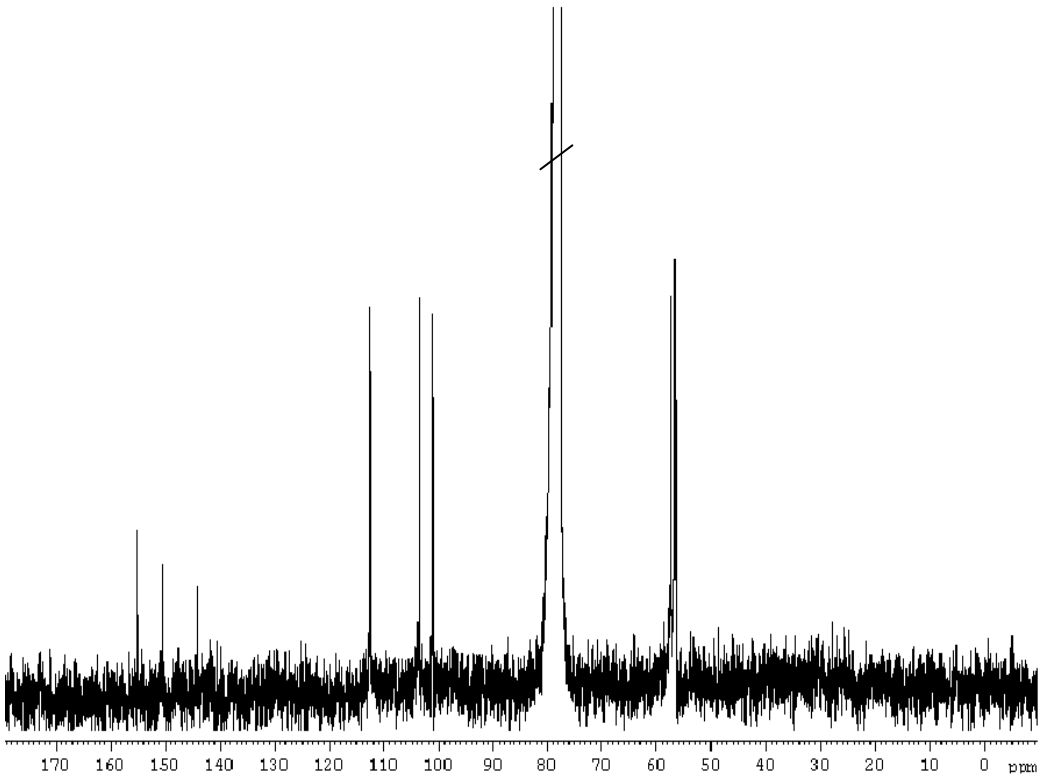

Compound 14 (isosclerone), *Stachyllidium* sp.,$CDCl_3$.

^{1}H NMR

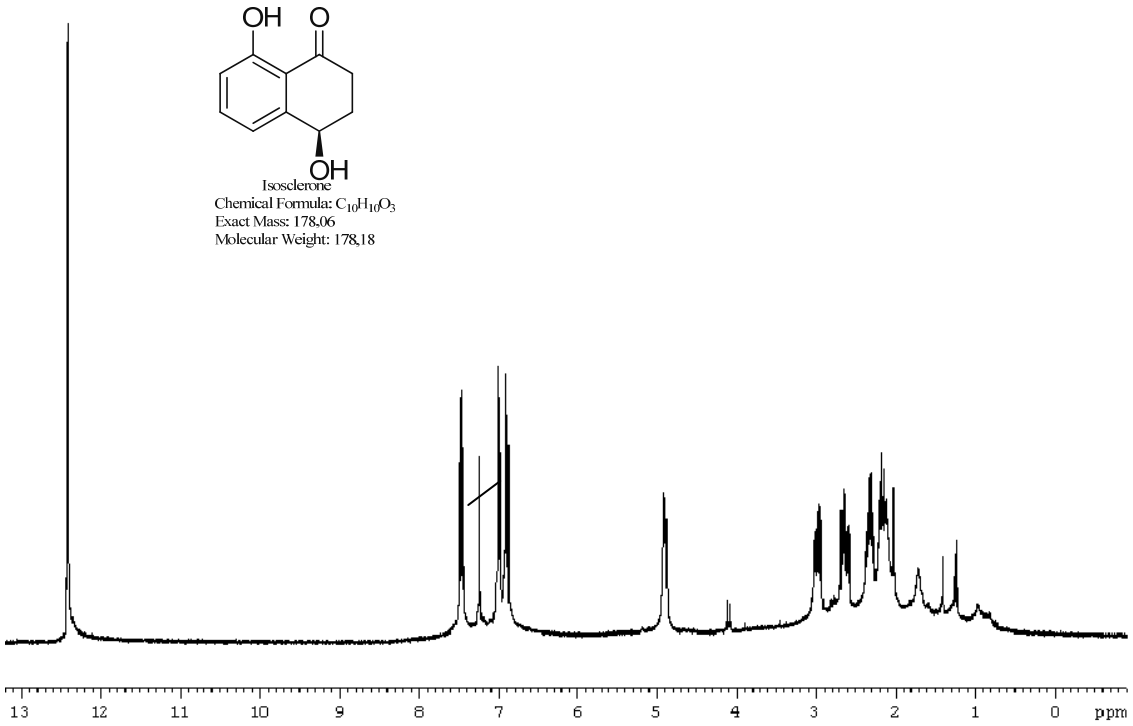

^{13}C NMR

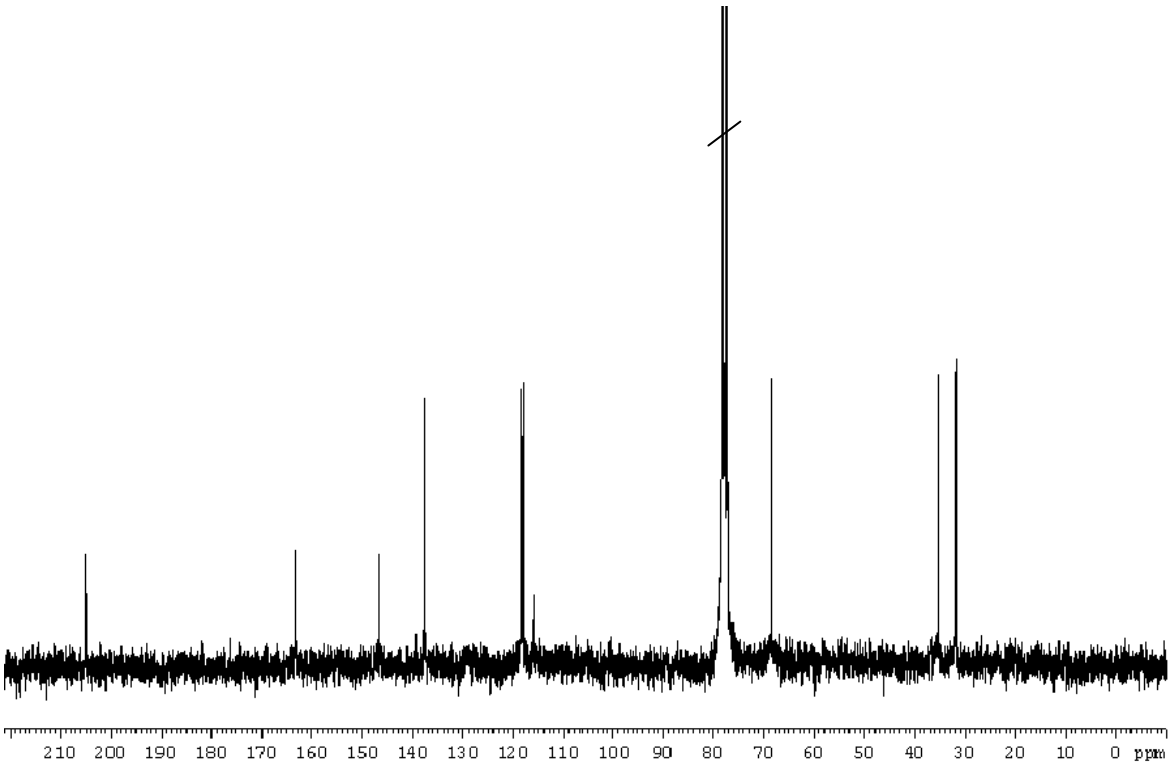

Compound 15, (tirosol), *Stachyllidium* sp.,$CDCl_3$. (H-NMR in MeOD, C-NMR in D-acetone)

^{1}H NMR

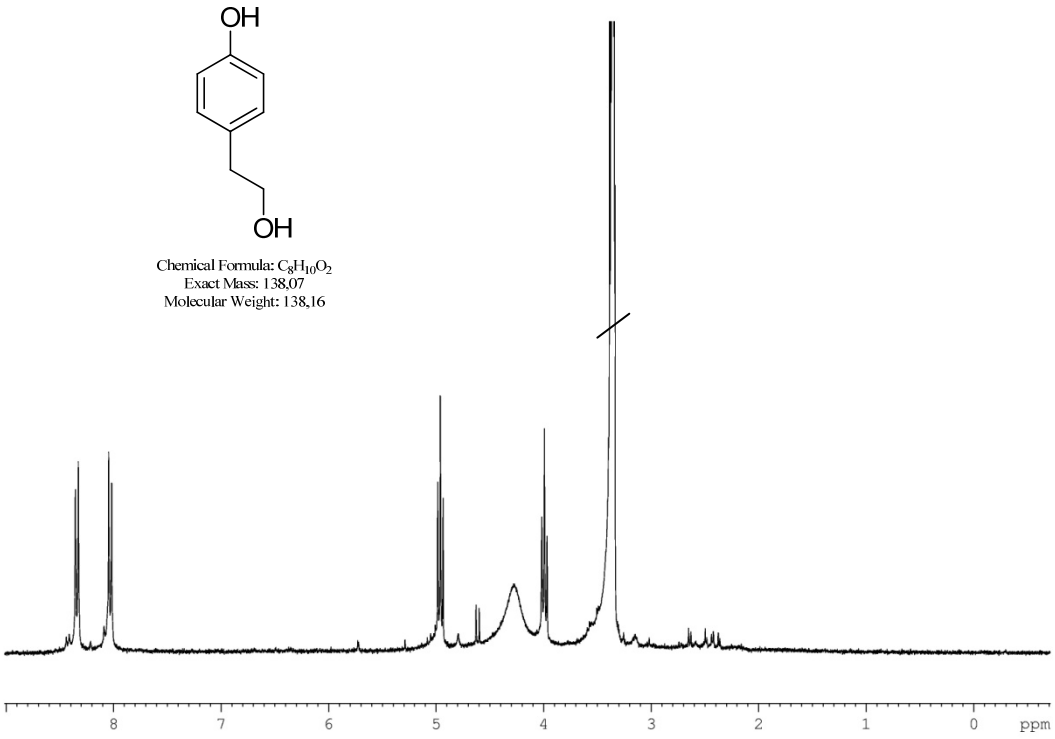

^{13}C NMR

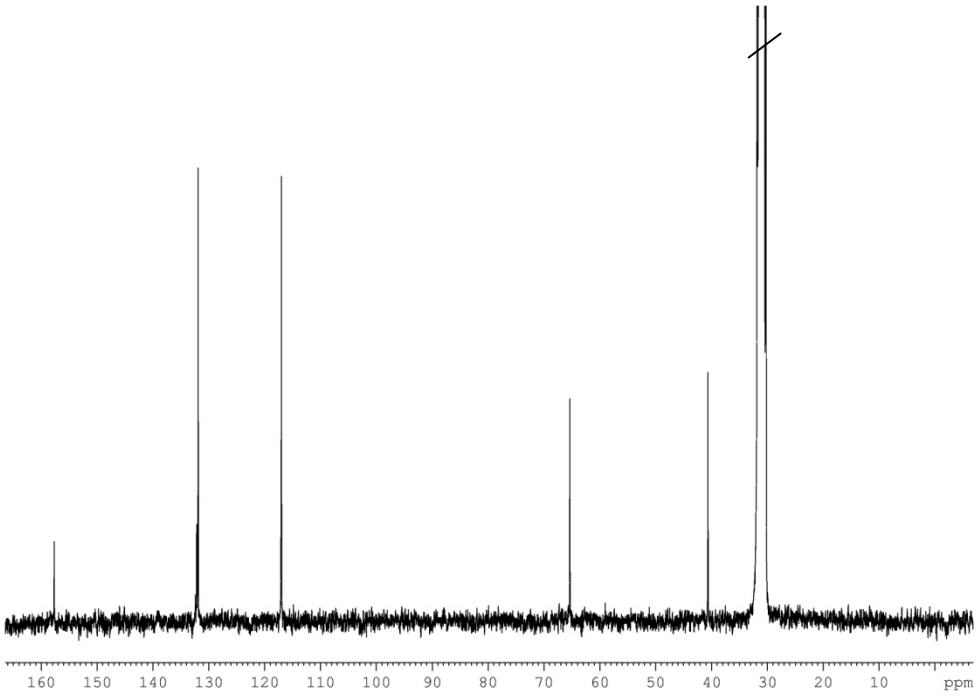

Compound 16, (sterol), *Stachyllidium* sp., D-acetone

^{1}H NMR

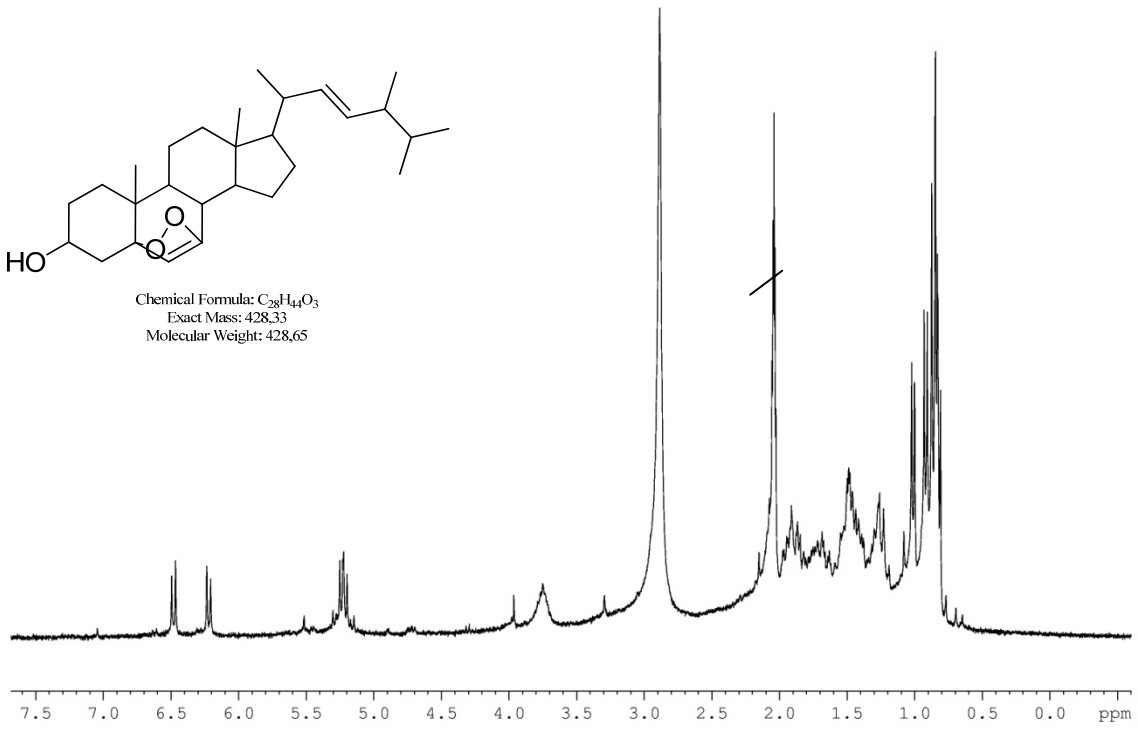

^{13}C NMR

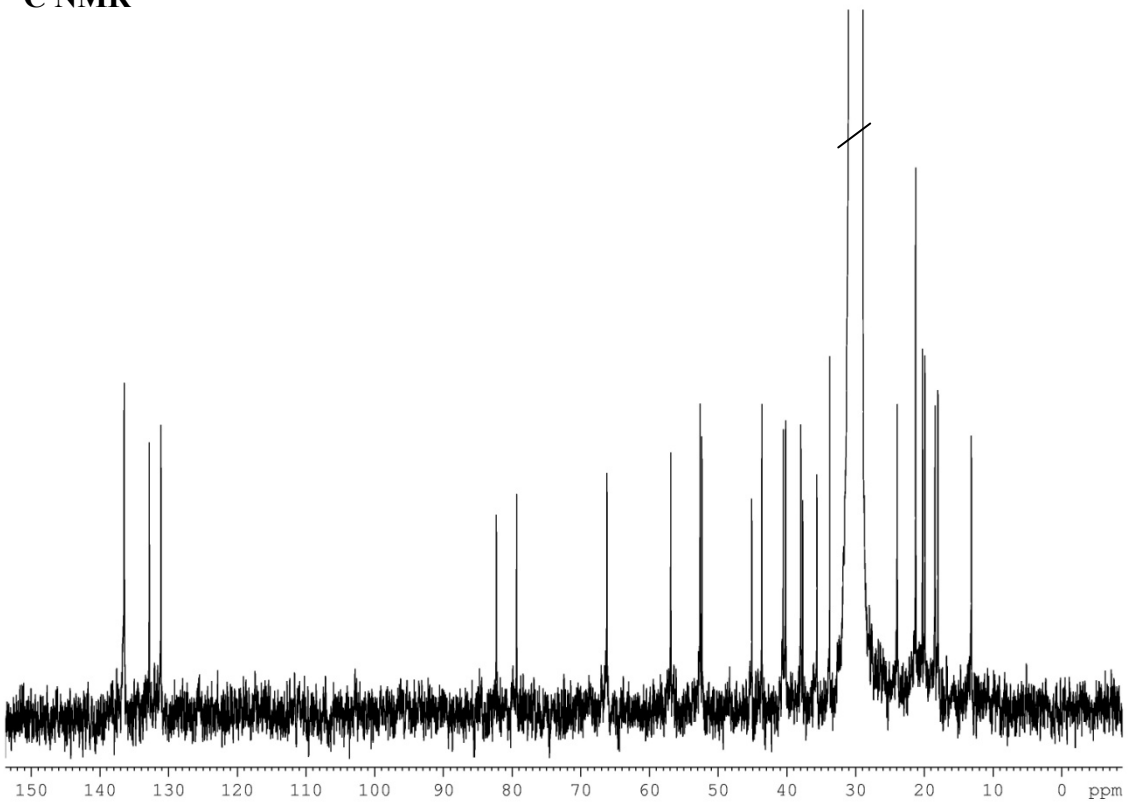

Compound 17, (nidulol), *Stachylidium* sp., D-acetone

^{1}H NMR

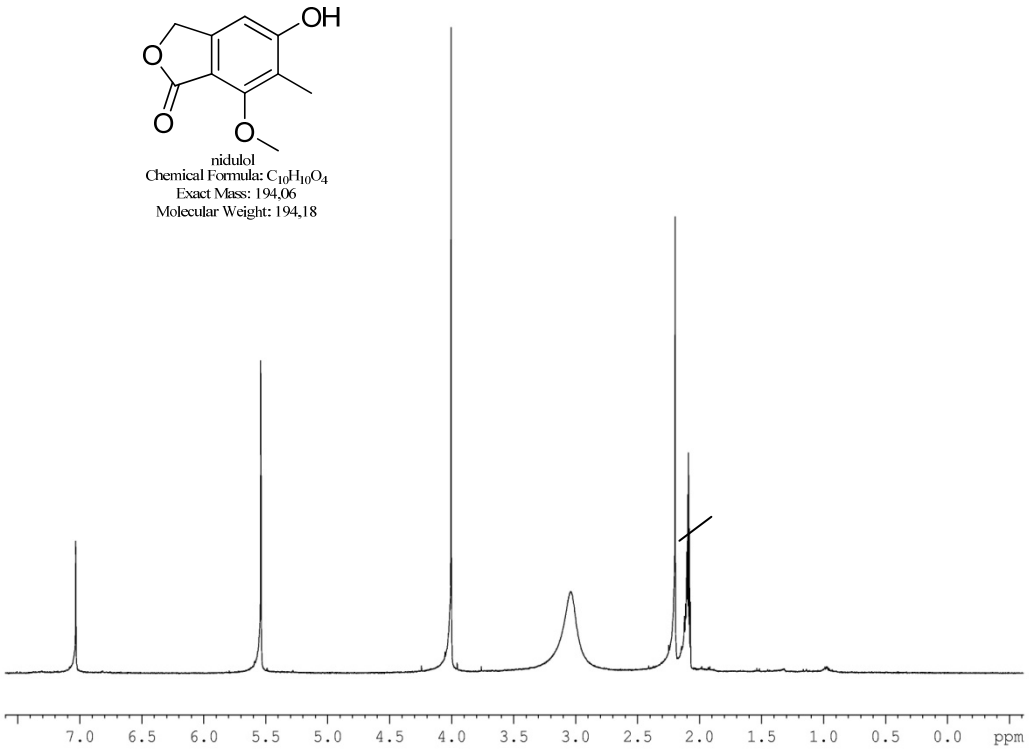

^{13}C NMR

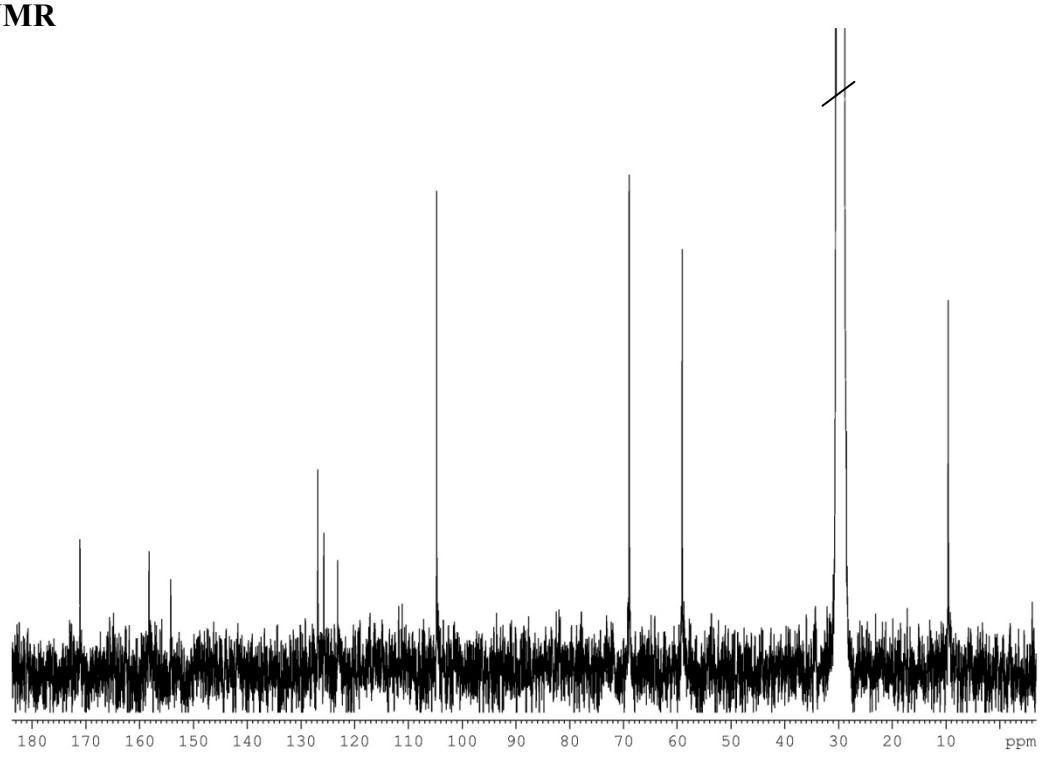

Compound (18) (furyl derivative) *Stachylidium* sp., MeoD

^{1}H NMR

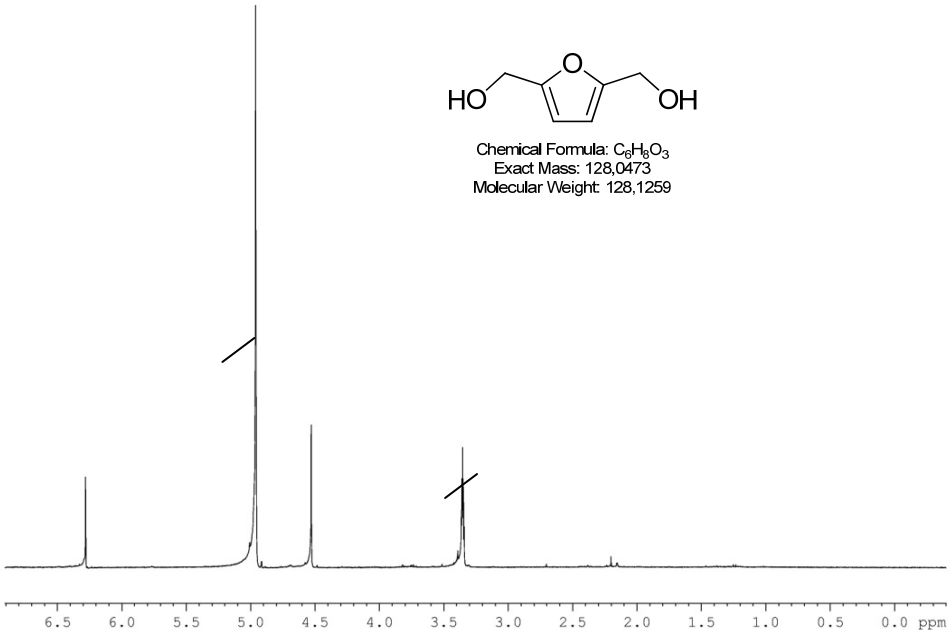

^{13}C NMR

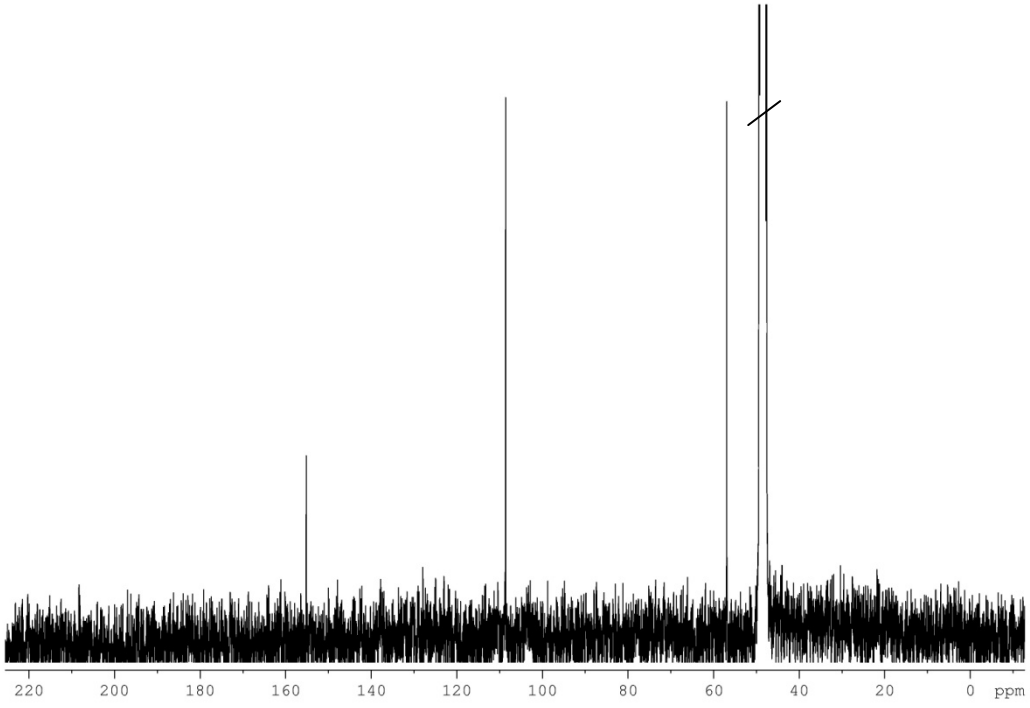

Compound (19), (tyrosine derivative), *Stachylidium* sp., MeoD

^{1}H NMR

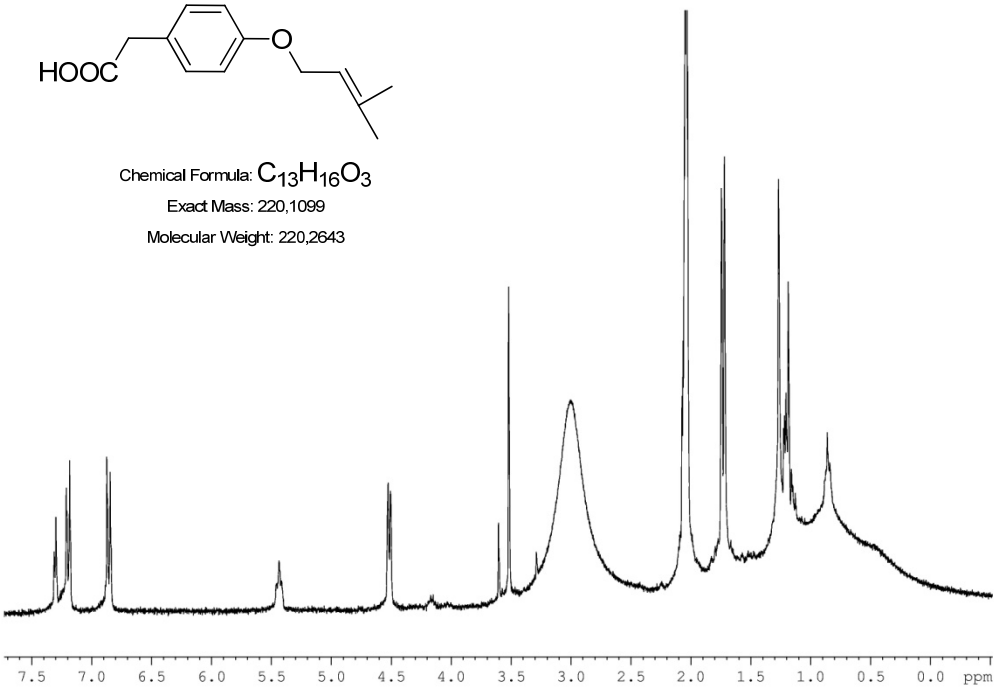

^{13}C NMR

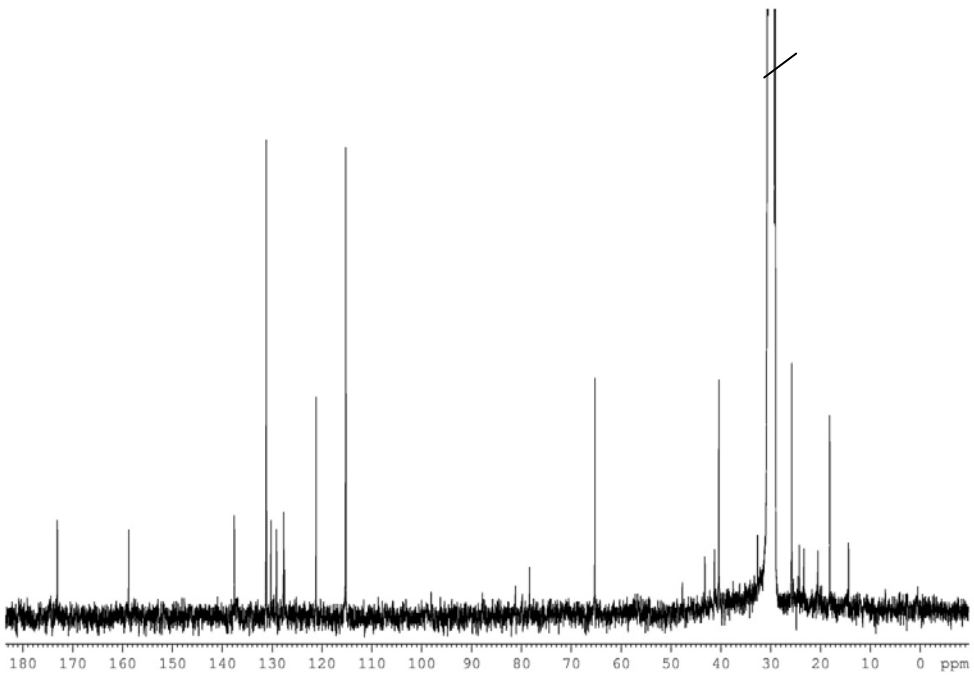

Compound 20, *para*-hydroxyphenylacetic acid, *Stachylidium* sp., MeoD

^{1}H NMR

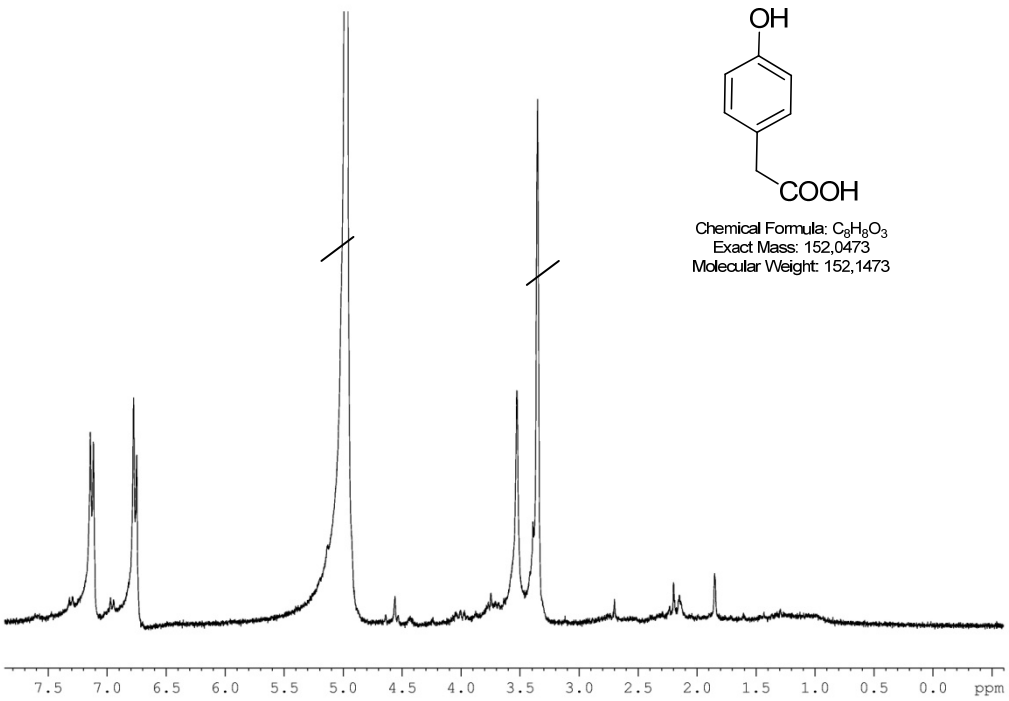

^{13}C NMR

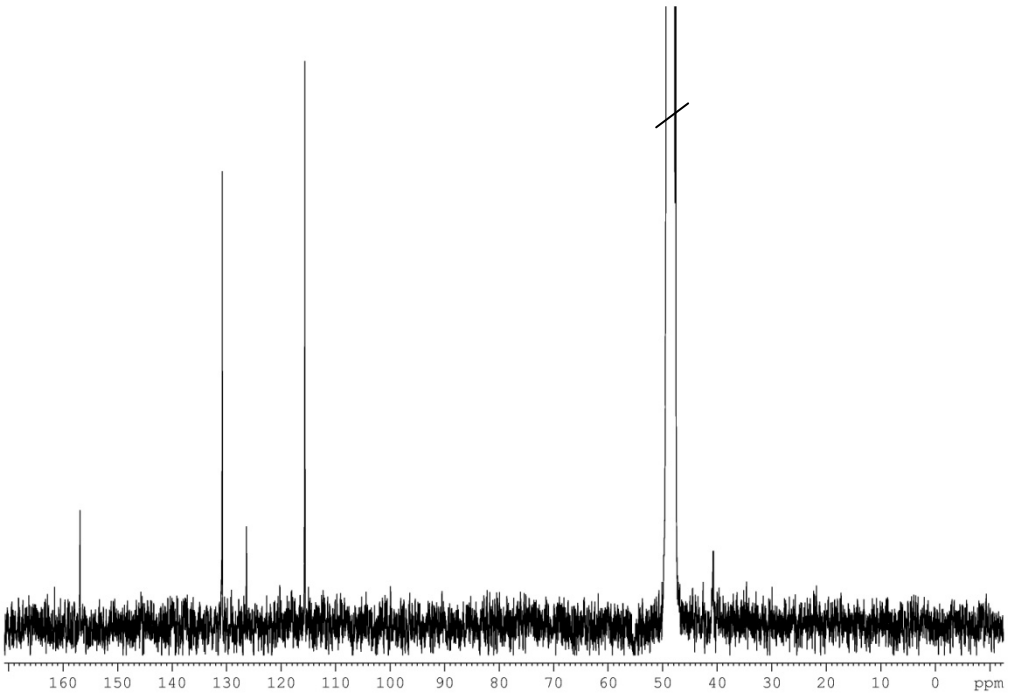

Compound 21, phenylacetic acid, *Stachylidium* sp., D-acetone

^{1}H NMR

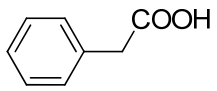

Chemical Formula: $C_8H_8O_2$
Exact Mass: 136,0524
Molecular Weight: 136,1479

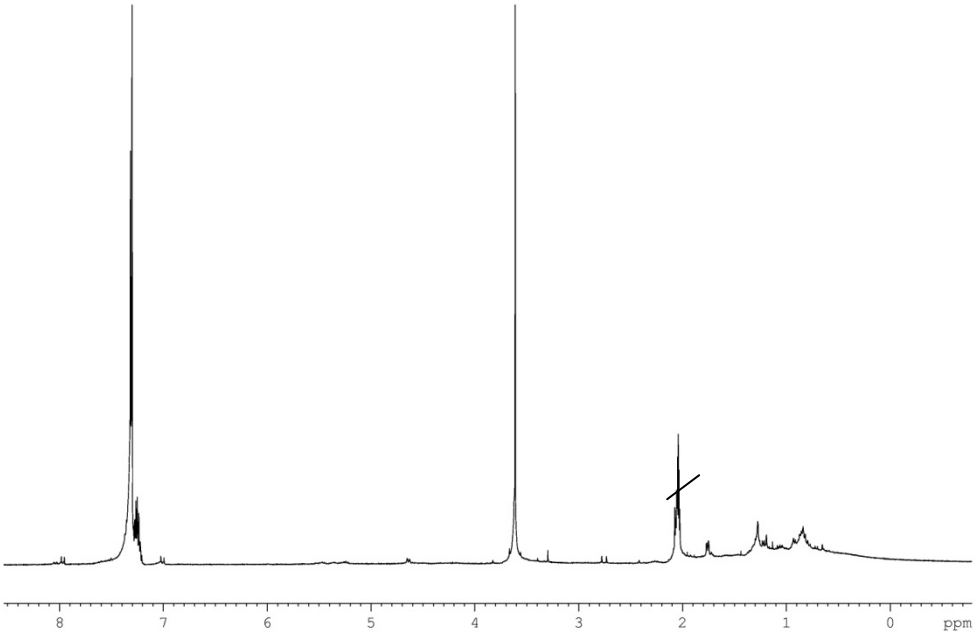

^{13}C NMR

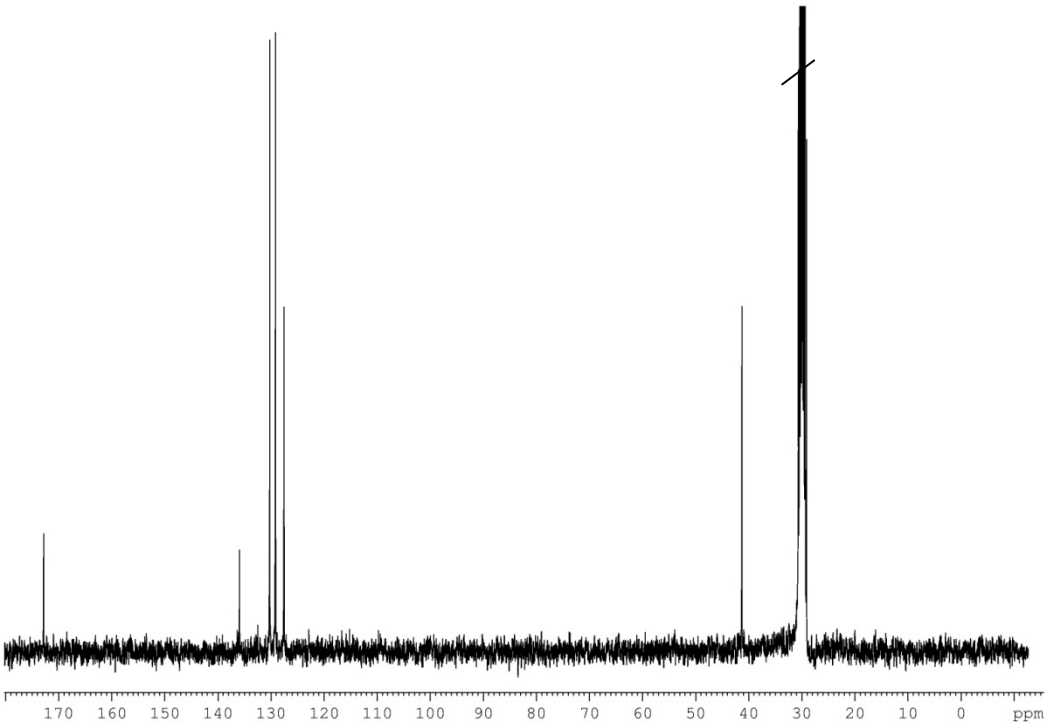

Compound 22, benzoic acid, *Stachylidium* sp., D-acetone

^{1}H NMR

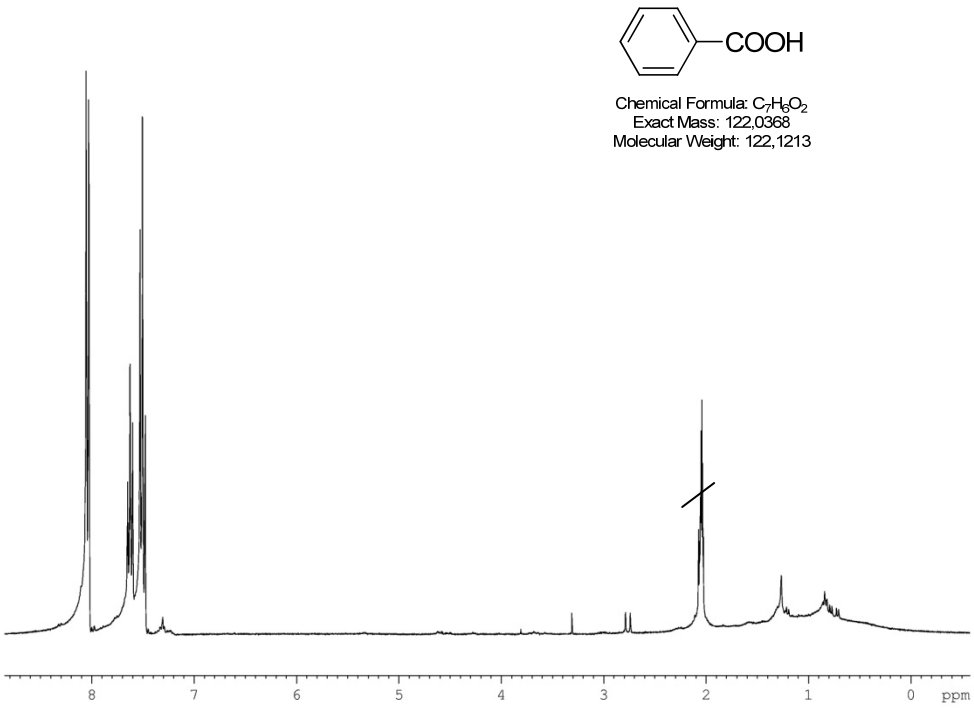

^{13}C NMR

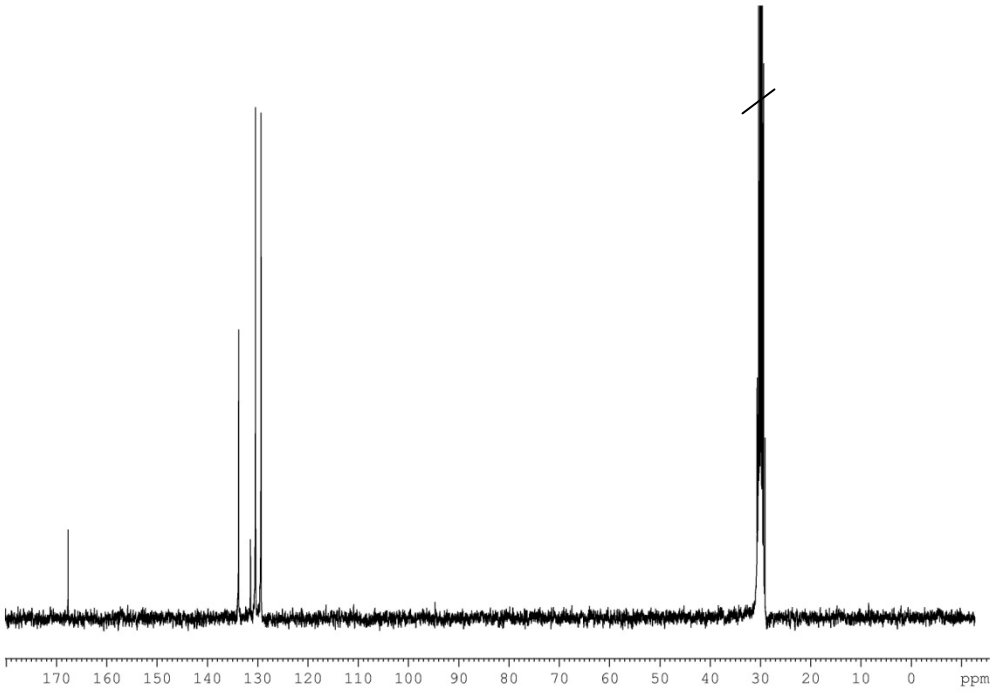

Compound 23, sterol, *Stachylidium* sp., D-acetone

^{1}H NMR

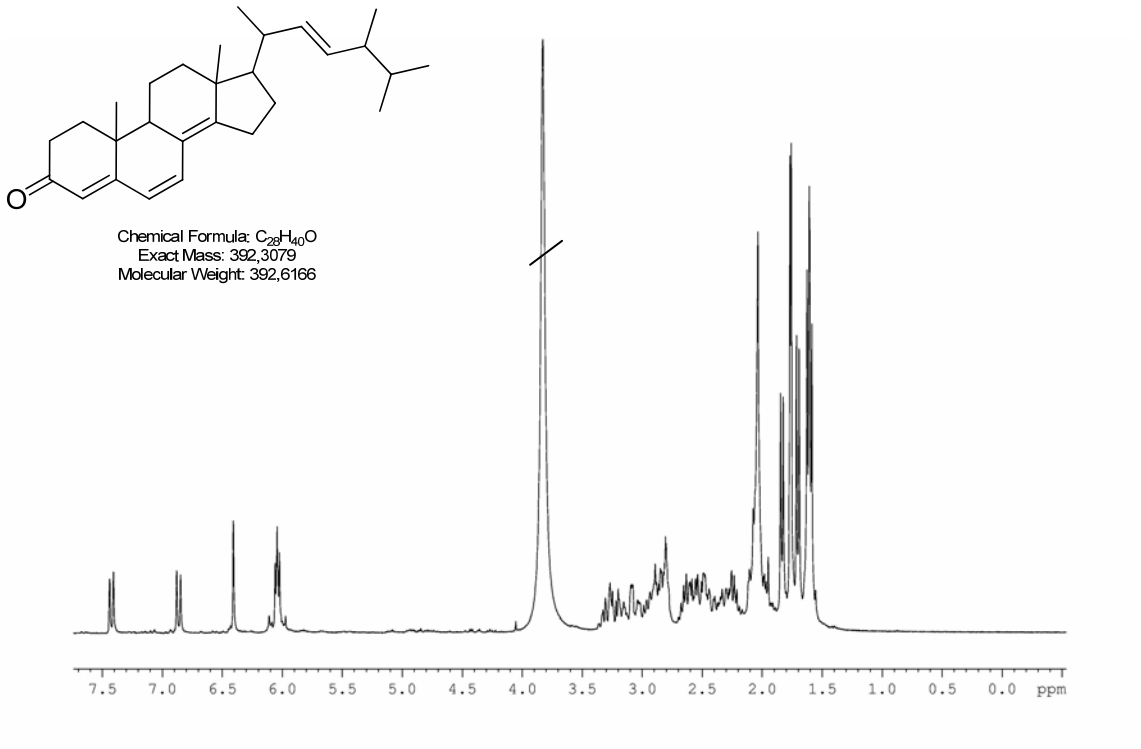

^{13}C NMR

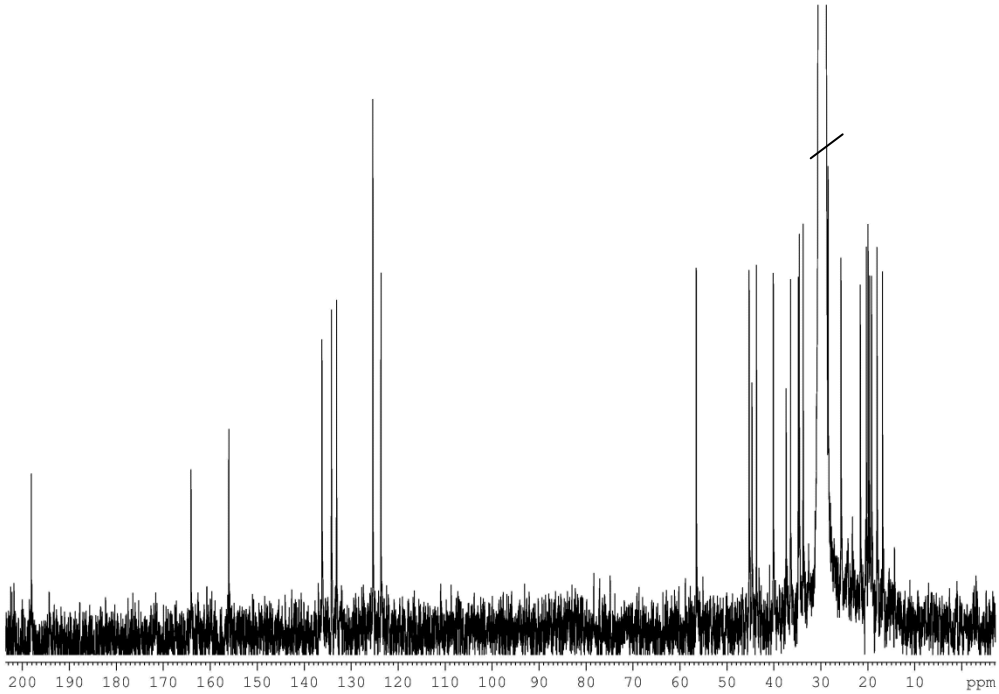

Compound 24, (2-furoic acid), *Stachylidium* sp., MeoD

^{1}H NMR

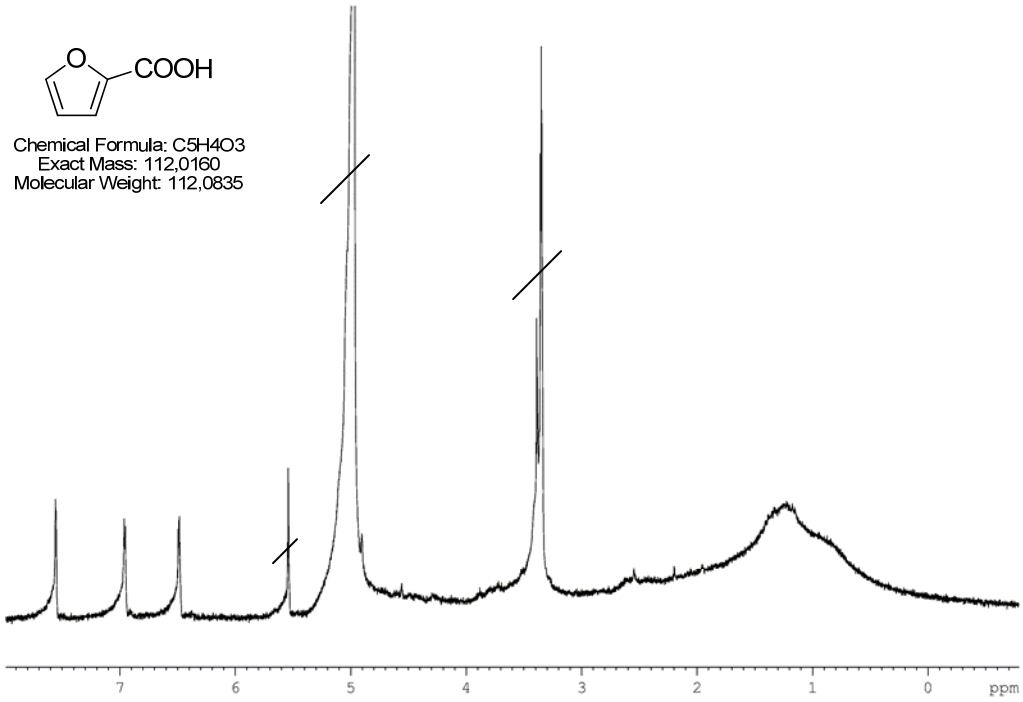

No ^{13}C NMR ; m/z 112.02; LR-LC-MS, found 110.8 $(M–H)^{+}$

The assignment of NMR shifts was supported using the ACD NMR predictor software (ACD/Labs®).

Compound 25, (3,4-dihydroxybenzoic acid/Catechuic acid), *Stachylidium* sp., MeoD

^{1}H NMR

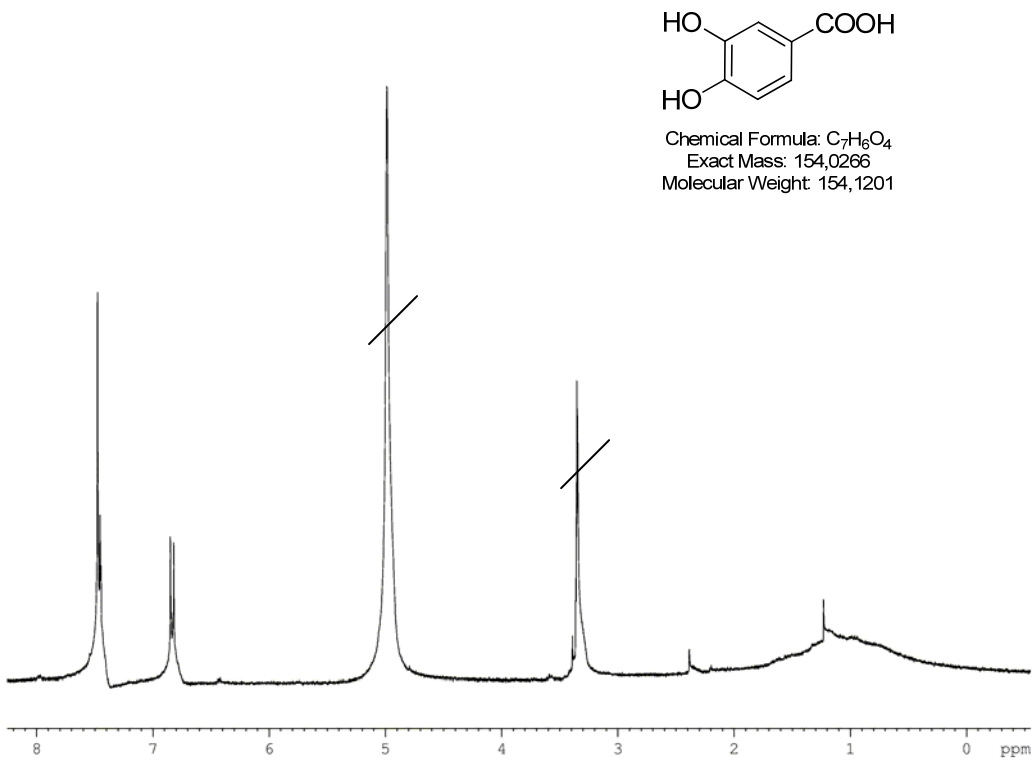

^{13}C NMR

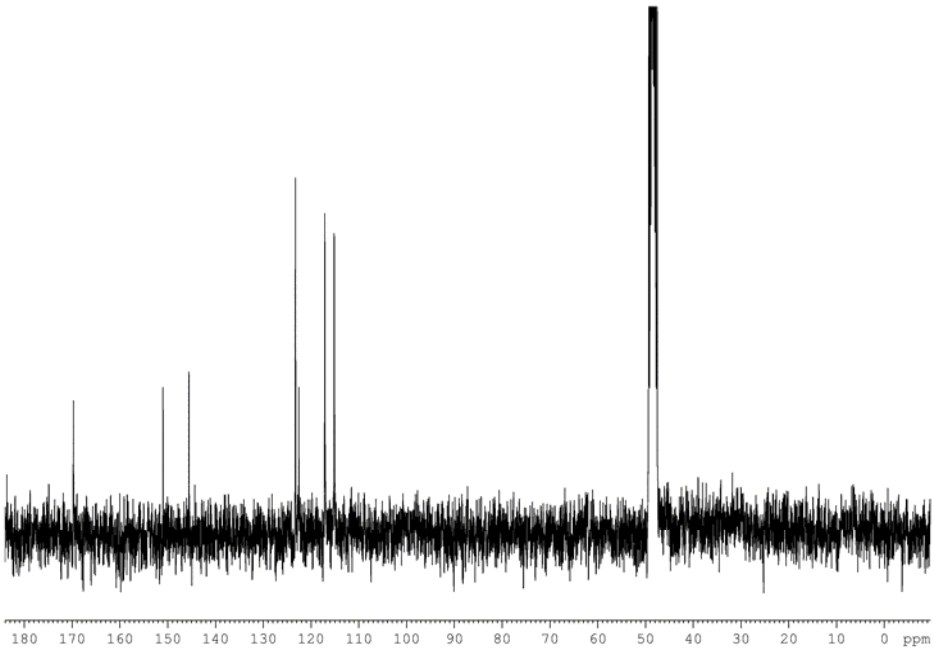

Compound **26, (**-(furan-2-yl)ethane-1,2-diol), *Stachylidium* sp., MeoD

^{1}H NMR

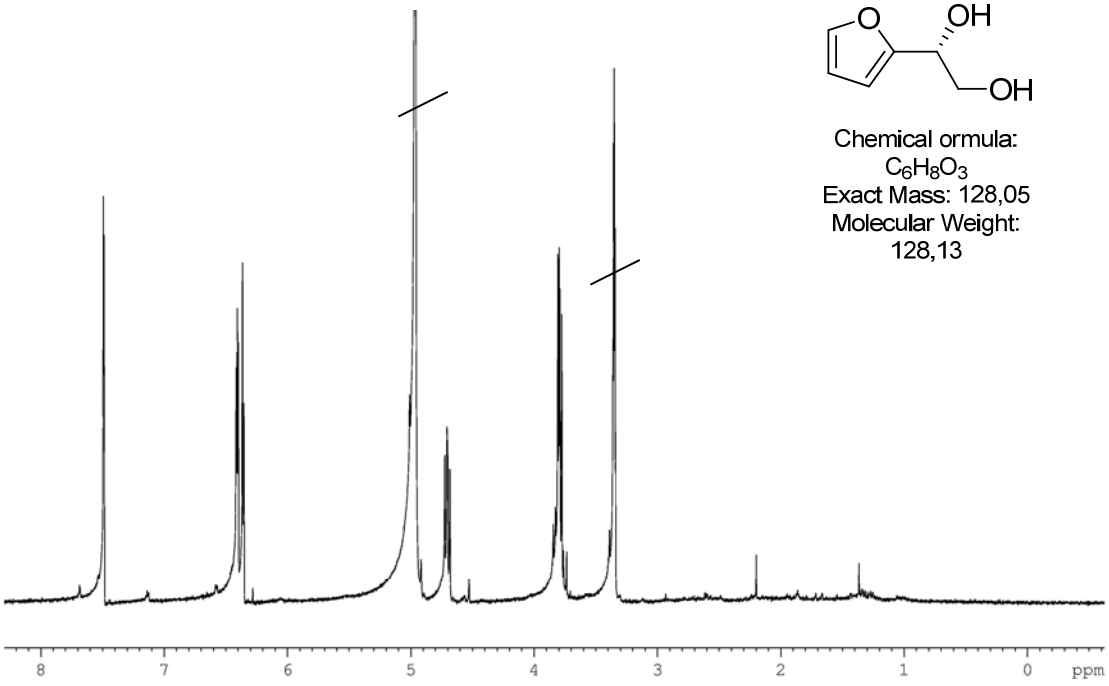

^{13}C NMR